Methods in Molecular Biology 2197

Springer Protocols

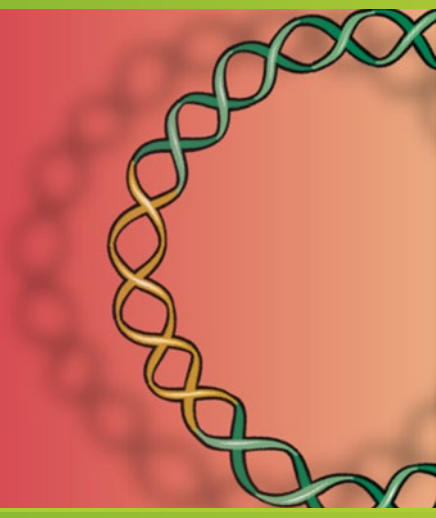

Ângela Sousa *Editor*

DNA Vaccines

Methods and Protocols

Humana Press

METHODS IN MOLECULAR BIOLOGY

Series Editor
John M. Walker
School of Life and Medical Sciences
University of Hertfordshire
Hatfield, Hertfordshire, UK

For further volumes:
http://www.springer.com/series/7651

For over 35 years, biological scientists have come to rely on the research protocols and methodologies in the critically acclaimed *Methods in Molecular Biology* series. The series was the first to introduce the step-by-step protocols approach that has become the standard in all biomedical protocol publishing. Each protocol is provided in readily-reproducible step-by-step fashion, opening with an introductory overview, a list of the materials and reagents needed to complete the experiment, and followed by a detailed procedure that is supported with a helpful notes section offering tips and tricks of the trade as well as troubleshooting advice. These hallmark features were introduced by series editor Dr. John Walker and constitute the key ingredient in each and every volume of the *Methods in Molecular Biology* series. Tested and trusted, comprehensive and reliable, all protocols from the series are indexed in PubMed.

DNA Vaccines

Methods and Protocols

Edited by

Ângela Sousa

CICS-UBI – Health Sciences Research Centre, University of Beira Interior, Covilhã, Portugal

Humana Press

Editor
Ângela Sousa
CICS-UBI – Health Sciences
Research Centre
University of Beira Interior
Covilhã, Portugal

ISSN 1064-3745 ISSN 1940-6029 (electronic)
Methods in Molecular Biology
ISBN 978-1-0716-0871-5 ISBN 978-1-0716-0872-2 (eBook)
https://doi.org/10.1007/978-1-0716-0872-2

This Humana imprint is published by the registered company Springer Science+Business Media, LLC, part of Springer Nature.
The registered company address is: 1 New York Plaza, New York, NY 10004, U.S.A.

Preface

Advances in molecular biology and the recombinant DNA technology are responsible for the emergence of a new paradigm for vaccination, providing tools to manipulate the organism's genome to design and produce DNA vaccines. These vaccines consist in the use of nonviral vectors of eukaryotic cell expression to transport a specific gene, which will encode a specific antigenic protein in the target cell, avoiding the use of the respective pathogen (or parts of the pathogen) dead or attenuated. In addition, DNA vaccines induce strong immune responses after the presentation of antigen genetic information to antigen-presenting cells (APCs), activating both humoral (prophylactic) and cellular (therapeutic) immune responses by the stimulation of T helper cells and cytotoxic and effector $CD8^+$ T cells, respectively. They can also act as adjuvants to the clinical response, for example due to the presence of CpG sequences, which are specific DNA immunostimulatory sequences. These considerations, together with the fact that conventional prophylactic vaccines do not exert any therapeutic effect against an ongoing infection, make DNA vaccination one of the most promising techniques for immunization against a variety of pathogens and tumors mainly induced by viral infections (such as HPV infection).

In general, vaccination has been regaining attention from members of the medical and scientific communities and also the broader public, including heads of state and public health. This level of public awareness of the fundamental relevance of vaccines for global human well-being has been rekindled by dramatic threats of rapidly emerging infectious diseases (predominantly by viruses, such as HIV or the recent coronavirus pandemic) and increasingly widespread multidrug-resistant bacterial infections. The use of DNA vaccines offers a series of economic, technical, and logistical advantages when compared to classical vaccines, especially when their use is considered under the conditions offered by developing countries. Despite the lack of reactivity and immunogenicity of DNA vaccines, they present rapid and low-cost manufacturing, thermostability, and easy distribution. For instance, large-scale production is much cheaper, maintaining quality control is easier, and marketing does not require a refrigeration network, as these vaccines are stable at room temperature. These factors facilitate transport and distribution and enable the transfer of this technology to these countries.

This new edition of *DNA Vaccines* aims to facilitate both efforts by assembling an overview of the field and practical hints for vaccinologists in academia and industry, providing broad and representative insights into recent developments of experimental approaches for DNA vaccines design, inclusion of adjuvants, manufacture, delivery to target cells, and evaluation of induced immune responses. To choose the best approach ahead, a basic understanding of the regulatory framework, including aspects of nonclinical safety testing and good manufacturing practice, is crucial.

The majority of chapters are designed to provide step-by-step protocols of particular DNA vaccines in combination with helpful technical notes and brief but informative introductions to the specific experimental or clinical approach. The notes section is where the reader can find little hints, tricks, observations, and detailed information that the expertise researcher learn from using a method regularly but does not appear in original research papers. This volume is also complemented by non-protocol contributions

providing overviews of different vaccine topologies, the role of CPG oligonucleotides, and important issues in the context of DNA vaccine transfer to clinical trials, such as ethical aspects and guidelines of how clinical studies should be designed.

Overall, we sincerely hope that this compendium may engender increased collaboration on DNA vaccines between basic and applied scientists in academia, government, and industry to develop future solutions for today's challenges, offering valuable tools and new technological platforms to develop suitable vaccines to treat and prevent diseases in both developed and developing nations.

Covilhã, Portugal *Ângela Sousa*

Contents

Contributors

Ana M. Almeida • *CICS-UBI—Health Sciences Research Centre, University of Beira Interior, Covilhã, Portugal*

Ana M. Azevedo • *Department of Bioengineering, Institute for Bioengineering and Biosciences, Instituto Superior Técnico, Universidade de Lisboa, Lisbon, Portugal*

Vasco Azevedo • *Laboratory of Cellular and Molecular Genetics, Federal University of Minas Gerais, Belo Horizonte, Minas Gerais, Brazil*

Fernanda A. L. Barroso • *Laboratory of Cellular and Molecular Genetics, Federal University of Minas Gerais, Belo Horizonte, Minas Gerais, Brazil*

Pablo Cáceres-Morgado • *Laboratory of Immunoncology, Fundación Ciencia & Vida, Santiago, Chile*

Miguel Castelo-Branco • *CICS-UBI—Health Sciences Research Centre, University of Beira Interior, Covilhã, Portugal; University Hospital Centre of Cova da Beira, Covilhã, Portugal*

Urh Černigoj • *BIA Separations d.o.o., Ajdovščina, Slovenia*

Janin Chandra • *The University of Queensland, Diamantina Institute, Translational Research Institute, Woolloongabba, QLD, Australia*

Nina D. Coelho-Rocha • *Laboratory of Cellular and Molecular Genetics, Federal University of Minas Gerais, Belo Horizonte, Minas Gerais, Brazil*

Diana Costa • *CICS-UBI—Health Sciences Research Centre, University of Beira Interior, Covilhã, Portugal*

Bruna Gregatti de Carvalho • *School of Chemical Engineering, University of Campinas, Campinas, SP, Brazil*

Ester S. S. dos Santos • *Laboratory of Cellular and Molecular Genetics, Federal University of Minas Gerais, Belo Horizonte, Minas Gerais, Brazil*

Lucimara Gaziola de la Torre • *School of Chemical Engineering, University of Campinas, Campinas, SP, Brazil*

Mariana M. Drumond • *Laboratory of Cellular and Molecular Genetics, Federal University of Minas Gerais, Belo Horizonte, Minas Gerais, Brazil; Center of Federal Education of Minas Gerais (CEFET-MG), Belo Horizonte, Minas Gerais, Brazil*

Ismail Eş • *School of Chemical Engineering, University of Campinas, Campinas, SP, Brazil*

Dalinda Eusébio • *CICS-UBI—Health Sciences Research Centre, University of Beira Interior, Covilhã, Portugal*

Rúben Faria • *CICS-UBI—Health Sciences Research Centre, University of Beira Interior, Covilhã, Portugal*

Barbara K. Felber • *Human Retrovirus Pathogenesis Section, Vaccine Branch, Center for Cancer Research, National Cancer Institute at Frederick, Frederick, MD, USA*

Amir Ghaemi • *Department of Influenza and Other Respiratory Viruses, Pasteur Institute of Iran, Tehran, Iran*

Sophie Gierak • *Department of Bioengineering, Institute for Bioengineering and Biosciences, Instituto Superior Técnico, Universidade de Lisboa, Lisbon, Portugal; Institut National des Sciences Appliquées de Rouen, Saint-Étienne-du-Rouvray, France*

Begum Horuluoglu • *National Cancer Institute, NIH, Frederick, MD, USA*

Xintao Hu • *Human Retrovirus Pathogenesis Section, Vaccine Branch, Center for Cancer Research, National Cancer Institute at Frederick, Frederick, MD, USA*
Yanlong Jiang • *College of Animal Science and Technology, Jilin Provincial Engineering Research Center of Animal Probiotics, Jilin Agricultural University, Changchun, China*
Neslihan Kayraklioglu • *National Cancer Institute, NIH, Frederick, MD, USA*
Dennis M. Klinman • *Leitman Klinman Consulting, Potomac, MD, USA; National Cancer Institute, NIH, Frederick, MD, USA*
Alvaro Lladser • *Laboratory of Immunoncology, Fundación Ciencia & Vida, Santiago, Chile; Facultad de Medicina y Ciencia, Universidad San Sebastián, Santiago, Chile*
Kenneth Lundstrom • *PanTherapeutics, Lutry, Switzerland*
Pamela Mancha-Agresti • *Laboratory of Cellular and Molecular Genetics, Federal University of Minas Gerais, Belo Horizonte, Minas Gerais, Brazil*
Ana Raquel Neves • *CICS-UBI—Health Sciences Research Centre, University of Beira Interior, Covilhã, Portugal*
Norbert Pardi • *Department of Medicine, University of Pennsylvania, Philadelphia, PA, USA*
Luís A. Passarinha • *UCIBIO, Departamento de Química, Faculdade de Ciências e Tecnologia, Universidade Nova de Lisboa, Caparica, Portugal*
Gabriel Perli • *Institute of Chemistry, University of Campinas, Campinas, SP, Brazil*
Amanda Costa Silva Noronha Pessoa • *School of Chemical Engineering, University of Campinas, Campinas, SP, Brazil*
Duarte Miguel F. Prazeres • *Department of Bioengineering, Institute for Bioengineering and Biosciences, Instituto Superior Técnico, Universidade de Lisboa, Lisbon, Portugal*
João A. Queiroz • *CICS-UBI—Health Sciences Research Centre, University of Beira Interior, Covilhã, Portugal*
Ana Cristina Ramalhinho • *CICS-UBI—Health Sciences Research Centre, University of Beira Interior, Covilhã, Portugal; University Hospital Centre of Cova da Beira, Covilhã, Portugal*
Sara Sousa Rosa • *Department of Bioengineering, Institute for Bioengineering and Biosciences, Instituto Superior Técnico, Universidade de Lisboa, Lisbon, Portugal*
Ailar Sabbaghi • *Department of Influenza and Other Respiratory Viruses, Pasteur Institute of Iran, Tehran, Iran*
A. Rita Silva-Santos • *Department of Bioengineering, Institute for Bioengineering and Biosciences, Instituto Superior Técnico, Universidade de Lisboa, Lisbon, Portugal*
Ângela Sousa • *CICS-UBI—Health Sciences Research Centre, University of Beira Interior, Covilhã, Portugal*
Fani Sousa • *CICS-UBI—Health Sciences Research Centre, University of Beira Interior, Covilhã, Portugal*
Aleš Štrancar • *BIA Separations d.o.o., Ajdovščina, Slovenia*
Thiago Bezerra Taketa • *School of Chemical Engineering, University of Campinas, Campinas, SP, Brazil*
Laísa M. Tavares • *Laboratory of Cellular and Molecular Genetics, Federal University of Minas Gerais, Belo Horizonte, Minas Gerais, Brazil*
István Tombácz • *Department of Medicine, University of Pennsylvania, Philadelphia, PA, USA*
Antonio Valentin • *Human Retrovirus Section, Vaccine Branch, Center for Cancer Research, National Cancer Institute at Frederick, Frederick, MD, USA*

Alexandra Wagner • *Department of Bioengineering, Institute for Bioengineering and Biosciences, Instituto Superior Técnico, Universidade de Lisboa, Lisbon, Portugal*
Chunfeng Wang • *College of Animal Science and Technology, Jilin Provincial Engineering Research Center of Animal Probiotics, Jilin Agricultural University, Changchun, China*
Drew Weissman • *Department of Medicine, University of Pennsylvania, Philadelphia, PA, USA*
Guilian Yang • *College of Animal Science and Technology, Jilin Provincial Engineering Research Center of Animal Probiotics, Jilin Agricultural University, Changchun, China*
Meihua Yu • *The University of Queensland, Diamantina Institute, Translational Research Institute, Woolloongabba, QLD, Australia*

Part I

Vector Design for Vaccination

Chapter 1

A Novel Cre Recombinase-Mediated In Vivo Minicircle (CRIM) DNA Vaccine Platform for Veterinary Application

Yanlong Jiang, Guilian Yang, and Chunfeng Wang

Abstract

Minicircle DNA (mcDNA) has been considered to be an alternative choice of traditional DNA vaccine due to its much smaller size, resulting in more efficient antigen synthesis, enhanced and long-lasting adaptive immune response, especially cellular immune response. However, the disadvantages such as relative high cost and labor intensiveness severely restrict its direct application in the field of veterinary vaccine. Here, we describe a novel *C*re *R*ecombinase-mediated *I*n vivo *M*cDNA platform, named CRIM, in which the parental plasmid could spontaneously transform into mcDNA by itself after transfection or oral administration. This CRIM vaccine platform might serve as a novel oral antigen delivery system for any infectious diseases, especially for veterinary application.

Key words Cre recombinase, CRIM platform, Minicircle DNA, Parental plasmid, Veterinary DNA vaccine

1 Introduction

Emerging infectious diseases have drawn increased demands to develop novel alternative approaches to design novel vaccine candidates. Among these, DNA vaccine has drawn more and more attentions due to its specific advantages such as easy manipulation and stability for transportation [1]. To date, there have been five species of veterinary DNA vaccine available in market, including the West Nile virus [2], hematopoietic necrosis virus in salmon [3], melanoma in dogs [4], growth hormone-releasing hormone (GHRH) gene therapy for swine [5], and H5N1 DNA vaccine for birds [6]. To note, there are also a number of disadvantages regarding to the application of veterinary DNA vaccine in field. For example, the DNA vaccines usually result in lower antibody titers compared with traditional inactivated vaccine [7]. In addition, the use of DNA vaccine still relies on direct injection which is considered to be labor intensive.

Ângela Sousa (ed.), *DNA Vaccines: Methods and Protocols*, Methods in Molecular Biology, vol. 2197,
https://doi.org/10.1007/978-1-0716-0872-2_1,

Minicircle DNA (mcDNA) is a novel technical platform for improved protein synthesis followed by increased immune response [8]. The parental plasmid could be transformed to mcDNA and another miniplasmid in the presence of recombinase, such as Cre [9], ParA [10], and PhiC31 [11], resulting in dramatically decreased plasmid size. The much smaller mcDNA have a number of advantages compared with parental plasmid, including more efficient entrance into cell nucleus, resulting in increased protein synthesis and long-lasting immune response [12, 13]. In addition, mcDNA vaccine has been shown to induce robust $CD8^+$ T-cell-mediated cellular immune response compared with traditional DNA vaccine [14], indicating its potential application in the control of infectious diseases caused by intracellular pathogens. Since the occurrence of mcDNA, it has been used mainly in the field of human application, such as the stem cell research, Hepatitis B Virus (HBV), and Human Immunodeficiency Virus (HIV) vaccine studies [15, 16], which belong to human being areas. To date, there is still no report regarding its application in veterinary vaccine due to its high cost and labor-intensive processes to purify mcDNA.

In this study, we designed a novel Cre recombinase-mediated in vivo mcDNA production system, named CRIM, in which the plasmid could transform to mcDNA by itself after entrance into host cells [17]. In this case, there is no need to purify mcDNA in vitro. This novel platform provides us en elegant choice to apply mcDNA technology directly in veterinary vaccine study.

2 Materials

2.1 Construction of CRIM Plasmid

1. *Plasmid, strains and cells*: Eukaryotic expression vector pcDNA3.1/NT-GFP-TOPO, Cre recombinase expression plasmid pPGK-Cre-bpA (a gift from Klaus Rajewsky, plasmid 11543, Addgene), competent *Escherichia coli* (*E. coli*) TopDH5α cells (*see* **Note 1**).
2. *Culture medium*: Luria-Bertani (LB) medium.
3. *Antibiotics*: 1000 × Ampicillin (100 mg/mL): Add 5 g ampicillin to 50 mL Milli-Q water.
4. *Enzymes*: PrimeSTAR Max Premix for PCR reaction; Quickcut digestion enzyme: SacII, SalI, PacI, XmaI; T4 DNA ligase.
5. *Other reagents*: 10 × DNA loading buffer: 30 mM EDTA, 50% (v/v) Glycerol, 0.25% (w/v) Xylene Cyanol FF, 0.25% (w/v) Bromophenol Blue. 5× TBE (Tris-Borate electrophoresis buffer): 54 g of Tris base(Tris), 27.5 g of boric acid, 20 mL of 0.5 M EDTA (pH 8.0), prepare in 1 L ddH_2O. 1% agarose

gel: add 0.3 g agarose to 30 mL 1 × TBE buffer. Ethidium bromide (5 mg/mL): EtBr; Electrophoresis equipment; LB-Ampicillin plate: LB agar plate with 100 μg/mL ampicillin.

6. *Kits*: DNA cleanup kit, Gel extraction kit, PurePlasmid Mini Kit.

2.2 Determination of Synthesis of Cre Recombinase

1. *Cells*: human embryo kidney cell HEK293T.
2. *Culture medium*: Dulbecco's Modified Eagle's Medium (DMEM), supplemented with 10% fetal bovine serum (FBS), 100 units/mL penicillin, 100 μg/mL streptomycin. 1 × PBS (phosphate buffered saline): 137 mM NaCl, 2.7 mM KCL, 8 mM Na_2HPO_4, 2 mM KH_2PO_4, pH 7.4. Trypsin solution: 0.25% trypsin-0.02% EDTA.
3. *Kits*: GoldHi EndoFree Plasmid Midi Kit, Whole cell protein extraction kit, ECL Western Blotting Substrate Kit.
4. *Transfection reagents*: Lipofectamine 3000, Opti-MEM medium.
5. *Materials (reagents, instruments, and equipment) for SDS–polyacrylamide and western blot*: Total cell protein extraction kit, 10% SDS-PAGE gel; SDS-PAGE gel electrophoresis equipment; SDS-PAGE running buffer: 25 mM Tris, 192 mM glycine, 0.1% SDS, pH 8.3. Protein ladder molecular weight standards; Laemmli buffer: 10% SDS, 50% glycerol, 0.25% bromophenol blue, and 250 mM Tris–HCl pH 6.8. Before use add 2-mercaptoethanol to a final concentration of 12.5%. 1 × PBST buffer: 137 mM NaCl, 2.7 mM KCL, 8 mM Na_2HPO_4, 2 mM KH_2PO_4, 0.05% Tween-20 (V/V), pH 7.4.
6. *Antibodies*: Rabbit anti-Cre antibody, HRP-conjugated goat anti-rabbit secondary antibody.
7. 25-cm^2 tissue culture flask, six-well cell culture plates.

2.3 Determination of the mcDNA Production

1. *Cell culture and transfection reagents*: Materials and medium are as described above.
2. *Kits*: QIAprep Spin Plasmid Kit.

2.4 Preparation of Bacteria Harboring CRIM Plasmid

1. *Strain*: attenuated *Salmonella* or other intracellular bacteria.
2. *Reagents for preparation of competent cell*: ddH_2O, 10% glycerol.
3. *Equipment*: electrometer; spectrophotometer; centrifuge.
4. *Others*: LB + 100 μg/mL ampicillin agar plate; LB medium; 1 × PBS (phosphate buffered saline): 137 mM NaCl, 2.7 mM KCL, 8 mM Na_2HPO_4, 2 mM KH_2PO_4, pH 7.4.

3 Methods

3.1 Construction of CRIM Plasmid

Ideally, any eukaryotic expression plasmid could be used as a backbone for the construction of CRIM vector (*see* **Note 2**). Here we take use of the classic eukaryotic vector pcDNA3.1/NT-GFP-TOPO as an example (*see* **Note 3**).

1. Use PrimeSTAR Max Premix for amplification of the CMV-GFP-SV40polyA cassette (*see* **Note 2**) with primers loxP-SacII-F and loxP-StuI-R (*see* **Note 4**). At the same time, use primers pcDNA -SacII and pcDNA -StuI (*see* **Note 5**) to amplify the backbone using pcDNA3.1/NT-GFP-TOPO as template. The underlined sequences indicate the restriction sites, whereas the italic letters indicate the loxP site.
   loxP-SacII-F:

   TATGCCGCGG TAATATAACTTCGTATAGCATACATTAT ACGAAGTTAT GGGGTCATTAGGGGACTTTC.

   loxP-StuI-R:

   ACCAGGCCT ATAACTTCGTATAGCATACATTATACGAA GTTAT CCACCGCATCCCCACATGCTTTG.

   pcDNA-SacII: AATACCGCGGAGGCAAGGCTTGACCGAC.

   pcDNA -StuI: GTAAGGCCTGGGCGCGTGGGGATACCCC.
2. Add 10 μL 10 × DNA loading buffer to 90 μL PCR product, load onto 1% agarose gel and separate by agarose gel electrophoresis.
3. Cut out the expected DNA fragment and purify the DNA by gel extraction kit.
4. Digest 1 μg both of the purified PCR products with Quickcut SacII and StuI at 37 °C for 4 h.
5. Purify the digested products by DNA clean up kit according to instruction.
6. Ligate the insert and vector at a ratio of 5:1 using T4 DNA ligase for overnight at 16 °C.
7. Transform *E. coli* DH5α with the ligation product according to instruction. Incubate the LB- Ampicillin plate overnight at 37 °C.
8. Pick a single colony and inoculate into a 15 mL glass tube containing 5 mL LB medium with 50 μg/mL of ampicillin. Incubate the tube in a shaking incubator overnight at 200 rpm and 37 °C.
9. Extract plasmid DNA using PurePlasmid Mini Kit according to the manufacturer's instructions. The generated plasmid is named pcDNA-loxP, which contains two loxP sites located outside the CMV-GFP-polyA cassette (*see* **Note 6**).

10. To amplify the Cre recombinase expression cassette, PGK-cre-polyA plasmid (*see* **Note 7**) is used as template with the primers PGK-F-XmaI/PGK-R-PacI (*see* **Note 5**). At the same time, primers pcDNA-loxP-XmaI and pcDNA-loxP-PacI are used to amplify vector backbone using the above pcDNA-loxP plasmid as template. The underlined sequences correspond to the recognition sequences for the respective restriction enzymes:

    PGK-F-XmaI: TCCCCCGGGTCGAGGTCGACGGTATCG.

    PGK-R-PacI: CCTTAATTAACCAGCTGGTTCTTTCCTCAG.

    pcDNA-loxP-XmaI: TCCCCCGGGCCGCTCACAATTCCACAC.

    pcDNA-loxP-PacI: CCTTAATTAACAGTGAGCGAGGAAGCGG.

11. Repeat **steps 2** and **3** to purify amplified PCR products.
12. Digest 1 μg both of the purified PCR products with XmaI and PacI at 37 °C for 4 h.
13. Repeat **steps 5**–**7** to transform *E. coli* DH5α competent cells using the ligation of two fragments mentioned above.
14. Pick a single colony and inoculate into a 15 mL glass tube containing 5 mL LB medium with 50 μg/mL of ampicillin. Incubate the tube in a shaking incubator overnight at 200 rpm and 37 °C.
15. Extract plasmid DNA using miniplasmid kit according to the manufacturer's instructions. The generated plasmid is named CRIM plasmid pcDNA-loxP-Cre.

3.2 Determination of Synthesis of Cre Recombinase by Western Blot

To determine the production of Cre recombinase by pcDNA-loxP-Cre, HEK293T cells are used for transfection and further analysis.

1. Maintain HEK293T cells in DMEM containing 10% FBS. On the day before transfection, aspirate culture medium, and wash each plate with 5 mL PBS. Then 2 mL of trypsin-EDTA is used to incubate cells for 10 min at 37 °C.
2. After the cells are detached from plate, resuspend cells in fresh DMEM-10% FBS.
3. Count the cells and plate 1×10^6 cells in each well of six-well plate. Incubate cells at 37 °C and 5% CO_2. On the day of transfection, cells should be 70–80% confluent which is optimal for transfection efficiency.
4. Plasmids are extracted by GoldHi EndoFree Plasmid Midi Kit according to the instruction. Cells are transfected with purified plasmid using Lipofectamine 3000 in Opti-MEM medium according to the instructions.

5. After 48 h post transfection, trypsinize the cells with 100 μL of trypsin-EDTA per well and incubate for 5 min at 37 °C.
6. Collected cells are lysed by whole cell protein extraction kit to extract total protein samples and subject to sodium dodecyl sulfate polyacrylamide gel electrophoresis (SDS-PAGE) in 10% acrylamide gels, followed by western blot. To note, rabbit anti-Cre antibody is used as primary antibody, followed by HRP-conjugated goat anti-rabbit secondary antibody.
7. Extract whole cell protein using commercial kit.
8. Add 50 μL of Laemmli buffer to the lysate and mix well. Boil the samples at 95 °C in a heat block for 5 min.
9. Subject the samples (10 μL) to SDS-PAGE in 10% acrylamide gels and then transfer the proteins to PVDF membranes.
10. For western blot, the PVDF membrane is incubated with rabbit anti-Cre antibody as primary antibody for 1 h at room temperature. After washing three times with PBST, the membrane is incubated with HRP-conjugated goat anti-rabbit secondary antibody for 1 h at room temperature. After further washing three times with PBST, the membrane is observed using ECL substrate.

3.3 Confirmation of the Production of mcDNA

After transfection, the total DNA components are extracted from HEK293T cells to confirm the production of mcDNA.

1. HEK293T cells in 6 well plates are transfected with purified plasmid pcDNA-loxP-Cre as described above.
2. After 24 h post transfection (*see* **Note 8**), the supernatants are discarded and cells are digested with 100 μL of trypsin-EDTA per well and incubate for 5 min at 37 °C.
3. Then, cells are collected by centrifuge at 350 × *g* for 10 min at 4 °C. The total DNA components are then extracted using QIAprep Spin Plasmid Kit according to manufacturer's instructions (*see* **Note 9**).
4. The extracted DNA is used as template to amplify either parental plasmid or mcDNA using primers CMV-F and CMV-R (*see* **Note 10**).

   CMV-F: ATGCCAAGTACGCCCCCT.

   CMV-R: ATACACTTGATGTACTGC.
5. The PCR products are separated by 1% DNA gel to determine the presence of mcDNA (Fig. 1) (*see* **Note 11**).

3.4 Bacterial Delivery of mcDNA In Vivo

The novel CRIM plasmid can be delivered by bacterial vectors for oral immunization in veterinary application, for example, the attenuated *Salmonella* strain C500 [18] (*see* **Note 12**). Firstly, we can transform the CRIM plasmid into the competent cells of *Salmonella* and then use the recombinant strain to immunize animals.

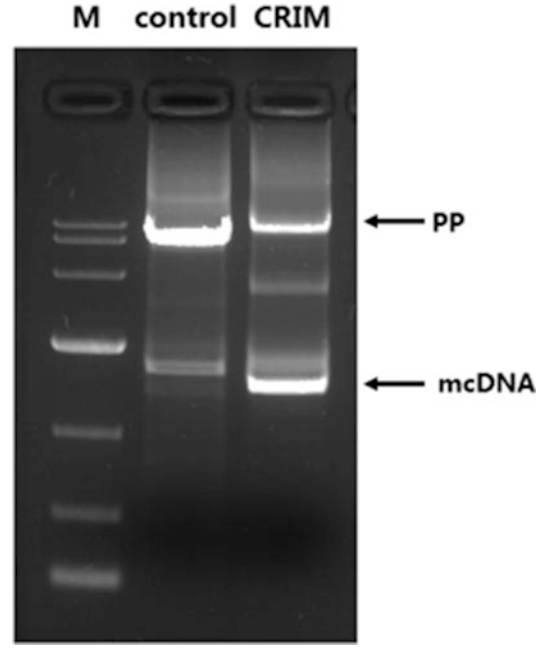

Fig. 1 Presence of mcDNA after transfection of CRIM plasmid into HEK293T cells. Control plasmid (without Cre recombinase cassette) is also included. For CRIM plasmid, the presences of mcDNA as well as parental plasmid (PP) could be observed due to the remaining of non-cut complete plasmid

1. *Preparation of Salmonella electronic competent cells:* Inoculate a single colony of C500 from LB agar plate into 50 mL LB medium and incubate at 37 °C with shaking at the speed of 180 rpm until the OD_{600} reaches 0.8–1.0. Collect bacteria by centrifuge at 6000 × *g* for 15 min at room temperature and resuspend in 10 mL chilled sterilized ddH_2O. After centrifuge at the same condition, resuspend and wash bacteria in 10 mL chilled sterilized 10% glycerol twice. After the final centrifuge, resuspend the pellet with 1 mL chilled sterilized 10% glycerol and separate into 100 μL/tube for storage in −80 °C.
2. *Electronic transformationof CRIM plasmid:* Transform 1 μL CRIM plasmid into 100 μL *Salmonella* competent cells using electrometer according to the instruction. Plating transformed cells on LB + 100 μg/mL ampicillin agar plate for selection of single colony.
3. *Preparation of recombinant strain for orally immunization:* Inoculate the *Salmonella* strain freezer stock into a 5 mL culture of LB with 100 μg/mL ampicillin. Grow at 37 °C statically for 14–16 h. Use the overnight culture(s) to inoculate 50 mL fresh pre-warmed Luria-broth with 100 μg/mL ampicillin at a 1:100 dilution. Grow with aeration at 37 °C until the OD_{600} reaches 0.8. Centrifuge the culture(s) at 6000 × *g* for 15 min at

room temperature and resuspend the pellet(s) in 500 μL sterile PBS. Immunize groups of mice orally by pipetting 20 μL of resuspended cells (approximately 1×10^9 CFU) (*see* **Note 13**).

4 Notes

1. DH5α or other regular competent cells are adequate for this procedure, such as Top10.
2. Dependent on your own purpose, any eukaryotic expression vector could be used to make a CRIM plasmid, for example, pVAX series, pcDNA series, or plasmid with pCAGGS promoter.
3. The reason to use pcDNA3.1/NT-GFP-TOPO plasmid is that it contains GFP reporter gene, which would facilitate its further detection.
4. Two loxP sites or other relative sequences such as lox66/lox71 could be used, both sequences work well in the present study. To increase the production of mcDNA and decrease the reverse transformation from mcDNA to parental plasmid, one could use lox66/lox71 instead of loxP, yielding lox72 site.
5. The enzyme sites used in this study were based on the sequences of pcDNA3.1/NT-GFP-TOPO plasmid, CMV-GFP-polyA cassette and PGK-cre-polyA cassette. In your own study, you can choose any potential enzymes which do not cut your own plasmid.
6. The GFP gene could be replaced with any interested foreigner antigen gene for the construction of mcDNA vaccine.
7. In this study, the PGK-cre-polyA plasmid was selected based on previous paper [19] in which the results demonstrated that PGK promoter rarely express gene in *E. coli* strain, whereas the CMV promoter has strong expression ability even in *E. coli*. Actually in a previous attempt, we firstly insert the Cre recombinase cassette under the CMV promoter. After extraction of plasmid, we found that the parental plasmid already transformed to mcDNA even in *E. coli* strain, which was not consistent with our main purpose. In addition, some other in vivo regulated promoters, such as PpagC or *araC* P_{BAD} were also included; all these promoters appeared to be leaky expressed in *E. coli* strain. Only the PGK promoter could be used for our purpose.
8. Different time points could be selected, for example, we had extracted DNA components from cells at 12, 24, and 48 h post transfection, and found that the presence of mcDNA at any time, indicating that the production of mcDNA could be achieved even at 12 h post transfection.

9. There is no specific commercial kit to isolate DNA components from transfected cells, then we selected a commercial kit to fulfill our purpose according to ref. 20.
10. To confirm the presence of mcDNA in transfected cells, we firstly try to run DNA gel directly after we extracted the DNA from cells, without any expected bands. Then we designed a pair of primers located in the region of CMV promoter, then the extracted DNA components were used as template for amplification of either mcDNA or parental plasmid.
11. There could be a few of nonspecific bands after PCR amplification, the reason is possible due to that we take use of extracted total DNA components from transfected cells as template and our designed primers have some nonspecific binding sites. This could be optimized by redesigning PCR primers.
12. A number of bacteria strains could be selected for the purpose of DNA vaccine. But the critical point is that it has to be intracellular survival bacteria, such as attenuated *Salmonella* or *Listeria monocytogenes* strains, for release of plasmid DNA into the cytoplasm of infected cells. For the bacteria which do not invade into host cells, for example the *E. coli* strain, should not be suitable for our purpose.
13. In addition to mice, other experimental animals such as chicken can also be used. The only difference is that usually it takes at least 100 μL resuspended bacteria for immunization, which require that the final resuspended volume of PBS is five times more than previous description to keep the final immunized dose of 1×10^9 CFU.

Acknowledgments

This work was supported by the National Natural Science Foundation of China (31602092).

References

1. Heppell J, Davis HL (2000) Application of DNA vaccine technology to aquaculture. Adv Drug Deliv Rev 43:29–43
2. Davis BS, Chang GJ, Cropp B et al (2001) West Nile virus recombinant DNA vaccine protects mouse and horse from virus challenge and expresses in vitro a noninfectious recombinant antigen that can be used in enzyme-linked immunosorbent assays. J Virol 75:4040–4047
3. Garver KA, LaPatra SE, Kurath G (2005) Efficacy of an infectious hematopoietic necrosis (IHN) virus DNA vaccine in Chinook Oncorhynchus tshawytscha and sockeye *O. nerka* salmon. Dis Aquat Org 64:13–22
4. Bergman PJ, Camps-Palau MA, McKnight JA et al (2006) Development of a xenogeneic DNA vaccine program for canine malignant melanoma at the animal medical center. Vaccine 24:4582–4585
5. Draghia-Akli R, Ellis KM, Hill LA et al (2003) High-efficiency growth hormone-releasing hormone plasmid vector administration into skeletal muscle mediated by electroporation in pigs. FASEB J 17:526–528

6. Jiang Y, Yu K, Zhang H et al (2007) Enhanced protective efficacy of H5 subtype avian influenza DNA vaccine with codon optimized HA gene in a pCAGGS plasmid vector. Antivir Res 75:234–241
7. Li L, Saade F, Petrovsky N (2012) The future of human DNA vaccines. J Biotechnol 162:171–182
8. Munye MM, Tagalakis AD, Barnes JL et al (2016) Minicircle DNA provides enhanced and prolonged transgene expression following airway gene transfer. Sci Rep 6:23125
9. Tolmachov O, Palaszewski I, Bigger B et al (2006) RecET driven chromosomal gene targeting to generate a RecA deficient *Escherichia coli* strain for Cre mediated production of minicircle DNA. BMC Biotechnol 6:17
10. Simcikova M, Alves CPA, Brito L et al (2016) Improvement of DNA minicircle production by optimization of the secondary structure of the 5′-UTR of ParA resolvase. Appl Microbiol Biotechnol 100:6725–6737
11. Kay MA, He CY, Chen ZY (2010) A robust system for production of minicircle DNA vectors. Nat Biotechnol 28:1287–1289
12. Schleef M, Schirmbeck R, Reiser M et al (2015) Minicircle: next generation DNA vectors for vaccination. Methods Mol Biol 1317:327–339
13. Stenler S, Blomberg P, Smith CI (2014) Safety and efficacy of DNA vaccines: plasmids vs. minicircles. Hum Vaccin Immunother 10:1306–1308
14. Dietz WM, Skinner NE, Hamilton SE et al (2013) Minicircle DNA is superior to plasmid DNA in eliciting antigen-specific CD8+ T-cell responses. Mol Ther 21:1526–1535
15. Li F, Cheng L, Murphy CM et al (2016) Minicircle HBV cccDNA with a Gaussia luciferase reporter for investigating HBV cccDNA biology and developing cccDNA-targeting drugs. Sci Rep 6:36483
16. Wang Q, Jiang W, Chen Y et al (2014) In vivo electroporation of minicircle DNA as a novel method of vaccine delivery to enhance HIV-1-specific immune responses. J Virol 88:1924–1934
17. Jiang Y, Gao X, Xu K et al (2019) A novel Cre recombinase-mediated in vivo Minicircle DNA (CRIM) vaccine provides partial protection against Newcastle disease virus. Appl Environ Microbiol 85:e00407–e00419
18. Zhao Z, Xue Y, Wu B et al (2008) Subcutaneous vaccination with attenuated *Salmonella enterica* serovar Choleraesuis C500 expressing recombinant filamentous hemagglutinin and pertactin antigens protects mice against fatal infections with both S. enterica serovar Choleraesuis and Bordetella bronchiseptica. Infect Immun 76:2157–2163
19. Li MZ, Elledge SJ (2005) MAGIC, an in vivo genetic method for the rapid construction of recombinant DNA molecules. Nat Genet 37:311–319
20. Gregor Siebenkotten H, Christine R, Radbruch A (1995) Isolation of plasmid DNA from mammalian cells using QIAprep kit. QIAGEN News 2, page 11 2:2

Chapter 2

Vaccination with Messenger RNA: A Promising Alternative to DNA Vaccination

István Tombácz, Drew Weissman, and Norbert Pardi

Abstract

The first proof-of-concept studies about the feasibility of genetic vaccines were published over three decades ago, opening the way for future development. The idea of nonviral antigen delivery had multiple advantages over the traditional live or inactivated pathogen-based vaccines, but a great deal of effort had to be invested to turn the idea of genetic vaccination into reality. Although early proof-of-concept studies were groundbreaking, they also showed that numerous aspects of genetic vaccines needed to be improved. Until the early 2000s, the vast majority of effort was invested into the development of DNA vaccines due to the potential issues of instability and low in vivo translatability of messenger RNA (mRNA). In recent years, numerous studies have demonstrated the outstanding abilities of mRNA to elicit potent immune responses against infectious pathogens and different types of cancer, making it a viable platform for vaccine development. Multiple mRNA vaccine platforms have been developed and evaluated in small and large animals and humans and the results seem to be promising. RNA-based vaccines have important advantages over other vaccine approaches including outstanding efficacy, safety, and the potential for rapid, inexpensive, and scalable production. There is a substantial investment by new mRNA companies into the development of mRNA therapeutics, particularly vaccines, increasing the number of basic and translational research publications and human clinical trials underway. This review gives a broad overview about genetic vaccines and mainly focuses on the past and present of mRNA vaccines along with the future directions to bring this potent vaccine platform closer to therapeutic use.

Key words DNA, Cancer, Clinical trial, Infectious disease, mRNA, Vaccine

1 Introduction

Undoubtedly, vaccines are one of the cornerstones of modern medicine, keeping dozens of life-threatening diseases in check and preventing hundreds of millions of cases of illness, thus saving millions of lives every year [1]. A long way from Jenner's groundbreaking experiments, the development of genetic vaccines is a current hot topic of biomedical studies, made possible by such advances of the previous century as nucleic acid sequencing, amplification, and synthesis. Considered to be one of the pioneering first steps, a report by Wolff et al. showed that protein is readily

Ângela Sousa (ed.), *DNA Vaccines: Methods and Protocols*, Methods in Molecular Biology, vol. 2197,
https://doi.org/10.1007/978-1-0716-0872-2_2,

expressed by intramuscularly injected, naked plasmid DNA or mRNA, thus ushering in a new era of vaccine research [2]. And understandably so: genetic vaccines have many potential benefits over their conventional counterparts; these will be briefly discussed later.

DNA-based vaccines have shown great promise in preclinical studies, inducing potent immune responses in small animals [3, 4]. However, large animal experiments and clinical trials have mostly been less successful so far, with immunogenicity remaining below expectations [5–7]. This is currently one of the major issues genetic vaccines need to overcome, and RNA-based vaccines are sure to benefit from the knowledge and experience already accumulated in DNA vaccine studies in this and other regards as well.

RNA-based vaccines are a relatively new addition to the field of genetic vaccines—dismissed for a long time as non-feasible mainly because of stability issues. While they share some basic features with DNA vaccines, RNA vaccines may offer solutions to some of the concerns and limitations of the former. In this review, we will attempt to summarize the advancements that make RNA-based vaccines a viable alternative to DNA, pointing out possible advantages of each over the other, and of both over conventional vaccines. Furthermore, we will elucidate on the current and possible future applications of RNA vaccines and on the challenges that need to be overcome in this regard.

2 The Emergence of Genetic Vaccination

Conventional vaccines, despite their clear value, face limitations in areas of safety (live attenuated vaccines), lack of broad and/or durable protective efficacy against many pathogens, and ease and time of production. As recombinant DNA techniques developed and became widespread, delivering genetic material as a vaccine seemed feasible. Paoletti et al. [8] modified vaccinia virus to express hepatitis B virus surface antigen or Herpes simplex virus glycoprotein D, then inoculated rabbits and observed antigen production along with the appearance of high-titer antibodies [8]. This study can be considered as a stepping stone between conventional whole virus vaccines and genetic vaccines. In 1990, pure genetic material—both DNA and RNA, as a means of protein expression—was delivered by Wolff et al. into mouse muscle, and protein production was detected [2]. Comparing plasmid DNA and mRNA encoding firefly luciferase, the authors found that peak activities reached similar levels for both, however, mRNA-encoded luciferase activity rapidly diminished, whereas substantial amounts of luciferase were detected for 60 days in the case of plasmid DNA. Concerns about the stability, difficult delivery, and overall low translatability of RNA-steered gene therapy and genetic vaccine research toward

the study and development of DNA-based approaches. In 1993, Ulmer and colleagues used plasmid DNA to express a conserved internal influenza protein in mice, and protection from lethal heterologous influenza virus challenge was demonstrated [9]. Multiple medical fields, like vaccine and cancer immunotherapy research, were eager to adapt the DNA platform thereafter. Although, in the same year, a study showed that antigen-specific cytolytic T cells could be induced by delivering influenza virus nucleoprotein-encoding mRNA formulated into liposomes [10], mRNA platforms were not intensively pursued for some time.

One of the most important milestones of vaccination, genetic or conventional, was the leap in gene and whole organism sequencing. In 1995, the genome sequence of *Haemophilus influenzae* was published [11], and many more have followed in the years. Sequencing and annotating a genome can provide a large number of potential targets for recombinant protein vaccines or genetic vaccines. Candidate antigens can then be screened and tested. One of the notable achievements of this "reverse vaccinology" method was the development of a universal vaccine against serogroup B meningococcus using recombinant proteins [12]. With advances in whole genome sequencing technologies, pathogens can be sequenced in a matter of days, enabling almost instant access to prospective targets for genetic vaccination.

Recent technological innovations enabled RNA to be a feasible alternative to both conventional and DNA-based vaccines. Nucleoside modification, stringent purification, and optimization of the coding and untranslated regions of RNA were demonstrated to drastically improve in vivo translatability by allowing synthetic RNA to evade toll-like receptors and a variety of other RNA sensors that trigger inflammatory reactions and consequently block mRNA translation [13–16]. While the majority of genetic vaccine research focused on DNA vaccines in the 1990s and 2000s, RNA vaccines emerged as a viable alternative in the last decade, and today both approaches are vigorously pursued.

3 Pros and Cons of DNA and mRNA Vaccines

One of the reasons why genetic vaccination (whether DNA or RNA) holds such promise is that it generally shows much greater ability to induce $CD4^+$ and $CD8^+$ T-cell responses than other noninfectious vaccine formats, e.g., protein subunit and whole inactivated pathogens [9, 17–20]. An important factor in determining the quality of the T-cell response appears to be the route by which antigens are taken up and presented by antigen-presenting cells (APCs). This is particularly well-documented in the case of $CD8^+$ T-cell activation, where direct presentation of antigens on Major Histocompatibility Complex (MHC) class I that are

translated within an APC can be much more efficient [21, 22] in stimulating $CD8^+$ T-cell proliferation and effector functions compared to "cross" presentation [23] of proteins or pathogens that are endocytosed from the extracellular space by the APC. While it is conventionally thought that $CD4^+$ T cells are mainly activated via an exogenous, endolysosomal pathway, there is now mounting evidence that $CD4^+$ T cells are also activated most efficiently by direct, endogenous presentation, though the relevant pathways are incompletely understood [24]. One possible explanation for these phenomena is the greater magnitude and half-life of peptide/MHC complex presentation that is expected in the case of continuous, direct presentation [25, 26]. It should also be noted that T cells activated by exogenous pathways may not recognize epitopes that are presented on cells infected by the target pathogens, since the different proteolytic activities of different cellular compartments (e.g., cytosolic proteasome vs. late endosome) likely select for separate populations of peptides that can be presented on MHC molecules. Both DNA- and RNA-based vaccines may therefore promote high-quality T-cell responses in part by mimicking intracellular infections.

Still, there are some important differences in antigen presentation between DNA and RNA vaccines, and there are still many unknowns. DNA delivered into the muscle by electroporation is believed to transfect mainly myocytes as opposed to professional APCs such as dendritic cells (DCs) and macrophages [2, 27], and in this way may mostly rely on the less efficient cross-presentation pathways [28] for T-cell activation. However, DCs can also be directly transfected by DNA and prime $CD8^+$ T cells [29], and DNA-transfected myocytes can upregulate MHC class I and co-stimulatory molecules, thus priming them to activate naïve $CD8^+$ T cells [30]. The contribution of these various antigen presentation pathways to DNA vaccine immunogenicity is not well understood. mRNA, on the other hand, is generally efficient in transfecting DCs, macrophages and other cell types and is thus, in theory, well positioned to induce robust, direct antigen presentation. To be sure, more research is needed to investigate the antigen presentation and T-cell activation pathways at play for both of these categories of vaccine.

Stemming from their closely tied function and role in gene expression, DNA and RNA share other advantages over conventional live attenuated, killed, or subunit vaccines, the most obvious being safety: delivery of a single protein component of a pathogen encoded as a piece of nucleic acid carries no risk of the vaccine itself converting to a pathogenic form and causing illness, which is a concern in case of live attenuated vaccines, especially in immunocompromised patients [31]. Secondly, production of nucleic acids is undoubtedly simpler and quicker than either large-scale protein production and purification, or live pathogen proliferation

technologies. For example, current influenza virus vaccines take about 6 months to produce (which may cause the deployment of a given batch to miss the peak of the number of incidents in a given influenza season) [32, 33], but nucleic acid-based vaccines could be deployed in a fraction of that time, as in vitro manufacturing is rapid, cost-effective and scalable. Moreover, once the manufacturing process is in place for a specific type of genetic vaccine, it can theoretically be used to produce any antigen-encoding vaccine of the same format—a level of simplicity and versatility that does not exist for the production of viral or protein subunit vaccines. This is also an important point in the case of emerging pathogens, as quick response is critical in preventing an epidemic. Thirdly, using the host's own transcription–translation machinery may be beneficial in some cases to allow natural protein folding or posttranslational modifications, including the potential generation of defective ribosomal products [34], thus increasing T-cell epitope availability compared to in vitro antigen production. It also needs to be mentioned that, for obvious reasons, both DNA and mRNA vaccines are only able to deliver protein antigens. Although in the majority of cases proteins serve as targets for recognition during pathogen infection, sometimes other molecules, e.g., bacterial polysaccharides, are also important antigens [35].

Stability is a critical requirement of pharmaceutical products, since long periods of time may pass between production and administration, not to mention the desirable option of stockpiling certain seasonal, large-demand vaccines. Another serious consideration is the possible need for cold-chain transport and storage, especially in economically developing countries where necessary infrastructure is limited. In this regard DNA has a clear advantage, as it is certainly more stable both in vivo and in vitro, RNA being very sensitive to contamination—ever-present RNases are able to degrade RNA in minutes. However, RNA nucleoside modifications, addition of suitable 5′ and 3′ untranslated region (UTR) elements, cap structure and a sufficiently long poly(A) tail can stabilize cytoplasmic RNA and ensure high levels of translation in vivo and in vitro. Additionally, appropriate manufacturing conditions can ensure that synthetic mRNA is free of RNase contaminants, and encapsulation of RNA by a wide variety of new methods [36] can effectively protect RNA from degradation by RNases in vivo. Instability, however, can also be turned into an advantage, in cases where more control over the duration of protein expression is desired. DNA, once delivered, can persist for months [2, 37, 38] without the option for removal, whereas with mRNA, controlled short intervals or bursts of expression can be achieved by modifying the above-mentioned stabilizing elements.

Persistence of DNA brings up a serious concern for safety, as it is theoretically possible for DNA to integrate into genomic DNA. This is a particular concern for virus-derived DNA, but plasmid DNA has also been rarely associated with genomic integration [39]. DNA-based expression constructs need to have, in principle, transcription-driving elements (i.e., a strong promoter). When integrated near e.g., proto-oncogenes, these elements can cause oncogenic transformation, leading to cancer, like in some cases of non-plasmid DNA therapeutics [40, 41]. Simple knock-out of a tumor suppressor can have similar consequences. Transformation of the host's germline genome is even more of an issue, as this may be inherited by offspring [42, 43]. It needs to be emphasized that the possibility of DNA integration in the case of DNA-based vaccines is, as of yet, theoretical, with data pointing to no significant integration in some studies [37, 39, 40]. However, formulation and individual DNA sequences may show different behavior in this regard, thus requiring strict investigation for each DNA-based therapeutic [39]. RNA, on the other hand, has no known way of integrating into DNA, unless reverse-transcribed into DNA first. Again, there is a theoretical possibility of reverse transcriptase being present in a human cell (e.g., in case of retroviral infection or from retrotransposons), but this necessary (and unlikely) extra step taken together with short persistence of RNA make RNA-based integration a highly improbable event. Also, since mRNA molecules do not need to contain transcription-driving elements, integration of their cDNA would not cause overexpression of genes near the integration site. Investigation may be needed to clarify whether RNA-based integration in special cases (e.g., retroviral infection) can occur.

Furthermore, while DNA needs to be localized to the nucleus, translation of RNA occurs in the cytoplasm, simplifying delivery strategies.

Large-scale manufacturing of DNA constructs is straightforward and well-established under Good Manufacturing Practice (GMP) conditions [44, 45]. Production of mRNA also requires production of a DNA template, in addition to several extra steps, namely in vitro transcription of mRNA, formation of a cap structure (which may be accomplished during transcription or done separately) [46–48], and removal of aberrant transcription products, such as short, aborted mRNA and double-stranded RNA fragments [14, 15]. Furthermore, most RNA-based vaccines are protected from RNase and delivered to the cytoplasm by lipid or polymer-based carriers, which also must be produced under GMP conditions. Although this extended pipeline carries additional costs and infrastructure relative to DNA purification alone, it is important to note that in vitro transcription of mRNA is a highly processive enzymatic reaction, in which a given amount of DNA template can yield one or two orders of magnitude more mRNA. Therefore,

Table 1
Comparison of beneficial and detrimental features of DNA and RNA vaccines

DNA vaccines	RNA vaccines
Advantages	
Simple, scalable manufacturing, rapid deployment Safety (no chance of infection compared to live/attenuated pathogen vaccines) Better cellular and humoral immune response (compared to humoral only with subunit vaccines)	
Persistence, prolonged expression Stable under normal conditions, ease of storage	Short half-life allows controlled expression kinetics Amplification during manufacturing No need to enter the nucleus No chance of genomic integration Cell-free, in vitro synthesis
Disadvantages	
Immunogenicity below expectations in human clinical trials to date	
Theoretical possibility of adverse events from genomic integration Nuclear delivery required	Additional steps required in production Susceptible to degradation ex vivo and in vivo

extremely large quantities of mRNA can in theory be produced from a relatively small amount of plasmid DNA, decreasing costs associated with the upstream DNA production. Advantages and disadvantages of DNA and RNA vaccines are summarized in Table 1.

4 mRNA Vaccine Types and Delivery

Current RNA vaccines are engineered in two basic forms: nonreplicating and self-amplifying [13, 49]. In principle, DNA vaccines are more closely related to nonreplicating mRNA vaccines, and thus are compared to them in this review. However, it is useful to elucidate on the differences of these two types of RNA vaccines. Nonreplicating mRNA vaccines use an RNA molecule containing the open reading frame of interest flanked by 5′ and 3′ UTRs, a cap structure and a poly(A) tail. Self-amplifying RNA vaccines carry additional elements derived from positive-strand RNA viruses [50]. The sequences encoding viral structural proteins are replaced by the gene of interest, while components of the RNA replication machinery are retained. When the vaccine is delivered into cells, the RNA-dependent RNA polymerase complex is expressed and begins replicating the antigen-encoding RNA. The obvious advantage of this mechanism is that a lower dose of the vaccine is required to achieve the same or even higher level of protein expression. While expression is delayed compared to nonreplicating mRNA vaccines

because of an initial lower number of molecules present, overall expression is more durable [51]. Nonreplicating mRNA vaccines on the other hand produce a short, strong burst of protein expression, and may be more advantageous if tighter control of persistence is required. Nonreplicating mRNA vaccines can be produced with unmodified or modified ribonucleotides, while self-amplifying mRNA vaccines use the unmodified nucleotides present in cells for their replication.

As with any therapeutic, delivery is a crucial aspect of genetic vaccine applications. In the case of mRNA vaccines, delivery has proven to be a challenge, bottlenecking efficiency for a long time. Although the most straightforward method—naked mRNA administration by intramuscular injection—was used by a number of studies [2, 52], susceptibility to RNases and low overall efficacy necessitated the development of new approaches. One of the early attempts was the use of the "gene gun" —mRNA-coated gold particles penetrating the cell membrane with high velocity [53–55]. Protection of mRNA and increased delivery efficiency can also be achieved by protamine condensation, with the added benefit of higher levels of immune response stimulation [56–60]; however, protamine was found to bind RNA too tightly, which inhibited translation [61, 62], thus, this complexing agent is no longer commonly used for the delivery of protein-encoding mRNA. Electroporation has been used for DNA vaccine delivery, and it is also an option for mRNA vaccines, both in vivo and in vitro [63]. Current delivery strategies favor nanoparticles with cationic lipids (lipid nanoparticle, LNP) or polymer-based approaches. Many of these have been used for over a decade for siRNA administration [64], and have been adapted to mRNA in recent years [65]. Cationic lipids have been used in a plethora of nucleic acid delivery studies, and have provided promising results [13, 36, 66]. They may also be combined with polymers for different formulation strategies [67]. Cationic polymers/dendrimers form complexes with negatively charged mRNA spontaneously, are easy to manufacture and modify, and hold great potential, but their use is not as widespread as that of LNPs in clinical applications. Current efforts focus on creating biodegradable formulations with minimal cytotoxicity [36, 68].

5 Current Standing of the Field of mRNA Vaccines

Currently, mRNA vaccines are mainly used in two therapeutic approaches: cancer immunotherapy and infectious disease vaccines. Several detailed reviews have recently been published on this topic [13, 36, 51, 66, 69–71], thus, we will only briefly discuss the current standing of these fields and highlight the most critical findings.

5.1 mRNA-Based Cancer Vaccines

RNA can be used in two quite different strategies in cancer immunotherapy: total tumor RNA or single tumor-associated antigens can be delivered (reviewed in [72]). Total RNA can be extracted from patients' tumors and used to generate anticancer immune responses against the set of antigens expressed by the particular tumor. Advantages of this approach include the lack of need to identify individual tumor antigens and lower chances of immune evasion by the tumor via immune escape mutations. On the other hand, autoimmunity is a possible issue, as total RNA includes targets also expressed by healthy cells. Multiple clinical trials on different cancer models have been completed using this approach [68, 73–79]. However, this strategy is very different from the principle of DNA vaccines, which serve as a basis for comparison in this review. Thus, we will focus on tumor-associated antigen RNA cancer vaccines, highlighting the most important results in this vast and intensively investigated field.

Dendritic cells are ideal targets for cancer vaccine delivery, since they play a key role in inducing antigen-specific immune responses, and strategies for their therapeutic use in conjunction with mRNA vaccines have been evaluated in recent decades. DCs can be directly purified from patients' samples, or monocytes can be extracted and stimulated with granulocyte-macrophage colony stimulating factor and interleukin-4 to differentiate into DCs [80, 81]. These are then transfected with mRNA ex vivo, and finally re-infused into the host. Direct in vivo delivery of RNA cancer vaccines is also possible. While it is more cost effective and rapid than ex vivo DC transfection, targeting of desired cells can be challenging [82].

In 1996, Boczkowski and coworkers electroporated DCs with in vitro synthesized chicken ovalbumin (OVA)-encoding mRNA or OVA protein, and mRNA proved to be more effective at stimulating CTL responses against OVA-expressing tumor cells in vitro [83]. In 2002, a phase I clinical trial was performed to evaluate an mRNA cancer vaccine for safety, feasibility, and efficacy in the treatment of metastatic prostate cancer. Thirteen study subjects received different doses of DCs transfected with prostate-specific antigen (PSA)-encoding mRNA; no adverse effects were observed. PSA-specific T-cell responses were detected in all patients, and 6 out of 7 evaluable patients exhibited a significant decrease in serum PSA levels. Analysis of circulating tumor cells of 3 patients showed transient molecular clearance in all 3 cases [84]. Discovery of several immune regulatory proteins has contributed to better efficacy of DC cancer vaccines: electroporation of DCs with mRNA encoding costimulatory molecules such as CD83, tumor necrosis factor receptor superfamily member 4 (TNFRSF4, also known as OX40) or 4-1BB ligand (4-1BBL) led to measurable increase in immune stimulation via DCs [75, 85–87]. mRNA can also be used to modulate the function of DCs by delivering pro-inflammatory cytokines or trafficking-associated molecules. TriMix, developed by

Etherna, is a three-component adjuvant containing CD70, CD40L and constitutively active toll-like receptor 4 (TLR4) encoded as mRNA. It can be readily combined with antigen-encoding mRNAs and delivered into DCs via electroporation [88]. In one study, this formulation was successfully used to treat stage III and IV melanoma patients, resulting in the regression of tumor in 27% of treated individuals [89]. Completed cancer clinical trials using DC vaccines include metastatic prostate cancer, metastatic lung cancer, renal cell carcinoma, multiple types of brain cancer, melanoma, acute myeloid leukemia, and pancreatic cancer, among others [70, 90, 91].

As individual cancer cases can vary widely in terms of the phenotype (and of course genotype) of the affected cells, a universal vaccination method is not feasible. Thus, it has been a long-standing goal in the field to develop methodologies that can produce personalized therapeutics. A current leader in mRNA pharmaceuticals, BioNTech, has developed a platform called Individualized Vaccines Against Cancer (IVAC) that either uses a combination of pre-manufactured mRNA-encoded antigens based on the RT-qPCR profile of the tumor, or, alternatively, a vaccine that is tailored to an individual's unique tumor antigens resulting from tumor-specific mutations identified by next generation sequencing of the tumor [92]. These studies have been crucial in demonstrating the feasibility of GMP-grade, large scale manufacturing and safety of mRNA vaccines and have pioneered the way for the application of mRNA to other therapeutic indications.

5.2 Infectious Disease mRNA Vaccines

The field of infectious disease vaccines offers useful points of reference for judging the effectiveness of new mRNA platforms, since they can be directly compared to conventional vaccine formats—a benchmark that is absent in the cancer vaccine field. Although fewer in number than mRNA cancer vaccines as of today, there are multiple ongoing or completed preclinical and clinical studies with mRNA infectious disease vaccines, and the field is rapidly expanding. mRNA vaccines have been developed against multiple viruses and several bacterial and parasitic targets. A detailed review on infectious disease mRNA vaccines has recently been published [66]. Here, we will briefly summarize the most relevant findings and mention the advantages of particular mRNA vaccines compared to current vaccine formats in the field.

HIV is one of the most difficult vaccine targets, which no approach has been able to effectively tackle so far. Several mRNA vaccine studies used DC vaccines, where DCs were electroporated with HIV antigens encoded as mRNA and injected into HIV-1 infected patients on antiretroviral therapy. Although the treatment gave rise to antigen-specific $CD4^+$ and $CD8^+$ T-cell responses, no clinical benefit was observed [93–98]. Attempts at directly

injectable HIV vaccines have resulted in similarly suboptimal outcomes. Multiple studies using different formulations of mRNA vaccines have demonstrated HIV-specific T- and B-cell responses; however, antibodies induced by these vaccines could almost exclusively neutralize tier 1 (easy-to-neutralize) viruses and none of these vaccines could induce durable neutralizing antibody responses [99–103].

Influenza virus causes frequent, worldwide epidemics, but despite intensive research and decades of experience, conventional vaccines are limited in their ability to respond to rapidly changing viral strains. Most currently used influenza vaccines are produced in eggs, which may not be ideal in case of certain virus strains (e.g., H5N1, which affects chickens), and can also give rise to egg-adaptive mutations, further decreasing the efficacy of currently used vaccine formats [104, 105]. As mentioned above, conventional influenza vaccines could take about 6 months to deploy, whereas in 2013, Hekele et al. produced an mRNA-based influenza vaccine within 8 days after the coding sequences became available for the hemagglutinin (HA) and neuraminidase (NA) of the H7N9 strain causing an outbreak in China. Mice treated with the vaccine exhibited protective HA inhibition titers after two injections in 4 weeks [106]. The first demonstration of protection from influenza virus infection involving an mRNA vaccine was described by Petsch et al. in 2012. Immunogenicity at a similar level to a licensed inactivated virus vaccine was observed in mice, ferrets, and pigs [107]. Recently, in a publication by Pardi et al., nucleoside-modified, HPLC-purified mRNA encoding full length HA elicited durable antibody responses against the more conserved, but generally immunosubdominant stalk region of HA that is one of the targets of “universal” influenza vaccine research. A single immunization was protective against both homologous and heterologous influenza viruses, and two immunizations protected against heterosubtypic virus challenge in mice [108]. Two human clinical trials have been completed with LNP-complexed, nucleoside-modified HA mRNA influenza vaccine. 100 μg H10N8 HA mRNA was injected intramuscularly (IM), and 100% and 87% of 23 study subjects showed measurable levels of HAI and microneutralization titers, respectively, with side effects similar to conventional adjuvanted vaccines. For H7N9, 25 and 50 μg IM doses achieved measurable HAI titers in 96.3% and 89.7% of participants, and microneutralization titers reached 100% and 96.6%, respectively [109]. While these results are promising, antibody titers were significantly lower than in previous animal models, an issue that requires attention.

Following the outbreak and publicity of Zika viral infections in 2015–2016, efforts were made by many groups to quickly develop a vaccine, and the mRNA platform has shown more than promising results. Two groups independently demonstrated the efficacy of

their own LNP-formulated, nucleoside-modified mRNA vaccines delivering Zika virus pre-membrane and envelope (prM-E)-encoding mRNA. Richner et al. observed high levels of neutralizing titers and protection from Zika virus challenge after 2 immunizations in mice [110]. Pardi et al. achieved similar results in both mice and NHPs after administration of a single dose [111]. Evaluation of the vaccine by Richner et al. has moved into the clinical phase (NCT03014089).

Animal studies of a rabies virus glycoprotein mRNA vaccine had shown promise, inducing protective immune responses against lethal challenge in mice, and raising significant levels of antibody titers in pigs [112]. Based on the promising preclinical data, a human study was initiated, using different doses and delivery routes. The vaccine failed to live up to expectations when delivered via needle injection either intradermal or intramuscular independent of dosage. Needle-free administration induced adequate antibody responses, but they declined after 1 year [113]. Optimization of the delivery system has been shown to increase durability of this vaccine. An LNP-formulated version of the vaccine was administered to NHPs, and adequate neutralization titers were observed, and remained stable for at least 5 months [114]. Testing of the vaccine has recently moved to phase I clinical trial (NCT03713086).

A limited number of mRNA vaccines against bacterial pathogens have also been evaluated. Lorenzi and colleagues intranasally administered naked, unmodified mRNA encoding *Mycobacterium tuberculosis* heat shock protein 65 (Hsp65) into mice and challenged them 30 days later. Bacterial loads were measured 4 weeks post-challenge, and a significant decrease was observed in mRNA-immunized animals [115]. Maruggi and colleagues demonstrated the efficacy of a self-amplifying mRNA vaccine approach against Streptococcus group A and B [116]. Streptolysin-O (group A) and pilus 2a backbone protein (group B) were administered, and the treatment conferred partial protection in a mouse challenge model.

Three reports have recently demonstrated that multiple mRNA-encoded antigens can be encapsulated into a single vaccine formulation and induce equally potent immune responses against each antigen [117–119]. This critical feature of mRNA vaccines offers the advantage of hitting a pathogen at multiple points, which could result in improved breadth and protective efficacy. Awasthi et al. used a trivalent nucleoside-modified mRNA-LNP vaccine against HSV-2, and compared it to an adjuvanted trivalent protein vaccine containing the same antigens the mRNA vaccine coded for [117]. The mRNA vaccine completely protected mice from HSV-2 challenge. No virus in vaginal cultures and no HSV-2 DNA in dorsal root ganglia was detected after vaginal infection with a viral dose at which trivalent protein vaccine was not effective. Chahal

et al. reported on a multivalent mRNA vaccine against Toxoplasma gondii, an intracellular pathogen that expresses variable antigens throughout its life cycle. Six self-replicating mRNAs were co-formulated and administered, inducing protective immunity in mice [118]. John et al. combined five conventional mRNAs encoding the five subunits of the human cytomegalovirus (HCMV) pentameric complex, and robust immune responses were observed in NHPs. Addition of a sixth mRNA, one against HCMV glycoprotein B, did not interfere with responses, suggesting that mRNAs encoding different antigens can be efficiently combined [119]. This six-component vaccine is currently investigated in a phase I clinical trial (NCT03382405).

Eukaryotic unicellular parasites represent an important group of human pathogens, causing deadly diseases such as malaria, leishmaniasis, or trypanosomiasis. Malaria kills approximately one million people each year, and conventional approaches to create a vaccine have not been successful so far [120]. A self-amplifying mRNA vaccine was demonstrated to be effective in disabling an immune evasion mechanism of the malaria parasite in which the parasite produces macrophage migration inhibitory factor (PMIF) to suppress memory T cells. mRNA-encoded PMIF was delivered to mice, and both cellular and humoral responses were observed, and the animals were protected against reinfection [121]. A self-amplifying mRNA vaccine against Leishmania was tested by Duthie and colleagues. A heterologous prime-boost regimen using LEISH-F2 RNA and protein significantly reduced Leishmania infection in the liver of mice compared to homologous immunizations by either RNA or protein (two administrations in each case) alone [122].

6 Challenges and Future Directions

To date, genetic vaccines have only been approved for veterinary products [69]. One of the main issues with human applications, as stated above, is that clinical genetic vaccine studies so far have reported more modest immunogenicity in humans than in preclinical animal models. Three recent phase I clinical trials using mRNA vaccines against influenza and rabies viruses reported mediocre results [109, 113, 123], an issue shared with previous DNA vaccine trials [7, 124]. Since the field of RNA vaccines is relatively new, there is currently not enough clinical data to compare and evaluate the multiple RNA platforms available today in this regard. This is sure to change in the near future, as new formulations with different expressional and immunostimulatory profiles are tested. Further studies will need to focus on adapting the very encouraging results of preclinical trials to human applications. For DNA vaccines, some of the strategies for improving responses currently

being tried are: increasing protein expression, addition of different adjuvants and immunostimulants, various prime-boost combinations (e.g., DNA prime with viral vector or protein boost), optimization of plasmid components (e.g., promoter, codon optimization), different delivery routes and delivery methods [69]. Similar strategies may be attempted for the improvement of RNA vaccines, in addition to the optimization of the RNA-specific structures (cap, 5′ and 3′ UTR, poly(A) tail) [13, 71, 125, 126].

Efficient delivery of mRNA as vaccines is of the utmost importance [36]. Recent advances in lipid and polymer biochemistry opened up new possibilities of delivery and targeting, benefiting RNA vaccines greatly. Optimization of RNA vaccines must involve the development and testing of as many different carrier molecules as possible, since different applications may require different delivery protocols.

Excitement about the prospects of RNA vaccines can be seen by the establishment of multiple pharmaceutical companies investing in RNA vaccine research, development and manufacture. BioNTech GmbH, CureVac AG and Moderna Therapeutics, partnering with such giants as Roche, Bayer, Sanofi, and Merck, are the current leading developers of the field, with billions of dollars channeled into RNA vaccine development.

Undoubtedly, RNA vaccines offer a more than promising alternative to conventional vaccines. While development of a truly effective genetic vaccine seems to be proving more difficult than originally imagined, the possible benefits are obvious. As both DNA and RNA vaccines are relatively novel in comparison to conventional platforms, and some infectious diseases have been unable to be tackled by conventional vaccines even with a significantly longer history of attempts, there is little reason to be discouraged by the as of yet unsatisfactory results of human trials. Genetic vaccine design and formulations offer a multitude of options for improvement.

Acknowledgement

The authors thank Michael J Hogan for valuable feedback on the manuscript. N.P. was supported by the National Institute of Allergy and Infectious Diseases (1R01AI146101).

References

1. World Health Organization (2018) Immunization coverage. https://www.who.int/news-room/fact-sheets/detail/immunization-coverage
2. Wolff JA, Malone RW, Williams P et al (1990) Direct gene transfer into mouse muscle in vivo. Science 247:1465–1468
3. Alarcon JB, Waine GW, McManus DP (1999) DNA vaccines: technology and application as anti-parasite and anti-microbial agents. Adv Parasitol 42:343–410
4. Smooker PM, Rainczuk A, Kennedy N et al (2004) DNA vaccines and their application against parasites--promise, limitations and

potential solutions. Biotechnol Annu Rev 10:189–236

5. Pierini S, Perales-Linares R, Uribe-Herranz M et al (2017) Trial watch: DNA-based vaccines for oncological indications. Onco Targets Ther 6:e1398878
6. Suschak JJ, Williams JA, Schmaljohn CS (2017) Advancements in DNA vaccine vectors, non-mechanical delivery methods, and molecular adjuvants to increase immunogenicity. Hum Vaccin Immunother 13:2837–2848
7. Hobernik D, Bros M (2018) DNA vaccines-how far from clinical use? Int J Mol Sci 19:3605
8. Paoletti E, Lipinskas BR, Samsonoff C et al (1984) Construction of live vaccines using genetically engineered poxviruses: biological activity of vaccinia virus recombinants expressing the hepatitis B virus surface antigen and the herpes simplex virus glycoprotein D. Proc Natl Acad Sci U S A 81:193–197
9. Ulmer JB, Donnelly JJ, Parker SE et al (1993) Heterologous protection against influenza by injection of DNA encoding a viral protein. Science 259:1745–1749
10. Martinon F, Krishnan S, Lenzen G et al (1993) Induction of virus-specific cytotoxic T lymphocytes in vivo by liposome-entrapped mRNA. Eur J Immunol 23:1719–1722
11. Fleischmann RD, Adams MD, White O et al (1995) Whole-genome random sequencing and assembly of Haemophilus influenzae Rd. Science 269:496–512
12. Giuliani MM, Adu-Bobie J, Comanducci M et al (2006) A universal vaccine for serogroup B meningococcus. Proc Natl Acad Sci U S A 103:10834–10839
13. Pardi N, Hogan MJ, Porter FW et al (2018) mRNA vaccines - a new era in vaccinology. Nat Rev Drug Discov 17:261–279
14. Baiersdorfer M, Boros G, Muramatsu H et al (2019) A facile method for the removal of dsRNA contaminant from in vitro-transcribed mRNA. Mol Ther Nucleic Acids 15:26–35
15. Kariko K, Muramatsu H, Ludwig J et al (2011) Generating the optimal mRNA for therapy: HPLC purification eliminates immune activation and improves translation of nucleoside-modified, protein-encoding mRNA. Nucleic Acids Res 39:e142
16. Sahin U, Kariko K, Tureci O (2014) mRNA-based therapeutics--developing a new class of drugs. Nat Rev Drug Discov 13:759–780
17. Pardi N, Hogan MJ, Naradikian MS et al (2018) Nucleoside-modified mRNA vaccines induce potent T follicular helper and germinal center B cell responses. J Exp Med 215:1571–1588
18. Kowalczyk DW, Ertl HC (1999) Immune responses to DNA vaccines. Cell Mol Life Sci 55:751–770
19. Tang DC, DeVit M, Johnston SA (1992) Genetic immunization is a simple method for eliciting an immune response. Nature 356:152–154
20. Xiang ZQ, Spitalnik S, Tran M et al (1994) Vaccination with a plasmid vector carrying the rabies virus glycoprotein gene induces protective immunity against rabies virus. Virology 199:132–140
21. Moore MW, Carbone FR, Bevan MJ (1988) Introduction of soluble protein into the class I pathway of antigen processing and presentation. Cell 54:777–785
22. Xu RH, Remakus S, Ma X et al (2010) Direct presentation is sufficient for an efficient antiviral CD8+ T cell response. PLoS Pathog 6: e1000768
23. Embgenbroich M, Burgdorf S (2018) Current concepts of antigen cross-presentation. Front Immunol 9:1643
24. Miller MA, Ganesan AP, Luckashenak N et al (2015) Endogenous antigen processing drives the primary CD4+ T cell response to influenza. Nat Med 21:1216–1222
25. Sei JJ, Haskett S, Kaminsky LW et al (2015) Peptide-MHC-I from endogenous antigen outnumber those from exogenous antigen, irrespective of APC phenotype or activation. PLoS Pathog 11:e1004941
26. Gett AV, Sallusto F, Lanzavecchia A et al (2003) T cell fitness determined by signal strength. Nat Immunol 4:355–360
27. Liu MA (2011) DNA vaccines: an historical perspective and view to the future. Immunol Rev 239:62–84
28. Fu TM, Ulmer JB, Caulfield MJ et al (1997) Priming of cytotoxic T lymphocytes by DNA vaccines: requirement for professional antigen presenting cells and evidence for antigen transfer from myocytes. Mol Med 3:362–371
29. Elnekave M, Furmanov K, Nudel I et al (2010) Directly transfected langerin+ dermal dendritic cells potentiate CD8+ T cell responses following intradermal plasmid DNA immunization. J Immunol 185:3463–3471

30. Shirota H, Petrenko L, Hong C et al (2007) Potential of transfected muscle cells to contribute to DNA vaccine immunogenicity. J Immunol 179:329–336
31. Ljungman P (2012) Vaccination of immunocompromised patients. Clin Microbiol Infect 18(Suppl 5):93–99
32. Krammer F, Palese P (2015) Advances in the development of influenza virus vaccines. Nat Rev Drug Discov 14:167–182
33. Racaniello V (2010) Pandemic influenza vaccine was too late in 2009. http://www.virology.ws/2010/12/09/pandemic-influenza-vaccine-was-too-late-in-2009/
34. Yewdell JW, Anton LC, Bennink JR (1996) Defective ribosomal products (DRiPs): a major source of antigenic peptides for MHC class I molecules? J Immunol 157:1823–1826
35. Weintraub A (2003) Immunology of bacterial polysaccharide antigens. Carbohydr Res 338:2539–2547
36. Kowalski PS, Rudra A, Miao L et al (2019) Delivering the messenger: advances in Technologies for Therapeutic mRNA delivery. Mol Ther 27:710–728
37. Wolff JA, Ludtke JJ, Acsadi G et al (1992) Long-term persistence of plasmid DNA and foreign gene expression in mouse muscle. Hum Mol Genet 1:363–369
38. Armengol G, Ruiz LM, Orduz S (2004) The injection of plasmid DNA in mouse muscle results in lifelong persistence of DNA, gene expression, and humoral response. Mol Biotechnol 27:109–118
39. Wang Z, Troilo PJ, Wang X et al (2004) Detection of integration of plasmid DNA into host genomic DNA following intramuscular injection and electroporation. Gene Ther 11:711–721
40. Deyle DR, Russell DW (2009) Adeno-associated virus vector integration. Curr Opin Mol Ther 11:442–447
41. Hacein-Bey-Abina S, von Kalle C, Schmidt M et al (2003) A serious adverse event after successful gene therapy for X-linked severe combined immunodeficiency. N Engl J Med 348:255–256
42. Gura T (2002) Gene therapy and the germ line. Mol Ther 6:2–4
43. Schuettrumpf J, Liu JH, Couto LB et al (2006) Inadvertent germline transmission of AAV2 vector: findings in a rabbit model correlate with those in a human clinical trial. Mol Ther 13:1064–1073
44. Tejeda-Mansir A, Montesinos RM (2008) Upstream processing of plasmid DNA for vaccine and gene therapy applications. Recent Pat Biotechnol 2:156–172
45. Xenopoulos A, Pattnaik P (2014) Production and purification of plasmid DNA vaccines: is there scope for further innovation? Expert Rev Vaccines 13:1537–1551
46. Martin SA, Paoletti E, Moss B (1975) Purification of mRNA guanylyltransferase and mRNA (guanine-7-) methyltransferase from vaccinia virions. J Biol Chem 250:9322–9329
47. Stepinski J, Waddell C, Stolarski R et al (2001) Synthesis and properties of mRNAs containing the novel "anti-reverse" cap analogs 7-methyl(3'-*O*-methyl)GpppG and 7-methyl (3'-deoxy)GpppG. RNA 7:1486–1495
48. Vaidyanathan S, Azizian KT, Haque A et al (2018) Uridine depletion and chemical modification increase Cas9 mRNA activity and reduce immunogenicity without HPLC purification. Mol Ther Nucleic Acids 12:530–542
49. Brito LA, Kommareddy S, Maione D et al (2015) Self-amplifying mRNA vaccines. Adv Genet 89:179–233
50. Geall AJ, Verma A, Otten GR et al (2012) Nonviral delivery of self-amplifying RNA vaccines. Proc Natl Acad Sci U S A 109:14604–14609
51. Zhang C, Maruggi G, Shan H et al (2019) Advances in mRNA vaccines for infectious diseases. Front Immunol 10:594
52. Conry RM, LoBuglio AF, Wright M et al (1995) Characterization of a messenger RNA polynucleotide vaccine vector. Cancer Res 55:1397–1400
53. Qiu P, Ziegelhoffer P, Sun J et al (1996) Gene gun delivery of mRNA in situ results in efficient transgene expression and genetic immunization. Gene Ther 3:262–268
54. Dileo J, Miller TE Jr, Chesnoy S et al (2003) Gene transfer to subdermal tissues via a new gene gun design. Hum Gene Ther 14:79–87
55. Steitz J, Britten CM, Wolfel T et al (2006) Effective induction of anti-melanoma immunity following genetic vaccination with synthetic mRNA coding for the fusion protein EGFP.TRP2. Cancer Immunol Immunother 55:246–253
56. Scheel B, Aulwurm S, Probst J et al (2006) Therapeutic anti-tumor immunity triggered by injections of immunostimulating single-stranded RNA. Eur J Immunol 36:2807–2816
57. Scheel B, Teufel R, Probst J et al (2005) Toll-like receptor-dependent activation of several human blood cell types by protamine-condensed mRNA. Eur J Immunol 35:1557–1566
58. Skold AE, van Beek JJ, Sittig SP et al (2015) Protamine-stabilized RNA as an ex vivo

stimulant of primary human dendritic cell subsets. Cancer Immunol Immunother 64:1461–1473

59. Hoerr I, Obst R, Rammensee HG et al (2000) In vivo application of RNA leads to induction of specific cytotoxic T lymphocytes and antibodies. Eur J Immunol 30:1–7
60. Weide B, Pascolo S, Scheel B et al (2009) Direct injection of protamine-protected mRNA: results of a phase 1/2 vaccination trial in metastatic melanoma patients. J Immunother 32:498–507
61. Fotin-Mleczek M, Duchardt KM, Lorenz C et al (2011) Messenger RNA-based vaccines with dual activity induce balanced TLR-7 dependent adaptive immune responses and provide antitumor activity. J Immunother 34:1–15
62. Schlake T, Thess A, Fotin-Mleczek M et al (2012) Developing mRNA-vaccine technologies. RNA Biol 9:1319–1330
63. Johansson DX, Ljungberg K, Kakoulidou M et al (2012) Intradermal electroporation of naked replicon RNA elicits strong immune responses. PLoS One 7:e29732
64. Kanasty R, Dorkin JR, Vegas A et al (2013) Delivery materials for siRNA therapeutics. Nat Mater 12:967–977
65. Pardi N, Tuyishime S, Muramatsu H et al (2015) Expression kinetics of nucleoside-modified mRNA delivered in lipid nanoparticles to mice by various routes. J Control Release 217:345–351
66. Maruggi G, Zhang C, Li J et al (2019) mRNA as a transformative Technology for Vaccine Development to control infectious diseases. Mol Ther 27:757–772
67. Guan S, Rosenecker J (2017) Nanotechnologies in delivery of mRNA therapeutics using nonviral vector-based delivery systems. Gene Ther 24:133–143
68. McNamara MA, Nair SK, Holl EK (2015) RNA-based vaccines in cancer immunotherapy. J Immunol Res 2015:794528
69. Liu MA (2019) A comparison of plasmid DNA and mRNA as vaccine technologies. Vaccines (Basel) 7:37
70. Pastor F, Berraondo P, Etxeberria I et al (2018) An RNA toolbox for cancer immunotherapy. Nat Rev Drug Discov 17:751–767
71. Iavarone C, O'Hagan DT, Yu D et al (2017) Mechanism of action of mRNA-based vaccines. Expert Rev Vaccines 16:871–881
72. Gilboa E, Vieweg J (2004) Cancer immunotherapy with mRNA-transfected dendritic cells. Immunol Rev 199:251–263
73. Bonehill A, Van Nuffel AM, Corthals J et al (2009) Single-step antigen loading and activation of dendritic cells by mRNA electroporation for the purpose of therapeutic vaccination in melanoma patients. Clin Cancer Res 15:3366–3375
74. Caruso DA, Orme LM, Neale AM et al (2004) Results of a phase 1 study utilizing monocyte-derived dendritic cells pulsed with tumor RNA in children and young adults with brain cancer. Neuro-Oncology 6:236–246
75. Dannull J, Nair S, Su Z et al (2005) Enhancing the immunostimulatory function of dendritic cells by transfection with mRNA encoding OX40 ligand. Blood 105:3206–3213
76. Kyte JA, Kvalheim G, Aamdal S et al (2005) Preclinical full-scale evaluation of dendritic cells transfected with autologous tumor-mRNA for melanoma vaccination. Cancer Gene Ther 12:579–591
77. Nair SK, Morse M, Boczkowski D et al (2002) Induction of tumor-specific cytotoxic T lymphocytes in cancer patients by autologous tumor RNA-transfected dendritic cells. Ann Surg 235:540–549
78. Schuurhuis DH, Verdijk P, Schreibelt G et al (2009) In situ expression of tumor antigens by messenger RNA-electroporated dendritic cells in lymph nodes of melanoma patients. Cancer Res 69:2927–2934
79. Su Z, Dannull J, Heiser A et al (2003) Immunological and clinical responses in metastatic renal cancer patients vaccinated with tumor RNA-transfected dendritic cells. Cancer Res 63:2127–2133
80. Saxena M, Bhardwaj N (2018) Re-emergence of dendritic cell vaccines for cancer treatment. Trends Cancer 4:119–137
81. Baar J (1999) Clinical applications of dendritic cell cancer vaccines. Oncologist 4:140–144
82. Kranz LM, Diken M, Haas H et al (2016) Systemic RNA delivery to dendritic cells exploits antiviral defence for cancer immunotherapy. Nature 534:396–401
83. Boczkowski D, Nair SK, Snyder D et al (1996) Dendritic cells pulsed with RNA are potent antigen-presenting cells in vitro and in vivo. J Exp Med 184:465–472
84. Heiser A, Coleman D, Dannull J et al (2002) Autologous dendritic cells transfected with prostate-specific antigen RNA stimulate CTL responses against metastatic prostate tumors. J Clin Invest 109:409–417

85. De Keersmaecker B, Heirman C, Corthals J et al (2011) The combination of 4-1BBL and CD40L strongly enhances the capacity of dendritic cells to stimulate HIV-specific T cell responses. J Leukoc Biol 89:989–999
86. Aerts-Toegaert C, Heirman C, Tuyaerts S et al (2007) CD83 expression on dendritic cells and T cells: correlation with effective immune responses. Eur J Immunol 37:686–695
87. Grunebach F, Kayser K, Weck MM et al (2005) Cotransfection of dendritic cells with RNA coding for HER-2/neu and 4-1BBL increases the induction of tumor antigen specific cytotoxic T lymphocytes. Cancer Gene Ther 12:749–756
88. Bonehill A, Tuyaerts S, Van Nuffel AM et al (2008) Enhancing the T-cell stimulatory capacity of human dendritic cells by co-electroporation with CD40L, CD70 and constitutively active TLR4 encoding mRNA. Mol Ther 16:1170–1180
89. Wilgenhof S, Van Nuffel AM, Benteyn D et al (2013) A phase IB study on intravenous synthetic mRNA electroporated dendritic cell immunotherapy in pretreated advanced melanoma patients. Ann Oncol 24:2686–2693
90. Van Lint S, Renmans D, Broos K et al (2015) The ReNAissanCe of mRNA-based cancer therapy. Expert Rev Vaccines 14:235–251
91. Benteyn D, Heirman C, Bonehill A et al (2015) mRNA-based dendritic cell vaccines. Expert Rev Vaccines 14:161–176
92. Sahin U, Derhovanessian E, Miller M et al (2017) Personalized RNA mutanome vaccines mobilize poly-specific therapeutic immunity against cancer. Nature 547:222–226
93. Routy JP, Boulassel MR, Yassine-Diab B et al (2010) Immunologic activity and safety of autologous HIV RNA-electroporated dendritic cells in HIV-1 infected patients receiving antiretroviral therapy. Clin Immunol 134:140–147
94. Van Gulck E, Vlieghe E, Vekemans M et al (2012) mRNA-based dendritic cell vaccination induces potent antiviral T-cell responses in HIV-1-infected patients. AIDS 26:F1–F12
95. Allard SD, De Keersmaecker B, de Goede AL et al (2012) A phase I/IIa immunotherapy trial of HIV-1-infected patients with tat, rev and Nef expressing dendritic cells followed by treatment interruption. Clin Immunol 142:252–268
96. Gandhi RT, Kwon DS, Macklin EA et al (2016) Immunization of HIV-1-infected persons with autologous dendritic cells transfected with mRNA encoding HIV-1 gag and Nef: results of a randomized, placebo-controlled clinical trial. J Acquir Immune Defic Syndr 71:246–253
97. Jacobson JM, Routy JP, Welles S et al (2016) Dendritic cell immunotherapy for HIV-1 infection using autologous HIV-1 RNA: a randomized, double-blind, placebo-controlled clinical trial. J Acquir Immune Defic Syndr 72:31–38
98. Gay CL, DeBenedette MA, Tcherepanova IY et al (2018) Immunogenicity of AGS-004 dendritic cell therapy in patients treated during acute HIV infection. AIDS Res Hum Retrovir 34:111–122
99. Bogers WM, Oostermeijer H, Mooij P et al (2015) Potent immune responses in rhesus macaques induced by nonviral delivery of a self-amplifying RNA vaccine expressing HIV type 1 envelope with a cationic nanoemulsion. J Infect Dis 211:947–955
100. Pollard C, Rejman J, De Haes W et al (2013) Type I IFN counteracts the induction of antigen-specific immune responses by lipid-based delivery of mRNA vaccines. Mol Ther 21:251–259
101. Zhao M, Li M, Zhang Z et al (2016) Induction of HIV-1 gag specific immune responses by cationic micelles mediated delivery of gag mRNA. Drug Deliv 23:2596–2607
102. Li M, Zhao M, Fu Y et al (2016) Enhanced intranasal delivery of mRNA vaccine by overcoming the nasal epithelial barrier via intra- and paracellular pathways. J Control Release 228:9–19
103. Pardi N, LaBranche CC, Ferrari G et al (2019) Characterization of HIV-1 nucleoside-modified mRNA vaccines in rabbits and rhesus macaques. Mol Ther Nucleic Acids 15:36–47
104. Zost SJ, Parkhouse K, Gumina ME et al (2017) Contemporary H3N2 influenza viruses have a glycosylation site that alters binding of antibodies elicited by egg-adapted vaccine strains. Proc Natl Acad Sci U S A 114:12578–12583
105. Wu NC, Zost SJ, Thompson AJ et al (2017) A structural explanation for the low effectiveness of the seasonal influenza H3N2 vaccine. PLoS Pathog 13:e1006682
106. Hekele A, Bertholet S, Archer J et al (2013) Rapidly produced SAM((R)) vaccine against H7N9 influenza is immunogenic in mice. Emerg Microbes Infect 2:e52
107. Petsch B, Schnee M, Vogel AB et al (2012) Protective efficacy of in vitro synthesized,

specific mRNA vaccines against influenza a virus infection. Nat Biotechnol 30:1210–1216

108. Pardi N, Parkhouse K, Kirkpatrick E et al (2018) Nucleoside-modified mRNA immunization elicits influenza virus hemagglutinin stalk-specific antibodies. Nat Commun 9:3361
109. Feldman RA, Fuhr R, Smolenov I et al (2019) mRNA vaccines against H10N8 and H7N9 influenza viruses of pandemic potential are immunogenic and well tolerated in healthy adults in phase 1 randomized clinical trials. Vaccine 37:3326–3334
110. Richner JM, Himansu S, Dowd KA et al (2017) Modified mRNA vaccines protect against Zika virus infection. Cell 168:1114–1125. e10
111. Pardi N, Hogan MJ, Pelc RS et al (2017) Zika virus protection by a single low-dose nucleoside-modified mRNA vaccination. Nature 543:248–251
112. Schnee M, Vogel AB, Voss D et al (2016) An mRNA vaccine encoding rabies virus glycoprotein induces protection against lethal infection in mice and correlates of protection in adult and newborn pigs. PLoS Negl Trop Dis 10:e0004746
113. Alberer M, Gnad-Vogt U, Hong HS et al (2017) Safety and immunogenicity of a mRNA rabies vaccine in healthy adults: an open-label, non-randomised, prospective, first-in-human phase 1 clinical trial. Lancet 390:1511–1520
114. Lutz J, Lazzaro S, Habbeddine M et al (2017) Unmodified mRNA in LNPs constitutes a competitive technology for prophylactic vaccines. NPJ Vaccines 2:29
115. Lorenzi JC, Trombone AP, Rocha CD et al (2010) Intranasal vaccination with messenger RNA as a new approach in gene therapy: use against tuberculosis. BMC Biotechnol 10:77
116. Maruggi G, Chiarot E, Giovani C et al (2017) Immunogenicity and protective efficacy induced by self-amplifying mRNA vaccines encoding bacterial antigens. Vaccine 35:361–368
117. Awasthi S, Hook LM, Pardi N et al (2019) Nucleoside-modified mRNA encoding HSV-2 glycoproteins C, D, and E prevents clinical and subclinical genital herpes. Sci Immunol 4:eaaw7083
118. Chahal JS, Khan OF, Cooper CL et al (2016) Dendrimer-RNA nanoparticles generate protective immunity against lethal Ebola, H1N1 influenza, and toxoplasma gondii challenges with a single dose. Proc Natl Acad Sci U S A 113:E4133–E4142
119. John S, Yuzhakov O, Woods A et al (2018) Multi-antigenic human cytomegalovirus mRNA vaccines that elicit potent humoral and cell-mediated immunity. Vaccine 36:1689–1699
120. Centers for Disease Control and Prevention (2019) Malaria. https://www.cdc.gov/malaria/malaria_worldwide/reduction/vaccine.html
121. Baeza Garcia A, Siu E, Sun T et al (2018) Neutralization of the plasmodium-encoded MIF ortholog confers protective immunity against malaria infection. Nat Commun 9:2714
122. Duthie MS, Van Hoeven N, MacMillen Z et al (2018) Heterologous immunization with defined RNA and subunit vaccines enhances T cell responses that protect against Leishmania donovani. Front Immunol 9:2420
123. Bahl K, Senn JJ, Yuzhakov O et al (2017) Preclinical and clinical demonstration of immunogenicity by mRNA vaccines against H10N8 and H7N9 influenza viruses. Mol Ther 25:1316–1327
124. Liu MA, Ulmer JB (2005) Human clinical trials of plasmid DNA vaccines. Adv Genet 55:25–40
125. Hajj KAW, K.A. (2017) Tools for translation: Non-viral materials for therapeutic mRNA delivery. Nat Rev Mater 2
126. Hajj KA, Ball RL, Deluty SB et al (2019) Branched-tail lipid nanoparticles potently deliver mRNA in vivo due to enhanced ionization at endosomal pH. Small 15:e1805097

Chapter 3

Impact of a Plasmid DNA-Based Alphavirus Vaccine on Immunization Efficiency

Kenneth Lundstrom

Abstract

Alphavirus vectors have been engineered for high-level gene expression relying originally on replication-deficient recombinant particles, more recently designed for plasmid DNA-based administration. As alphavirus-based DNA vectors encode the alphavirus RNA replicon genes, enhanced transgene expression in comparison to conventional DNA plasmids is achieved. Immunization studies with alphavirus-based DNA plasmids have elicited specific antibody production, have generated tumor regression and protection against challenges with infectious agents and tumor cells in various animal models. A limited number of clinical trials have been conducted with alphavirus DNA vectors. Compared to conventional plasmid DNA-based immunization, alphavirus DNA vectors required 1000-fold less DNA to elicit similar immune responses in rodents.

Key words Alphaviruses, Antibody production, DNA vaccines, Layered RNA/DNA vectors, RNA replicons, Protection against challenges with infectious agents and tumor cells, Tumor regression

1 Introduction

Since the introduction of genetic engineering, vaccine development has in addition to the classical approach of immunization with live attenuated or inactivated infectious agents [1] included recombinantly expressed antigens and immunogens [2], first validated in animal models followed by human clinical trials [3]. Immunization with either non-viral or viral vectors has elicited humoral and cellular immune responses and has provided protection of vaccinated animals against challenges with infectious agents [4] or tumor cells [5]. Generally, conventional plasmid DNA vectors have been applied for immunization to induce antibody responses against the expressed antigen [6]. In attempts to improve the delivery, polymer- and liposome-based coating of microparticles and nanoparticles has been utilized [7, 8]. In the context of microparticles, size exclusion provides passive targeting of antigen-presenting cells (APCs) and support of sustained presentation of DNA

Ângela Sousa (ed.), *DNA Vaccines: Methods and Protocols*, Methods in Molecular Biology, vol. 2197,
https://doi.org/10.1007/978-1-0716-0872-2_3,

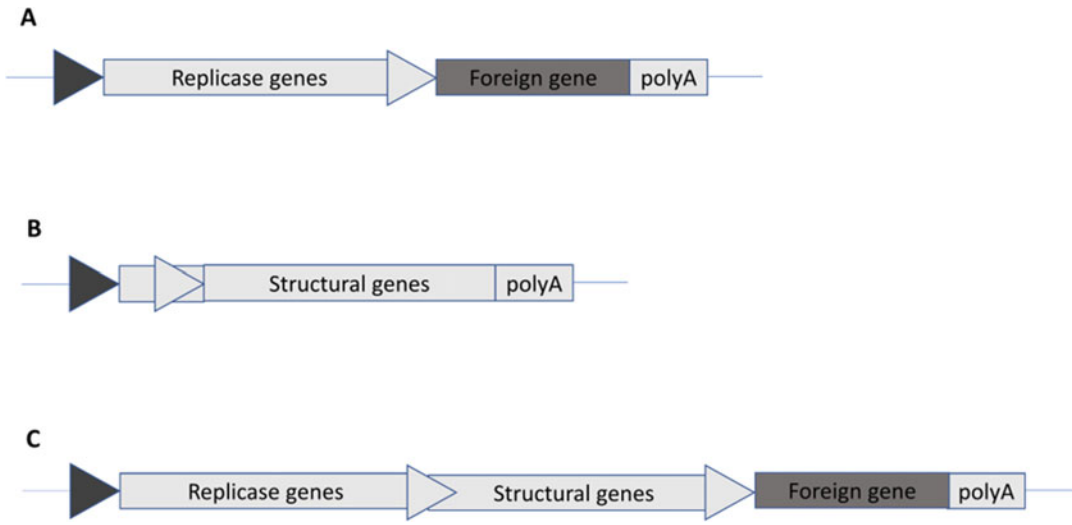

Fig. 1 Schematic presentation of DNA-based alphavirus replicon vectors. (**a**) pSCA1 DNA expression vector containing a CMV promoter (black arrowhead), the nsP1-4 nonstructural replicase genes, the subgenomic 26S promoter (gray arrowhead), the foreign gene of interest, polyA tail. (**b**) pSCA-helper vector with alphavirus structural genes. (**c**) pCMV-SFV4 expression vector with full-length alphavirus genome and the foreign gene of interest

to cells though release of encapsulated vaccines [7]. In the case of nanoparticles, increased internalization, improved transfection efficacy, and better uptake across mucosal surfaces can be achieved [7]. Furthermore, enhanced immune stimulation and activation can be triggered through innate immune response receptors by selection of appropriate biomaterials. The humoral and cellular protective immune responses can also be affected by encapsulation approaches, which adds flexibility to administration routes [7].

An attractive alternative for improved DNA-based vaccine relates to the application of alphavirus replicon vectors. This approach provides enhanced antigen expression due to the self-amplifying nature of alphavirus replicons. Moreover, the superior expression compared to levels observed from conventional DNA plasmids allows up to 1000-fold lower DNA quantities to be used for immunization, still achieving similar immune responses [9]. All alphavirus expression vectors are based on self-amplifying replicon sequences coding for the four nonstructural alphavirus proteins nsP1-4 [10] (Fig. 1). The proteins expressed from the nsP1-4 genes form the replicase complex responsible for highly efficient RNA replication in host cells. It has been estimated that a single copy of replicon RNA can generate up to 200,000 copies of RNA ready for immediate translation in the cytoplasm, which together with the utilized alphavirus subgenomic promoter will provide extreme levels of expression of the gene of interest. Originally, expression vectors for three typical alphaviruses, Semliki Forest

virus (SFV) [11], Sindbis virus (SIN) [12], and Venezuelan equine encephalitis virus (VEE) [13], were engineered. The initial application involved either direct immunization with in vitro transcribed RNA or recombinant alphavirus particles produced in BHK cells after co-transfection of alphavirus expression vector and helper RNAs [11]. To facilitate the use and to ensure high biosafety standards of alphaviruses, direct immunization of plasmid DNA vectors was enabled by introduction of a mammalian host cell-compatible eukaryotic RNA polymerase II type promoter such as CMV upstream of the replicon region [14]. Due to the presence of the replicon, DNA-based alphavirus vectors provide superior expression levels, which can be further enhanced by the introduction of a nuclear localization signal (NLS) in the vector to facilitate the transfer of DNA to the nucleus [15]. To verify any potential stable chromosomal integration, an alphavirus DNA vector carrying the luciferase reporter gene was administered intramuscularly [16]. Reporter gene expression was detected in the skeletal muscle for more than 19 months, but the DNA was only present as an extrachromosomal plasmid. However, low-level random chromosomal integration occurred when the intramuscular injection was followed by electroporation, although the frequency was significantly lower than seen for spontaneous gene mutations [17]. It was further demonstrated that only minor spread of DNA to other organs occurred after administration into skeletal muscles without any genomic integration [18]. Additional studies have confirmed that neither anti-DNA antibodies [19] nor prokaryotic antibiotic resistance genes [20] were detected after repeated intramuscular administration in primates.

A number of immunization studies have been conducted based on alphavirus DNA vectors (Table 1) [21]. In the context of infectious diseases, immunization with a SIN DNA vector expressing the herpes simplex virus type I glycoprotein B (HSV-1-gB) elicited virus-specific antibodies and cytotoxic T-cell responses in mice [22]. Additionally, a single intramuscular injection provided protection against challenges with lethal doses of HSV-1. In another study, expression of the bovine viral diarrhea virus (BVDV) from an SFV-DNA vector generated cytotoxic T-lymphocyte (CTL) activity and cell-mediated immune (CMI) responses against cytopathic and noncytopathic BVDV in BALB/c mice [23]. Furthermore, immunization with a SIN DNA vector expressing the measles virus (MV) hemagglutinin (PMSIN-H) provided protection against pulmonary measles in cotton rats [24]. SFV and adenovirus DNA immunizations were compared for the classical swine fever virus (CSFV) E2 glycoprotein in pigs, resulting in significantly higher titers of CSFV-specific neutralizing antibodies after heterologous prime-boosting regimen with SFV and adenovirus in comparison to immunization with only adenovirus [25]. In the context of human immunodeficiency virus (HIV), a

Table 1
Examples of immunization with DNA-based alphavirus vectors in animal models

Disease	DNA vector	Amount (μg)	Target	Model/delivery	Response	Ref
Viral infections						
HSV	SIN	0.01–3	HSV-1-gB	Mouse/i.m.	Protection against HSV-1 challenges	[22]
BVDV	SFV	100	BVDV p80	Mouse/i.m.	CTL and CMI immune responses	[23]
MV	SIN	100	MV-H	Rat/i.m.	Protection against MV challenges	[24]
CSFV	SFV	100	CSV E2 + rADV	Pig/i.m.	No viremia in immunized pigs	[25]
HIV	SFV	0.2	Env, Gag-Pol-Nef	Mouse/i.m.	Efficient low dose priming	[9]
HCV	SFV	0.5–50	Core-E1-E2 + MVA	Mouse/i.m.	Humoral immune response	[26]
EBOV	SFV	5	EBOV GP, VP40	Mouse/i.d.	Binding & neutralizing antibodies	[27]
EBOV	SFV	10	EBOV GP + VP40	Mouse/i.m	Humoral & cellular responses	[28]
Bacterial infections						
TB	SIN	0.5–50	Ag85A	Mouse/s.c.	Protecion against *M. tuberculosis*	[29]
TB	VEE	20	Acr-Ag85B fusion	Mouse/i.m.	Protecion against *M. tuberculosis*	[30]
TP	SFV	100	TgNTPase-II	Mouse/i.m.	Protecion against *T. gondii*	[31]
Toxins						
BoNT/A	SFV	100	BoNT/A + GM-CSF	Mouse/i.m.	Prolonged survival	[32]
Cancer						
Metastasis	SFV	2	HPV E7/Hsp70	Mouse/gg	Potency against metastatic tumors	[33]
Cervix	SFV	0.05	HPV E6-E7	Mouse/i.d.	Protection against HPV	[34]
Breast	SIN	100	Neu	Mouse/i.m.	Reduced tumor incidence and mass	[35]
Breast	SIN	100	Neu	Mouse/i.d.	Superior effect compared to i.m.	[35]

Breast	SIN	100	Neu + Dox or Pac	Mouse/i.m.	Tumor reduction	[36]
Breast	SIN	100	Neu + Ad-neu	Mouse/i.m.	Prolonged survival in mice	[37]
Lung	SIN	100	Neu + Ad-neu	Mouse/i.m.	Tumor metastasis regression	[37]
Breast	SIN	3	TRP1	Mouse/gg	Innate immune pathway activation	[38]
Melanoma	SFV	50	MUC18	Mouse/i.m.	Protection against tumor challenges	[39]
Melanoma	SIN	50	VEGFR2-IL-12 + Survivin-βhCG Ag	Mouse/i.m.	Prolonged survival in mice	[40]
Brain	SIN	100	gp100, IL-18	Mouse	Anti-tumor and protective effects	[41]

Acr α-crystallin, *Ad* adenovirus, *Ag* antigen, *BoNT/A* Botulinum neurotoxin serotype A, *BVDV* bovine viral diarrhea virus, *CMI* cell-mediated immune, *CSFV* classical swine fever virus, *CTL* cytotoxic T-lymphocyte, *Dox* doxorubcin, *EBOV* Ebola virus, *gB* glycoprotein B, *gg* gene gun, *GM-CSF* granulocyte-macrophage colony-stimulating factor, *GP* glycoprotein, *H* hemagglutinin, *HCV* hepatitis C virus, *HPV E7* human papilloma virus E7 protein, *Hsp70* heat shock protein 70 from *Mycobacterium tuberculosis*, *HSV* herpes simplex virus, *i.d.* intradermal, *IL-18* interleukin-18, *i.m.* intramuscular, *MV* measles virus, *MVA* modified vaccinia virus Ankara, *MV-HFdU* measles virus hemagglutinin fusion protein, *MUC18* melanoma cell adhesion molecule, *neu* neu oncogene, *Pac* paclitaxel, *s.c.* subcutaneous, *SFV* Semliki Forest virus, *SIN* Sindbis virus, *TB* tuberculosis, *TgNTPase-II Toxoplasma gondii* nucleoside triphosphate hydrolase-II, *TP* toxoplasmosis, *TRP1* tyrosine-related protein-1, *VEE* Venezuelan equine encephalitis virus, *VEGFR2* vascular epithelial growth factor receptor-2, *VP40* matrix viral protein

prime-boost regimen for an SFV-DNA plasmid and a poxvirus Ankara (MVA) vector expressing HIV Env and a Gag-Pol-Nef fusion protein demonstrated efficient priming of HIV-specific T cell and IgG responses with a low dose of 0.2 μg SFV DNA, which seemed to rather be related to the number of doses than the quantity of the dose [9]. In another approach, prime immunization with an SFV-DNA vector expressing hepatitis C virus (HCV) Core-E1-E2 followed by a heterologous boost with an MVA vector expressing the nearly full-length HCV genome resulted in long-lasting T-cell responses in mice suggesting an interesting approach for HCV vaccine development [26]. Related to Ebola virus (EBOV), binding and neutralizing antibodies were detected in mice intradermally injected with an SFV-DNA plasmid expressing the EBOV glycoprotein (GP) alone or together with EBOV VP40, showing superior immunogenicity in comparison to recombinant MVA vaccines [27]. Moreover, co-expression of EBOV GP and VP40 from SFV-DNA vectors generated significantly higher antibody levels than when applied alone [28]. In the context of bacterial infections, a SIN DNA vector expressing the *Mycobacterium tuberculosis* p85 antigen generated strong immune responses in mice and provided long-term protection against challenges with lethal doses of *M. tuberculosis* [29]. Moreover, immunization with a DNA-based VEE vector containing a fusion of the *M. tuberculosis* α-crystallin (Acr) and Ag85B antigens, elicited $CD4^+$ and $CD8^+$ T-cell responses and inhibited bacterial growth in lungs and spleen after an aerosol-based *M. tuberculosis* challenge [30]. In another approach, the nucleoside triphosphate hydrolase-II of *Toxoplasma gondii* (TgNTPase-II) expressed from a DNA-based SFV vector provided partial protection against acute infection and toxoplasmosis in immunized mice [31]. Another target for vaccine development relates to the *Clostridium botulinum* neurotoxin serotype A (BoNT/A), which co-delivered or co-expressed with granulocyte-macrophage colony-stimulating factor (GM-CSF) from an SFV-DNA vector improved immunogenicity and significantly prolonged survival after challenges with lethal doses of BoNT/A [32].

DNA-based alphavirus vectors have also been applied for the development of cancer vaccines. For instance, expression of the human papilloma virus type 16 (HPV-16) E7 protein as a fusion protein with the *M. tuberculosis* heat shock protein 70 (Hsp70) elicited significantly stronger immune responses compared to E7 alone in vaccinated mice [33]. Furthermore, the fusion construct provided superior potency in E7-expressing metastatic tumors. Intradermal administration of an SFV-DNA vector carrying the HPV E6 and E7 antigens followed by electroporation resulted in therapeutic anti-tumor activity and rendering 85% of immunized mice tumor-free [34]. In the context of breast cancer, intramuscular administration of a DNA-based SIN-neu vector elicited strong antibody responses against A2L2 breast tumor cells and reduced

tumor incidence and tumor mass in immunized mice [35]. The importance of the route of administration was demonstrated by intradermal administration, which required 80% less SIN DNA to reach the same efficacy as intramuscular injections. This approach also protected against the development of spontaneous breast tumors and reduction of metastasis. In another approach, mice implanted with A2L2 tumors were subjected to combination therapy with SIN-neu and doxorubicin or paclitaxel [36]. Neither individual treatment reduced tumor growth, but the chemotherapy followed by vaccination resulted in significant tumor regression. Immunization of mice with SIN-neu DNA or an Adenovirus (Ad-neu) vector prior to challenges with A2L2 tumor cells in a solid mammary tumor model and a lung metastasis model resulted in significant inhibition of tumor growth [37]. However, if the vaccination took place 2 days after the tumor cell challenge the treatment was inefficient. On the other hand, SIN-neu DNA priming followed by Ad-neu boosting provided a significantly prolonged survival. In another breast cancer study, a DNA-based SIN vector expressing the self/tumor antigen tyrosine-related protein-1 (TRP1) showed activation of innate immune pathways to trigger antiviral immune responses, to improve immunization efficacy, and to provide immunity to melanoma [38]. Furthermore, the melanoma cell adhesion molecule (MCAM/MUC18) introduced into a SIN DNA vector (SIN-MUC18), provided protection against lethal challenges in both primary and metastatic mouse tumor models [39]. The synergistic effect of SFV-DNA vectors was evaluated in mice by targeting tumor cells and angiogenesis by administration of one DNA vector expressing domains of the murine vascular epidermal growth factor receptor-2 (VEGFR2) and interleukin-12 (IL12) and another vector expressing survivin and β-hCG antigens [40]. The combination therapy elicited strong humoral and cellular immune responses, inhibited tumor growth and prolonged survival in a B16 mouse melanoma model. Finally, a SIN DNA vector expressing human gp100 and interleukin-18 (IL-18) provided both protective and therapeutic activity in implanted B16 tumors in mice [41]. The immunostimulatory effect on $CD4^+$ and $CD8^+$ T cells and interferon-γ generated antitumor activity, which resulted in a significantly improved survival rate.

2 Materials

2.1 Reagents and Equipment

1. Phosphate buffered saline (PBS).
2. 1 mM ethylenediamine tetra-acetic acid (EDTA) containing 0.25% Trypsin.
3. Tissue culture flasks (T25, T75, and T175).

4. Microwell plates (6-, 12-, and 24-well plates).
5. Falcon tubes (15 and 50 mL).
6. Plastic syringes (1, 10, and 50 mL).
7. Dulbecco's modified F-12 medium.
8. Iscove's modified Dulbecco's medium.
9. Opti-MEM I reduced-serum medium.
10. X-gal stock solution: 50 mM K ferricyanide, 50 mM K ferrocyanide, 1 M MgCl, 2% X-gal in DMF or DMSO.
11. X-gal staining solution: 1× PBS, 5 mM K ferricyanide, 5 mM K ferrocyanide, 2 mM MgCl, 1 mg/mL X-gal.
12. Moviol 4-88 containing 2.5% DABCO (1,4-diazobicyclo-[2.2.2]-octane).
13. Lysis buffer: 50 mM Tris–HCl pH 7.6, 150 mM NaCl, 2 mM EDTA, 1% (v/v) Nonidet P-40 (NP40).
14. Hybond ECL nitrocellulose filter.
15. TBST: Tris-buffered saline with 0.1% Tween 20.
16. Starvation medium: Methionine-free MEM, 2 mM glutamine, 20 mM HEPES.
17. Chase medium: E-MEM, 2 mM glutamine, 20 mM HEPES, 150 μg/mL unlabelled Methionine.

2.2 Cell Lines

The following cell lines can be used for alphavirus production and studies on expression of recombinant proteins (*see* **Note 1**):

1. BHK-21 cells (Baby hamster kidney) (ATCC-CCL-10).
2. CHO-K1 cells (Chinese ovary cells) (ATCC-CCL-61).
3. COS7 cells (African green monkey cells) (ATCC-CRL-1651).
4. HEK293 cells (Human embryonic kidney) (ATCC CRL-1573).

2.3 Cell Culture Media

1. BHK-21, CHO-K1, and HEK293 cells are cultured in a 1:1 mixture of Dulbecco's modified F-12 medium and Iscove's modified Dulbecco's medium supplemented with 4 mM glutamine and 10% fetal calf serum (FCS).
2. COS7 cells are cultured in DMEM (Dulbecco's Modified Eagles Medium) supplemented with 5% fetal calf serum, 5 mM glutamine, and 0.1% penicillin/streptomycin.

2.4 Alphavirus Plasmid Vectors

Similar expression vectors have been engineered for the three most commonly used alphaviruses, SFV, SIN, and VEE. As the methods are similar for all three alphaviruses, the focus here is on SFV only and more detailed information on SIN [42] and VEE [43] can be

found elsewhere. The following vectors can be applied for DNA transfections in cell lines and for immunization studies:

1. pSCA1 (layered DNA-RNA vector with CMV promoter) [14].
2. pSCA-Helper (layered DNA-RNA helper vector with CMV promoter) [44].
3. pCMV-SFV4 (full-length layered DNA-RNA vector) [45].

The pSCA1 layered DNA-RNA vector can be used directly for transfection of host cells for recombinant proteins and immunization studies for vaccine development [14] (*see* **Note 2**). Alternatively, co-transfection of pSCA1 and the pSCA-Helper vector or transfection of the full-length pCMV-SFV4 vector generates replication-deficient and proficient particles, respectively.

3 Methods

3.1 Subcloning into SFV Vectors

Introduction of foreign genes can take place in the cloning sites of the chosen SFV expression vector and restriction endonuclease digestions and nucleotide sequencing can be used for verification of inserts (*see* **Note 3**). Preparation of high purity DNA (Midiprep or Maxiprep DNA) is highly recommended to provide the best possible quality and yields for DNA transfection and immunization studies.

3.2 Transfection of Alphavirus Plasmid DNA

Transient alphavirus plasmid DNA transfections can be achieved with the *Trans*IT®-LT1 transfection reagent as follows:

1. Plate cells at a density of 0.8–3.0 $\times$ 10^5 cells/mL on 6-well plates in 2.5 mL complete growth medium per well and culture cells for 18–24 h to approximately 80% confluency prior to transfection.
2. Prepare the *Trans*IT®-LT1 reagent-DNA complex as follows. Add 250 μL of Opti-MEM I Reduced-Serum Medium in a sterile tube. Add 2.5 μg plasmid DNA (1 μg/μL) and mix gently. Add 7.5 μL *Trans*IT®-LT1 to the diluted DNA mixture and mix completely and incubate at room temperature for 15–30 min.
3. Transfer the *Trans*IT®-LT1 reagent–DNA complex to complete growth medium dropwise to different areas of the wells. Gently rock the plate back and forth for even distribution. Incubate for 24–72 h.
4. Harvest cells for the evaluation of transfection efficacy and expression activity.

3.3 Verification of Transfection Efficiency

The transfection efficiency can be verified by reporter gene expression based on green fluorescent protein (GFP) and β-galactosidase (*see* **Note 4**). Alternatively, immunofluorescence can be applied in case of available antibodies for the recombinant protein in question. DNA transfected cells prepared as described in Subheading 3.2 are subjected to the following verification and preparation.

3.3.1 GFP Detection

1. Count the number of GFP-positive cells applying fluorescence microscopy.
2. Estimate the transfection efficacy based on the ratio between the total number of cells and GFP-positive cells.
3. The relative GFP fluorescence (RLU) can provide an indication of the level of recombinant protein expression.

3.3.2 X-Gal Staining

1. Wash DNA transfected cells with PBS, fix in cold methanol (99.8%) at −20 °C for 5 min and wash again three times with PBS.
2. Stain cells for at least 2 h in X-gal staining solution at 37 °C or at room temperature.
3. Count the number of β-galactosidase (blue) positive cells applying light microscopy.
4. Estimate the transfection efficacy based on the ratio between the total number of cells and β-galactosidase positive cells.

3.3.3 Immunofluorescence

If antibodies are available against the recombinant protein itself, or against tags engineered in the vector construct, immunofluorescence methods can be used for the determination of transfection efficiency.

1. Culture SFV-transfected cells on sterile coverslips, rinse twice with PBS, and fix for 6 min at −20 °C in methanol.
2. Wash the coverslips three times in PBS and incubate for 30 min at room temperature in PBS containing 0.5% gelatin and 0.25% BSA to prevent nonspecific binding.
3. Replace the blocking buffer with a primary antibody in the same buffer for 30 min at room temperature, wash three times with PBS and incubate with a secondary antibody for 30 min at room temperature.
4. Rewash the coverslips three times with PBS, once more with H_2O, and air dry.
5. Mount the coverslips on glass slides using 10 μL Moviol 4-88 containing 2.5% DABCO (1,4-diazobicyclo-[2.2.2]-octane).
6. Count the ratio between the total number of cells and positive cells to estimate the transfection efficiency.

3.4 Evaluation of Gene Expression

Initial confirmation of recombinant protein expression is recommended before proceeding to immunization studies as it enables verification of expression levels and the size of gene products. Expression evaluation can be performed by Western blotting if antibodies are available against the target protein or engineered tag fusions. Alternatively, expression can be evaluated by metabolic labeling of SFV-DNA transfected cells with ^{35}S-methionine.

3.4.1 Western Blotting

1. Transfect host cells (BHK-21, CHO-K1, HEK293) cultured on 6-, 12-, or 24-well plates with SFV-DNA vectors and incubate for 1–2 days at 37 °C.
2. Lyse cells with 250, 125, and 62.5 μL of lysis buffer per 6-, 12-, and 24-well plate, respectively, incubate for 10 min on ice and load samples onto 10–12% SDS-PAGEs (polyacrylamide gel electrophoresis).
3. Transfer electrophoresed protein material to Hybond ECL nitrocellulose filters for 30 min.
4. Treat filters with 5% nonfat dry milk at +4 °C for 30 min followed by primary and secondary antibody treatment, each for 30 min at room temperature.
5. Apply the ECL Chemiluminescence kit for the visualization of specific bands.

3.4.2 Metabolic Labeling

1. Transfect host cells (BHK-21, CHO-K1, or HEK293) cultured on 6-, 12-, or 24-well plates with SFV-DNA vectors and incubate for 1–2 days at 37 °C.
2. Remove the medium, wash cells once with PBS, add Starvation medium, and incubate cells for 30 min at 37 °C.
3. Replace the medium with Starvation medium containing 50–100 μCi/mL of ^{35}S-methionine and incubate cells for 20 min at 37 °C.
4. Remove the medium, wash cells twice with PBS, and add Chase medium for appropriate time (e.g., 15 min to 3 h).
5. Remove the Chase medium, wash cells once with PBS, add 250 μL lysis buffer per 6-well plate, and incubate cells for 10 min on ice.
6. Load samples on 10–12% SDS-PAGEs under standard conditions, fix in 10% acetic acid, 30% methanol for 30 min at room temperature and replace with Amplify® for 30 min at room temperature.
7. Dry the gel and expose it on Hyperfilm-MP for 2–24 h (depending on signal) at room temperature or at −80 °C applying radioactivity-intensifying screens for visualization (*see* **Note 5**).

3.5 Immunizations

In the context of prophylactic and therapeutic efficacy of DNA-based alphavirus vaccinations, the following immunization processes and methods for therapeutic evaluation can be set up (*see* **Note 6**) [4].

3.5.1 DNA Immunization of C57BL/6 Mice

1. Immunize C57BL/6 mice with 3 μg layered DNA-RNA plasmid vectors by five weekly intramuscular injections, which can be enhanced by plasmid-coated gold particles applying gene gun technology [38].
2. Inoculate vaccinated mice with 1×10^5 B16F10 tumor cells 1 week after the last immunization and monitor for tumor growth for at least 3 weeks.

3.5.2 DNA Immunization of BALB/c Mice

1. Dilute SFV plasmid DNA vectors expressing membrane proteins PrM and E of Murray Valley encephalitis virus (MVE) in saline to a concentration of 1 mg/mL and inject doses of 100–125 μg DNA intramuscularly into BALB/c mice [46].
2. Challenge immunized mice intraperitoneally with 1.3×10^8 PFU of MVE and monitor for signs of encephalitis for 21 days. Alternatively, immunize SPF mice intramuscularly with 100 mg DNA into multiple sites in the hind leg muscles and boost after 21 days.
3. Challenge mice intracranially with 1000 $TCID_{50}$ of MVE 2 weeks after the final immunization and monitor for signs of encephalitis for 21 days.
4. The evaluation of tumor protection of mice immunized with DNA-based alphavirus vectors can be performed by intravenous administration of 5×10^5 CT26.CL25 tumor cells (from mouse colon) in mice and evaluate tumor protection at 21 days post-immunization.
5. Count the number of pulmonary metastases after 12 days.
6. In case of pre-established tumors, inject 1×10^5 CT26.CL25 cells intravenously into BALB/c mice let tumors grow for 2 days before immunization with DNA vectors.
7. Assess animal survival.

3.5.3 DNA Immunization of Pigs

1. Immunize pigs intramuscularly with 100 μg SFV-DNA-based alphavirus vector, for example SFV-CSFV E2 DNA [25].
2. The vaccination regime can consist of a priming administration followed by a booster injection 4 weeks later.
3. Collect blood from pigs from the superior vena cava for antibody analysis.
4. Challenge pigs with the virulent CSFV Shimen strain and follow clinical symptoms of viremia.

3.6 Future Directions and Potential for Other Applications

The presence of the alphavirus replicon in the DNA-based vectors has warranted high levels of recombinant protein and antigen production, providing the basis for strong immune responses in immunized animal models. The enhanced expression has supported immune responses and also allowed immunization with up to 1000-fold lower concentrations compared to conventional DNA plasmids [9]. The next steps of DNA-based vaccine development should include additional vector development and evaluation of vaccine efficiency in clinical trials.

4 Notes

1. BHK-21 cells are robust, easy to culture and suitable for expression studies. The advantage of using HEK293 cells relates to their human origin.
2. In addition to the vectors described in Subheading 2.4, mutant vectors providing enhanced and prolonged expression due to lower cytotoxicity of replicated RNA [47, 48] or presence of translation enhancement signals in the vector are available [49].
3. Subcloning of genes/gene fragments into the alphavirus expression vectors can be facilitated by initial cloning into conventional small size commercial plasmids followed by excision by restriction enzymes and re-cloning into to the final alphavirus vectors.
4. Reporter gene expression should be visible already 6 h post-transfection and generally reaches maximum expression at 24 h post-transfection. However, mutant alphavirus vectors may provide enhanced expression levels at 48 h post-infection.
5. Visualization of radioactively labeled proteins via SDS-PAGE can efficiently be enhanced by application of film cassettes with double-sided X-ray intensifying screens [50].
6. Although suggestions for appropriate doses of vaccine are indicated for the various DNA immunization protocols, a dose optimization exercise is recommended to define the optimal dose providing maximal immune responses.

References

1. Delrue I, Verzele D, Madder A et al (2012) Inactivated virus vaccines: from chemistry to prophylaxis: merits, risks and challenges. Expert Rev Vaccines 11:695–719
2. Deng MP, Hu ZH, Wang HL et al (2012) Developments of subunit and VLP vaccines against influenza a virus. Virol Sin 27:145–153
3. Apostolopoulos V (2016) Vaccine delivery methods into the future. Vaccine 4:9. https://doi.org/10.3390/vaccines4020009
4. Lundstrom K (2014) Alphavirus-based vaccines. Viruses 6:2392–2415
5. Zajakina A, Spunde K, Lundstrom K (2017) Application of Alphaviral vectors for

immunomodulation in cancer therapy. Curr Pharmaceut Design 23:1–27

6. Chiarella P, Massi E, De Robertis M et al (2008) Strategies for effective naked-DNA against infectious diseases. Recent Pat Antiinfect Drug Discov 3:93–101
7. Farris E, Brown DM, Ramer-Tait AE et al (2016) Micro- and nano-particulates for DNA vaccine delivery. Exp Biol Med 241:919–929
8. Tejeda-Mansir A, Garcia-Rendon A, Guerrero-German P (2018) Plasmid-DNA lipid and polymer nanovaccines: a new strategic in vaccines development. Biotechnol Genet Eng Rev 26:1–23
9. Knudsen ML, Ljungberg K, Tatoud R et al (2015) Alphavirus replicon DNA expressing HIV antigens is an excellent prime for boosting with recombinant Ankara (MVA) or with HIV gp140 protein antigen. PLoS One 10: e0117042
10. Strauss JH, Strauss EG (1994) The alphaviruses: gene expression, replication and evolution. Micobiol Rev 58:491–562
11. Liljestrom P, Garoff H (1991) A new generation of animal cell expression vectors based on the Semliki Forest virus replicon. Biotechnology 9:1356–1361
12. Xiong C, Levis R, Shen P et al (1989) Sindbis virus: an efficient, broad host range vector for gene expression in animal cells. Science 243:1188–1191
13. Davis NL, Willis LV, Smith JF et al (1989) In vitro synthesis of infectious Venezuelan equine encephalitis virus RNA from a cDNA clone: analysis of a viable deletion mutant. Virology 171:189–204
14. DiCiommo DP, Bremner R (1998) Rapid, high level protein production using DNA-based Semliki Forest virus vectors. J Biol Chem 273:18060–18066
15. Lechardeur D, Lukacs GL (2006) Nucleocytoplasmic transport of plasmid DNA: a perilous journey from the cytoplasm to the nucleus. Hum Gene Ther 17:882–889
16. Wolff JA, Ludtke JJ, Acsadi G et al (1992) Long-term persistence of plasmid DNA and foreign gene expression in mouse muscle. Hum Mol Genet 1:363–369
17. Wang Z, Troilo PJ, Wang X et al (2004) Detection of integration of plasmid DNA into host genomic DNA following intramuscular injection and electroporation. Gene Ther 11:711–721
18. Manam S, Ledwith BJ, Barnum AB et al (2000) Plasmid DNA vaccines: tissue distribution and effects of DNA sequence, adjuvants and delivery method on integration into host DNA. Intervirology 43:273–281
19. Jiao S, Williams P, Berg RK et al (1992) Direct gene transfer into nonhuman primate myofibers in vivo. Hum Gene Ther 3:21–33
20. Mairhofer J, Lara AR (2014) Advances in host and vector development for the production of plasmid DNA vaccines. Methods Mol Biol 1139:505–541
21. Lundstrom K (2019) Plasmid DNA-based Alphavirus Vaccines. Vaccines (Basel) 7:E29. https://doi.org/10.3390/vaccines7010029
22. Hariharan MJ, Driver DA, Townsend K et al (1998) DNA immunization against herpes simplex virus: enhanced efficacy using a Sindbis virus-based vector. J Virol 72:950–958
23. Reddy JR, Kwang J, Varthakavi V et al (1999) Semliki Forest virus vector carrying the bovine viral diarrhea virus NS3 (p80) cDNA induced immune responses in mice and expressed BVDV protein in mammalian cells. Comp Immunol Microbiol Infect Dis 22:231–246
24. Pasetti MF, Ramirez K, Resendiz-Albor A et al (2009) Sindbis virus-based measles DNA vaccines protect cotton rats against respiratory measles: relevance of antibodies, mucosal and systemic antibody-secreting cells, memory B cells, and Th1-type cytokines as correlates of immunity. J Virol 83:2789–2794
25. Sun Y, Li N, Li HY et al (2010) Enhanced immunity against classical swine fever in pigs induced by prime-boost immunization using an alphavirus replicon-vectored DNA vaccine and a recombinant adenovirus. Vet Immunol Immunopathol 137:20–27
26. Marin MQ, Perez P, Ljungberg K et al (2019) Potent anti-hepatitis C (HCV) T cell immune responses induced in mice vaccinated with DNA-launched RNA replicons and MVA-HCV. J Virol 93:e00055–e00019. https://doi.org/10.1128/JVI.00055
27. Öhlund P, Garcia-Arriaza J, Zusinaite E et al (2018) DNA-launched RNA replicon vaccines induce potent anti-ebolavirus immune responses that can be further improved by a recombinant MVA boost. Sci Rep 8:12459
28. Ren S, Wei Q, Cai L et al (2018) Alphavirus replicon DNA vectors expressing Ebola GP and VP40 antigens induce humoral and cellular immune responses in mice. Front Microbiol 8:2662
29. Kirman JR, Turon T, Su H et al (2003) Enhanced immunogenicity to *Mycobacterium tuberculosis* by vaccination with an alphavirus plasmid replicon expressing antigen 85A. Infect Immun 71:575–579

30. Dalmia N, Klimstra WB, Mason C et al (2015) DNA-launched alphavirus replicons encoding a fusion of mycobacterial antigens Acr and Ag85B are immunogenic and protective in a murine model of TB infection. PLoS One 10: e0136635
31. Zheng L, Hu Y, Hua Q et al (2017) Protective immune response in mice induced by a suicidal DNA vaccine encoding NTPase-II gene of toxoplasma gondii. Acta Trop 166:336–342
32. Li N, Yu YZ, Yu WY et al (2011) Enhancement of the immunogenicity of DNA replicon vaccine of clostridium botulinum neurotoxin serotype A by GM-CSF gene adjuvant. Immunopharmacol Immunotoxicol 33:211–219
33. Hsu KF, Hung CF, Cheng WF et al (2001) Enhancement of suicidal DNA vaccine potency by linking *Mycobacterium tuberculosis* heat shock protein 70 to an antigen. Gene Ther 8:376–383
34. Van de Wall S, Ljungberg K, Ip PP et al (2018) Potent therapeutic efficacy of an alphavirus replicon DNA vaccine expressing human papilloma virus E6 and E7 antigens. Onco Targets Ther 7:e1487913
35. Lachman LB, Rao XM, Kremer RH et al (2001) DNA vaccination against neu reduces breast cancer incidence and metastasis in mice. Cancer Gene Ther 8:259–268
36. Eralp Y, Wang X, Wang JP et al (2004) Doxorubicin and paclitaxel enhance the antitumor efficacy of vaccines directed against HER2/neu in a murine mammary carcinoma model. Breast Cancer Res 6:R275–R283
37. Wang X, Wang JP, Rao XM et al (2005) Prime-boost vaccination with plasmid and adenovirus gene vaccines control HER2/neu+ metastatic breast cancer in mice. Breast Cancer Res 7: R580–R588
38. Leitner WW, Hwang LN, deVeer MJ et al (2003) Alphavirus-based DNA vaccine breaks immunological tolerance by activating innate antiviral pathways. Nat Med 9:33–39
39. Leslie MC, Zhao YJ, Lachman LB et al (2007) Immunization against MUC18/MCAM, a novel antigen that drives melanoma invasion and metastasis. Gene Ther 14:316–323
40. Yin X, Wang W, Zhu X et al (2015) Synergistic antitumor efficacy of combined DNA vaccines targeting tumor cells and angiogenesis. Biochem Biophys Res Commun 465:239–244
41. Yamanaka R, Xanthopoulos KG (2005) Induction of antigen-specific immune responses against malignant brain tumors by intramuscular injection of Sindbis DNA encoding gp100 and IL-18. DNA Cell Biol 24:317–324
42. Ehrengruber MU, Lundstrom K (2016) Recombinant Alphavirus-mediated expression of ion channels and receptors in the brain. In: Luján R, Ciruela F (eds). Neuromethods Receptor and ion channel detection in the brain: methods and protocols, vol 110. Springer Science + Business Media, New York. https://doi.org/10.1007/978-1-4939-3064-7_7
43. https://www.addgene.org/58970/
44. DiCiommo DP, Duckett A, Burcescu I et al (2004) Retinoblastoma protein purification and transduction of retina and retinoblastoma cells using improved alphavirus vectors. Invest Ophthalmol Vis Sci 45:3320–3329
45. Ulper L, Sarand I, Rausalu K et al (2008) Construction, properties, and potential application of infectious plasmids containing Semliki Forest virus full-length cDNA with a n inserted intron. J Virol Methods 148:265–270
46. Colombage G, Hall R, Pavy M et al (1998) DNA-based and alphavirus-vectored immunization with PrM and E proteins elicits long-lived and protective immunity against the flavivirus, Murray Valley encephalitis virus. Virology 250:151–163
47. Lundstrom K, Abenavoli A, Malgaroli A et al (2003) Novel Semliki Forest virus vectors with reduced toxicity and temperature-sensitivity for long-term enhancement of transgene expression. Mol Ther 7:202–209
48. Agapov EV, Frolov I, Lindenbach BD et al (1998) Noncythopathic Sindbis virus RNA vectors for heterologous gene expression. Proc Natl Acad Sci U S A 95:12989–12994
49. Sjöberg EM, Suomalainen M, Garoff H (1994) A significantly improved Semliki Forest virus expression system based on translation enhancer segments from the viral capsid gene. Bio/Technology 12:1127–1131
50. Voytas D, Ke N (2001) Detection and quantitation of radiolabeled proteins and DNA in gels and blot. Curr Protoc Mol Biol Appendix 3:3A

Part II

DNA Vaccine Adjuvants and Immunostimulatory Response

Chapter 4

CpG Oligonucleotides as Vaccine Adjuvants

Neslihan Kayraklioglu, Begum Horuluoglu, and Dennis M. Klinman

Abstract

CpG Oligonucleotides (ODN) are immunomodulatory synthetic oligonucleotides specifically designed to stimulate Toll-like receptor 9. TLR9 is expressed on human plasmacytoid dendritic cells and B cells and triggers an innate immune response characterized by the production of Th1 and pro-inflammatory cytokines. This chapter reviews recent progress in understanding the mechanism of action of CpG ODN and provides an overview of human clinical trial results using CpG ODN to improve vaccines for the prevention/treatment of cancer, allergy, and infectious disease.

Key words Adjuvant, Allergy, Cancer, CpG motif, DNA vaccine, Infection, TLR9, Toll-like receptors

1 Introduction

Vaccines have saved millions of lives by preventing innumerable infections. Vaccine efficacy is determined by the magnitude, duration, and quality of the induced immune response. The innate and adaptive arms of the immune system both contribute to protection, depending upon the nature of the infectious agent. The innate immune response involves multiple cell types including dendritic cells, macrophages, monocytes, neutrophils, basophils, eosinophils, lymphocytes, and/or natural killer (NK) cells. Innate immunity serves to rapidly clear infectious pathogens and subsequently helps heal inflammatory tissue damage [1]. Cells of the adaptive immune system include primarily B and T lymphocytes. The adaptive immunity they mediate develops slowly but is highly specific and critical to achieving sterilizing immunity and long-term memory.

Successful vaccination involves a complex series of immune interactions. Professional antigen presenting cells (APCs include dendritic cells and macrophages) and certain other immune cells (e.g., B lymphocytes) take up the antigen (Ag) present in the vaccine. This Ag is then processed and immunogenic fragments presented to T lymphocytes via cell–cell interactions in a process

Ângela Sousa (ed.), *DNA Vaccines: Methods and Protocols*, Methods in Molecular Biology, vol. 2197,
https://doi.org/10.1007/978-1-0716-0872-2_4,

dependent upon specific surface receptors. Ag-activated $CD4^+$ T cells provide help to Ag-specific B cells, supporting their proliferation, switch recombination and somatic hypermutation. These events result in the production of high-affinity antibody (Ab) (an outcome measured in many clinical trials) [2–5]. $CD8^+$ T cells are also stimulated to proliferate and mature into cytotoxic effectors. These are typically monitored by their production of Th1 cytokines such as IFNγ, or lytic factors such as perforin and granzyme B. Over the course of a vaccine-induced response, Ag-specific memory B and T lymphocytes arise that persist long-term and provide protection from subsequent infection by the target pathogen [6–8].

Adjuvants are agents that enhance the magnitude, breadth, quality, and/or longevity of the immune response induced by co-administered Ag. Adjuvants can also reduce the dose of Ag and/or frequency of immunizations required to achieve protective immunity. Historically, vaccines were produced from live attenuated or heat-inactivated organisms [9]. While not appreciated at the time, such vaccines contained bacterial contaminants that served as intrinsic adjuvants [10].

Adjuvants can promote immunity in several ways including: (1) stabilizing or entrapping the Ag thereby extending the duration of immune stimulation; (2) promoting an inflammatory response at the site of Ag deposition thereby attracting activated macrophages and dendritic cells to improve Ag uptake and presentation; (3) presenting co-stimulatory signals to T and B cells to enhance the induction of Ag-specific immunity [11].

There is considerable interest in identifying safer and more effective adjuvants to enhance the utility of the next generation of vaccines targeting pathogens, allergy, and cancer. In support of these goals, immunologists and microbiologists have sought to elucidate the mechanism(s) of action of adjuvants. Notable success was achieved through the discovery of Toll-like receptors (TLRs) and their role is promoting innate and adaptive immune responses, leading to a Nobel prize for Drs. Hoffmann and Beutler in 2011 [12, 13].

Members of the TLR family become activated upon recognition of pathogen-associated molecular patterns (PAMPs). PAMPs are conserved structures expressed by many different infectious microorganisms. These include the lipopolysaccharides and lipoproteins commonly found on bacterial cell walls (recognized by TLR4 and TLR2), flagellin, which is the dominant component of bacterial flagellae (recognized by TLR5) and nucleic acids of bacterial and viral origin. Double stranded viral RNA is recognized by TLR3 while single stranded RNA is detected by TLRs 7/8. Unmethylated CpG motifs present in bacterial and viral DNA (referred to as CpG DNA) are recognized by TLR9 [14]. To date, 10 human (TLRs 1–10) and 12 mouse TLRs (TLRs 1–9

and TLRs 11–13) have been identified. Human TLRs 1, 2, 4, 5, 6, and 10 are located on the exterior cell membrane and recognize PAMPs present in the milieu surrounding the cell whereas TLRs 3, 7, 8, 9, 11, 12, and 13 are embedded in intracellular vesicles and respond to PAMPs released by intracellular pathogens [15–17].

The structure of TLRs includes an extracellular leucine-rich repeat region, a transmembrane domain, and a cytosolic Toll/Interleukin-1 receptor domain. TLR stimulation triggers an innate immune response that supports the generation of adaptive immunity including long-term pathogen-specific memory [18, 19]. TLRs are expressed primarily by immune cells although other cell types involved in host protection (such as barrier epithelial cells) can also express these receptors. TLR recognition induces the rapid production of pro-inflammatory cytokines and chemokines that support the recruitment of additional inflammatory cells that produce type I interferons and antimicrobial peptides [18, 20].

The ability of TLR agonists to support both innate and adaptive immunity piqued interest in their potential to act as vaccine adjuvants. Early studies suggested that certain TLR ligands might pose a safety hazard by increasing susceptibility to toxic shock or autoimmune disease. Ligands for TLR2 and TLR4 were of particular concern in this context, as they induced a septic shock like syndrome in animal models [21]. Similarly, TLR2 and TLR4 ligands elicited a Th2 (pro-allergic) immune response that exacerbated asthma in experimental models [22–24]. Subsequent studies identified TLR agonists with better safety profiles, among which the TLR9 agonist CpG ODN stood out for their ability to induce strong Th1 immune responses. Th1 immunity reduces host susceptibility to allergic asthma without triggering toxic shock or autoimmunity [25–27]. The remainder of this chapter will describe the structure and mechanism of action of CpG ODN and summarize results of preclinical and clinical studies concerning their utility as vaccine adjuvants.

2 Activation of TLR9

2.1 The TLR9 Signaling Cascade

TLR9 recognizes "CpG motifs" (consisting of a central unmethylated CG dimer flanked by 5′ purines and 3′ pyrimidines) that are present at high frequency in bacterial DNA. Such motifs are rare in mammalian DNA due to a combination of CG suppression and CG methylation [16]. TLR9 receptors are located in the late endosomal and lysosomal compartments of the endoplasmic reticulum (ER). They are triggered when bacterial or viral DNA is released within an infected cell or taken up from the surrounding milieu [28].

TLR9 receptors differ between species, with the structure of human versus mouse TLR9 varying by 24% [16]. The cell types expressing TLR9 also varies between species. TLR9 is present in plasmacytoid DC (pDC) and B cells of all mammals (including

humans) but is expressed by macrophages and myeloid-derived dendritic cells (mDC) of rodents but not primates [18, 29–31]. Thus, murine studies may overestimate the activity that CpG ODN will have in humans.

The binding of CpG DNA to TLR9 induces the receptor to undergo proteolytic cleavage [32, 33]. After exiting the ER, the TLR9 ectodomain is cleaved by asparagine endopeptidase and/or cathepsins [34, 35]. If this cleavage step is blocked, adaptor molecules cannot be recruited and signaling does not occur. The requirement for ectodomain cleavage thus provides an ancillary mechanism to restrict receptor activation to endolysosomal compartments and prevent TLR9 from responding to self-DNA. The truncated form of TLR9 recruits myeloid differentiation factor 88 (MyD88), IRAK, and TRAF6 which in turn recruit various MAP kinases and transcription factors (including NF-κB, AP1, and IRF-7) that upregulate the expression of pro-inflammatory genes [36].

Changes in the expression of genes encoding TNFα, IL-1ß, and IL-1α occur within 30 min of in vivo CpG ODN administration [37]. Global gene expression peaks 3 h after CpG ODN treatment, at which time nearly 1000 genes are upregulated [38]. These genes fall into functional categories (as defined by Ingenuity Pathway Analysis) including immune response (e.g., *IL1A, IL1B, TLR9,* and *TNFA*), cell signaling (e.g., *NFKB1A, MYD88, IRAK3,* and *A20*) and cell movement (e.g., *BFL1, NAP-1, NAK,* and *EGFR*) [39]. Gene expression levels then decline over a 3 day period before rising again at day 5. Of interest, the function of genes activated at 3 h differs from those at 5 days. The second peak of gene activation primarily involves genes in the functional groups cell cycle regulation (*PLK1, WEE1, CHK2,* and *TOPO2A*) and DNA damage response (*BRCA1, GADD4A, E2F4,* and *RPA1*) and appear to be part of a counter-regulatory mechanism that returns the immune system to homeostasis [39].

2.2 CpG ODN

Four distinct classes of CpG ODN have been identified. Although each class contains at least one "CpG motif," they otherwise differ in structure and immunological activity. K-type ODN (also referred to as B-type) contain 1–5 CpG motifs embedded in a phosphorothioate (PS) backbone. The PS backbone enhances resistance to digestion by nucleases and substantially prolongs in vivo half-life (30–60 min versus 5–10 min for phosphodiester backbone ODN in plasma) [40]. K-type ODN trigger pDC to differentiate and produce TNFα while stimulating B cells to proliferate and secrete IgM [41, 42]. K-type ODN have been the most extensively characterized in clinical trials (described below).

D-type ODN (also referred to as A-type) typically express a single CpG motif flanked by palindromic sequences that enables the formation of a stem-loop structure. The central nucleotides are

phosphodiester (PO) while the ends are capped with PS poly G motifs that facilitate concatamer formation. D-type ODN trigger pDC to mature and secrete IFNα but have no effect on B cells [41–43]. The differences in biological activity of K- versus D-type ODN are largely explained by where they localize [44, 45]. K-type ODN are rapidly transported through early endosomes into late endosomes whereas D-type ODN persist in the early endosome. D-type ODN interact with MyD88/IRF-7 complexes in the early endosome to trigger a signaling cascade that supports IFNα production [45]. D-type ODN tend to form multimers in solution (due to the formation of Hoogsteen bonds between their poly-G tails) which complicates the synthesis of a consistent product for clinical use. D-type ODN were successfully packaged into stable virus-like particles (VLP) and used as adjuvants in several preclinical and clinical studies [46–48].

C-type ODN resemble K-type in being composed entirely of PS nucleotides but resemble D-type in containing palindromic CpG motifs that can form stem-loop structures or dimers. This class of ODN stimulates B cells to secrete IL-6 and pDC to produce IFNα. C-type ODN interact with TLR9 in both early and late endosomes, and thus express properties in common with both K- and D-type ODN [49, 50]. PO linkages can be introduced into their CG dinucleotides (referred to as semi-soft C), a modification reported to further enhance the activity of C-type ODN.

P-type CpG ODN contain double palindromes that can form hairpins at their GC-rich 3′ ends as well as concatamerize due to the presence of the 5′ palindromes. These highly ordered structures are credited with inducing the strongest type I IFN production of any class of CpG ODN [51, 52].

2.3 Cellular Immunology

TLR9 activation by K-Type CpG ODN stimulates mature human B cells to enter the G1 phase of the cell cycle, undergo class switching to IgG2a and secrete pro-inflammatory cytokines and Abs in a T-cell-independent manner. CpG activation also stimulates B cells to increase expression of Fcγ receptor and co-stimulatory molecules including class II MHC, CD80, and CD86 [53–55]. The effect of CpG ODN on naive B cells is less clear. Some studies suggest that multiple signals are required to stimulate naive B cells yet recent work indicates that CpG ODN alone can initiate IgM production and improve naive B-cell survival [31, 56–59]. Primary B cells stimulated with Ag upregulate TLR9 and thus become even more responsive to CpG [31, 60]. Mice immunized with CpG-Ag complexes produce class-switched Abs in vivo, consistent with CpG acting as adjuvants for coadministered proteins [60]. The upregulation of CD40 by CpG ODN also downregulates Fas expression by B cells, reducing their susceptibility to Fas-mediated apoptosis [61].

The only type of dendritic cell in humans that responds directly to CpG ODN activation is the plasmacytoid DC. Both K- and D-type CpG ODNs induce pDC to increase surface expression of MHC class II, ICAM-1, CD40, CD54, CD80, and CD86. They also stimulate the production of various cytokines and chemokines (TNFα, IL-6, IL-8, IP-10) while inducing pDC to mature and become resistant to apoptosis [62, 63]. D-type CpG ODN induce IFNα secretion by pDCs [41–43]. In mice, bone-marrow-derived DCs and Langerhans cells express TLR9 and are activated by K-type CpG ODN to secrete IL-12 and IL-6 [64–66]. CpG-activated Langerhans cells and splenic DC change morphology and migrate to secondary lymphoid organs where they play a key role in mediating Th1 cell activation [66, 67].

Purified human monocytes and macrophages do not express TLR9 and are not activated by CpG ODN [30]. Nevertheless, CpG DNA treatment of human peripheral blood mononuclear cells (PBMC) secondarily activates monocytes to increase CD40 and CD69 expression and produce IL-6 and TNFα [68, 69]. Murine monocytes express TLR9 and respond directly to CpG ODN stimulation [70] by producing cytokines (including TNFα) and differentiating into M1-like (inflammatory) macrophages [71].

Neither T nor NK cells respond directly to CpG ODN. However, the type I interferons produced by CpG stimulated pDC induce T cells to upregulate co-stimulatory molecule expression. They also improve the proliferative response of T cells following TCR ligation [72, 73]. K-type CpG create a Th1-biased immune milieu in the secondary lymphoid organs that promotes cross-priming of cytotoxic T cells, supports NK cell activation, and improves Ab responses [74–79].

3 CpG ODN as Vaccine Adjuvants

3.1 Results from Preclinical Studies

Shortly after CpG ODN were discovered, in vivo studies showed that immunizing mice with a combination of K-type ODN plus protein (such as ovalbumin or hen egg lysozyme) led to the induction of significantly stronger humoral and cell-mediated immune responses [77, 80]. Subsequent studies established that the adjuvant-like properties of CpG ODN were optimized by presenting them to the immune system in close spatial and temporal proximity with the immunogen.

More than 1500 preclinical studies examining the immunogenicity of CpG-adjuvanted vaccines have since been published. CpG ODN were shown to boost the humoral immune response induced by vaccines targeting a plethora of pathogens, including *B. anthracis*, *Helicobacter pylori* [81], *L. major*, influenza [82], rabies [83], herpes simplex virus (HSV) [84], measles, lymphocytic choriomeningitis virus, multiple orthopox viruses [85], human papilloma virus (HPV) [86, 87], hepatitis B virus (HBV), and

tetanus toxoid, with Ag-specific Ab titers improved by up to three orders of magnitude [72, 77, 88–94].

There have been fewer studies of their effect on T-cell responses but those also documented a significant benefit to CpG ODN adjuvants. For example, adding CpG ODN to a leishmania vaccine against metacyclic promastigotes accelerated the generation and increased the number of IFNγ-producing $CD4^+$ and $CD8^+$ T cells by two- to threefold in mice [95]. This pathogen-specific IFNγ response had a significant effect on disease, reducing parasite load by >1000-fold while reducing the extent and duration of disease ($p < 0.001$).

While vaccines are typically administered prophylactically to reduce host susceptibility to infection, there are situations in which pathogen-specific immunity is needed after exposure (e.g., following the release of a biothreat pathogen). In such cases, accelerating the induction of protective immunity is critical. There is considerable evidence that CpG ODN accelerate the development of vaccine-induced responses. For example, mice and rhesus macaques immunized with the FDA-approved anthrax vaccine (AVA) supplemented with CpG ODN developed humoral immunity up to three times faster, neutralizing titers that were five to ten times higher, and were significantly better protected from infection than those immunized with AVA alone [96, 97].

As pathogens may gain access to the host through the respiratory, gastrointestinal, vaginal and/or rectal mucosa, the ability of CpG ODN to boost mucosal immunity was also examined. Animals immunized intravaginally with an HSV-2 vaccine combined with CpG ODN rapidly developed strong mucosal and systemic Th1 immune responses that protected against lethal HSV-2 challenge [98]. They also generated MHC-restricted, Ag-specific cytotoxic T cells (CTL), replicating the effect of delivering the CpG ODN augmented vaccine systemically. Administering CpG ODN in combination with recombinant HSV-1 glycoprotein B via the nasal route significantly increased Ag-specific IgA levels and anti-HSV CTLs in the genital tract and protected mice from genital HSV challenge [99]. Using CpG ODN as adjuvant with intranasally delivered enterovirus 71 (EV71) vaccine induced higher amounts of EV71-specific IgG and IgA titers in serum and mucosa when compared to EV71 alone and protected mice from subsequent lethal challenge [100]. Titers of virus-neutralizing IgA and IgG were increased in both the tears and serum of rabbits vaccinated by intraocular delivery of CpG-adjuvanted HSV-1 vaccine. HSV-1 vaccine alone failed to induce Ag-specific T-cell immunity whereas the CpG-adjuvanted vaccine generated local and systemic Ag-specific T-cell responses polarized toward Th1 immunity [101].

Oral delivery is a favored route for vaccine administration. Several studies evaluated the effect of adding CpG ODN to oral vaccines. Newborn mice orally immunized with sonicated

salmonella proteins (SSPs) plus CpG developed both mucosal and systemic immune responses and were better protected than those vaccinated with SSP alone [102]. Combining SSP with CpG ODN induced six-fold higher pathogen-specific serum IgG ($p < 0.05$), markedly (but not significantly) increased serum IgA and showed significantly enhanced survival following enteric challenge with live *Salmonella enteritidis*. The same vaccine lacking CpG was nonprotective [102]. CpG ODN improved the systemic (IgG, CTL, T-cell proliferation) and mucosal (IgA) immune responses elicited by Hepatitis B Antigen (HBsAg) and tetanus toxoid vaccines when delivered orally [103]. As CpG ODN are susceptible to degradation by the harsh conditions present in the gastrointestinal tract (low pH and digestive enzymes), their adjuvant activity is lower when delivered orally vs parenterally [104]. Efforts to modify ODN to enable oral delivery will be described later in this chapter.

The ability of CpG ODN to act as adjuvants in animal models of immune deficiency triggered interest in their potential to improve the response of geriatric animals whose cellular and humoral immune responses were diminished [105, 106]. Vaccines for the elderly must compensate for the progressive decline in immune function that accompanies aging. Several studies found that CpG ODN significantly boosted the immunogenicity of vaccines delivered to aged mice, in some cases restoring T-cell priming and humoral immunity to levels found in young adults [107–110]. Newborns are also less capable of mounting robust vaccine responses due to the immaturity of their immune system. For example, neonates respond poorly when immunized with hepatitis B surface Ag, attenuated measles virus, or tetanus toxoid [90, 111]. Improved Ab and CTL responses were elicited when CpG ODN were used as adjuvants with these vaccines in young mice [102, 111, 112].

CpG ODN were effective as vaccine adjuvants in multiple species. CpG ODN adjuvanted AVA induced a rapid and protective toxin-neutralizing Ab response in guinea pigs [113]. Calves immunized with a formalin-inactivation bovine respiratory syncytial virus vaccine plus CpG ODN generated higher Ag-specific Ab responses and cleared virus from their lungs better than animals immunized with vaccine alone [114]. Vaccinating calves intranasally with CpG-adjuvanted recombinant outer membrane protein H of *Pasteurella multocida* improved IgG and IgA Ab levels and protection from subsequent infection [115]. Oral vaccination of newborn piglets with live attenuated pseudorabies virus plus CpG ODN generated 18-fold higher serum IgG and ten-fold higher mucosal IgA levels when compared with animals immunized with pseudorabies virus alone [116]. CpG ODN also improved the immunogenicity of a vaccine targeting Newcastle disease in chickens, increasing the Ag-specific IgG response by three-fold and protecting animals from challenge by an otherwise lethal dose of Newcastle disease virus [117]. Similarly, adding CpG ODN to a formalin-

inactivated H9N2 avian influenza vaccine or a reticuloendotheliosis virus (REV) subunit vaccine-improved virus-specific Ab responses in chickens [118, 119]. The addition of CpG ODN (formulated in Emulsigen) to the equine influenza virus vaccine (Encevac TC4) enhanced Ag-specific Ab responses in horses [120]. CpG ODN also reduced allergic symptoms in horses affected by recurrent airway obstruction (an asthma-like disease) [121, 122]. Adding CpG ODN to the aluminum-adjuvanted rabies vaccines (IARV) boosted specific Ab titers in dogs and protected them from lethal rabies challenge [123].

As mentioned above, TLR9 is expressed in a more diverse group of immune cells in rodents than primates. Thus, the response of mice may not accurately reflect the activity of CpG adjuvants in humans. To circumvent this problem, preclinical testing was conducted in monkeys that express TLR9 on the same cell types and mount a response that closely mimics humans [124–126]. Those studies established the ability of CpG ODN to act as vaccine adjuvants in primates [56, 125–128]. As noted above, adding CpG ODN to AVA significantly accelerated and boosted immunity to anthrax in rhesus macaques [97]. The resultant neutralizing Abs were of high avidity and provided significantly greater protection against anthrax infection than those induced by AVA alone [93, 96, 97]. Similarly, K-type ODN significantly increased the Ag-specific serum IgG response of Aotus monkeys immunized with a peptide-based malaria vaccine [126]. These effects were sequence specific, as control ODN had no effect on vaccine immunogenicity [126].

Immunodeficiency is a hallmark of human immunodeficiency virus (HIV)-induced AIDS. HIV infection in humans (and simian immunodeficiency virus (SIV) infection in macaques) reduces the number and functional activity of $CD4^+$ T cells, resulting in suboptimal responses to many vaccines [129–131]. For example, both HIV-infected patients and SIV-infected macaques respond poorly to Engerix-B® vaccination (the licensed hepatitis B virus vaccine from GlaxoSmithKline) [129, 130]. Yet retrovirus infection has a greater effect on the adaptive than innate arms of the immune system [127], with PBMC from HIV-infected individuals maintaining their response to CpG stimulation despite declines in Ag-specific immunity [127]. The ability of CpG ODN to boost the response of macaques with SIV viral loads $<10^7$ copies/mL to Engerix-B® was therefore investigated. While lower than the neutralizing titers achieved in immunized uninfected animals, adding CpG ODN to the Engerix-B® boosted Ab levels to protective levels in these SIV-infected macaques, suggesting that CpG ODN can boost the immunogenicity of vaccines in immunocompromised as well as normal hosts [127].

The ability of CpG ODN to induce a Th1-biased immune response that supports CTL generation suggests they might be useful as adjuvants for cancer vaccines [132–134]. Early studies

found that systemic delivery of CpG adjuvanted vaccines significantly increased tumor-specific CTL frequency [135–140]. CpG treatment was successful in eradicating small tumors (<300 mm^3) but only slowed the growth of large established tumors despite continued generation of tumor-specific CTL in the periphery. This was because large tumors (in mice and humans) create an immunosuppressive micromilieu that downregulates CTL activity, preventing immune cells from eradicating the cancer. To overcome this limitation, CpG ODN were injected directly into the tumor bed with the goal of activating local DCs and facilitating Ag presentation in situ. Unexpectedly, intra-tumoral injection of CpG ODN not only boosted T-cell immunity but also reduced the number and suppressive activity of monocyte-derived suppressor cells (MDSC) in the tumor bed [141]. CpG ODN inhibited the production of arginase 1 and nitric oxide (factors critical to their suppression of T-cell activity) while inducing MDSC to differentiate into tumoricidal macrophages [141, 142]. Intra-tumoral CpG administration also stimulated the rapid expansion of the $CD8^+$ T cells, reduced their susceptibility to proliferative exhaustion, and resulted in durable control of primary and metastatic tumor growth in murine models [143].

3.1.1 Impact of Delivery Method

The response induced by adding CpG ODN to vaccines is optimized by insuring that APCs are exposed to Ag and adjuvant simultaneously [144]. This was initially established in murine studies involving the model Ag ovalbumin [145] and verified in experiments involving a multitude of vaccine candidates. For example, when CpG ODN plus Hepatitis B Ag were administered concurrently to the same site, protective Ab titers were significantly increased when compared to Ag alone. In contrast, no increase in titer was observed if the CpG was delivered to a different site than the Ag [40].

Adding CpG ODN to weak protein Ags magnified the resultant immune response by up to 100-fold [26, 146, 147]. Conjugating CpG ODN to complex vaccines (such as whole apoptotic tumor cells) enhanced antitumor immunity [148]. CpG-conjugated tumor cells triggered the expansion of tumor-specific CTL that delayed tumor growth and prevented metastatic spread in mice. The mechanism by which CpG-Ag conjugates enhanced immunogenicity was twofold: (1) it insured co-internalization within the same APC and (2) it improved the uptake of Ag via DNA-binding receptors on the APCs (the latter effect is independent of the nature of the ODN but requires physical conjugation of DNA to target Ag) [149, 150].

One challenge faced by CpG-based adjuvants is their susceptibility to in vivo elimination by adsorption onto serum proteins and/or degradation by nucleases. While the speed of degradation is reduced by the use of PS nucleotides, further protection is gained

by incorporating the vaccine/adjuvant complexes into liposomes, polymeric nanoparticles (NP), biodegradable microparticles (such as alginate and cationic microparticles) or multicomponent nanorods [151–153]. The advantages provided by these delivery vehicles reduce degradation thereby prolonging circulation time and improving uptake by APCs. Co-delivery of CpG ODN plus Ag in NP yielded vaccines that were generally superior at generating protective CTL and/or Ab responses. In vivo murine studies documented the greater activity of multiple types of NP in tumor therapy models. CpG ODN can also be encapsulated into liposomes with high efficiency, with their rate of release determined by pH of the liposomes when formulated [151, 154, 155]. Liposome-encapsulated CpG ODN showed superior immunogenicity when used as mucosal vaccines, anti-parasite vaccines, and in cancer treatment [156–161].

Another limitation of ODN-based therapies is their reliance on parenteral routes of administration. Although PS modification reduces ODN sensitivity to DNase digestion, it does little to alter susceptible to the harsh environment of the GI tract. Virtually every clinical trial delivered ODN-based vaccines by injection [162, 163]. Efforts were made to formulate ODN for oral delivery. This required that the ODN be (1) protected from DNases, digestive acids, and enzymes in the GI tract and (2) delivered in a form readily adsorbed through the gut while retaining immunomodulatory properties. In 2012, Zhu et al. incorporated ODN in pH-dependent PLGA (poly-D,L-lactide-*co*-glycolide) NP for delivery to the large intestines [164]. These NP remained intact when passing through the upper gut but released their cargo when the pH changed in the lower GI tract. Yamamoto et al. showed that carbonate apatite microparticles formulated in a high glucose environment could protect ODN from the low pH and DNA degrading enzymes in the gut [165]. In vitro studies showed that immune cells recognized and responded to CpG ODN adsorbed onto calcium carbonate NP (CaNP) while an in vivo study showed that they could protect against the development of atopic dermatitis [166]. Unfortunately, that experiment failed to include free CpG ODN as a control. When free versus calcium carbonate encapsulated CpG ODN were directly compared, no difference in activity was observed in vivo following oral delivery (with both being far less effective than parenteral administration) [104].

3.1.2 Use of CpG ODN in Combination with Other Immune Modifiers

Identifying TLR agonist combinations that synergize to achieve optimal humoral and cellular responses is desirable in this era of combination immunotherapy. Finding synergistic agonists is facilitated by an understanding of the downstream signaling pathways triggered by TLR ligands. For example, TLR3 signals via a MyD88-independent pathway and thus might synergize with TLR9 which

relies on MyD88 signaling [167, 168]. Microarray analysis of gene expression patterns showed that these ligands synergistically enhanced the activation of genes associated with immune function [169]. Co-delivery of CpG ODN plus Poly (I:C) with a DNA-encoded HIV vaccine increased protection against viral challenge, enhanced the avidity and magnitude of Ag-specific $CD8^+$ T-cell responses and increased IL-12/IL-15 production by DC in murine studies [170–173]. Liposome co-encapsulation of TLR3 and TLR9 ligands in combination with a cancer Ag boosted specific immunity and led to long-term protection in mice [174]. A combination of CpG ODN with the TLR4 ligand monophosphoryl lipid A (MPLA) in liposomes is being evaluated clinically for the treatment of non-small-cell lung cancer (NSCLS) and melanoma [175–177]. Our group examined the effect of combining TLR7/8 agonists with CpG ODN. While each agonist alone slowed tumor growth, the combination of TLR9 with TLR7 eradicated large established tumors in 87% of mice [178, 179].

The effect of combining CpG ODN with non-TLR adjuvants has also been examined. Co-administering CpG ODN with cGAMP, the cyclic dinucleotide adaptor molecule of STING, enhanced Ag-specific responses and reduced tumor growth more effectively than either agent alone [180]. Administering Ag plus CpG ODN to mice in Incomplete Freud's adjuvant (IFA) or alum also in improved humoral and cellular immunity when compared to either adjuvant alone [53, 77, 111, 181–185]. Similarly, TLR9 agonists enhanced the immune response to vaccine Ag presented in Quil A; Emulsigen® (a mineral oil-in-water emulsion) [186, 187], and Montanide® (a water-in-mineral oil emulsion) [126, 144, 188, 189].

More recently, the possibility of co-administering CpG ODN with checkpoint inhibitors was investigated. Two of the best characterized checkpoint inhibitors are monoclonal Abs targeting cytotoxic T lymphocyte antigen 4 (CTLA-4) and programmed cell death protein 1 (PD-1). Therapies involving checkpoint inhibitors have shown efficacy in clinical trials yet only a minority of patients and tumor types respond. Adding CpG ODN might improve the activation and infiltration of $CD8^+$ T cells into the tumor [190, 191]. Such T-cell synergy was observed in multiple studies involving the combination of CpG ODN plus inhibitors of CTLA-4 or PD1. This included murine models of melanoma, bladder cancer, and colon carcinoma [143, 192, 193]. Based on these studies, several Phase I clinical trials of CpG ODN plus checkpoint inhibitors have been initiated [190].

3.2 Results from Clinical Studies

More than 100 clinical trials studying K-type CpG ODN as adjuvants are currently underway or have been completed (https://clinicaltrials.gov/). The vaccines involved target infectious agents, allergens, and cancer.

3.2.1 Vaccines Targeting Infectious Agents

Human clinical trials have evaluated the utility of adding CpG ODN to vaccines against HBV, *B. anthracis*, *Plasmodium* spp., influenza virus, and *S. pneumonia*. HBV is a hepadnavirus that predominantly infects hepatocytes. Infection can cause acute or chronic hepatitis, the latter being associated with long-term complications including cirrhosis of the liver and hepatocellular carcinoma. Although vaccination has reduced the incidence of and complications from HBV infection, the disease remains a major public health issue among individuals who respond poorly to the originally licensed vaccines [194]. Approved vaccines against HBV, Engerix-B® and Recombivax-HB®, use HbsAg as their major antigenic component and alum as adjuvant. HbsAg is expressed on the surface of HBV and is released into the serum following infection. Those vaccines require three immunizations over a period of 6 months to generate protective Ab titers. 5–10% of immunocompetent individuals fail to achieve long lasting seroprotection after completing the full vaccination series [195]. Immunocompromised patients do even more poorly: protective titers are achieved by only 45–60% of vaccinated elderly individuals [196, 197], 35–87% of patients with chronic kidney disease (depending on disease severity) [198] and 55% of patients with chronic liver disease caused by Hepatitis C infection [199].

As noted above, rodents and nonhuman primates treated with HBsAg vaccines adjuvanted with CpG ODN had higher response rates and produced two- to ten-fold more ($p = 0.005$) IgG anti-HBsAg Ab compared to those receiving vaccine alone [88, 125, 200]. In vitro, CpG ODN increased the recognition of HBV epitopes [201] and triggered a two- to four-fold increase in the production of IFNγ and IL-4 by PBMC from patients with chronic HBV infection [202]. Similar effects were observed in clinical trials: normal volunteers generated three- to ten-fold higher anti-HBsAg Ab titers when immunized with CpG-adjuvanted vaccine versus vaccine alone [181, 182, 200]. The first CpG-containing HBV vaccine to complete Phase III trials was HEPLISAV-B®. HEPLISAV-B® elicited higher Ab titers with fewer immunizations than did previously licensed alum-adjuvanted vaccines [203–205].

Two doses of HEPLISAV-B® elicited faster (3 vs. 7 months) protective immunity in more subjects (95% vs. 81%) than 3 doses of Engerix-B® in a trial involving over 2000 18–55 year olds [203]. In a subsequent Phase III trial evaluating nearly 1500 40–70 year olds, the seroprotection rate was 90% with HEPLISAV-B® versus 70% with Engerix-B® [206]. In adults with type-2 diabetes mellitus, 90% versus 65% achieved seroprotection with HEPLISAV-B® versus Engerix-B®. Minor adverse event rates were 35.4% versus 36.2% ((primarily injection site pain (23–39%), fatigue (11–17%) and headache (8–17%) [207]) while serious adverse event rates were 3.9% versus 4.8% in HEPLISAV-B® versus Engerix-B® groups,

respectively over 12 months of follow-up [206]. HEPLISAV-B® was licensed by the US FDA in 2017 for use in adults 18 years of age and older.

Anthrax is caused by toxin-producing Gram-positive *Bacillus anthracis*. The spores of this pathogen are highly resistant to environmental degradation (desiccation, heat, UV light) and most disinfectants [208]. Protection against anthrax is provided by Abs against the protective antigen (PA) component of the toxin. The licensed human vaccine, Anthrax Vaccine Adsorbed (AVA, BioThrax®), is made from sterile, cell free filtrates of avirulent nonencapsulated *Bacillus anthracis* cultures containing PA protein. BioThrax® is administered as 6 subcutaneous (sc) injections over 18 months followed by annual boosters [209, 210]. For biodefense preparedness in the US, there is considerable interest in a vaccine capable of inducing faster, stronger, and longer lasting immunity against anthrax.

In animal studies, combining CpG ODN with AVA significantly increased the speed, magnitude, and duration of the resultant immune response, generating PA-specific Abs that provided significantly greater protection from challenge when compared to animals vaccinated with the AVA alone ($p < 0.001$) [93, 96, 97]. Of importance, a majority of mice immunized with the CpG-adjuvanted vaccine maintained resistance to anthrax for >1 year, despite Ab titers declining below protective levels. This prolonged survival was mediated by the rapid de novo production of protective Abs by long-lived memory B cells. That pool was three-fold larger and contained six-fold more high-affinity B cells in mice immunized with CpG-adjuvanted AVA vs AVA alone [211].

Phase I clinical trials showed that adding CpG to BioThrax® accelerated and enhanced the immune response of healthy vaccines. Those who received the adjuvanted vaccine developed six- to eight-fold higher Ab titers 3 weeks more rapidly than recipients of BioThrax® alone. No serious AEs related to the study agents were reported and the combination was reasonably well tolerated [183, 212]. A Phase 2 safety and immunogenicity study comparing different doses and schedules of CpG-containing BioThrax® vaccine (AV7909) showed that 2 doses of AV7909 yielded similar levels of toxin-neutralizing Ab as 3 doses of BioThrax® alone while having a similar safety profile. A Phase III clinical trial investigating lot-to-lot consistency, safety, and immunogenicity of the 2-dose adjuvanted AV7909 was recently initiated (https://clinicaltrials.gov/ct2/show/NCT03877926).

Malaria vaccines typically induce immune responses against proteins present on the surface of the parasite, such as merozoite surface protein 1 (MSP1) or apical membrane antigen 1 (AMA1). A number of clinical trials evaluated CpG ODN as an adjuvant for vaccines targeting these proteins [213, 214]. CpG adjuvants

enhanced anti-MSP1 Ab responses by 49-fold after two immunizations and eight-fold after three immunizations when compared to an MSP1 vaccine formulated in Alhydrogel alone ($p < 0.0001$) [215]. In a separate study, AMA1-C1/Alhydrogel® supplemented with CpG ODN improved the anti-AMA-1 Ab response by two- to three-fold ($p = 0.013$) [216, 217]. An even greater improvement in AMA1-specific Ab titers (up to 14-fold) was observed when this CpG adjuvanted vaccine was administered to malaria naive individuals [215, 218, 219]. Unfortunately, the response induced with the CpG adjuvanted AMA1-C1 vaccine did not protect against malaria challenge [220].

CpG ODN improved the immunogenicity of licensed influenza vaccines in multiple animal models [221–223]. Adding CpG ODN to the human influenza vaccine Fluviral® induced higher virus-specific Ab titers resulting in a 20% reduction of viral load in challenged ferrets when compared to Fluviral® alone [223]. A randomized, blinded, Phase Ib trial was conducted wherein subjects were vaccinated with either a $1/10^{th}$ or full dose of Fluarix® alone or in combination with CpG ODN. The inclusion of CpG did not improve hemagglutin inhibition (HI) Ab titers or total serum IgG levels. However, recipients of the $1/10^{th}$ dose of Fluarix® vaccine combined with CpG had four- to seven-fold more IFNγ-producing PBMCs compared to low dose vaccine recipients alone, which was nearly equivalent to a full dose of Fluarix® in the absence of adjuvant. These results are consistent with a dose-sparing effect of CpG ODN in humans [184].

Chronic HIV infection is characterized by reduced $CD4^+$ T-cell number and function and reduced cytolytic activity by $CD8^+$ T cells. This contributes to a diminution in the immunogenicity of standard vaccines, placing HIV patients at greater risk of infection [224, 225]. Since CpG ODN boosted the responsiveness of mice with depressed adaptive immune systems, studies examined whether they would have the same effect in HIV-infected patients. Care was taken, since it was possible that CpG-mediated stimulation of latently infected T cells might increase virus replication [226–230].

Since CpG adjuvanted Engerix-B® vaccine was safe and effective in normal volunteers, its activity in patients with HIV infection was examined [231–233]. The anti-HBsAg Ab response of patients immunized twice with the CpG adjuvanted vaccine was eightfold higher than recipients of Engerix-B® alone. 89% of the CpG adjuvanted group responded to vaccination and they achieved protective titers 4 weeks earlier than recipients of Engerix-B® alone. Seroprotective titers (>10 mL U/L) were reached by all individuals in the CpG group by week 10% versus 89% in the control group. Protective titers persisted in 80% of the CpG group versus 40% in the non-CpG group over 5 years of follow-up. There were no

significant differences in peripheral blood $CD4^+$ or $CD8^+$ T cell counts or plasma viremia between vaccination groups. However, helper T cells from recipients of the adjuvanted vaccine mounted two- to three-fold higher Ag-specific responses following ex vivo stimulation when compared to those vaccinated with Engerix-B® alone [231–233].

The effect of adding CpG to pneumococcal vaccines was also evaluated in HIV-infected individuals. Significantly more patients immunized with a combination of Prevnar followed by CpG-adjuvanted Pneumo Novum generated high IgG responses than those vaccinated without CpG (although CpG ODN did not enhance the response to Prevnar alone) [234]. Immunization did not alter the titer of anti-HIV Abs or $CD4^+$ T-cell count [235].

3.2.2 Vaccines Targeting Allergens

Allergic diseases including asthma, allergic rhinitis, eczema, and anaphylaxis affect 10–30% of people in the developed world. Allergic inflammation is triggered when an allergen (such as pollen) initiates a strong Th2 response. Th2 cells produce cytokines (IL-4, IL-13) that support the production of IgE Abs that in turn trigger mast cells, basophils, and eosinophils to release soluble mediators of inflammation (histamine, prostaglandins, and leukotirenes) that cause disease symptoms. Disease can be prevented by shifting the immune response against the allergen from Th2- to Th1-dominated. Th1 cells secrete cytokines (such as IFNγ) that inhibit Th2-mediated allergy. As CpG ODN preferentially support the induction of Th1 responses, mice were vaccinated with CpG-adjuvanted allergens and the effect monitored [25, 26, 138]. Results showed that even animals with pre-existing Th2 immunity responded to vaccination and subsequent allergen exposure by preferentially mounting a non-allergic Th1 response (with a concomitant lessening of allergic signs and symptoms) [26].

These findings were followed by clinical trials examining the effect of a CpG-based vaccine against ragweed allergy. Phase II studies showed that CpG ODN coupled to ragweed allergen (TOLAMBA) reduced the response of immune cells in the nasal mucosa to allergen stimulation, reduced disease severity for two seasons, and led to a prolonged shift from Th2 immunity toward Th1 immunity [236, 237]. Despite these encouraging results, a multicenter multi-year Phase III trial yielded inconclusive results and failed to achieve the primary efficacy endpoint. This lack of reproducibility was attributed to the low level of active disease among participants in the second study and a problem in the timing of vaccine administration (which did not match the onset of ragweed season) [238].

In a Phase I study, an A/D class CpG ODN was incorporated into a VLP and used as an adjuvant for sc immunotherapy in combination with the house dust mite allergen, QbG10. All

patients achieved nearly complete alleviation of their allergic symptoms after 10 weeks of immunotherapy. This promising clinical outcome awaits confirmation in a placebo-controlled Phase II trial [239, 240].

3.2.3 Vaccines Targeting Cancer

Large established cancers create an immunosuppressive microenvironment that limits the tumoricidal activity of CTL and NK cells [241]. Myeloid-derived suppressor cells (MDSC) are key contributors to this inhibitory milieu [242]. Recent studies show that CpG ODN can induce murine MDSC (which express TLR9) to differentiate into tumoricidal macrophages and lose their ability to suppress $CD8^+$ T-cell function [141, 179, 243]. CpG ODN were evaluated as stand-alone antitumor agents in several clinical trials (based on the hypothesis that they would improve host recognition of and response to endogenous tumor Ags). Initial studies of healthy volunteers showed that CpG ODN treatment was well tolerated, caused no significant toxicity, yet increased serum levels of IP-10, IFNγ, MIP-1A and IL-12p40 [244]. In most trials, CpG ODN was administrated SQ or IV. The route of administration affected the nature/strength of the subsequent response and adverse effects in patients, with SC administration yielding higher serum cytokine levels and injection site reactions when compared to the IV route [244].

Based on animal studies showing that intra-tumoral injections of CpG ODN elicited a stronger protective response than did systemic delivery, the effect of intra-tumoral CpG ODN was also investigated [141, 245, 246]. CpG ODN delivered intra-tumorally to treat malignant skin tumors or lymphoma yielded promising results [247]. Most of those studies used K-type CpG 7909 (also referred as PF-3512676). Clinical trials confirmed that stronger long-term immunity and enhanced tumor regression was observed when CpG ODN was administrated intra-tumorally versus systemically. Hofmann et al. reported that half of all patients with basal cell carcinoma or melanoma had complete or partial tumor remission upon intra-tumoral administration of CpG ODN. Molenkamp et al. and Brody et al. reported that systemic tumor regression was induced by the improved generation of tumor-specific $CD8^+$ T cells in lymphoma and melanoma patients who received intra-tumoral CpG ODN [248, 249]. Kim et al. showed enhanced numbers of $CD123^+$ pDC accompanied by decreased numbers of $FoxP3^+$ T cells (Tregs) at the site of delivery when radiation therapy was combined with intra-tumoral CpG ODN, and tumor regression was observed even at distant sites in patients with lymphoma [250].

CpG ODN treatment has also been delivered in combination with conventional cancer treatments including checkpoint inhibitors. Intra-tumoral administration of CpG ODN increased the

response of cancer patients to PD-1 blockade and increased the frequency of tumor-specific $CD8^+$ T cells [143]. Moreover, CpG ODN given to cancer patients in combination with radiation and chemotherapy improved the uptake of tumor Ags released by dying cells and improved immune responses against tumor Ags [251, 252]. Studies of patients with malignant glioma and lymphoma support the prediction that local TLR9 can safely enhance the efficacy of conventional antitumor strategies [250, 253]. Local adverse events were generally mild to moderate and well tolerated. The most frequent systemic side effect was lymphopenia. CpG ODN improved the antitumor response and prolonged survival in a Phase II study targeting stage IIIb–IV NSCLC using platinum-based chemotherapy [254]. CpG ODN upregulated CD20 expression on malignant human B cells, improving the activity of CD20-specific MAb (Rituximab) and increasing the expression of IFN-inducible genes [255, 256].

The safety and activity of CpG ODN combined with rituximab was further evaluated in a phase II study of 23 patients with relapsed/refractory follicular lymphoma. Minimal adverse effects were observed, primarily grade 1–2 fatigue and erythema at the site of injection. There was a single episode of grade III menorrhagia. Nine patients responded with a significant increase in tumor infiltrating $CD8^+$ T cells, 11 achieved a partial response (PR) and 6 a complete response (CR) to therapy [257].

A number of clinical trials examined the utility of adding CpG ODN adjuvants to peptide-based vaccines targeting tumor-associated antigens (TAAs). Combining CpG ODN with the MART-1 peptide vaccine in patients with melanoma resulted in a tenfold increase in the frequency of Ag-specific $CD8^+$ T cells in a Phase I trial that did not assess tumor progression [185, 258]. Vaccination with the tumor Ag NY-ESO-1 plus CpG ODN improved the Ag-specific Ab response and enhanced $CD8^+$ T-cell responses in patients with melanoma, NSCLC, prostate, and breast cancer (when those tumors expressed NY-ESO-1) in trials that did not evaluate disease progression [139, 259, 260]. Addition of CpG ODN to a MAGE-3 vaccine enhanced anti-MAGE-3 Ab titers in a Phase I/II trial and when used in combination with high dose IL-12 controlled melanoma in >60% of patients and led to complete response in 19% of patients in a Phase II trial [261]. Vaccination with autologous tumor cells followed by a combination of CpG ODN, GM-CSF and then IFNγ led to a partial response (PR) or stable disease (SD) in 42% of patients with solid tumors [262]. In another trial, 22 patients with stage III–IV melanoma were vaccinated with a combination of MART-1, gp100, and tyrosinase peptides emulsified in Montanide® ISA-51 with CpG 7909 and GM-CSF. Over 2–7 months of follow up, 10% of these patients had PR and 38% SD. The median progression free survival time in

this study was 1.9 months and the median overall survival (OS) was 13.4 months. These outcomes were not superior to the therapeutic alternatives commonly used in patients with stage IV and recurrent melanoma [263, 264].

There was also a phase I/II trial involving a virus like nanoparticle that included A/D-type CpG ODN coupled to a Melan-A/MART-1 peptide (also referred as MelQbg10) tested in melanoma patients with stage II–IV disease. Results indicated the vaccine was safe and that it induced a Melan-A/MART-1-specific T-cell response in 66% patients. The inclusion of CpG ODN significantly increased the percentage of central memory T cells.

While patients whose tumor was surgically resected generally remained tumor free, vaccination was largely ineffective at preventing tumor metastases from progressing [48].

3.3 CpG ODN as Adjuvants for DNA Vaccines

DNA vaccines consist of a bacterial plasmid that encodes an Ag of interest [265]. When taken up by host cells, the plasmid coding region is transcribed, translated and the resulting protein presented to the immune system in the context of self MHC [266]. DNA vaccines offer the advantages of stability, low cost, ease of manufacture, and safety when compared to conventional protein-based vaccines [267, 268].

Interest in DNA vaccines spiked in the 1990s when plasmid DNA vaccination was shown to induce Ab and CTL responses against many different Ags in animal studies [269–273]. Over the next 20 years, animal models showed that DNA vaccines might be useful for the prophylaxis and treatment of cancer, infection, and allergy [274]. DNA vaccines were approved for veterinary use against West Nile Virus in horses and melanoma in dogs [275, 276]. To date, DNA vaccines have been evaluated in 72 Phase I, 20 Phase II, and 2 Phase III human trials. Unfortunately, they proved to be considerably less immunogenic in primates than most other species. While generally found to be safe, the magnitude of the humoral and cellular response they elicited in Man was substantially lower than competing protein-based strategies [269].

Considerable effort was therefore invested in improving the potency of DNA vaccines. One strategy involved increasing the amount of CpG DNA in the plasmid backbone to enhance immunogenicity [277, 278]. That approach showed promise in animal studies, with CpG-enriched plasmids inducing stronger T- and B-cell responses to various Ags [279]. Studies in pathogen and tumor challenged mice showed that these stronger responses provided greater protection [280, 281]. Yet such improvements were not observed when similar vaccines were tested in Man. It is likely that differences in TLR9 expression (particularly the broader range of cell types responsive to CpG in mice vs. Man) accounted for the greater immunogenicity of these vaccines in rodents.

96 clinical trials evaluating the safety and immunogenicity of DNA vaccines were initiated in the past decade (www.clinicaltrials.gov). Results from only a small fraction of those trials have been published. A phase IIb study involving a DNA vaccine targeting HPV 16 and 18 proteins for cervical intraepithelial neoplasia grade 2/3 (VGX-3100) reported that the vaccine was well tolerated and significantly increased Ag-specific $CD8^+$ T-cell responses [282]. Two phase III trials using VGX3100 are ongoing (NCT03185013 and NCT03721978). In a phase I trial using a different DNA vaccine targeting the same HPV Ags (referred as GX-118E), Ag-specific $CD8^+$ T-cell responses were enhanced in 8 out of 9 patients, virus was cleared from the circulation, and lesions completely regressed in 7 out of 9 individuals over 36 weeks follow-up [283]. A phase I trial involving a DNA vaccine encoding mammaglobin-A (Mam-A, a tumor-specific secretory protein over-expressed in 80% of human breast cancers) reported enhanced Ag-specific T-cell responses and improved progression free survival compared to the control group [284]. Thus, available data indicate that DNA vaccines promote the generation of Ag-specific T cells and do not cause major adverse events.

3.4 Safety

Preclinical studies in which mice were treated daily with high doses of CpG ODN (2.5 mg/kg) resulted in a number of serious adverse effects (AE) including liver toxicity, enlargement of the spleen and lymph nodes, extramedullary hematopoiesis, and systemic inflammation [285, 286]. In contrast, the lower doses typical of human trials (ranging from 1.5 to 15 μg/kg) administered weekly or monthly were well tolerated [163]. The possibility that immunostimulatory CpG ODN might trigger or worsen autoimmune disease and inflammatory syndromes was also investigated [287, 288]. Murine studies found that lymphocytes stimulated with CpG ODN were more resistant to undergoing apoptosis, an effect linked to the development of systemic lupus erythematosus (SLE) in some strains [289–291]. Moreover, B cells from lupus prone mice increased the production of pro-inflammatory cytokines and autoAbs by two- to three-fold after CpG stimulation, resulting in a 60% rise in serum IgG anti-DNA Ab titers (although disease was not accelerated or worsened in those animals) [292, 293]. A number of organ-specific autoimmune diseases are promoted by the Th1 immune responses elicited by CpG ODN. In an experimental encephalomyelitis model (mimicking multiple sclerosis), mice treated with CpG DNA and challenged with autoAg developed autoreactive Th1 effector cells and developed disease. Mice treated with autoAg alone remained disease free [294, 295]. In another study, CpG DNA co-administered with a Chlamydia-derived Ag induced an autoimmune myocarditis [296]. CpG ODN also increased the susceptibility of mice to arthritis [297]. These preclinical findings suggested that CpG motifs had the potential to promote autoreactivity.

In clinical trials involving thousands of human participants, the most common reactions induced by CpG-containing vaccines were minor and localized to the injection site, consisting of erythema, edema, inflammation, and pain. Minor systemic flu-like symptoms (headache, rigors, pyrexia, nausea, and fever) were also observed [135, 144]. Such symptoms generally arose within 24 h of administration and lasted for less than 2 days. When patients received multiple doses of CpG adjuvanted vaccines, the likelihood of injection site reactions rose although their severity remained mild to moderate [231]. No major AEs occurred in healthy recipients of CpG-adjuvanted vaccines [135, 162].

The possibility that CpG stimulation might increase the risk of autoimmune disease in humans was examined in multiple studies. Most found that serum autoAb levels against double stranded DNA (dsDNA), rheumatoid factor, thyroglobulin, and nuclear Abs did not change nor did symptoms of autoimmune disease arise [217, 263, 298–301]. In a study of CpG-adjuvanted Engerix-B®, 1 out of 56 healthy volunteers developed increased anti-dsDNA Abs at week 6 and these returned to baseline by week 24 [181]. Elevated antinuclear antibody (ANA) and anti-dsDNA Ab levels were found in 10% of patients that received AMA1-C1/Alhydrogel® plus CpG ODN but these also returned to baseline within 6 weeks [217]. Thus, it appears that CpG ODN adjuvants are safe and well tolerated in normal individuals.

In contrast to their safety in normal volunteers, serious AEs were reported in studies of HIV-infected and cancer patients treated with CpG ODN. Whether these adverse reactions were caused by vaccination or were secondary to the underlying diseases (such as the heart attack observed in one subject in one trial) is uncertain. 10% of HIV-infected patients vaccinated with Engerix-B® plus CpG 7909 developed a severe AE. Yet neither the nature nor timing of those events (occurring 2–16 weeks post-vaccination) were consistent with their being CpG related [231]. 14% of patients in the same study developed elevated serum anti-ds DNA autoAb levels although no clinical symptoms of autoimmunity were observed [231]. An increase in anti-dsDNA Abs was found in 50% of melanoma patients after four vaccinations with Melan-A, Montanide® ISA-51, and CpG 7909, yet none developed clinical signs of autoimmune disease [185]. When 10–40 mg of CpG ODN was administrated intracerebrally to glioblastoma patients, treatment-related general and partial seizures developed in 10% of patients [302]. 2% of those patients also developed grade 3–4 hematologic events [302]. In a study of 50 patients with refractory B-cell non-Hodgkin's lymphoma, one case of Sjorgen's syndrome was reported. Symptoms possibly related to the development of a paraneoplastic autoimmune disease included inflammation of the salivary glands and kerato-conjunctivitis sicca after treatment with rituximab plus CpG 7909 [256]. The ability to draw definitive

conclusions concerning CpG ODN safety from these tumor vaccine trials is compromised by several deficiencies, including (1) low patient number (leaving most trials underpowered), (2) short duration (providing insufficient temporal follow up to determine whether therapy altered tumor growth) and (3) inclusion of patients with different types and severity of cancer (preventing intra-group comparisons). Thus, the possibility that CpG ODN may cause or worsen autoimmune disease in patients with preexisting conditions has not been resolved.

4 Conclusion

CpG ODN trigger the innate immune system by binding to intracellular cognate TLR9 receptors. The resultant immune response is characterized by the production of pro-inflammatory Th1 cytokines and chemokines that support the induction of an adaptive immune response to co-delivered Ag. The diverse effects of CpG ODN support their ability to act as vaccine adjuvants in healthy individuals and those with compromised immune systems [181, 231, 232].

CpG ODN accelerate and increase the titer, affinity, and persistence of protective Abs against co-administered Ag while improving cellular immunity [182, 183, 212]. FDA approval of the HEPLISAV-B® vaccine targeting Hepatitis B speaks to the success of CpG as a vaccine adjuvant [303].

Less definitive conclusions can be drawn concerning the use of CpG ODN in cancer vaccines. In most studies, CpG DNA increased the immunogenicity of co-administered peptide vaccines. Patients who received adjuvanted cancer vaccines generated stronger Ag-specific serum Ab, $CD8^+$ and $CD4^+$ T-cell responses when compared to peptide vaccines alone [139, 185, 258–260]. Antitumor immunity also arose more rapidly in patients vaccinated with CpG adjuvanted vaccines. However, these immune responses rarely led to a significant improvement in clinical outcome [263, 264].

The success of CpG adjuvanted vaccines targeting infectious agents but not tumors suggests that the magnitude of the immune response needed to eliminate large established tumors exceeds that required to halt an ongoing infection. The current generation of cancer vaccine plus CpG ODN combinations does not induce immune responses strong enough to eradicate established tumors. Data from animal models suggests that CpG adjuvanted tumor vaccines will be more effective if administered early in the disease process (rather than waiting for all conventional therapies to fail), as they are more effective against small/slow growing tumors [304]. It also appears that intra-tumoral delivery will be more successful than systemic administration [248, 249].

Treatment of advanced tumors improved with the discovery of checkpoint inhibitors. Results from preclinical and clinical studies using CpG ODN in combination with checkpoint inhibitors (and other treatment modalities such as monoclonal antibodies, chemo/radiotherapy) suggest the response rate may be further increased [254–256].

CpG ODN are also be combined with surgery to prevent tumor recurrence and metastasis. In murine models, CpG adjuvanted tumor vaccines prevented metastatic spread after removal of the primary cancer. Thus, multiple strategies for harnessing the immunomodulatory properties of CpG ODN are being pursued in the clinic. Additional progress may accompany the testing of newer classes of CpG ODN, whose activity in humans is still poorly understood.

References

1. Julier Z, Park AJ, Briquez PS et al (2017) Promoting tissue regeneration by modulating the immune system. Acta Biomater 53:13–28
2. Klein U, la-Favera R (2008) Germinal centres: role in B-cell physiology and malignancy. Nat Rev Immunol 8:22–33
3. Wienands J, Engels N (2016) Control of memory B cell responses by extrinsic and intrinsic mechanisms. Immunol Lett 178:27–30
4. Engels N, Wienands J (2018) Memory control by the B cell antigen receptor. Immunol Rev 283:150–160
5. Schmidlin H, Diehl SA, Blom B (2009) New insights into the regulation of human B-cell differentiation. Trends Immunol 30:277–285
6. Sarkander J, Hojyo S, Tokoyoda K (2016) Vaccination to gain humoral immune memory. Clin Transl Immunology 5:e120
7. Cockburn IA, Chen YC, Overstreet MG et al (2010) Prolonged antigen presentation is required for optimal CD8+ T cell responses against malaria liver stage parasites. PLoS Pathog 6:e1000877
8. Vezys V, Yates A, Casey KA et al (2009) Memory CD8 T-cell compartment grows in size with immunological experience. Nature 457:196–199
9. Shah RR, Hassett KJ, Brito LA (2017) Overview of vaccine adjuvants: introduction, history, and current status. Methods Mol Biol 1494:1–13
10. Dresser DW (1961) Effectiveness of lipid and lipidophilic substances as adjuvants. Nature 191:1169–1171
11. Sarkar I, Garg R, van den Hurk v DL (2019) Selection of adjuvants for vaccines targeting specific pathogens. Expert Rev Vaccines 18:505–521
12. Lemaitre B, Nicolas E, Michaut L et al (1996) The dorsoventral regulatory gene cassette spatzle/toll/cactus controls the potent antifungal response in drosophila adults. Cell 86:973–983
13. Poltorak A, He X, Smirnova I et al (1998) Defective LPS signaling in C3H/HeJ and C57BL/10ScCr mice: mutations in Tlr4 gene. Science 282:2085–2088
14. Janeway CA Jr, Medzhitov R (2002) Innate immune recognition. Annu Rev Immunol 20:197–216
15. Xiao H, Peng Y, Hong Y et al (2013) Local administration of TLR ligands rescues the function of tumor-infiltrating CD8 T cells and enhances the antitumor effect of lentivector immunization. J Immunol 190:5866–5873
16. Hemmi H, Takeuchi O, Kawai T et al (2000) A toll-like receptor recognizes bacterial DNA. Nature 408:740–745
17. O'Neill LA, Golenbock D, Bowie AG (2013) The history of toll-like receptors - redefining innate immunity. Nat Rev Immunol 13:453–460
18. Hornung V, Rothenfusser S, Britsch S et al (2002) Quantitative expression of toll-like receptor 1–10 mRNA in cellular subsets of human peripheral blood mononuclear cells and sensitivity to CpG oligodeoxynucleotides. J Immunol 168:4531–4537

19. Kanzler H, Barrat FJ, Hessel EM et al (2007) Therapeutic targeting of innate immunity with toll-like receptor agonists and antagonists. Nat Med 13:552–559
20. Akira S, Takeda K (2004) Toll-like receptor signalling. Nat Rev Immunol 4:499–511
21. Lorne E, Dupont H, Abraham E (2010) Toll-like receptors 2 and 4: initiators of non-septic inflammation in critical care medicine? Intensive Care Med 36:1826–1835
22. Redecke V, Hacker H, Datta SK et al (2004) Cutting edge: activation of toll-like receptor 2 induces a Th2 immune response and promotes experimental asthma. J Immunol 172:2739–2743
23. Dabbagh K, Dahl ME, Stepick-Biek P et al (2002) Toll-like receptor 4 is required for optimal development of Th2 immune responses: role of dendritic cells. J Immunol 168:4524–4530
24. Farrokhi S, Abbasirad N, Movahed A et al (2017) TLR9-based immunotherapy for the treatment of allergic diseases. Immunotherapy 9:339–346
25. Shirota H, Sano K, Kikuchi T et al (2000) Regulation of T-helper type 2 cell and airway eosinophilia by transmucosal coadministration of antigen and oligodeoxynucleotides containing CpG motifs. Am J Respir Cell Mol Biol 22:176–182
26. Shirota H, Sano K, Kikuchi T et al (2000) Regulation of murine airway eosinophilia and Th2 cells by antigen-conjugated CpG oligodeoxynucleotides as a novel antigen-specific immunomodulator. J Immunol 164:5575–5582
27. Kim YH, Girardi M, Duvic M et al (2010) Phase I trial of a toll-like receptor 9 agonist, PF-3512676 (CPG 7909), in patients with treatment-refractory, cutaneous T-cell lymphoma. J Am Acad Dermatol 63:975–983
28. Latz E, Schoenemeyer A, Visintin A et al (2004) TLR9 signals after translocating from the ER to CpG DNA in the lysosome. Nat Immunol 5:190–198
29. Suzuki Y, Wakita D, Chamoto K et al (2004) Liposome-encapsulated CpG oligodeoxynucleotides as a potent adjuvant for inducing type 1 innate immunity. Cancer Res 64:8754–8760
30. Kadowaki N, Ho S, Antonenko S et al (2001) Subsets of human dendritic cell precursors express different toll-like receptors and respond to different microbial antigens. J Exp Med 194:863–869
31. Bernasconi NL, Onai N, Lanzavecchia A (2003) A role for toll-like receptors in acquired immunity: up-regulation of TLR9 by BCR triggering in naive B cells and constitutive expression in memory B cells. Blood 101:4500–4504
32. Ewald SE, Lee BL, Lau L et al (2008) The ectodomain of toll-like receptor 9 is cleaved to generate a functional receptor. Nature 456:658–662
33. Park B, Brinkmann MM, Spooner E et al (2008) Proteolytic cleavage in an endolysosomal compartment is required for activation of Toll-like receptor 9. Nat Immunol 9:1407–1414
34. Ewald SE, Engel A, Lee J et al (2011) Nucleic acid recognition by Toll-like receptors is coupled to stepwise processing by cathepsins and asparagine endopeptidase. J Exp Med 208:643–651
35. Sepulveda FE, Maschalidi S, Colisson R et al (2009) Critical role for asparagine endopeptidase in endocytic Toll-like receptor signaling in dendritic cells. Immunity 31:737–748
36. Kumagai Y, Takeuchi O, Akira S (2008) TLR9 as a key receptor for the recognition of DNA. Adv Drug Deliv Rev 60:795–804
37. Klaschik S, Tross D, Klinman DM (2009) Inductive and suppressive networks regulate TLR9-dependent gene expression *in vivo*. J Leukoc Biol 85:788–795
38. Saitoh S, Miyake K (2009) Regulatory molecules required for nucleotide-sensing toll-like receptors. Immunol Rev 227:32–43
39. Klaschik S, Tross D, Shirota H et al (2010) Short- and long-term changes in gene expression mediated by the activation of TLR9. Mol Immunol 47:1317–1324
40. Mutwiri GK, Nichani AK, Babiuk S et al (2004) Strategies for enhancing the immunostimulatory effects of CpG oligodeoxynucleotides. J Control Release 97:1–17
41. Verthelyi D, Ishii KJ, Gursel M et al (2001) Human peripheral blood cells differentially recognize and respond to two distinct CPG motifs. J Immunol 166:2372–2377
42. Hartmann G, Battiany J, Poeck H et al (2003) Rational design of new CpG oligonucleotides that combine B cell activation with high IFN-alpha induction in plasmacytoid dendritic cells. Eur J Immunol 33:1633–1641
43. Krug A, Towarowski A, Britsch S et al (2001) Toll-like receptor expression reveals CpG DNA as a unique microbial stimulus for plasmacytoid dendritic cells which synergizes with CD40 ligand to induce high amounts of IL-12. Eur J Immunol 31:3026–3037
44. Guiducci C, Ott G, Chan JH et al (2006) Properties regulating the nature of the

plasmacytoid dendritic cell response to Toll-like receptor 9 activation. J Exp Med 203:1999–2008

45. Honda K, Ohba Y, Yanai H et al (2005) Spatiotemporal regulation of MyD88-IRF-7 signalling for robust type-I interferon induction. Nature 434:1035–1040
46. Storni T, Ruedl C, Schwarz K et al (2004) Nonmethylated CG motifs packaged into virus-like particles induce protective cytotoxic T cell responses in the absence of systemic side effects. J Immunol 172:1777–1785
47. Goldinger SM, Dummer R, Baumgaertner P et al (2012) Nano-particle vaccination combined with TLR-7 and -9 ligands triggers memory and effector CD8(+) T-cell responses in melanoma patients. Eur J Immunol 42:3049–3061
48. Speiser DE, Schwarz K, Baumgaertner P et al (2010) Memory and effector CD8 T-cell responses after nanoparticle vaccination of melanoma patients. J Immunother 33:848–858
49. Marshall JD, Fearon K, Abbate C et al (2003) Identification of a novel CpG DNA class and motif that optimally stimulate B cell and plasmacytoid dendritic cell functions. J Leukoc Biol 73:781–792
50. Vollmer J, Weeratna R, Payette P et al (2004) Characterization of three CpG oligodeoxynucleotide classes with distinct immunostimulatory activities. Eur J Immunol 34:251–262
51. Vollmer J, Krieg AM (2009) Immunotherapeutic applications of CpG oligodeoxynucleotide TLR9 agonists. Adv Drug Deliv Rev 61:195–204
52. Samulowitz U, Weber M, Weeratna R et al (2010) A novel class of immune-stimulatory CpG oligodeoxynucleotides unifies high potency in type I interferon induction with preferred structural properties. Oligonucleotides 20:93–101
53. Davis HL, Weeranta R, Waldschmidt TJ et al (1998) CpG DNA is a potent enhancer of specific immunity in mice immunized with recombinant hepatitis B surface antigen. J Immunol 160:870–876
54. Kobayashi H, Horner AA, Takabayashi K et al (1999) Immunostimulatory DNA pre-priming: a novel approach for prolonged Th1-biased immunity. Cell Immunol 198:69–75
55. Krieg AM, Yi A, Matson S et al (1995) CpG motifs in bacterial DNA trigger direct B-cell activation. Nature 374:546–548
56. Hartmann G, Weeratna RD, Ballas ZK et al (2000) Delineation of a CpG phosphorothioate oligodeoxynucleotide for activating primate immune responses in vitro and *in vivo*. J Immunol 164:1617–1624
57. Ruprecht CR, Lanzavecchia A (2006) Toll-like receptor stimulation as a third signal required for activation of human naive B cells. Eur J Immunol 36:810–816
58. Huggins J, Pellegrin T, Felgar RE et al (2007) CpG DNA activation and plasma-cell differentiation of. Blood 109:1611–1619
59. Jiang W, Lederman MM, Harding CV et al (2007) TLR9 stimulation drives naive B cells to proliferate and to attain enhanced antigen presenting function. Eur J Immunol 37:2205–2213
60. Eckl-Dorna J, Batista FD (2009) BCR-mediated uptake of antigen linked to TLR9 ligand stimulates B-cell proliferation and antigen-specific plasma cell formation. Blood 113:3969–3977
61. Wang Z, Karras JG, Colarusso TP et al (1997) Unmethylated CpG motifs protect murine B lymphocytes against Fas-mediated apoptosis. Cell Immunol 180:162–167
62. Kerkmann M, Rothenfusser S, Hornung V et al (2003) Activation with CpG-A and CpG-B oligonucleotides reveals two distinct regulatory pathways of type I IFN synthesis in human plasmacytoid dendritic cells. J Immunol 170:4465–4474
63. Krieg AM (2002) CpG motifs in bacterial DNA and their immune effects. Annu Rev Immunol 20:709–760
64. Jakob T, Walker PS, Krieg AM et al (1998) Activation of cutaneous dendritic cells by CpG containing oligodeoxynucleotides: a role for dendritic cells in the augmentation of Th1 responses by immunostimulatory DNA. J Immunol 161:3042–3049
65. Sparwasser T, Koch E, Vabulas RM et al (1998) Bacterial DNA and immunostimulatory CpG oligonucleotides trigger maturation and activation of murine dendritic cells. Eur J Immunol 28:2045–2054
66. Ban E, Dupre L, Hermann E et al (2000) CpG motifs induce Langerhans cell migration *in vivo*. Int Immunol 12:737–745
67. Behboudi S, Chao D, Klenerman P et al (2000) The effects of DNA containing CpG motif on dendritic cells. Immunology 99:361–366
68. Hartmann G, Krieg AM (1999) CpG DNA and LPS induce distinct patterns of activation in human monocytes. Gene Ther 6:893–903
69. Pichyangkul S, Yongvanitchit K, Kum-arb U et al (2001) Whole blood cultures to assess the immunostimulatory activities of CpG oligodeoxynucleotides. J Immunol Methods 247:83–94

70. Stacey KJ, Sweet MJ, Hume DA (1996) Macrophages ingest and are activated by bacterial DNA. J Immunol 157:2116–2120
71. Sato T, Shimosato T, Ueda A et al (2015) Intrapulmonary delivery of CpG microparticles eliminates lung tumors. Mol Cancer Ther 14:2198–2205
72. Sun S, Zhang X, Tough DF, Sprent J (1998) Type I interferon-mediated stimulation of T cells by CpG DNA. J Exp Med 188:2335–2342
73. Bendigs S, Salzer U, Lipford GB et al (1999) CpG-oligodeoxynucleotides co-stimulate primary T cells in the absence of antigen-presenting cells. Eur J Immunol 29:1209–1218
74. Kranzer K, Bauer M, Lipford GB et al (2000) CpG-oligodeoxynucleotides enhance T-cell receptor-triggered interferon-gamma production and up-regulation of CD69 via induction of antigen-presenting cell-derived interferon type I and interleukin-12. Immunology 99:170–178
75. Sparwasser T, Vabulas RM, Villmow B et al (2000) Bacterial CpG DNA activates dendritic cells *in vivo*: T helper cell-independent cytotoxic T cell responses to soluble proteins. Eur J Immunol 30:3591–3597
76. Vabulas RM, Pircher H, Lipford GB et al (2000) CpG-DNA activates *in vivo* T cell epitope presenting dendritic cells to trigger protective anti-viral cytotoxic T cell responses. J Immunol 164:2372–2378
77. Chu RS, Targoni OS, Krieg AM et al (1997) CpG oligodeoxynucleotides act as adjuvants that switch on T helper 1 (Th1) immunity. J Exp Med 186:1623–1631
78. Sun S, Zhang X, Tough D et al (2000) Multiple effects of immunostimulatory DNA on T cells and the role of type I interferons. Springer Semin Immunopathol 22:77–84
79. Tascon RE, Ragno S, Lowrie DB et al (2000) Immunostimulatory bacterial DNA sequences activate dendritic cells and promote priming and differentiation of CD8+ T cells. Immunology 99:1–7
80. Lipford GB, Bauer M, Blank C et al (1997) CpG-containing synthetic oligonucleotides promote B and cytotoxic T cell responses to protein antigen: a new class of vaccine adjuvants. Eur J Immunol 27:2340–2344
81. Yang WC, Sun HW, Sun HQ et al (2018) Intranasal immunization with immunodominant epitope peptides derived from HpaA conjugated with CpG adjuvant protected mice against helicobacter pylori infection. Vaccine 36:6301–6306
82. Hayashi T, Momota M, Kuroda E et al (2018) DAMP-inducing adjuvant and PAMP adjuvants parallelly enhance protective Type-2- anD-type-1 immune responses to influenza split vaccination. Front Immunol 9:2619
83. Yu P, Yan J, Wu W et al (2018) A CpG oligodeoxynucleotide enhances the immune response to rabies vaccination in mice. Virol J 15:174
84. Hensel MT, Marshall JD, Dorwart MR et al (2017) Prophylactic herpes simplex virus 2 (HSV-2) vaccines Adjuvanted with stable emulsion and toll-like receptor 9 agonist induce a robust HSV-2-specific cell-mediated immune response, protect against symptomatic disease, and reduce the latent viral reservoir. J Virol 91:e02257-16
85. Reeman S, Gates AJ, Pulford DJ et al (2017) Protection of mice from lethal vaccinia virus infection by vaccinia virus protein subunits with a CpG adjuvant. Viruses 9:378
86. Da Silva DM, Skeate JG, Chavez-Juan E et al (2019) Therapeutic efficacy of a human papillomavirus type 16 E7 bacterial exotoxin fusion protein adjuvanted with CpG or GPI-0100 in a preclinical mouse model for HPV-associated disease. Vaccine 37:2915–2924
87. Yang Y, Che Y, Zhao Y et al (2019) Prevention and treatment of cervical cancer by a single administration of human papillomavirus peptide vaccine with CpG oligodeoxynucleotides as an adjuvant *in vivo*. Int Immunopharmacol 69:279–288
88. McCluskie MJ, Davis HL (1998) CpG DNA is a potent enhancer of systemic and mucosal immune responses against hepatitis B surface antigen with intranasal administration to mice. J Immunol 161:4463–4466
89. von HC, Mariotti S, Teloni R et al (2001) The adjuvant effect of synthetic oligodeoxynucleotide containing CpG motif converts the anti-Haemophilus influenzae type b glycoconjugates into efficient anti-polysaccharide and anti-carrier polyvalent vaccines. Vaccine 19:3058–3066
90. Kovarik J, Bozzotti P, Love-Homan L et al (1999) CpG oligodeoxynucleotides can circumvent the Th2 polarization of neonatal responses to vaccines but may fail to fully redirect Th2 responses established by neonatal priming. J Immunol 162:1611–1617
91. Eastcott JW, Holmberg CJ, Dewhirst FE et al (2001) Oligonucleotide containing CpG motifs enhances immune response to mucosally or systemically administered tetanus toxoid. Vaccine 19:1636–1642

92. Al-Mariri A, Tibor A, Mertens P et al (2001) Protection of BALB/c mice against *Brucella abortus* 544 challenge by vaccination with bacterioferritin or P39 recombinant proteins with CpG oligodeoxynucleotides as adjuvant. Infect Immun 69:4816–4822
93. xie H, Gursel I, Ivins BE et al (2005) CpG oligodeoxynucleotides adsorbed onto polylactide-co-glycolide microparticles improve the immunogenicity and protective activity of the licensed anthrax vaccine. Infect Immun 73:828–833
94. Fogg CN, Americo JL, Lustig S et al (2007) Adjuvant-enhanced antibody responses to recombinant proteins correlates with protection of mice and monkeys to orthopoxvirus challenges. Vaccine 25:2787–2799
95. Mendez S, Tabbara K, Belkaid Y et al (2003) Coinjection with CpG-containing immunostimulatory oligodeoxynucleotides reduces the pathogenicity of a live vaccine against cutaneous Leishmaniasis but maintains its potency and durability. Infect Immun 71:5121–5129
96. Klinman DM, Currie D, Lee G et al (2007) Systemic but not mucosal immunity induced by AVA prevents inhalational anthrax. Microbes Infect 9:1478–1483
97. Klinman DM, xie H, Little SF et al (2004) CpG oligonucleotides improve the protective immune response induced by the anthrax vaccination of rhesus macaques. Vaccine 22:2881–2886
98. Tengvall S, Lundqvist A, Eisenberg RJ et al (2006) Mucosal administration of CpG oligodeoxynucleotide elicits strong CC and CXC chemokine responses in the vagina and serves as a potent Th1-tilting adjuvant for recombinant gD2 protein vaccination against genital herpes. J Virol 80:5283–5291
99. Gallichan WS, Woolstencroft RN, Guarasci T et al (2001) Intranasal immunization with CpG oligodeoxynucleotides as an adjuvant dramatically increases IgA and protection against herpes simplex virus-2 in the genital tract. J Immunol 166:3451–3457
100. Lin YL, Chow YH, Huang LM et al (2018) A CpG-adjuvanted intranasal enterovirus 71 vaccine elicits mucosal and systemic immune responses and protects human SCARB2-transgenic mice against lethal challenge. Sci Rep 8:10713
101. Nesburn AB, Ramos TV, Zhu X et al (2005) Local and systemic B cell and Th1 responses induced following ocular mucosal delivery of multiple epitopes of herpes simplex virus type 1 glycoprotein D together with cytosine-phosphate-guanine adjuvant. Vaccine 23:873–883
102. Huang CF, Wang CC, Wu TC et al (2008) Neonatal sublingual vaccination with salmonella proteins and adjuvant cholera toxin or CpG oligodeoxynucleotides induces mucosal and systemic immunity in mice. J Pediatr Gastroenterol Nutr 46:262–271
103. McCluskie MJ, Weeratna RD, Krieg AM et al (2000) CpG DNA is an effective oral adjuvant to protein antigens in mice. Vaccine 19:950–957
104. Kayraklioglu N, Scheiermann J, Alvord WG et al (2017) Effect of calcium carbonate encapsulation on the activity of orally administered CpG oligonucleotides. Mol Ther Nucleic Acids 8:243–249
105. Miller RA (1989) The cell biology of aging: immunologic models. J Gerontol 44:B4
106. Thoman ML, Weigle WO (1989) The cellular and subcellular bases of Immunosenescence. Adv Immunol 46:221–261
107. Qin W, Jiang J, Chen Q et al (2004) CpG ODN enhances immunization effects of hepatitis B vaccine in aged mice. Cell Mol Immunol 1:148–152
108. Siegrist CA, Pihlgren M, Tougne C et al (2004) Co-administration of CpG oligonucleotides enhances the late affinity maturation process of human anti-hepatitis B vaccine response. Vaccine 23:615–622
109. Sen G, Chen Q, Snapper CM (2006) Immunization of aged mice with a pneumococcal conjugate vaccine combined with an unmethylated CpG-containing oligodeoxynucleotide restores defective immunoglobulin G antipolysaccharide responses and specific CD4+-T-cell priming to young adult levels. Infect Immun 74:2177–2186
110. Fukuyama Y, Ikeda Y, Ohori J et al (2015) A molecular mucosal adjuvant to enhance immunity against pneumococcal infection in the elderly. Immune Netw 15:9–15
111. Brazolot Millan CL, Weeratna R, Krieg AM et al (1998) CpG DNA can induce strong Th1 humoral and cell-mediated immune responses against hepatitis B surface antigen in young mice. Proc Natl Acad Sci U S A 95:15553–15558
112. van Haren SD, Ganapathi L, Bergelson I et al (2016) In vitro cytokine induction by TLR-activating vaccine adjuvants in human blood varies by age and adjuvant. Cytokine 83:99–109
113. Savransky V, Shearer JD, Gainey MR et al (2017) Correlation between anthrax lethal toxin neutralizing antibody levels and survival in Guinea pigs and nonhuman primates

vaccinated with the AV7909 anthrax vaccine candidate. Vaccine 35:4952–4959

114. Mapletoft JW, Oumouna M, Townsend HG et al (2006) Formulation with CpG oligodeoxynucleotides increases cellular immunity and protection induced by vaccination of calves with formalin-inactivated bovine respiratory syncytial virus. Virology 353:316–323
115. Muangthai K, Tankaew P, Varinrak T et al (2018) Intranasal immunization with a recombinant outer membrane protein H based Haemorrhagic septicemia vaccine in dairy calves. J Vet Med Sci 80:68–76
116. Linghua Z, Xingshan T, Fengzhen Z (2008) *In vivo* oral administration effects of various oligodeoxynucleotides containing synthetic immunostimulatory motifs in the immune response to pseudorabies attenuated virus vaccine in newborn piglets. Vaccine 26:224–233
117. Linghua Z, Xingshan T, Fengzhen Z (2007) Vaccination with Newcastle disease vaccine and CpG oligodeoxynucleotides induces specific immunity and protection against Newcastle disease virus in SPF chicken. Vet Immunol Immunopathol 115:216–222
118. Singh SM, Alkie TN, Hodgins DC et al (2015) Systemic immune responses to an inactivated, whole H9N2 avian influenza virus vaccine using class B CpG oligonucleotides in chickens. Vaccine 33:3947–3952
119. Yuan F, Chu Y, Qi L et al (2017) Immunoprotection induced by CpG-ODN/poly(I:C) combined with recombinant gp90 protein in chickens against reticuloendotheliosis virus infection. Antivir Res 147:1–10
120. Lopez AM, Hecker R, Mutwiri G et al (2006) Formulation with CpG ODN enhances antibody responses to an equine influenza virus vaccine. Vet Immunol Immunopathol 114:103–110
121. Klier J, Lehmann B, Fuchs S et al (2015) Nanoparticulate CpG immunotherapy in RAO-affected horses: phase I and IIa study. J Vet Intern Med 29:286–293
122. Klier J, Fuchs S, May A et al (2012) A nebulized gelatin nanoparticle-based CpG formulation is effective in immunotherapy of allergic horses. Pharm Res 29:1650–1657
123. Ren J, Sun L, Yang L et al (2010) A novel canine favored CpG oligodeoxynucleotide capable of enhancing the efficacy of an inactivated aluminum-adjuvanted rabies vaccine of dog use. Vaccine 28:2458–2464
124. Verthelyi D, Kenney RT, Seder RA et al (2002) CpG oligodeoxynucleotides as vaccine adjuvants in primates. J Immunol 168:1659–1663
125. Davis HL, Suparto II, Weeratna RR et al (2000) CpG DNA overcomes hyporesponsiveness to hepatitis B vaccine in orangutans. Vaccine 18:1920–1924
126. Jones TR, Obaldia N III, Gramzinski RA et al (1999) Synthetic oligodeoxynucleotides containing CpG motifs enhance immunogenicity of a peptide malaria vaccine in Aotus monkeys. Vaccine 17:3065–3071
127. Verthelyi D, Gursel M, Kenney RT et al (2003) CpG oligodeoxynucleotides protect normal and SIV-infected macaques from Leishmania infection. J Immunol 170:4717–4723
128. Verthelyi D, Wang VW, Lifson JD et al (2004) CpG oligodeoxynucleotides improve the response to hepatitis B immunization in healthy and SIV-infected rhesus macaques. AIDS 18:1003–1008
129. Diamant EP, Schechter C, Hodes DS et al (1993) Immunogenicity of hepatitis B vaccine in human immunodeficiency virus-infected children. Pediatr Infect Dis J 12:877–878
130. Wong EK, Bodsworth NJ, Slade MA et al (1996) Response to hepatitis B vaccination in a primary care setting: influence of HIV infection, CD4+ lymphocyte count and vaccination schedule. Int J STD AIDS 7:490–494
131. Pacanowski J, Kahi S, Baillet M et al (2001) Reduced blood $CD123^+$ (lymphoid) and $CD11c^+$ (myeloid) dendritic cell numbers in primary HIV-1 infection. Blood 98:3016–3021
132. Stern BV, Boehm BO, Tary-Lehmann M (2002) Vaccination with tumor peptide in CpG adjuvant protects via IFN-gamma-dependent CD4 cell immunity. J Immunol 168:6099–6105
133. Sandler AD, Chihara H, Kobayashi G et al (2003) CpG oligonucleotides enhance the tumor antigen-specific immune response of a granulocyte macrophage colony-stimulating factor-based vaccine strategy in neuroblastoma. Cancer Res 63:394–399
134. Wille-Reece U, Flynn BJ, Lore K et al (2006) Toll-like receptor agonists influence the magnitude and quality of memory T cell responses after prime-boost immunization in nonhuman primates. J Exp Med 203:1249–1258
135. Krieg AM (2006) Therapeutic potential of toll-like receptor 9 activation. Nat Rev Drug Discov 5:471–484
136. Rothenfusser S, Hornung V, Ayyoub M et al (2004) CpG-A and CpG-B oligonucleotides differentially enhance human peptide-specific primary and memory CD8+ T-cell responses in vitro. Blood 103:2162–2169

137. Baines J, Celis E (2003) Immune-mediated tumor regression induced by CpG-containing oligodeoxynucleotides. Clin Cancer Res 9:2693–2700
138. Tighe H, Takabayashi K, Schwartz D et al (2000) Conjugation of immunostimulatory DNA to the short ragweed allergen amb a 1 enhances its immunogenicity and reduces its allergenicity. J Allergy Clin Immunol 106:124–134
139. Fourcade J, Kudela P, ndrade Filho PA et al (2008) Immunization with analog peptide in combination with CpG and montanide expands tumor antigen-specific CD8+ T cells in melanoma patients. J Immunother 31:781–791
140. Mukherjee P, Pathangey LB, Bradley JB et al (2007) MUC1-specific immune therapy generates a strong anti-tumor response in a MUC1-tolerant colon cancer model. Vaccine 25:1607–1618
141. Shirota Y, Shirota H, Klinman DM (2012) Intratumoral injection of CpG oligonucleotides induces the differentiation and reduces the immunosuppressive activity of myeloid-derived suppressor cells. J Immunol 188:1592–1599
142. Sato-Kaneko F, Yao S, Ahmadi A et al (2017) Combination immunotherapy with TLR agonists and checkpoint inhibitors suppresses head and neck cancer. JCI Insight 2:e93397
143. Wang S, Campos J, Gallotta M et al (2016) Intratumoral injection of a CpG oligonucleotide reverts resistance to PD-1 blockade by expanding multifunctional CD8+ T cells. Proc Natl Acad Sci U S A 113:E7240–E7249
144. Shirota H, Klinman DM (2014) Recent progress concerning CpG DNA and its use as a vaccine adjuvant. Expert Rev Vaccines 13:299–312
145. Sacks T, Klinman DM (1997) Long-term effect of primary immunization on subsequent immune responsiveness. Cell Immunol 177:162–168
146. Cho HJ, Takabayashi K, Cheng PM et al (2000) Immunostimulatory DNA-based vaccines induce cytotoxic lymphocyte activity by a T-helper cell-independent mechanism. Nat Biotechnol 18:509–514
147. Heit A, Schmitz F, O'Keeffe M et al (2005) Protective CD8 T cell immunity triggered by CpG-protein conjugates competes with the efficacy of live vaccines. J Immunol 174:4373–4380
148. Shirota H, Klinman DM (2011) CpG-conjugated apoptotic tumor cells elicit potent tumor-specific immunity. Cancer Immunol Immunother 60:659–669
149. Shirota H, Sano K, Hirasawa N et al (2001) Novel roles of CpG oligodeoxynucleotides as a leader for the sampling and presentation of CpG-tagged antigen by dendritic cells. J Immunol 167:66–74
150. Shirota H, Sano K, Hirasawa N et al (2002) B cells capturing antigen conjugated with CpG oligodeoxynucleotides induce Th1 cells by elaborating IL-12. J Immunol 169:787–794
151. Klinman DM, Sato T, Shimosato T (2016) Use of nanoparticles to deliver immunomodulatory oligonucleotides. Wiley Interdiscip Rev Nanomed Nanobiotechnol 8:631–637
152. Wilson KD, Tam YK (2009) Lipid-based delivery of CpG oligodeoxynucleotides for cancer immunotherapy. Expert Rev Clin Pharmacol 2:181–193
153. Hanagata N (2012) Structure-dependent immunostimulatory effect of CpG oligodeoxynucleotides and their delivery system. Int J Nanomedicine 7:2181–2195
154. Heffernan MJ, Murthy N (2005) Polyketal nanoparticles: a new pH-sensitive biodegradable drug delivery vehicle. Bioconjug Chem 16:1340–1342
155. Fiore VF, Lofton MC, Roser-Page S et al (2010) Polyketal microparticles for therapeutic delivery to the lung. Biomaterials 31:810–817
156. Tada R, Muto S, Iwata T et al (2017) Attachment of class B CpG ODN onto DOTAP/DC-chol liposome in nasal vaccine formulations augments antigen-specific immune responses in mice. BMC Res Notes 10:68
157. Shivahare R, Vishwakarma P, Parmar N et al (2014) Combination of liposomal CpG oligodeoxynucleotide 2006 and miltefosine induces strong cell-mediated immunity during experimental visceral leishmaniasis. PLoS One 9:e94596
158. Puangpetch A, Anderson R, Huang YY et al (2012) Cationic liposomes extend the immunostimulatory effect of CpG oligodeoxynucleotide against Burkholderia pseudomallei infection in BALB/c mice. Clin Vaccine Immunol 19:675–683
159. Kim DH, Moon C, Oh SS et al (2015) Liposome-encapsulated CpG enhances antitumor activity accompanying the changing of lymphocyte populations in tumor via intratumoral administration. Nucleic Acid Ther 25:95–102
160. Lu Y, Wang Y, Miao L et al (2016) Exploiting in situ antigen generation and immune modulation to enhance chemotherapy response in advanced melanoma: a combination nanomedicine approach. Cancer Lett 379:32–38

161. Mansourian M, Badiee A, Jalali SA et al (2014) Effective induction of anti-tumor immunity using p5 HER-2/neu derived peptide encapsulated in fusogenic DOTAP cationic liposomes co-administrated with CpG-ODN. Immunol Lett 162:87–93
162. Krieg AM, Efler SM, Wittpoth M et al (2004) Induction of systemic TH1-like innate immunity in normal volunteers following subcutaneous but not intravenous administration of CPG 7909, a synthetic B-class CpG oligodeoxynucleotide TLR9 agonist. J Immunother 27:460–471
163. Scheiermann J, Klinman DM (2014) Clinical evaluation of CpG oligonucleotides as adjuvants for vaccines targeting infectious diseases and cancer. Vaccine 32:6377–6389
164. Zhu Q, Talton J, Zhang G et al (2012) Large intestine-targeted, nanoparticle-releasing oral vaccine to control genitorectal viral infection. Nat Med 18:1291–1296
165. Yamamoto H, Wu X, Nakanishi H et al (2015) A glucose carbonate apatite complex exhibits in vitro and *in vivo* anti-tumour effects. Sci Rep 5:7742
166. Wang Y, Yamamoto Y, Shigemori S et al (2015) Inhibitory/suppressive oligodeoxynucleotide nanocapsules as simple oral delivery devices for preventing atopic dermatitis in mice. Mol Ther 23:297–309
167. Alexopoulou L, Holt AC, Medzhitov R et al (2001) Recognition of double-stranded RNA and activation of NF-kappaB by toll-like receptor 3. Nature 413:732–738
168. Hoebe K, Janssen EM, Kim SO et al (2003) Upregulation of costimulatory molecules induced by lipopolysaccharide and double-stranded RNA occurs by Trif-dependent and Trif-independent pathways. Nat Immunol 4:1223–1229
169. Tross D, Petrenko L, Klaschik S et al (2009) Global changes in gene expression and synergistic interactions induced by TLR9 and TLR3. Mol Immunol 46:2557–2564
170. Zheng R, Cohen PA, Paustian CA et al (2008) Paired toll-like receptor agonists enhance vaccine therapy through induction of interleukin-12. Cancer Res 68:4045–4049
171. Whitmore MM, DeVeer MJ, Edling A et al (2004) Synergistic activation of innate immunity by double-stranded RNA and CpG DNA promotes enhanced antitumor activity. Cancer Res 64:5850–5860
172. He H, Genovese KJ, Nisbet DJ et al (2007) Synergy of CpG oligodeoxynucleotide and double-stranded RNA (poly I:C) on nitric oxide induction in chicken peripheral blood monocytes. Mol Immunol 44:3234–3242
173. Zhu Q, Egelston C, Gagnon S et al (2010) Using 3 TLR ligands as a combination adjuvant induces qualitative changes in T cell responses needed for antiviral protection in mice. J Clin Invest 120:607–616
174. Bayyurt B, Tincer G, Almacioglu K et al (2017) Encapsulation of two different TLR ligands into liposomes confer protective immunity and prevent tumor development. J Control Release 247:134–144
175. Cluff CW (2010) Monophosphoryl lipid A (MPL) as an adjuvant for anti-cancer vaccines: clinical results. Adv Exp Med Biol 667:111–123
176. Kruit WH, Suciu S, Dreno B et al (2013) Selection of immunostimulant AS15 for active immunization with MAGE-A3 protein: results of a randomized phase II study of the European Organisation for Research and Treatment of Cancer melanoma Group in Metastatic Melanoma. J Clin Oncol 31:2413–2420
177. Hamilton E, Blackwell K, Hobeika AC et al (2012) Phase 1 clinical trial of HER2-specific immunotherapy with concomitant HER2 kinase inhibition [corrected]. J Transl Med 10:28
178. Zhao BG, Vasilakos JP, Tross D et al (2014) Combination therapy targeting toll like receptors 7, 8 and 9 eliminates large established tumors. J Immunother Cancer 2:12
179. Shirota H, Tross D, Klinman DM (2015) CpG oligonucleotides as cancer vaccine adjuvants. Vaccines (Basel) 3:390–407
180. Temizoz B, Kuroda E, Ohata K et al (2015) TLR9 and STING agonists synergistically induce innate and adaptive type-II IFN. Eur J Immunol 45:1159–1169
181. Cooper CL, Davis HL, Morris ML et al (2004) CPG 7909, an immunostimulatory TLR9 agonist oligodeoxynucleotide, as adjuvant to Engerix-B HBV vaccine in healthy adults: a double-blind phase I/II study. J Clin Immunol 24:693–701
182. Halperin SA, Van NG, Smith B et al (2003) A phase I study of the safety and immunogenicity of recombinant hepatitis B surface antigen co-administered with an immunostimulatory phosphorothioate oligonucleotide adjuvant. Vaccine 21:2461–2467
183. Rynkiewicz D, Rathkopf M, Sim I et al (2011) Marked enhancement of the immune response to BioThrax(R) (anthrax vaccine adsorbed) by the TLR9 agonist CPG 7909 in healthy volunteers. Vaccine 29:6313–6320
184. Cooper CL, Davis HL, Morris ML et al (2004) Safety and immunogenicity of CPG

7909 injection as an adjuvant to Fluarix influenza vaccine. Vaccine 22:3136–3143

185. Speiser DE, Lienard D, Rufer N et al (2005) Rapid and strong human CD8+ T cell responses to vaccination with peptide, IFA, and CpG oligodeoxynucleotide 7909. J Clin Invest 115:739–746
186. Ioannou XP, Griebel P, Hecker R et al (2002) The immunogenicity and protective efficacy of bovine herpesvirus 1 glycoprotein D plus Emulsigen are increased by formulation with CpG oligodeoxynucleotides. J Virol 76:9002–9010
187. Ioannou XP, Gomis SM, Karvonen B et al (2002) CpG-containing oligodeoxynucleotides, in combination with conventional adjuvants, enhance the magnitude and change the bias of the immune responses to a herpesvirus glycoprotein. Vaccine 21:127–137
188. Hirunpetcharat C, Wipasa J, Sakkhachornphop S et al (2003) CpG oligodeoxynucleotide enhances immunity against blood-stage malaria infection in mice parenterally immunized with a yeast-expressed 19 kDa carboxyl-terminal fragment of *Plasmodium yoelii* merozoite surface protein-1 (MSP1(19) formulated in oil-based Montanides). Vaccine 21:2923–2932
189. Kumar S, Jones TR, Oakley MS et al (2004) CpG oligodeoxynucleotide and Montanide ISA 51 adjuvant combination enhanced the protective efficacy of a subunit malaria vaccine. Infect Immun 72:949–957
190. Adamus T, Kortylewski M (2018) The revival of CpG oligonucleotide-based cancer immunotherapies6. Contemp Oncol (Pozn) 22:56–60
191. Hu-Lieskovan S, Ribas A (2017) New combination strategies using programmed cell death 1/programmed cell death ligand 1 checkpoint inhibitors as a backbone. Cancer J 23:10–22
192. Davila E, Kennedy R, Celis E (2003) Generation of antitumor immunity by cytotoxic T lymphocyte epitope peptide vaccination, CpG-oligodeoxynucleotide adjuvant, and CTLA-4 blockade. Cancer Res 63:3281–3288
193. Mangsbo SM, Sandin LC, Anger K et al (2010) Enhanced tumor eradication by combining CTLA-4 or PD-1 blockade with CpG therapy. J Immunother 33:225–235
194. Lavanchy D (2004) Hepatitis B virus epidemiology, disease burden, treatment, and current and emerging prevention and control measures. J Viral Hepat 11:97–107
195. Walayat S, Ahmed Z, Martin D et al (2015) Recent advances in vaccination of non-responders to standard dose hepatitis B virus vaccine. World J Hepatol 7:2503–2509
196. Denis F, Mounier M, Hessel L et al (1984) Hepatitis-B vaccination in the elderly. J Infect Dis 149:1019
197. de RS, Heijtink RA, Bakker-Bendik M et al (1994) Immunogenicity of standard and low dose vaccination using yeast-derived recombinant hepatitis B surface antigen in elderly volunteers. Vaccine 12:532–534
198. Agarwal SK, Irshad M, Dash SC (1999) Comparison of two schedules of hepatitis B vaccination in patients with mild, moderate and severe renal failure. J Assoc Physicians India 47:183–185
199. Mattos AA, Gomes EB, Tovo CV et al (2004) Hepatitis B vaccine efficacy in patients with chronic liver disease by hepatitis C virus. Arq Gastroenterol 41:180–184
200. Freed DC, Towne VM, Casimiro DR et al (2011) Evaluating functional antibodies in rhesus monkeys immunized with hepatitis B virus surface antigen vaccine with novel adjuvant formulations. Vaccine 29:9385–9390
201. Bai JY, Yang YT, Zhu R et al (2012) CpG oligodeoxynucleotides discriminately enhance binding capacity of human naive B cells to hepatitis B virus epitopes. Can J Microbiol 58:752–759
202. Wang S, Han Q, Zhang G et al (2011) CpG oligodeoxynucleotide-adjuvanted fusion peptide derived from HBcAg epitope and HIV-tat may elicit favorable immune response in PBMCs from patients with chronic HBV infection in the immunotolerant phase. Int Immunopharmacol 11:406–411
203. Kuan RK, Janssen R, Heyward W et al (2013) Cost-effectiveness of hepatitis B vaccination using HEPLISAV in selected adult populations compared to Engerix-B(R) vaccine. Vaccine 31:4024–4032
204. Eng NF, Bhardwaj N, Mulligan R et al (2013) The potential of 1018 ISS adjuvant in hepatitis B vaccines: HEPLISAV review. Hum Vaccin Immunother 9:1661–1672
205. Cooper C, Mackie D (2011) Hepatitis B surface antigen-1018 ISS adjuvant-containing vaccine: a review of HEPLISAV safety and efficacy. Expert Rev Vaccines 10:417–427
206. Heyward WL, Kyle M, Blumenau J et al (2013) Immunogenicity and safety of an investigational hepatitis B vaccine with a toll-like receptor 9 agonist adjuvant (HBsAg-1018) compared to a licensed hepatitis B vaccine in healthy adults 40–70 years of age. Vaccine 31:5300–5305
207. Jackson S, Lentino J, Kopp J et al (2018) Immunogenicity of a two-dose investigational

hepatitis B vaccine, HBsAg-1018, using a toll-like receptor 9 agonist adjuvant compared with a licensed hepatitis B vaccine in adults. Vaccine 36:668–674

208. Kamal SM, Rashid AK, Bakar MA et al (2011) Anthrax: an update. Asian Pac J Trop Biomed 1:496–501
209. Geier DA, Geier MR (2002) Anthrax vaccination and joint related adverse reactions in light of biological warfare scenarios. Clin Exp Rheumatol 20:217–220
210. Ready T (2004) US soldiers refuse to fall in line with anthrax vaccination scheme. Nat Med 10:112
211. Tross D, Klinman DM (2008) Effect of CpG oligonucleotides on vaccine-induced B cell memory. J Immunol 181:5785–5790
212. Hopkins RJ, Daczkowski NF, Kaptur PE et al (2013) Randomized, double-blind, placebo-controlled, safety and immunogenicity study of 4 formulations of anthrax vaccine adsorbed plus CPG 7909 (AV7909) in healthy adult volunteers. Vaccine 31:3051–3058
213. Gupta S, Gunter JT, Novak RJ et al (2009) Patterns of plasmodium vivax and *Plasmodium falciparum* malaria underscore importance of data collection from private health care facilities in India. Malar J 8:227
214. Ellis RD, Sagara I, Doumbo O et al (2010) Blood stage vaccines for *Plasmodium falciparum*: current status and the way forward. Hum Vaccin 6:627–634
215. Ellis RD, Martin LB, Shaffer D et al (2010) Phase 1 trial of the *Plasmodium falciparum* blood stage vaccine MSP1(42)-C1/Alhydrogel with and without CPG 7909 in malaria naive adults. PLoS One 5:e8787
216. Dicko A, Diemert DJ, Sagara I et al (2007) Impact of a *Plasmodium falciparum* AMA1 vaccine on antibody responses in adult Malians. PLoS One 2:e1045
217. Sagara I, Ellis RD, Dicko A et al (2009) A randomized and controlled phase 1 study of the safety and immunogenicity of the AMA1-C1/Alhydrogel + CPG 7909 vaccine for *Plasmodium falciparum* malaria in semi-immune Malian adults. Vaccine 27:7292–7298
218. Crompton PD, Mircetic M, Weiss G et al (2009) The TLR9 ligand CpG promotes the acquisition of *Plasmodium falciparum*-specific memory B cells in malaria-naive individuals. J Immunol 182:3318–3326
219. Mullen GE, Ellis RD, Miura K et al (2008) Phase 1 trial of AMA1-C1/Alhydrogel plus CPG 7909: an asexual blood-stage vaccine for *Plasmodium falciparum* malaria. PLoS One 3:e2940
220. Duncan CJ, Sheehy SH, Ewer KJ et al (2011) Impact on malaria parasite multiplication rates in infected volunteers of the protein-in-adjuvant vaccine AMA1-C1/Alhydrogel +CPG 7909. PLoS One 6:e22271
221. Moldoveanu Z, Love-Homan L, Huang WQ et al (1998) CpG DNA, a novel immune enhancer for systemic and mucosal immunization with influenza virus. Vaccine 16:1216–1224
222. Rhee JW, Kim D, Park BK et al (2012) Immunization with a hemagglutinin-derived synthetic peptide formulated with a CpG-DNA-liposome complex induced protection against lethal influenza virus infection in mice. PLoS One 7:e48750
223. Fang Y, Rowe T, Leon AJ et al (2010) Molecular characterization of *in vivo* adjuvant activity in ferrets vaccinated against influenza virus. J Virol 84:8369–8388
224. Lopez-Palomo C, Martin-Zamorano M, Benitez E et al (2004) Pneumonia in HIV-infected patients in the HAART era: incidence, risk, and impact of the pneumococcal vaccination. J Med Virol 72:517–524
225. Hersperger AR, Pereyra F, Nason M et al (2010) Perforin expression directly ex vivo by HIV-specific CD8 T-cells is a correlate of HIV elite control. PLoS Pathog 6:e1000917
226. Agrawal S, Agrawal A, Doughty B et al (2003) Cutting edge: different toll-like receptor agonists instruct dendritic cells to induce distinct Th responses via differential modulation of extracellular signal-regulated kinase-mitogen-activated protein kinase and c-Fos. J Immunol 171:4984–4989
227. Scheller C, Ullrich A, McPherson K et al (2004) CpG oligodeoxynucleotides activate HIV replication in latently infected human T cells. J Biol Chem 279:21897–21902
228. Equils O, Schito ML, Karahashi H et al (2003) Toll-like receptor 2 (TLR2) and TLR9 signaling results in HIV-long terminal repeat trans-activation and HIV replication in HIV-1 transgenic mouse spleen cells: implications of simultaneous activation of TLRs on HIV replication. J Immunol 170:5159–5164
229. Sulkowski MS, Chaisson RE, Karp CL et al (1998) The effect of acute infectious illnesses on plasma human immunodeficiency virus (HIV) type 1 load and the expression of serologic markers of immune activation among HIV-infected adults. J Infect Dis 178:1642–1648
230. Rotchford K, Strum AW, Wilkinson D (2000) Effect of coinfection with STDs and of STD treatment on HIV shedding in genital-tract

secretions: systematic review and data synthesis. Sex Transm Dis 27:243–248

231. Cooper CL, Davis HL, Angel JB et al (2005) CPG 7909 adjuvant improves hepatitis B virus vaccine seroprotection in antiretroviral-treated HIV-infected adults. AIDS 19:1473–1479
232. Angel JB, Cooper CL, Clinch J et al (2008) CpG increases vaccine antigen-specific cell-mediated immunity when administered with hepatitis B vaccine in HIV infection. J Immune Based Ther Vaccines 6:4
233. Cooper CL, Angel JB, Seguin I et al (2008) CPG 7909 adjuvant plus hepatitis B virus vaccination in HIV-infected adults achieves long-term seroprotection for up to 5 years. Clin Infect Dis 46:1310–1314
234. Sogaard OS, Lohse N, Harboe ZB et al (2010) Improving the immunogenicity of pneumococcal conjugate vaccine in HIV-infected adults with a toll-like receptor 9 agonist adjuvant: a randomized, controlled trial. Clin Infect Dis 51:42–50
235. Winckelmann AA, Munk-Petersen LV, Rasmussen TA et al (2013) Administration of a Toll-like receptor 9 agonist decreases the proviral reservoir in virologically suppressed HIV-infected patients. PLoS One 8:e62074
236. Creticos PS, Schroeder JT, Hamilton RG et al (2006) Immunotherapy with a ragweed-toll-like receptor 9 agonist vaccine for allergic rhinitis. N Engl J Med 355:1445–1455
237. Simons FE, Shikishima Y, Van NG et al (2004) Selective immune redirection in humans with ragweed allergy by injecting Amb a 1 linked to immunostimulatory DNA. J Allergy Clin Immunol 113:1144–1151
238. Kundig TM, Klimek L, Schendzielorz P et al (2015) Is the allergen really needed in allergy immunotherapy? Curr Treat Options Allergy 2:72–82
239. Senti G, Johansen P, Haug S et al (2009) Use of A-type CpG oligodeoxynucleotides as an adjuvant in allergen-specific immunotherapy in humans: a phase I/IIa clinical trial. Clin Exp Allergy 39:562–570
240. Klimek L, Willers J, Hammann-Haenni A et al (2011) Assessment of clinical efficacy of CYT003-QbG10 in patients with allergic rhinoconjunctivitis: a phase IIb study. Clin Exp Allergy 41:1305–1312
241. Vasievich EA, Huang L (2011) The suppressive tumor microenvironment: a challenge in cancer immunotherapy. Mol Pharm 8:635–641
242. Ostrand-Rosenberg S, Sinha P (2009) Myeloid-derived suppressor cells: linking inflammation and cancer. J Immunol 182:4499–4506
243. Zoglmeier C, Bauer H, Noerenberg D et al (2011) CpG blocks immunosuppression by myeloid-derived suppressor cells in tumor-bearing mice. Clin Cancer Res 17:1765–1775
244. Krieg AM (2004) Antitumor applications of stimulating toll-like receptor 9 with CpG oligodeoxynucleotides. Curr Oncol Rep 6:88–95
245. Carpentier AF, Chen L, Maltonti F et al (1999) Oligodeoxynucleotides containing CpG motifs can induce rejection of a neuroblastoma in mice. Cancer Res 59:5429–5432
246. Carpentier AF, Xie J, Mokhtari K et al (2000) Successful treatment of intracranial gliomas in rat by oligodeoxynucleotides containing CpG motifs. Clin Cancer Res 6:2469–2473
247. Brody JD, Ai WZ, Czerwinski DK et al (2010) In situ vaccination with a TLR9 agonist induces systemic lymphoma regression: a phase I/II study. J Clin Oncol 28:4324–4332
248. Hofmann MA, Kors C, Audring H et al (2008) Phase 1 evaluation of intralesionally injected TLR9-agonist PF-3512676 in patients with basal cell carcinoma or metastatic melanoma. J Immunother 31:520–527
249. Molenkamp BG, Sluijter BJ, Van Leeuwen PA et al (2008) Local administration of PF-3512676 CpG-B instigates tumor-specific CD8+ T-cell reactivity in melanoma patients. Clin Cancer Res 14:4532–4542
250. Kim YH, Gratzinger D, Harrison C et al (2012) In situ vaccination against mycosis fungoides by intratumoral injection of a TLR9 agonist combined with radiation: a phase 1/2 study. Blood 119:355–363
251. Carson WE III, Shapiro CL, Crespin TR et al (2004) Cellular immunity in breast cancer patients completing taxane treatment. Clin Cancer Res 10:3401–3409
252. Lake RA, Robinson BW (2005) Immunotherapy and chemotherapy--a practical partnership. Nat Rev Cancer 5:397–405
253. Carpentier A, Laigle-Donadey F, Zohar S et al (2006) Phase 1 trial of a CpG oligodeoxynucleotide for patients with recurrent glioblastoma. Neuro-Oncology 8:60–66
254. Manegold C, Gravenor D, Woytowitz D et al (2008) Randomized phase II trial of a toll-like receptor 9 agonist oligodeoxynucleotide, PF-3512676, in combination with first-line taxane plus platinum chemotherapy for advanced-stage non-small-cell lung cancer. J Clin Oncol 26:3979–3986
255. Friedberg JW, Kim H, McCauley M et al (2005) Combination immunotherapy with a CpG oligonucleotide (1018 ISS) and

rituximab in patients with non-Hodgkin lymphoma: increased interferon-alpha/beta-inducible gene expression, without significant toxicity. Blood 105:489–495

256. Leonard JP, Link BK, Emmanouilides C et al (2007) Phase I trial of toll-like receptor 9 agonist PF-3512676 with and following rituximab in patients with recurrent indolent and aggressive non-Hodgkin's lymphoma. Clin Cancer Res 13:6168–6174
257. Friedberg JW, Kelly JL, Neuberg D et al (2009) Phase II study of a TLR-9 agonist (1018 ISS) with rituximab in patients with relapsed or refractory follicular lymphoma. Br J Haematol 146:282–291
258. Baumgaertner P, Jandus C, Rivals JP et al (2012) Vaccination-induced functional competence of circulating human tumor-specific CD8 T-cells. Int J Cancer 130:2607–2617
259. Bioley G, Guillaume P, Luescher I et al (2009) Vaccination with a recombinant protein encoding the tumor-specific antigen NY-ESO-1 elicits an A2/157-165-specific CTL repertoire structurally distinct and of reduced tumor reactivity than that elicited by spontaneous immune responses to NY-ESO-1-expressing tumors. J Immunother 32:161–168
260. Valmori D, Souleimanian NE, Tosello V et al (2007) Vaccination with NY-ESO-1 protein and CpG in Montanide induces integrated antibody/Th1 responses and CD8 T cells through cross-priming. Proc Natl Acad Sci U S A 104:8947–8952
261. McQuade JL, Homsi J, Torres-Cabala CA et al (2018) A phase II trial of recombinant MAGE-A3 protein with immunostimulant AS15 in combination with high-dose Interleukin-2 (HDIL2) induction therapy in metastatic melanoma. BMC Cancer 18:1274
262. Haining WN, Davies J, Kanzler H et al (2008) CpG oligodeoxynucleotides alter lymphocyte and dendritic cell trafficking in humans. Clin Cancer Res 14:5626–5634
263. Tarhini AA, Leng S, Moschos SJ et al (2012) Safety and immunogenicity of vaccination with MART-1 (26-35, 27L), gp100 (209-217, 210M), and tyrosinase (368-376, 370D) in adjuvant with PF-3512676 and GM-CSF in metastatic melanoma. J Immunother 35:359–366
264. Del VM, Di GL, Ascierto PA et al (2014) Efficacy and safety of ipilimumab 3mg/kg in patients with pretreated, metastatic, mucosal melanoma. Eur J Cancer 50:121–127
265. McCluskie MJ, Weeratna RD, Davis HL (2000) The role of CpG in DNA vaccines. Springer Semin Immunopathol 22:125–132
266. Klinman DM (2003) CpG DNA as a vaccine adjuvant. Expert Rev Vaccines 2:305–315
267. Hobernik D, Bros M (2018) DNA vaccines-how far from clinical use? Int J Mol Sci 19:3605
268. Prazeres DMF, Monteiro GA (2014) Plasmid Biopharmaceuticals. Microbiol Spectr 2
269. Ferraro B, Morrow MP, Hutnick NA et al (2011) Clinical applications of DNA vaccines: current progress. Clin Infect Dis 53:296–302
270. Tang DC, DeVit M, Johnston SA (1992) Genetic immunization is a simple method for eliciting an immune response. Nature 356:152–154
271. Ulmer JB, Donnelly JJ, Parker SE et al (1993) Heterologous protection against influenza by injection of DNA encoding a viral protein. Science 259:1745–1749
272. Wang B, Agadjanyan MG, Srikantan V et al (1993) Molecular cloning, expression, and biological characterization of an HTLV-II envelope glycoprotein: HIV-1 expression is permissive for HTLV-II-induced cell fusion. AIDS Res Hum Retrovir 9:849–860
273. Fynan EF, Webster RG, Fuller DH et al (1993) DNA vaccines: protective immunizations by parenteral, mucosal, and gene-gun inoculations. Proc Natl Acad Sci U S A 90:11478–11482
274. Klinman DM, Klaschik S, Tross D et al (2010) FDA guidance on prophylactic DNA vaccines: analysis and recommendations. Vaccine 28:2801–2805
275. Dauphin G, Zientara S (2007) West Nile virus: recent trends in diagnosis and vaccine development. Vaccine 25:5563–5576
276. Witter MP, Groenewegen HJ, Lopes da Silva FH et al (1989) Functional organization of the extrinsic and intrinsic circuitry of the parahippocampal region. Prog Neurobiol 33:161–253
277. Krieg AM, Wu T, Weeratna R et al (1998) Sequence motifs in adenoviral DNA block immune activation by stimulatory CpG motifs. Proc Natl Acad Sci U S A 95:12631–12636
278. Sato Y, Roman M, Tighe H et al (1996) Immunostimulatory DNA sequences necessary for effective intradermal gene immunization. Science 273:352–354
279. Kojima Y, Xin KQ, Ooki T et al (2002) Adjuvant effect of multi-CpG motifs on an HIV-1 DNA vaccine. Vaccine 20:2857–2865
280. Schneeberger A, Wagner C, Zemann A et al (2004) CpG motifs are efficient adjuvants for DNA cancer vaccines. J Invest Dermatol 123:371–379

281. Ma Y, Jiao YY, Yu YZ et al (2018) A built-in CpG adjuvant in RSV F protein DNA vaccine drives a Th1 polarized and enhanced protective immune response. Viruses 10:38
282. Trimble CL, Morrow MP, Kraynyak KA et al (2015) Safety, efficacy, and immunogenicity of VGX-3100, a therapeutic synthetic DNA vaccine targeting human papillomavirus 16 and 18 E6 and E7 proteins for cervical intraepithelial neoplasia 2/3: a randomised, double-blind, placebo-controlled phase 2b trial. Lancet 386:2078–2088
283. Kim TJ, Jin HT, Hur SY et al (2014) Clearance of persistent HPV infection and cervical lesion by therapeutic DNA vaccine in CIN3 patients. Nat Commun 5:5317
284. Tiriveedhi V, Tucker N, Herndon J et al (2014) Safety and preliminary evidence of biologic efficacy of a mammaglobin-a DNA vaccine in patients with stable metastatic breast cancer. Clin Cancer Res 20:5964–5975
285. Heikenwalder M, Polymenidou M, Junt T et al (2004) Lymphoid follicle destruction and immunosuppression after repeated CpG oligodeoxynucleotide administration. Nat Med 10:187–192
286. Sparwasser T, Hultner L, Koch ES et al (1999) Immunostimulatory CpG-oligodeoxynucleotides cause extramedullary murine hemopoiesis. J Immunol 162:2368–2374
287. Le HC, Cohen P, Bousser MG et al (1999) Suspected hepatitis B vaccination related vasculitis. J Rheumatol 26:191–194
288. Allen MB, Cockwell P, Page RL (1993) Pulmonary and cutaneous vasculitis following hepatitis B vaccination. Thorax 48:580–581
289. Gilkeson GS, Ruiz P, Howell D et al (1993) Induction of immune-mediated glomerulonephritis in normal mice immunized with bacterial DNA. Clin Immunol Immunopathol 68:283–292
290. Steinberg AD, Krieg AM, Gourley MF et al (1990) Theoretical and experimental approaches to generalized autoimmunity. Immunol Rev 118:129–163
291. Gilkeson GS, Pippen AM, Pisetsky DS (1995) Induction of cross-reactive anti-dsDNA antibodies in preautoimmune NZB/NZW mice by immunization with bacterial DNA. J Clin Invest 95:1398–1402
292. Gilkeson GS, Conover J, Halpern M et al (1998) Effects of bacterial DNA on cytokine production by (NZB/NZW)F1 mice. J Immunol 161:3890–3895
293. Mor G, Singla M, Steinberg AD et al (1997) Do DNA vaccines induce autoimmune disease? Hum Gene Ther 8:293–300
294. Segal BM, Klinman DM, Shevach EM (1997) Microbial products induce autoimmune disease by an IL-12-dependent pathway. J Immunol 158:5087–5090
295. Segal BM, Chang JT, Shevach EM (2000) CpG oligonucleotides are potent adjuvants for the activation of autoreactive encephalitogenic T cells *in vivo*. J Immunol 164:5683–5688
296. Bachmaier K, Meu N, Maza LM (1999) Chlamydia infections and heart disease linked through antigenic mimicry. Science 283:1335–1339
297. Zeuner RA, Verthelyi D, Gursel M et al (2003) Influence of stimulatory and suppressive DNA motifs on host susceptibility to inflammatory arthritis. Arthritis Rheum 48:1701–1707
298. Ellis RD, Mullen GE, Pierce M et al (2009) A phase 1 study of the blood-stage malaria vaccine candidate AMA1-C1/Alhydrogel with CPG 7909, using two different formulations and dosing intervals. Vaccine 27:4104–4109
299. Yi AK, Hornbeck P, Lafrenz DE et al (1996) CpG DNA rescue of murine B lymphoma cells from anti-IgM-induced growth arrest and programmed cell death is associated with increased expression of c-myc and bcl-xL1. J Immunol 157:4918–4925
300. Krieg AM, Vollmer J (2007) Toll-like receptors 7, 8, and 9: linking innate immunity to autoimmunity. Immunol Rev 220:251–269
301. Yu P, Musette P, Peng SL (2008) Toll-like receptor 9 in murine lupus: more friend than foe! Immunobiology 213:151–157
302. Carpentier A, Metellus P, Ursu R et al (2010) Intracerebral administration of CpG oligonucleotide for patients with recurrent glioblastoma: a phase II study. Neuro-Oncology 12:401–408
303. Splawn LM, Bailey CA, Medina JP et al (2018) Heplisav-B vaccination for the prevention of hepatitis B virus infection in adults in the United States. Drugs Today (Barc) 54:399–405
304. Madan RA, Bilusic M, Heery C et al (2012) Clinical evaluation of TRICOM vector therapeutic cancer vaccines. Semin Oncol 39:296–304

Chapter 5

Molecular Adjuvants for DNA Vaccines: Application, Design, Preparation, and Formulation

Ailar Sabbaghi and Amir Ghaemi

Abstract

Compared with conventional vaccines, the main advantage of DNA vaccine-based methods is its continued expression of the plasmid-encoded antigens followed by the induction of subsequent humoral and cellular immunities. DNA vaccines are currently used in animal models, but limited success has been obtained for use in clinical applications due to their poor immunogenicity. Various strategies are attempted to improve the induced immune response of DNA vaccines. It has been demonstrated that co-administration of molecular adjuvants with DNA vaccines is a promising approach to effectively elicit protective immunity by increasing the transfection efficiency of DNA vaccines. Genetic adjuvants are incorporated to promote activation of the transfected local antigen-presenting cells (APCs) and immune cells in the draining lymph node and polarization of T-cell subsets to decrease T-cell tolerance to the specific antigen. Here we provide an overview of different types of genetic adjuvants. The aim of the current chapter is to present a framework for the construction of a gene-based vaccine and adjuvant. Moreover, we describe the application of DNA vaccines co-administered with different types of genetic adjuvants and the methods to evaluate their potency in the mouse models.

Key words Adaptive immunity, Chemokine, Cytokine, DNA vaccine, Molecular adjuvant

1 Introduction

Plasmid DNA vaccines introduced as the third vaccine generation, encompass a gene which encodes desired antigen along with respective epitopes to promote cell- and antibody-mediated immunity [1]. According to the advantages attributed to DNA vaccines such as: (a) induction of immune responses by producing immunogenic proteins using the appropriate eukaryotic expression systems; (b) sustained corresponding epitopes presentation through major histocompatibility complex (MHC) class I and II pathways by promoting the long-term gene expression [2, 3]; (c) high stability; (d) less requirement to the cold chain during transportation [4]; (e) high safety profile and low manufacturing costs due to the lack of isolation and purification of the desired proteins from pathogens;

Ângela Sousa (ed.), *DNA Vaccines: Methods and Protocols*, Methods in Molecular Biology, vol. 2197,
https://doi.org/10.1007/978-1-0716-0872-2_5,

(f) mild inflammation at the injection site as the common side effect; and (g) ability to manipulate the DNA vaccines based on the recombinant DNA technology [5], have led to the development of gene vaccines as a promising approach in the vaccine industry.

Due to the poor induction of immunogenic cells especially in the large mammalians, the development of alternative strategies such as codon usage- and plasmid design-optimization, use of gene delivery systems, and vaccine adjuvants to improve the antigen immunogenicity seems inevitable. Among different strategies, immune-stimulating adjuvants are mainly favorable to be used to deal with the limited potency of vaccines [3, 6]. Regarding the modest effect of traditional adjuvants on the DNA vaccine immunogenicity, the advancement of novel adjuvants, namely molecular adjuvants, has come into the sharp focus of virologists [5, 7].

Molecular adjuvants (also designed genetic adjuvants) are substances introduced as regulators of the immune response through the several mechanisms, including activation of the innate immune system, enhancement of the antigen presentation, augmentation of the chemotactic responses, and proliferation, differentiation, and maturation of lymphocytes and dendritic cells [3, 8, 9].

In order to design the plasmid-based vaccines using the recombinant DNA technology, molecular adjuvants can be used as the individual plasmids encoding adjuvant along with the gene vaccines or vaccine cocktails by insertion of the adjuvant encoding gene into the structure of plasmid vaccines [5].

In the following sections, we will summarize the most investigated genetic adjuvants.

1.1 Cytokine-Encoding Plasmids

Cytokines are small secreted proteins, which play a key role in the intercellular communication and immune-signaling pathways. Adverse effects of cytokines can be limited via the moderate secretion of the recombinant cytokines by infected cells at the site of injection. In this condition, despite the short half-life of cytokines, the prolonged stimulation of the local immune cells (notably APCs) is also achieved through the long-lasting gene expression [5, 10].

Plasmid-encoded T helper (Th)-1 inducing cytokines comprising interleukin-2 (IL-2), IL-12, IL-15, IL-18, IL-23, and interferon γ (IFN-γ) can lead to Th1-based immune responses to DNA vaccines. In this way, the cytotoxic T-lymphocyte and the ratio of IgG2a/IgG1 are commonly augmented [3, 11, 12].

Plasmids containing Th-2 cytokine-induced genes consist of IL-4, IL-5, IL-6, IL-10, and IL-13 can mainly stimulate humoral responses as the genetic adjuvants. A lower ratio of IgG2a/IgG1 and the cellular immune responses can preferably occur when this type of adjuvants is delivered simultaneously with the desired DNA vaccine. In addition, co-administration of pro-inflammatory cytokines expression plasmids such as IL-1α, IL-1β, granulocyte-

macrophage colony-stimulating factor (GM-CSF), and tumor necrosis factor (TNF)-α with the genetic vaccine can usually induce both cellular and humoral responses without being skewed toward either Th-1 or Th-2 immune responses [3, 11, 12].

Given the synergistic effects of cytokines, the construction of the fusion plasmids through the insertion of multiple cytokine genes into the same plasmid may increase their adjuvant effects [3]. According to literature, GM-CSF is a cytokine whose adjuvant properties have been studied widely. However, the mechanism through which GM-CSF acts as an effective adjuvant has not been clarified precisely until now. In most studies, GM-CSF has slight effects on the Th1/Th2 balance alternation. However, in some cases, it has been suggested that the adjuvant properties of GM-CSF can be influenced by the time of administration. It has been reported that injection of a GM-CSF-encoding plasmid 3 days prior to DNA vaccination induced a predominant Th2 response, while injection of the same cytokine-encoding plasmid 3 days after DNA vaccination enhanced Th1 responses [12].

1.2 Chemokine-Encoding Plasmids

The superfamily of chemokines comprises a large number of the structurally related small proteins that act through binding to the G-protein-coupled receptors. Expression of the desired chemokine at the site of genetic vaccine injection can lead to activation, differentiation, and expansion of effector T-lymphocytes against co-administered antigens by the regulation of leukocyte trafficking cells [3, 7, 9].

Similar to cytokines, the incorporation of different chemokine genes into the structure of the genetic vaccines can be designed easily. Since chemokines are more stable and less toxic than cytokines, it seems that chemokines consider a better candidate for use as the vaccine adjuvants [3, 7, 9].

1.3 Co-Stimulatory Molecule-Encoding Plasmids

Co-stimulatory molecules that are expressed on the surface of APCs have a critical role in the development of adaptive immunity after the antigen recognition. In this way, the activation, differentiation, and proliferation of T-cells can be promoted by the interaction of CD80/86 receptors expressed on the activated APCs with the CD28 that is typically expressed on the surface of T-cells. Alternatively, the interaction of CD40 ligand (CD40L) on the activated T-cells with CD40 on the surface of dendritic cells and B-cells can regulate the maturation of dendritic cells, as well as the B-cell expansion and differentiation [3, 7, 13].

Since co-stimulatory molecules are commonly introduced as the membrane-bound proteins, the adjuvant effects of these molecules are limited to the vaccine administration site. Consequently, the employment of co-stimulatory molecules can consider as a promising approach to modulate the DNA vaccine responses. It has been shown that co-administration of the B7 molecules

(notably CD86) with DNA vaccines have a compelling impact on both $CD4^+$ and $CD8^+$ T-cell responses. Alternatively, CD40L plasmids have been reported to improve the cell- and antibody-mediated immunity induced by DNA vaccines. The plasmid expressing the extra domain of cytotoxic T lymphocyte-associated antigen 4 (CTLA-4) fusion protein can also enhance the humoral responses by targeting the CD80/86 on the APCs surface [3, 7, 13].

1.4 Plasmids Encoding Pathogen-Recognition Receptor (PRR) Ligands and Immune-Signaling Molecules

PRRs, which are introduced as the innate immune receptors, along with the respective signaling molecules play a critical role in the interaction between the innate and adaptive immune systems [3, 14].Therefore, binding between PRR ligands and specific innate immune receptors induce the activation of the innate immunity. Following recognition, signaling pathways initiate by the adaptive molecules, which results in the activation of transcription factors such as nuclear factor kappa B (NFκB), *interferon regulatory factor 3* (IRF-3), *IRF-7*, and mitogen-activated protein kinase (MAPKs). The adaptive immune system priming requires the production of cytokines and co-stimulatory molecules, which can be prompted by these transcription factors. In this way, type 1 IFNs derived IRF-3 and IRF-7 along with NFκB-dependent pro-inflammatory cytokines trigger the migration of dendritic cells to the nearest lymph node by providing critical signals for dendritic cells maturation. Maturated dendritic cells with increased expression of B7 molecules elicited by MAPKs have a direct role in the initiation of the adaptive immunity [3, 15].

Although PRR ligands- and signaling molecule-based plasmids (*see* Table 1) can potentially be used as molecular adjuvants for the enhancement of the adaptive immunity against the vaccine antigens, further studies are required to ensure that such approaches do not lead to any excess toxicity that may limit their deployment [3, 7].

It has been shown that other signaling factors can also act as an effective adjuvant. These include (a) T-box-containing protein expressed in T-cells (T-bet, a T-cell transcription factor); (b) high-mobility group box 1 protein (*HMGB1, an inflammatory mediator*); (c) 70 kDa heat-shock proteins (*Hsp70,* an anti-inflammatory protein); (d) melanoma differentiation-associated gene 5 (MDA-5, a retinoic acid inducible gene I (RIG-1) like dsRNA receptor); (e) programmed cell death protein 1 (PD-1, an immune regulator); (f) DNA-dependent activator of IFN-regulatory factors (DAI, the cytosolic DNA sensor) [3].

Overall, genetic adjuvants include cytokines, chemokines, PRR ligands, co-stimulatory molecules, and signaling factors are summarized in Table 1.

The current chapter will provide methods for the cloning and preparation of target adjuvant gene and DNA vaccine. The genetic adjuvant and DNA vaccine are further subjected to in vivo

Table 1
Overview of the current molecular adjuvants

Molecular adjuvants	Example	References
Cytokines	Th-1 inducing cytokines including IL-2, IL-7, IL-9, IL-12, IL-15, IL-18, IL-23, IL-33, and IFN-γ; Th-2 inducing cytokines including IL-4, IL-5, IL-6, IL-10, and IL-13; pro-inflammatory cytokines including IL-1α, IL-1β, GM-CSF, TNF-α, and TNF-β	[8, 11, 12, 16]
Chemokines	C-C motif chemokine ligand-19 (CCL-19), CCL-21, macrophage inflammatory protein (MIP)-1 alpha, MIP-3 alpha, MIP-3 beta, RANTES (regulated upon activation in normal T cell expressed, and secreted), interferon gamma-induced protein-10 (IP-10), C-C chemokine receptor type-7 (CCR-7), monocyte chemoattractant protein-1 (*MCP-1*), and the murine beta chemokine TCA3	[3, 7, 8, 12]
Co-stimulatory molecules	CD80 (B7.1), CD86 (B7.2), CD40, CD40L, extra domain of CTLA-4, and the adhesion molecules intracellular adhesion molecule-1 (ICAM-1)	[3, 7, 8, 12]
Pathogen-recognition receptor ligands	Poly (I:C) (toll-like receptor-3 (TLR-3) ligand), CPG (TLR-9 ligand), eRNA41H (RIG-1 ligand), and Sendai virus-derived 546 nucleotide-long RNA (RIG-1 ligand)	[5]
Immune-signaling molecules	Transcription factors including NFκB, IRF-1, IRF-3, IRF-7, and T-bet; adaptor proteins including myeloid differentiation primary response 88 (*MYD88*), and TIR-domain-containing adapter-inducing interferon-β (*TRIF*); inflammation signaling proteins including *HMGB1*, and *Hsp70*; pattern recognition receptors including melanoma differentiation-associated gene 5 (MDA-5), RIG-1, and DAI; PD-1 as an immune regulator	[3, 7, 12, 17]

vaccination studies using a mouse model followed by the evaluation of T-cell and B-cell responses, as well as cytokine levels. Here, we describe the approaches for examining adjuvant- and antigen-specific cell-mediated immunity (T-cell proliferation and cytokine ELISpot assay) as well as the measurement of the antigen-specific antibody titers using ELISA.

2 Materials

2.1 Target Gene Preparation to Use

1. Polymerase chain reaction (PCR): PCR reagents including a thermostable DNA polymerase with proof-reading ability (e.g., *Pfu*), deoxynucleotide triphosphates (dNTPs), DNA polymerase 10 × buffer, $MgCl_2$, and gene-specific primers.
2. Complementary DNA (cDNA) synthesis and the target gene amplification by PCR: The commercially available kits for total RNA extraction and cDNA synthesis, as well as PCR reagents for the amplification of the desired gene.

3. Other cloned vectors containing the gene of interest: Appropriate commercially available restriction enzymes and corresponding 10 × reaction buffers for the insert release.
4. In-silico designing: De novo creation of desired DNA sequences by gene design tools (e.g., Gene Designer) and online bioinformatics software such as http://genomes.urv.es/OPTIMIZER for gene design and codon optimization, respectively.

2.2 Directional Cloning

2.2.1 Double-Digestion

1. Desired commercial cloning vector (e.g., PCDNA 3.1) and the gene of interest: store at −20 °C.
2. Appropriate commercial restriction enzymes and corresponding 10 × reaction buffers: store at −20 °C.
3. 1 mg/mL acetylated bovine serum albumin (BSA).
4. Sterile double-distilled water and incubator.
5. Stop solution: 0.5 M Ethylenediaminetetraacetic acid (EDTA), pH 8.0.
6. Thermal block or water bath for enzyme inactivation.
7. 5 M NaCl for final salt concentration adjustment.
8. Agarose, appropriate commercial DNA size marker, DNA Loading Dye, and nucleic acid stain (e.g., ethidium bromide).
9. Agarose gel electrophoresis system and gel documentation system.

2.2.2 DNA Extraction and Clean-Up

1. Low-melting point agarose.
2. Tris-acetate-EDTA (TAE) buffer: Make 1 L of 10 × stock solution TAE buffer in ultrapure water with 48.4 g of Tris base, 3.72 g disodium EDTA, and adjust to pH 8.5 with glacial acetic acid. Prior to use, dilute 100 mL of 10 × stock to 1 L with ultrapure water to prepare 1 × TAE buffer.
3. DNA sample, appropriate commercial DNA size marker, DNA Loading Dye, and nucleic acid stain (e.g., ethidium bromide).
4. Agarose gel electrophoresis system and gel documentation system.
5. Thermal block or water bath for melting gel.
6. Low-Melting-Temperature (LMT) elution buffer: 20 mM Tris–Cl, 1 mM EDTA, pH 8.0.
7. Equilibrated Phenol, pH 8.0.
8. (1:1 v/v) Phenol:Chloroform.
9. 70% and 100% (v/v) ethanol.
10. 10 M Ammonium acetate.

11. Tris-EDTA (TE) buffer: 10 mM Tris–HCl and 1 mM EDTA, pH 8.0.
12. NanoDrop™ UV-Vis Spectrophotometer.
13. Available commercial clean-up kits.

2.2.3 Ligation Process

1. T4 DNA ligase: store at −20 °C.
2. T4 DNA ligase reaction buffer (10×): 300 mM Tris–HCl pH 7.8, 100 mM $MgCl_2$, 100 mM dithiothreitol (DTT), 10 mM ATP. Store working aliquots at −20 °C.
3. Purified DNA: store at −20 °C.
4. Sterile double-distilled water and incubator.
5. Thermal block or water bath for enzyme inactivation.

2.3 Introduction of the Recombinant Vector into the Competent Cell

1. Appropriate host bacterial strain (e.g., DH5α and JM109).
2. Luria-Bertani (LB) broth: Add 5 g tryptone, 10 g yeast extract, 5 g NaCl to 800 mL of distilled H_2O (dH_2O). Adjust to 1 L with distilled H_2O and sterilize by autoclaving.
3. 50 mL sterile centrifuge tube.
4. Shaker incubator for bacterial growth.
5. NanoDrop™ UV-Vis Spectrophotometer.
6. $MgCl_2$-$CaCl_2$ solution: 80 mM $MgCl_2$, 20 mM $CaCl_2$.
7. 0.1 M $CaCl_2$ solution: 0.735 g of calcium chloride ($CaCl_2 \cdot 2H_2O$) was dissolved in 50 mL dH_2O and sterilize by filtration.
8. A standard plasmid (e.g., pUC19) as positive control [18].
9. Water bath, 42 °C.
10. Super Optimal Broth with Catabolic repression (SOC) medium: Add 20 g BactoTryptone, 5 g Bacto Yeast Extract, 2 mL of 5 M NaCl, 2.5 mL of 1 M KCl, 10 mL of 1 M $MgCl_2$, 10 mL of 1 M $MgSO_4$, 20 mL of 1 M glucose to 900 mL dH_2O. Adjust to 1 L with dH_2O and sterilize by autoclaving.
11. Super Optimal Broth (SOB) agar plates containing 20 mM $MgSO_4$ and the appropriate antibiotic: Standard SOB contains 10 mM $MgSO_4$ and is identical to SOC medium, except that it does not contain 20 mM glucose.
12. Incubator for growth plate.
13. Plasmid mini kit.
14. Restriction site digestion to confirm the desired clone (*see* Subheading 2.2.1).
15. Agarose, appropriate commercial DNA size marker, DNA Loading Dye, and nucleic acid stain (e.g., ethidium bromide).

16. Agarose gel electrophoresis system and gel documentation system.
17. Endotoxin-free Plasmid Kit for DNA extraction at a large-scale (e.g., EndoFree® Plasmid Purification Giga kit).

2.4 Evaluation of the Desired Protein Expression

1. Cell line for transfection: Human embryonic kidney (HEK), or Monkey kidney fibroblast cells (COS-7).
2. Transfection agent: Lipofectamine 2000 reagent.
3. Appropriate culture medium, e.g., Dulbecco's Modified Eagle *Medium* (DMEM*)* and *Opti-MEM*® Reduced-Serum Medium.
4. Fetal bovine serum (FBS), 6-well plates, and 1.5 mL sterile tubes.
5. Phosphate-buffered saline (PBS): To 900 mL dH_2O add 0.2 g KCl, 0.2 g KH_2PO_4, 8 g NaCl, and 1.14 g $NaHPO_4$. Adjust to pH 7.2 and to a final volume of 1 L with distilled H_2O. Sterilize by autoclaving.
6. A positive control: GFP cloned into the eukaryotic expression vector.
7. The humidified incubator with 5% CO_2 for cell growth.
8. Trypsin-EDTA solution (1 ×): 0.25% (w/v) trypsin, 0.5 mM EDTA in Hank's Balanced Salt Solution (*HBSS*).
9. Total RNA isolation kit, e.g., High Pure RNA Isolation.
10. cDNA synthesis kit, e.g., PrimeScriptTM RT reagent Kit (Perfect Real Time).
11. NanoDrop™ UV-Vis Spectrophotometer.
12. Real-Time kit, e.g., SYBR® *Premix Ex Taq* ™ (Perfect Real Time).
13. Respective forward and reverse primers.

2.5 Evaluation of Immune Responses

2.5.1 Immunization

1. The appropriate mice strain.
2. ketamine-xylazine solution.
3. 27 G *needle* syringe for the intraperitoneal injection.

2.5.2 ELISA Assay

1. Pasteur pipette, micro-centrifuge, the humidified incubator with 5% CO_2 for the cell growth, and 96-well flat-bottomed plates.
2. Appropriate specific antigen.
3. Carbonate-bicarbonate coating buffer: 15 mM Na_2CO_3, 35 mM $NaHCO_3$, pH 9.6.
4. Washing buffer: Tris-*buffered* saline (TBS) containing 0.1% Tween 20 (TBS-T).
5. Blocking buffer: PBS containing 5% BSA, 0.1% Tween 20.

6. Secondary conjugated antibody: *Horseradish peroxidase* (HRP) goat anti-mouse IgG.
7. Peroxidase substrate: 3,3′,5,5′-tetramethylbenzidine (TMB).
8. Stop solution: 2 M H_2SO_4.
9. Automated ELISA reader.

2.5.3 Lymphocyte Proliferation Assay (LPA)

1. Sterile petri dish, 5 mL syringe, and PBS.
2. RBC lysis buffer: 0.15 M NH_4Cl, 1 mM $KHCO_3$, 0.1 mM Na_2EDTA, pH 7.2.
3. Washing buffer: RPMI 1640 medium.
4. Proliferation medium: RPMI 1640 medium supplemented with 10% fetal calf serum, 1% L-glutamine, 1% HEPES, 0.1% penicillin/streptomycin, and 25 mg/mL of amphotericin B.
5. Trypan blue dye.
6. Phytohemagglutinin (PHA) and appropriate specific antigen: Store at −20 °C.
7. 5 mg/mL MTT solution [(3-(4,5-Dimethylthiazol-2-yl)-2,5-diphenyltetrazolium bromide, a tetrazolium salt]: Add 25 mg MTT powder in 5 mL PBS and sterilized by filter.
8. Dimethyl sulfoxide (DMSO).

2.5.4 Cytokine ELISpot Assay

1. 35% (v/v) ethanol.
2. The Polyvinylidene fluoride (PVDF) membrane 96-well ELISpot plate.
3. Coating buffer: Carbonate-bicarbonate buffer or PBS.
4. Blocking buffer: 10 g BSA (1×) in 1 L PBS containing 0.1% Tween 20 (PBS-T), pH 7.2.
5. Washing buffer: Sterile PBS and PBS containing 0.1% Tween 20 (PBS-T), pH 7.2.
6. Proliferation medium: RPMI 1640 medium supplemented with 10% fetal calf serum, 1% L-glutamine, 1% HEPES, 0.1% penicillin/streptomycin, and 25 mg/mL of amphotericin B.
7. *Concanavalin* A (ConA) and appropriate specific antigen.
8. Appropriate primary monoclonal antibodies and biotinylated secondary antibodies.
9. Alkaline phosphatase conjugated streptavidin.
10. Alkaline phosphatase substrate: 5-bromo-4-chloro-3-indolyl phosphate (*BCIP*)/nitro blue tetrazolium (*NBT*).
11. Automated ELIspot reader.

3 Methods

3.1 Insertion of the DNA Fragment of Interest into the Desired Cloning Vector

The gene of interest can be obtained through diverse pathways. Four known approaches consist of (a) direct amplification of the desired gene by PCR; (b) synthesis of cDNA by reverse transcriptase and then use this as a template to amplify the target gene; (c) from other cloned vector containing the gene of interest by the digestion process; (d) by in-silico designing of the target DNA sequence [19, 20].

3.1.1 Double-Digestion

Double-digestion of both desired commercially available cloning vector and the gene of interest are preferably carried out by two different sticky-end restriction enzymes (*see* **Notes 1** and **2**).

If Single Compatible Buffer Is Available

1. Prepare a typical simultaneous double-digestion reaction with two different restriction enzymes in a total volume of 20 μL, following Table 2 (*see* **Note 3**).
2. Spin the digestion mixture briefly and incubate at the optimal temperature for 1 h or longer (*see* **Note 8**).
3. Inactive the enzymes by adding the stop solution containing EDTA or by heating the reaction mixture to prevent nonspecific degradation of the target DNA (*see* **Note 9**).
4. Store the digestion mixture at −20 °C until required.

If Single Compatible Buffer Is Not Available

1. Start the sequential double-digestion with a restriction enzyme that has the lowest salt concentration in its recommended buffer, following Table 3.
2. Spin the digestion mixture briefly and incubate at the first enzyme specific-temperature for 1 h or longer.

Table 2
Conditions to prepare a typical simultaneous double-digestion reaction with two different restriction enzymes in a total volume of 20 μL

<For 1 reaction> reagents:	Amount	Final concentration
DNA (1 μg) (*see* **Notes 3** and **4**)	*x* μL	
Restriction enzyme 1 (*see* **Note 5**)	1 μL	1–2 units/μL
Restriction enzyme 2	1 μL	1–2 units/μL
Appropriate 10× reaction buffer (*see* **Note 6**)	2 μL	1×
Acetylated BSA 1 mg/mL (*see* **Note 7**)	2 μL	
Sterile double-distilled water	–	
Total	20 μL	

Table 3
Conditions to start the sequential double-digestion with a restriction enzyme that has the lowest salt concentration in its recommended buffer

<For 1 reaction> reagents:	Amount	Final concentration
DNA (1 μg)	*x* μL	
Restriction enzyme 1	1 μL	1–2 units/μL
Appropriate 10× reaction buffer	2 μL	1×
Acetylated BSA 1 mg/mL	2 μL	
Sterile double-distilled water	–	
Total	20 μL	

3. Stop the reaction using the heat or by adding a stop solution containing EDTA.
4. Confirm the linearized vector by gel electrophoresis.
5. Adjust the final salt concentration of the reaction to prepare the appropriate conditions for the function of the second enzyme (*see* **Note 10**).
6. Add the second enzyme.
7. Spin the digestion mixture briefly and incubate at the specific-temperature of the secondary enzyme for 1 h or longer.
8. Stop the reaction using the heat or by adding a stop solution, such as EDTA.
9. Store the digestion mixture at −20 °C until required.

3.1.2 DNA Extraction and Clean-Up

1. Make an agarose gel for electrophoresis using low-melting point agarose in 1 × TAE buffer (*see* **Notes 11** and **12**).
2. Load the restriction enzyme digested DNA samples (DNA of interest and desired cloning vector) along with a DNA size marker in separate wells of the agarose gel.
3. Using a UV transilluminator to view digestion products.
4. Cut out the region of the gel containing the target DNA band.
5. Measure the weight of the gel slice.
6. Add five times volume of LMT elution buffer to the gel slice.
7. Heat for 5 min at 65 °C to melt the gel.
8. Let the solution cool down at room temperature. Then, add an equal volume of equilibrated phenol and vortex for 20 s to mix them thoroughly.
9. Extract the aqueous layer (DNA solution) by centrifuging the mixture (20 °C, 4000 × *g*, 10 min) (*see* **Note 13**) and repeat the same, once with phenol:chloroform, and once with chloroform (*see* **Note 14**).

Table 4
Conditions to perform the ligation reaction of the purified DNA inserts and vector molecules by the bacteriophage T4 DNA ligase (*see* Note 19)

<For 1 reaction> reagents:	Amount	Final concentration
Linearized vector (50–200 ng)	*x* μL	
Digested insert (*see* **Note 20**)	*x* μL	
Ligase 10× reaction buffer (*see* **Note 21**)	1 μL	1×
T4 DNA ligase (*see* **Note 22**)	1 μL	0.1 weiss unit
Sterile double-distilled water	–	
Total volume	10 μL	

10. Precipitate the DNA by adding 0.2 volumes 10 M ammonium acetate and 2 volumes absolute ethanol at 4 °C (*see* **Note 15**).
11. Incubate for 10 min at room temperature and recover the DNA by centrifugation (4 °C, 5000 × *g*, 20 min).
12. Using the ethanol to a final concentration of 70% (v/v) for washing the DNA pellet (*see* **Note 16**) and resuspend the DNA pellet in a suitable volume of TE buffer (*see* **Note 17**).
13. Evaluate the quantification and purification of the extracted DNA by measuring the absorbance at 260 nm and 280 nm (*see* **Note 4**).
14. The DNA aliquots can be stored at −20 °C or can directly be used for the ligation process [18, 21].
15. For further purification of the extracted DNA, use the commercially available clean-up kits according to protocols recommended by manufacturers (*see* **Note 18**).

3.1.3 Ligation of Purified DNA Inserts and Vector Molecules by the Bacteriophage T4 DNA Ligase (Preferably)

1. Set up the ligation reaction as presented in Table 4 (*see* **Note 19**).
2. Spin the ligation mixture briefly.
3. For sticky ends ligation, incubate the mixture at 22 °C (room temperature) for 3 h or at 4 °C overnight (*see* **Note 23**).
4. For blunt ends ligation, incubate the mixture at 22 °C for 4–16 h (*see* **Note 23**).
5. Heat-inactivation of the bacteriophage T4 DNA ligase (65 °C for 15 min).
6. Store the ligation mixture at −20 °C.
7. Set up a negative control ligation reaction (all components except the insert) to evaluate re-circularizing of incomplete digested vectors.

3.2 Introduction of the Recombinant Vector into the $CaCl_2$ Treated-Cells

3.2.1 Preparation of Component Cells

1. Inoculate a desired *E. coli* host strain into 100 mL LB broth and incubate at 37 °C in shaker incubator (200 rpm) for 2.5–3 h (*see* **Note 24**).
2. Control the bacterial growth by measuring the optical density (OD) of a bacterial culture at 600 nm using the spectrophotometer until it reaches 0.35–0.4 ng/μL (*see* **Note 25**).
3. Transfer the bacterial culture (OD_{600} 0.35–0.4 ng/μL) into the ice-cold 50 mL sterile centrifuge tube and cool the culture on ice for 10 min to stop bacterial growth.
4. Collect the cells by centrifugation (4 °C, 2700 × *g*, 10 min) and remove the supernatant.
5. Gently resuspend the cell pellet in 30 mL of ice-cold, sterile $MgCl_2$-$CaCl_2$ solution (per 50 mL tube) and incubate on ice for 10 min (*see* **Note 26**).
6. Collect the cells by centrifugation (4 °C, 2700 × *g*, 10 min) and remove the supernatant.
7. Gently resuspend the cell pellet in 2 mL of ice-cold, sterile 0.1 M $CaCl_2$ solution (per 50 mL tube) (*see* **Note 26**).
8. Competent cells can be stored at 4 °C for 24–48 h or can be used directly for heat-shock transformation.

3.2.2 Transformation of Competent Cells by Heat-Shock Method

1. Transfer 100 μL of prepared competent cells to a pre-chilled sterile micro-tube and add DNA (10 μL or less of the ligation mixture) to the $CaCl_2$ treated-cells. Prepare positive and negative controls using standard plasmid and an aliquot of competent cells without DNA, respectively (*see* **Note 27**).
2. Mix the mixture by gentle swirling and incubate on ice for 30 min.
3. Heat-shock by placing the tube in a water bath previously set at 42 °C and incubate for exactly 90 s (do not shake the tube in this stage) (*see* **Note 28**).
4. After incubation time, immediately chill the cells by placing the tube on ice for 1–2 min (*see* **Note 28**).
5. In order to let the cells recover and express the antibiotic resistance marker, add 800 μL pre-warmed liquid SOC medium (without antibiotic) and incubate for 45 min.
6. Spread transformed cells (up to 200 μL per 90-mm plate) onto an agar SOB medium containing 20 mM $MgSO_4$ and the selective antibiotic. Positive and negative controls should also be plated onto the selective agar plate.
7. Incubate at 37 °C overnight [18, 21, 22].

3.2.3 Selection of Bacteria Colonies Containing Recombinant Plasmids

1. Inoculate a single colony into 6 mL of the sterile LB medium containing the selective antibiotic and incubate at 37 °C overnight with vigorous shaking (200 rpm) to ensure good aeration.
2. Extract the plasmid DNA using Plasmid Mini Kit following the instructions recommended by the manufacturer.
3. Evaluate the quantification and purification of the extracted DNA by measuring the absorbance at 260 nm and 280 nm.
4. Digest the extracted plasmid with the same restriction enzymes used for the cloning (*see* Subheading 3.1.1).
5. Confirm the linearized vector and gene of interest by electrophoresis (*see* **Note 29**).
6. Inoculate the culture medium containing the appropriate antibiotic with the confirmed clone.
7. Extract the plasmid DNA at a large-scale using EndoFree® Plasmid Purification Giga kit according to the manufacturer's recommended protocol for in vitro and in vivo procedures (*see* **Note 30**).
8. Evaluate the quantification and purification of the extracted DNA by measuring the absorbance at 260 nm and 280 nm.
9. Store the DNA in aliquots at −20 °C until required [21, 23].

3.3 Evaluation of the Desired Protein Expression

Transfection of recombinant plasmids to eukaryotic cell lines using Lipofectamine ™ 2000 should be as follows (*see* **Note 31**):

1. The day before transfection, seed the cells of interest onto the 6-well plate; so that the cells reach 70-90% confluent density within 24 h (*see* **Note 32**).
2. On the transfection day, add 4 μg DNA of interest in 150 μL *Opti-MEM* (or other media) without serum (*see* **Note 33**). In another 1.5 mL tube, dilute 10 μL of Lipofectamine ™ 2000 in 150 μL Opti-MEM (or other media) without serum.
3. Incubate the tubes at room temperature for 5 min (*see* **Note 34**).
4. Following the 5 min incubation, combine two mixtures together and mix them gently.
5. Incubate the transfection mixture at room temperature for 25–30 min.
6. During incubation, gently discard the cell media and replace it with Opti-MEM (or other media) without serum.
7. After incubation time, add transfection mixture to cells in a drop-like manner.
8. Incubate at 37 °C in a humidified incubator with 5% CO_2 for 5–6 h.

9. If toxicity effects including the presence of dead cells or changes in the cell morphology is observed, remove the transfection mixture and replace with fresh growth medium, e.g., DMEM with 10% FBS and incubate at 37 °C.
10. Harvest the cells after 48–72 h by trypsinization and extract total RNA by High Pure RNA Isolation Kit. Use a positive control such as GFP cloned into the eukaryotic expression vector to monitor transfection efficiency [23, 24].
11. Evaluate the quantification and purification of the extracted RNA by measuring the absorbance at 260 nm and 280 nm (*see* **Note 35**).
12. cDNA synthesis using both oligo (dT) primer and Random Hexamer by PrimeScript™ RT reagent Kit (Perfect Real Time) according to the manufacturer's recommendations (*see* **Note 36**).
13. Protein expression confirmation by real-time PCR SYBR® *Premix Ex Taq* ™ (Perfect Real Time) with respective forward and reverse primers following instructions provided by the manufacturer (*see* **Note 37**) [23].

3.4 Evaluation of Immune Responses

3.4.1 Immunization

1. Randomly divide mice into multiple groups (both control and experimental groups) based on the study.
2. Prior to the vaccination or challenge, the mice should be anesthetized by the intraperitoneal administration of the ketamine-xylazine solution (*see* **Note 38**).
3. Immunize the mice three times at 2-week intervals with the DNA vaccine, with or without adjuvant (*see* **Note 39**).
4. Challenge the mice 2 weeks after the last immunization (in the case of viral infection).
5. Monitor the mice daily for morbidity/survival during the 14 days after the challenge.

3.4.2 Evaluation of Humoral Immune Responses

Determination of antigen-specific antibody titers by the standard antigen-specific enzyme-linked immunosorbent assay (ELISA) should be as follows:

1. Collect the blood from the orbital sinus of immunized and control groups using Pasteur pipette.
2. Obtain the mouse sera by micro-centrifugation of the collected blood.
3. Coat the 96-well flat-bottomed plates with 100 μL specific antigen in the carbonate-bicarbonate coating buffer and incubate at 4 °C overnight (*see* **Note 40**).
4. Following overnight incubation, remove the coating solution and wash the plate with TBS-T buffer three times (*see* **Note 41**).

5. Block the remaining protein-binding sites in each well by adding 300 μL blocking buffer per well and incubate the plate for at least 2 h at room temperature (*see* **Note 41**).
6. Wash the plate three times with TBS-T buffer.
7. Prepare two-fold serial dilutions of serum (control and experimental groups) and load 100 μL diluted serum per well in duplicate.
8. Incubate the plate at 37 °C for 2 h.
9. Wash the plate three times. Add 100 μL of HRP goat anti-mouse IgG secondary antibody to each well and incubate the plate at 37 °C for 2 h.
10. Remove the solution and wash the plate three times with TBS-T buffer.
11. Develop the colorimetric assay by adding 100 μL/well of TMB substrate and incubate for 20 min at room temperature.
12. Add 50 μL/well of 2 M H_2SO_4 to stop the reaction.
13. Measure the absorbance at 450 nm by an automated ELISA plate reader.
14. Since the intensity of the absorbance at 450 nm is directly proportional to the level of target protein concentration, the endpoint antibody titer is defined as the dilution of a sample which generates a stronger signal (at least three times), compared to the negative control signal (*see* **Note 42**) [6, 25].

3.4.3 Cellular Mediated Immune Responses by lymphocyte proliferation assay (LPA)

Assessment of the lymphocyte proliferation in response to specific antigen stimulation by lymphocyte proliferation assay (LPA) should be as follows:

1. Two weeks after the last immunization, sacrifice the mice and remove the spleen aseptically.
2. Place the spleen into the sterile petri dish on ice and add 10 mL sterile 1 × PBS.
3. Prepare the single-cell suspensions from mouse spleen by crushing the spleen using a 5 mL syringe plunger.
4. Collect the cell pellet by centrifugation (4 °C, 1000 × *g*, 10 min).
5. Discard the supernatant and subsequently vortex the pellet for 1 min immediately to avoid losing the cell viability.
6. Lyse the erythrocytes by adding 3 mL of a lysis buffer and incubate on ice for 5 min (*see* **Note 43**).
7. Following the incubation, stop the lysis reaction by adding 12 mL sterile 1 × PBS and centrifuge at 1000 × *g* for 10 min.
8. Decant the supernatant and wash the pellet twice with RPMI 1640 medium.

9. Resuspend the cells in 5 mL RPMI 1640 medium supplemented with 10% fetal calf serum, 1% L-glutamine, 1% HEPES, 0.1% penicillin/streptomycin, and 25 mg/mL of amphotericin B.
10. Count the cells with trypan blue (*see* **Note 44**) and seed splenocytes at a cell density of 2×10^5 cells/well in 96-well flat-bottomed plates in the presence of 1 μg/mL specific antigen, 5 μg/mL phytohemagglutinin (PHA, T-cell mitogen; as positive control) or in the absence of stimuli (medium only, as negative control). All samples should be tested in triplicate for each mouse.
11. Incubate at 37 °C in a humidified incubator with 5% CO_2 for 48 h.
12. Following incubation, add 30 μL of 5 mg/mL MTT solution per well and incubate for 4 h at 37 °C in 5% CO_2 to determine the lymphoproliferation (*see* **Note 45**).
13. Add 100 μL of dimethyl sulfoxide to each well (*see* **Note 46**).
14. Read the OD at the wavelength of 540 nm by an automated ELISA plate reader.
15. Determine stimulating index (SI) as follows:
    {OD values of stimulated cells (Cs) − relative cell numbers of unstimulated cells (Cu)}/relative OD values of unstimulated cells (SI = (Cs − Cu)/Cu) [25, 26].

3.4.4 Evaluation of the Cellular Mediated Immune Responses by ELISpot Assay

Determination of the secreted Th1/Th2 cytokines in response to the specific antigen stimulation by cytokine ELISpot (the enzyme-linked immunospot) assay using the PVDF membrane 96-well ELISpot plates (preferably) (*see* **Note 47**) should be as follows:

1. Prepare the splenic single-cell suspensions from immunized mice (*see* Subheading 3.4.3).
2. Add 15 μL/well of 35% ethanol for no more than 1 min to prepare the PVDF membrane in the 96-well ELISpot plate.
3. Wash the plate thoroughly with sterile water for five times to remove residual alcohol completely (*see* **Note 48**).
4. Coat the primary monoclonal antibodies in coating buffer according to the manufacturer's instructions for the respective cytokines onto the ethanol-treated PVDF membrane plate and incubate at 4 °C overnight.
5. Wash the plate five times with sterile PBS (200 μL/well).
6. Block the remaining protein-binding sites in each well by adding 200 μL/well blocking buffer and incubate for 2 h at room temperature.
7. Remove the blocking buffer and wash the plate five times with sterile PBS (200 μL/well).

8. Seed splenocytes at a cell density of 2×10^5 cells/well in 96-well ELISpot plates in the presence of 1 μg/mL of specific antigen, 5 μg/mL of *Concanavalin* A (Con A, T-cell mitogen; as positive control) or in the absence of stimuli (medium only, as negative control). All samples should be run in triplicate for each mouse (*see* **Note 49**).
9. Incubate the plate at 37 °C in a humidified incubator with 5% CO_2 for 24–48 h, stimulating the cells to secrete cytokines (*see* **Note 50**).
10. Wash with PBS (200 μL/well) two times and then with PBS-T (200 μL/well) three times (*see* **Note 51**).
11. Add 100 μL/well of diluted biotinylated cytokine-specific detection antibodies (as secondary conjugated antibody) in PBS-Tween with 1% BSA and incubate the plate at room temperature for 2 h.
12. Wash with sterile PBS-T (200 μL/well) five times.
13. Add 100 μL of alkaline phosphatase conjugated streptavidin or other streptavidin enzyme conjugates in PBS-Tween with 1% BSA per well as recommended by manufacturer and incubate at room temperature for 1–2 h.
14. Wash the plate three times with PBS-T (200 μL/well) and then three times with PBS (200 μL/well).
15. Spot development by adding 100 μL/well substrate solution (BCIP/NBT for streptavidin-alkaline phosphatase) and incubate for 10–15 min at room temperature.
16. Following incubation, stop the reaction by washing the plate with tap water.
17. Incubate at 4 °C overnight to air-dry the plate (*see* **Note 52**).
18. Count spots by automated ELISpot reader (each spot: one cell).
19. Calculate the frequency of the secreting cells as follows:

    The number of spots in control wells − the number of spots in experimental wells [23, 27–29].

4 Notes

1. The clonal insertion in the correct orientation and the correct open reading frame is reached by creating the incompatible termini at the opposite ends of the DNA insert and plasmid using the digestion with two different restriction enzymes. Moreover, the generation of self-ligated clones will also be limited by this strategy. Of note, in order to create noncommercial DNA molecules, different restriction sites can be

introduced by adding the synthetic linkers (adaptors) or by using primers with desirable incompatible restriction sites in 5′ termini [21, 30].

2. It is worth noting that use of the certain restriction enzymes called isocaudomers such as *Bam*HI, *Bgl*II, *Bcl*I, and *Sau*3AI simultaneously can induce self-ligation through the generation of the identical sticky ends [18]. On the other hand, cohesive ends especially longer overhang sequences produced by restriction enzymes, compared to the blunt ends enhance the ligation efficiency by annealing of the complementary regions and by promoting the chance of ligation via T4 DNA ligase. The base composition of the overhang sequences may also affect the ligation efficiency, so that AT-rich overhangs reduce the chance of ligation procedure [21, 31].
3. A typical digestion reaction is commonly carried out in a volume of 20 μL containing 1 μg of template [21].
4. The purity of target DNA and the absence of contaminants such as RNA, phenol, and chloroform can significantly affect the success of digestion reaction. Thus, the DNA purity should be quantitated spectrophotometrically through the measurement of the ratio of absorbance at 260 nm and 280 nm. A ratio of 1.8 ± 0.05 indicates the purity of the DNA sample [18, 21].
5. The amount of enzyme required to complete digestion of one microgram of DNA in an hour under the standard digestion conditions is called the enzyme unit [21]. Since the multiple freeze–thaw cycles can reduce the enzyme activity, the enzyme is supplied in 50% glycerol to prevent freezing at −20 °C. Regarding the concentration of glycerol, the enzyme volume should not exceed 10% of the final digestion reaction volume to avoid star activity. Star activity (nonspecific digestion of double-strand DNA) is usually induced by increase in incubation time, excessive enzyme concentration, incorrect buffer conditions, and glycerol concentration of higher than 5% [18, 32].
6. The information supplied by manufacturers on the activity of enzymes can be used to select the compatible buffers. As a rule, the best matching restriction buffer should be selected for the optimum digestion reaction. Furthermore, the use of buffers with an enzyme activity of less than 50% should be avoided.
7. Check the manufacturer's *recommendations* for optimal digestion conditions. Occasionally, adding some additional components to the reaction, such as acetylated bovine serum albumin (BSA) as the enzyme thermal stabilizer, may be required [33].
8. The experimental conditions especially incubation time and optimal temperature vary among various restriction enzymes. Therefore, follow *the* manufacturer's instructions to provide the optimal digestion conditions.

9. Inactivation of restriction enzymes is done using the heat or by adding EDTA (for heat-resistant enzymes) as recommended by the manufacturer [18, 34].
10. According to the recommended NEB protocol, sequential double-digestion is initiated using the enzyme which requires the lower salt concentration. Subsequently, the second digestion is performed by buffer adjustment using a small volume of the high salt buffer (second buffer) or a small volume of the concentrated saline solution such as 5 M NaCl. Therefore, check the buffer information sheet supplied by the restriction enzyme provider carefully.
11. Low-melting agarose gel, compared to standard agarose gel is a better choice for undamaged DNA extraction due to its low-melting temperature (65 °C) which is considerably lower than the melting temperature of double-stranded DNA [21].
12. Due to the presence of borate ions in TBE (Tris/Borate/EDTA) buffer and its inhibitory effect on the ligation process, the TAE (Tris/Acetate/EDTA) buffer preferably replaced for the DNA recovery from agarose gel [21].
13. Following centrifugation, the white layer between the aqueous and organic phase is agarose.
14. The use of phenol in combination with the chloroform can lead to a better separation of the aqueous and organic phases from each other. Of note, since the oxidation products of phenol can degrade the nucleic acids, residual phenol should be removed using the chloroform extraction [21, 35].
15. DNA precipitation can be triggered using ammonium acetate and absolute ethanol. In the presence of salt, ethanol induces the structural alterations in DNA, results in the aggregation and precipitation of DNA molecules [35].
16. Since salts are less soluble in absolute ethanol than in 70% ethanol, washing the pellet with 70% alcohol is recommended to remove the excess salts.
17. Compared to H_2O, TE (Tris-EDTA) buffer can lead to stabilization of the DNA and better dissolution of it by chelating the cationic ions and providing the alkaline conditions, respectively.
18. For further purification of the extracted DNA from the residual restriction enzymes, salts, and inhibitors, the clean-up procedure is typically recommended. These contaminations may cause a reduction in cloning efficiency through interfering with the ligation reaction [21, 36].
19. Reaction volumes larger than 20 μL are not suggested for the ligation process. The typical ligation reaction is usually performed at a final volume of 10 μL to achieve maximum

efficiency. Notice that the remove of the 5′-phosphate using a phosphatase enzyme, such as calf intestinal alkaline phosphatase (CIP) or shrimp alkaline phosphatase (SAP), prevents the re-ligation of the digested vector without any insert when using a single restriction digest or isocadomers [21].

20. The required amount of digested insert for a ligation reaction based on the amount of vector (typically 50–200 ng) and the desired insert/vector molar ratio is calculated as follows:

$$\text{ng of insert} = \frac{\text{ng of vector} \times \text{kb size of insert}}{\text{kb size of vector}} \times \text{Molar ratio of (insert/vector)}$$

Commonly, molar ratios of 1:1, 3:1, and 5:1 (insert/vector) are recommended for ligation reaction. However, the optimization of this ratio to increase the ligation efficiency may be required. Notice that the formation of long linear Concatemers consisting of the repeated subunit of the digested DNA may be induced by the excess DNA, leading to a decrease in the ligation efficiency [18, 21].

21. T4 DNA ligase is an ATP-dependent enzyme; therefore, avoid repeated freeze-thaw cycles of ligase buffer to prevent ATP degradation [21, 37].

22. One Weiss unite is defined as the amount of T4 DNA ligase required to catalyze the exchange of 1 nmole of 32P from inorganic pyrophosphate to ATP in 20 min at 37 °C. Of note, both bacteriophage T4 DNA ligase and *E. coli* DNA ligase can be used during the ligation to form phosphodiester bonds, but bacteriophage T4 DNA ligase is preferably used in the laboratory experiments due to its capacity to join either blunt ends or sticky ends [21, 37].

23. The optimal temperature and incubation time required for an effective ligation reaction can be influenced by factors such as length of ligating fragments and base composition of the overhang sequences. According to literature, blunt-end ligation is commonly performed at 15–25 °C for 4–16 h, whereas sticky ends are ligated efficiently at room temperature (22 °C) for 3 h or at 4 °C overnight [18, 21].

24. *E. coli* strains such as DH5α and JM109, which lack both recA and endA, are typically used for transformation [19]. On the other hand, incubation with gentle agitation at 37 °C ensures the adequate aeration of bacterial culture [21].

25. For maximum efficiency of transformation, the OD of the bacterial culture at 600 nm should not exceed 0.4 ng/μL. In this density, the present bacterial population is at the early- to mid-log phase or at the late logarithmic growth phase, which transformation occurs with the maximum efficiency. Thus,

measure the OD_{600} of the bacterial culture during incubation time by spectrophotometry every 15–20 min. Moreover, to ensure the high transformation efficiency, keep the temperature of the culture and other solutions at 4 °C [21].

26. DNA can bind to the cell surface through the formation of a cationic bridge between negatively charged groups in the lipopolysaccharides inner core and positively charged ions (Mg^{2+}, Ca^{2+}) under cold conditions [38].
27. It is crucial to use the positive and negative controls in the laboratory experiments to evaluate the transformation efficiency and detect the transformation contamination, respectively.
28. A sudden increase in temperature destabilizes the cell membrane and increases its permeability, resulting in the entry of DNA into the competent cells. Afterward, cooling the cells by placing them on ice allows the cell membrane to restore [39].
29. Positive bacteria colonies can be confirmed by the size of the separated insert on an agarose gel.
30. As recommended by plasmid purification protocols, up to 10 mg of endotoxin-free ultrapure plasmid DNA can bind to the Anion-Exchange Resins provided by the kits under appropriate binding conditions.
31. Lipofectamine 2000 is a cationic liposome-based delivery system which promotes DNA uptake by the formation of a complex with genetic materials (positive charges of the liposome vs negative charge of the nucleic acids) and by binding the transfection complex (with positive surface charge) to the negatively charged cell surface by means of electrostatic interactions. Due to the neutral co-lipid (helper-lipid) mediating fusion of the liposome and the cell membrane, the transfection complex can be fused to the cell membrane, resulting in the entry of nucleic acids to the host cytoplasm [24, 40].
32. Cell lines such as HEK (Human embryonic kidney) and COS-7 (Monkey kidney fibroblast cells) are mainly used to evaluate of the desired protein expression because of their high capacity of transfection [23].
33. Since the serum may adversely affect the transfection efficiency, it is recommended to use *Opti-MEM®* Reduced-Serum Medium instead of the other media such as DMEM. Opti-MEM is an improved Minimal Essential Medium (MEM) that allows keeping cells in the reduced serum conditions during the transfection with no change in growth rate or morphology.
34. The transfection efficiency can be influenced by factors such as cell density, the amount of DNA and transfection reagent, incubation time required for the formation of Lipofectamine-

DNA complex, and the presence or absence of components such as antibiotics and serum [24]. Thus, it is recommended to check the manufacturer's guidance for optimal transfection conditions.

35. 260 nm is the wavelength in which nucleic acids have maximum absorbance and the 260/280 ratio of ~2.0 indicates the purity of the RNA sample [41].
36. PrimeScriptTM RT reagent Kit is designed to perform the reverse transcription, optimized for real-time RT-PCR.
37. SYBR Premix Ex Taq (Tli RNaseH Plus) is designed for intercalator-based real-time PCR using SYBR Green I. It is supplied at 2 × concentration and includes SYBR Green I at the appropriate concentration for real-time monitoring.
38. The amount of anesthesia can be varied, depending on the strain, age, and weight of the mouse [42].
39. Determination of the appropriate route for vaccination can be affected by the factors such as the purpose of the study and the chemical and physical properties of the deployed vaccine or adjuvant [43]. On the other hand, it has been determined that the memory T-cells population can be primed following the subsequent encounter with the same antigen at 1- or 2-week intervals called as the memory checkpoint [44]. Therefore, the mice vaccination is carried out more than one time with appropriate intervals to promote the stronger cellular mediated immune response.
40. Carbonate-bicarbonate buffer is one the most common coating buffer used in ELISA procedure. The high pH of this buffer has an important role to facilitate binding proteins to a positively charged plate through deprotonation of proteins [45].
41. Tween 20 is a nonionic detergent commonly used in washing and blocking buffers to prevent nonspecific adsorption of proteins on the surface of ELISA Microwells by blocking the nonspecific sites, decreasing the nonspecific background signals, and increasing the sensitivity of the ELISA. Additionally, incorporation of Tween 20 in combination with other blocking reagents such as BSA improves its prevention ability [46].
42. Quantitative ELISA also can be used to determine the accurate concentration of antigen-specific antibody. In this procedure, standard proteins with known concentrations are used to draw a standard curve using the absorption data at 450 nm obtained from the serial diluted standard proteins. Consequently, the concentration of specific antibody can be determined by interpolating the ELISA data from the standard curve.

43. If incubation time lasts longer than 5 min, the lymphocyte cells will also be lysed.
44. Using the trypan blue staining method, live and dead cells appear colorless and blue, respectively.
45. The yellow MTT is reduced to purple formazan crystals by the dehydrogenase enzyme that is only produced by the mitochondria of active living cells.
46. Since the production of formazan crystals is proportional to the number of living cells, the intensity of the produced color is an appropriate indicator for the viability of the cells. The formazan crystals are insoluble in aqueous solutions and thus it is dissolved in DMSO or acidified isopropanol.
47. Due to the PVDF membrane's white color which provides an ideal backdrop for ELISpot enumeration and its high capacity to bind the particular antibodies, PVDF membrane-bottomed 96-well plates are considered as a good candidate to check the frequency of cytokine-positive cells [47].
48. The cell viability and antibody binding capacity can be adversely affected by ethanol.
49. If the expression level of the desired protein is low, more cells should be used to compensate for this deficiency.
50. According to the BioLegend protocol, 24 h incubation for IFN-γ, IL-2, and TNF-α, as well as 48 h incubation for IL-4, IL-5, and IL-10 is recommended. Of note, incubation with shaking can lead to the formation of undefined spots on the PVDF membrane. Therefore, do not shake or move the plate during the incubation time.
51. Tween 20 helps to wash the nonspecifically attached cells from the PVDF membrane during the overnight incubation [29]. Of note, the use of an automatic plate washer in this stage can lead to damage to the integrity of the PVDF membrane.
52. Incubation at 4 °C results in the sharper spots.

Acknowledgement

The authors would like to acknowledge Pasteur Institute of Iran for the financial support. This work was supported by Pasteur Institute of Iran (grant 1029).

References

1. Iurescia S, Fioretti D, Rinaldi M (2014) Strategies for improving DNA vaccine performance. Methods Mol Biol 1143:21–31
2. Raska M, Turanek J (2015) DNA vaccines for the induction of immune responses in mucosal tissues. Mucosal Immunol 2:1307–1335
3. Li L, Petrovsky N (2017) Molecular adjuvants for DNA vaccines. Curr Issues Mol Biol 22:17–40
4. Borja-Cabrera GP, Santos FB, Nico D et al (2012) The Leishmune® s nucleoside hydrolase DNA vaccine as an aid in immunotherapy of canine visceral leishmaniasis. Procedia Vaccinol 6:64–73
5. Li L, Petrovsky N (2016) Molecular mechanisms for enhanced DNA vaccine immunogenicity. Expert Rev Vaccines 15:313–329
6. Fotouhi F, Shaffifar M, Farahmand B et al (2017) Adjuvant use of the NKT cell agonist alpha-galactosylceramide leads to enhancement of M2-based DNA vaccine immunogenicity and protective immunity against influenza a virus. Arch Virol 162:1251–1260
7. Saade F, Petrovsky N (2012) Technologies for enhanced efficacy of DNA vaccines. Expert Rev Vaccines 11:189–209
8. Suschak JJ, Williams JA, Schmaljohn CS (2017) Advancements in DNA vaccine vectors, non-mechanical delivery methods, and molecular adjuvants to increase immunogenicity. Hum Vaccin Immunother 13:2837–2848
9. Kim JJ, Yang J-S, Dentchev T, Dang K et al (2000) Chemokine gene adjuvants can modulate immune responses induced by DNA vaccines. J Interf Cytokine Res 20:487–498
10. Okuda K, Kawamoto S, Fukushima J (2000) Cytokine and costimulatory factor-encoding plasmids as adjuvants for DNA vaccination. Methods Mol Med 29:197–204
11. Wang B, Kang Y, Ascione R (2012) Cytokine genes as molecular adjuvants for DNA vaccines. Gene Vaccines 1:89–107
12. Scheerlinck J-PY (2001) Genetic adjuvants for DNA vaccines. Vaccine 19:2647–2656
13. Bugeon L, Dallman MJ (2000) Costimulation of T cells. Am J Respir Crit Care Med 162: S164–S168
14. Dalod M, Chelbi R, Malissen B et al (2014) Dendritic cell maturation: functional specialization through signaling specificity and transcriptional programming. EMBO J 33:1104–1116
15. Cohn L, Delamarre L (2014) Dendritic cell-targeted vaccines. Front Immunol 5:255
16. Villarreal DO, Svoronos N, Wise MC et al (2015) Molecular adjuvant IL-33 enhances the potency of a DNA vaccine in a lethal challenge model. Vaccine 33:4313–4320
17. Lladser A, Mougiakakos D, Tufvesson H et al (2011) DAI (DLM-1/ZBP1) as a genetic adjuvant for DNA vaccines that promotes effective antitumor CTL immunity. Mol Ther 19:594–601
18. Casali N, Preston A (2003) *E coli* plasmid vectors: methods and applications, vol 235. Springer Science & Business Media, New York, pp 121–140
19. Humbert MV (2019) Cloning, expression, and purification of recombinant *Neisseria gonorrhoeae* proteins. Methods Mol Biol 1997:233–266
20. Madigan MT, Martinko JM, Bender KS et al (2014) Brock biology of microorganisms, 14th edn. Benjamin Cummings, San Francisco, pp 316–331
21. Sambrook J, Russell DW (2001) Molecular cloning: a laboratory manual, vol 1, 3th edn. Cold Spring Harbor Laboratory Press, New York, pp 1.84–1.119
22. Green MR, Sambrook J (2012) Molecular cloning: a laboratory manual, vol 1, 4th edn. Cold Spring Harbor Laboratory Press, New York, pp 157–261
23. Gupta SK, Dey S, Chellappa MM (2016) DNA vaccination in chickens. Methods Mol Biol 1404:165–178
24. Dalby B, Cates S, Harris A et al (2004) Advanced transfection with Lipofectamine 2000 reagent: primary neurons, siRNA, and high-throughput applications. Methods 33:95–103
25. Saeedi A, Ghaemi A, Tabarraei A et al (2014) Enhanced cell immune responses to hepatitis C virus core by novel heterologous DNA prime/lambda nanoparticles boost in mice. Virus Genes 49:11–21
26. Naderi M, Saeedi A, Moradi A et al (2013) Interleukin-12 as a genetic adjuvant enhances hepatitis C virus NS3 DNA vaccine immunogenicity. Virol Sin 28:167–173
27. Davtyan H, Petrushina I, Ghochikyan A (2014) Immunotherapy for Alzheimer's disease: DNA-and protein-based epitope vaccines. Methods Mol Biol 1143:259–281
28. Hjertner B, Bengtsson T, Morein B et al (2018) A novel adjuvant G3 induces both Th1 and Th2 related immune responses in mice after immunization with a trivalent

inactivated split-virion influenza vaccine. Vaccine 36:3340–3344

29. Fourati IS, Grenier A-J, Jolette É et al (2014) Development of an IFN-γ ELISpot assay to assess varicella-zoster virus-specific cell-mediated immunity following umbilical cord blood transplantation. J Vis Exp 89:e51643
30. Baumann T, Arndt KM, Müller KM (2013) Directional cloning of DNA fragments using deoxyinosine-containing oligonucleotides and endonuclease V. BMC Biotechnol 13:1–11
31. Bola G (2005) Evaluating the role of G, C-nucleotides and length of overhangs in T4 DNA ligase efficiency. J Exp Microbiol Immunol 8:1–7
32. Gerstein AS (2001) Molecular biology problem solver: a laboratory guide. John Wiley & Sons, Hoboken, New Jersey, pp 225–266
33. Farell EM, Alexandre G (2012) Bovine serum albumin further enhances the effects of organic solvents on increased yield of polymerase chain reaction of GC-rich templates. BMC Res Notes 5:257
34. Tong J, Barany F, Cao W (2000) Ligation reaction specificities of an NAD+-dependent DNA ligase from the hyperthermophile Aquifex aeolicus. Nucleic Acids Res 28:1447–1454
35. Moore D, Dowhan D (2002) Purification and concentration of DNA from aqueous solutions. Curr Protoc Mol Biol 59:2.1.1–2.1.10
36. Ihle Ø, Michaelsen TE (2000) Efficient purification of DNA fragments using a protein binding membrane. Nucleic Acids Res 28:e76
37. Tabor S (2001) DNA ligases. Curr Protoc Mol Biol. Chapter 3: 3.14.1-3.14.4
38. Chang AY, Chau V, Landas JA et al (2017) Preparation of calcium competent Escherichia coli and heat-shock transformation. JEMI Methods 1:22–25
39. Panja S, Aich P, Jana B et al (2008) How does plasmid DNA penetrate cell membranes in artificial transformation process of *Escherichia coli*? Mol Membr Biol 25:411–422
40. Escriou V, Ciolina C, Helbling-Leclerc A et al (1998) Cationic lipid-mediated gene transfer: analysis of cellular uptake and nuclear import of plasmid DNA. Cell Biol Toxicol 14:95–104
41. Desjardins P, Conklin D (2010) NanoDrop microvolume quantitation of nucleic acids. J Vis Exp 45:e2565
42. Gargiulo S, Greco A, Gramanzini M et al (2012) Mice anesthesia, analgesia, and care, part I: anesthetic considerations in preclinical research. ILAR J 53:E55–E69
43. Shimizu S (2004) Routes of administration. The laboratory mouse chapter 32:527–541
44. Devarajan P, Bautista B, Vong AM et al (2016) New insights into the generation of CD4 memory may shape future vaccine strategies for influenza. Front Immunol 7:1–7
45. TIP T (2010) ELISA technical guide and protocols. Thermo Fisher Scientific Inc USA, Bartlesville, OK
46. Steinitz M (2000) Quantitation of the blocking effect of tween 20 and bovine serum albumin in ELISA microwells. Anal Biochem 282:232–238
47. Weiss AJ (2012) Overview of membranes and membrane plates used in research and diagnostic ELISPOT assays. Method Mol Biol 792:243–256

Chapter 6

Assessing Antigen-Specific Cellular Immune Responses upon HIV/SIV Plasmid DNA Vaccination in the Nonhuman Primate Model

Xintao Hu, Barbara K. Felber, and Antonio Valentin

Abstract

Reliable detection and quantification of antigen-specific T cells are critical for assessing the immunogenicity of vaccine candidates. In this chapter, we describe the use of ELISpot and flow cytometry-based assays for efficient detection, mapping, and functional characterization of memory T lymphocytes in different tissues of rhesus macaques immunized with plasmid DNA. Flow cytometric assays provide a large amount of information, both phenotypic and functional, about individual cells, while the ELISpot is well suited for high throughput sample screening.

Key words CD4, CD8, DNA Vaccine, ELISpot, Flow cytometry, HIV, Macaque, Peptide, SIV, Tetramer

1 Introduction

The ability to recognize antigens and differentiate into memory cells is a function related to the specific interaction between specialized lymphocyte surface receptors, the T-cell receptor (TCR) and the surface immunoglobulins for T and B lymphocytes, respectively, and foreign molecules. Being able to monitor antigen binding to the TCR, and the downstream functional responses triggered by antigen recognition, provides a tool for the evaluation of the immunogenicity of any vaccine candidate. We and other groups designed and developed DNA-based vaccines for both prophylactic and therapeutic interventions against SIV/HIV infection (reviewed in [1–4]). Using the rhesus macaque animal model, we have shown that DNA vaccines induce potent, long-lasting cytotoxic T-cell responses that disseminate systemically, including mucosal sites, and efficiently contribute to control of viremia [5–12].

Ângela Sousa (ed.), *DNA Vaccines: Methods and Protocols*, Methods in Molecular Biology, vol. 2197,
https://doi.org/10.1007/978-1-0716-0872-2_6,

The two most commonly used techniques for the evaluation of antigen-specific T-cell responses are enzyme-linked immunospot assay (ELISpot), established in 1983 [13] and widely used in the HIV vaccine field [14–16] and flow cytometric analysis based on discovery by Fulwyler [17] and further developed to characterize cell subsets and their functional properties including measurements of intracellular cytokine production upon HIV vaccination and infection (reviewed in [18–22]). The ELISpot assay is very efficient for high throughput screening of samples and is also used for the identification of single peptides responsible for the T-cell responses identified upon stimulation with a complex peptide mixture (epitope mapping). Although ELISpot screening is efficient and reliable, the assay does not provide any information about the phenotype of the responding cells, and in most cases is restricted to the detection of a single secreted protein. In contrast, flow cytometry-based assays are able to combine many parameters simultaneously, including cell phenotype and functional responses, within the same sample, and accurately identify complex responses and polyfunctionality of single cells [23–25].

This chapter will address the analysis of antigen-specific responses by T lymphocytes, although similar technology can be used for monitoring antigen-specific B cells (reviewed in [26–28]). The following protocols were mainly used in the analysis of primary samples from DNA immunized macaques, but, obviously, the procedures can be implemented to monitor T-cell responses in many different systems (other vaccine platforms, other infection models or different species).

The ELISpot used in our studies is to map specific epitopes and, importantly, to address the ability to release perforin upon antigen recognition [9]. We used this functional assay to quantify the number of antigen-specific T cells releasing perforin more accurately than flow-based assays because the rapid degranulation induced by the peptide binding to the TCR rapidly empties the intracellular perforin from many of the interferon-γ (IFN-γ) secreting T cells [9]. The flow cytometry-based assays provide information about the phenotype of the antigen-specific T cells combined with the detection of several intracellular cytokines produced in response to the antigen, cytotoxic potential and proliferative responses. The use of tetramers allows the identification of antigen-specific $CD8^+$ T cells (class I tetramers) without the need of stimulating the cells in vitro [29, 30], which is an advantage for the analysis of the vaccine-induced T cells dissemination into anatomical locations [10], such as the gastrointestinal tract, that typically yield a fragile lymphocyte population for in vitro studies. It is worth to mention that tetramer staining can be combined with immune phenotyping using as many surface markers as desired, and also with intracellular cytokine staining in peptide-stimulated samples, collecting functional information of the diverse $CD8^+$ T cells with a single peptide specificity.

2 Materials

Precautions: All human and nonhuman primate (NHP) blood and tissue samples must be handled inside a Biosafety Cabinet (BSC) in a Biosafety Level-2* (BSL-2*) laboratory facility. Precise information and adequate training are mandatory for all personnel involved in the processing of human and monkey blood and tissues within the BSL-2* facility. All centrifugations must be performed using buckets equipped with aerosol containment lids. Placing and removal of tubes from the buckets must be performed inside a BSC. The BSC must be cleaned with CaviCide or other equivalent disinfectant before and after completion of the work. All the materials, bottles, and cryovials with the viable frozen cells must be cleaned with CaviCide or a similar disinfectant before bringing them to the BSC.

2.1 Common Reagents, Materials, and Equipment

1. Phosphate Buffer Saline (PBS) without calcium and magnesium, pH 7.4.
2. Distilled water.
3. RPMI medium 1640 (1×): with L-glutamine and phenol red, no sodium pyruvate, no HEPES.
4. R-10 medium: RPMI medium 1640 supplemented with 10% fetal calf serum (FCS), penicillin (100 U/mL) and streptomycin (100 μg/mL). Store at 4 °C.
5. Cell counting dye: 2 μL Ethidium Bromide (from 1% stock) and 2 μL Acridine Orange (from 10 mg/mL stock) into 10 mL of 1 × PBS. Store at 4 °C wrapped in foil for up to 2 months.
6. R-10/DNase I medium: R-10 medium containing DNase I (30 U/mL).
7. 15 mL and 50 mL conical tubes.
8. Disposable transfer pipettes.
9. CaviCide or other equivalent disinfectant.
10. Benchtop Centrifuge, for example we used Sorvall Legend XTR (roter: TX-1000) by Thermo Fisher.
11. Incubator (5% CO_2 and 37 °C).
12. Fluorescence Microscope.

2.2 Reagents and Materials for the Processing and Storage of NHP Blood Samples

1. Ficoll-Paque PLUS: density 1.077 g/mL (store at room temperature (RT) in the dark).
2. Lonza BioWhittaker™ ACK Lysing Buffer.
3. Freezing medium (90% FCS+ 10% DMSO). Freezing medium must be prepared the same day and kept at 4 °C until use.
4. Controlled-rate freezer or alternative (*see* **Note 1**).
5. −80 °C freezer.

6. Liquid nitrogen tank.
7. Floating cryotube rack.

2.3 Reagents for the Processing of NHP Tissues

1. 70% ethanol (store at RT for up to 1 week).
2. Sterile forceps and blunt-end scissors.
3. Digestion solution: R-10 medium containing DNase I (30 U/mL) and Liberase (5 μg/mL) or collagenase (200 U/mL).
4. Plunger of a 3 mL syringe.
5. 100 μm cell strainer.
6. Lab shaker or rocker able to hold 15 mL and 50 mL conical tubes.

2.4 Reagents List for ELISpot Assay

1. Monkey IFN-γ ELISpot^{PLUS} (Mabtech AB):

   Strip plates pre-coated with mAb MT126L (anti-human/monkey IFN-γ mAb) as capture antibody.

   Biotinylated detection mAb 7-B6-1(anti-human/monkey IFN-γ mAb) supplied in sterile filtered (0.2 μm) PBS with 0.02% sodium azide.

   Streptavidin-ALP provided in 0.1 M Tris buffer with 0.002% Kathon CG.

   Anti-human CD3 mAb CD3-1 (cross-reactive with cynomolgus and rhesus macaque) as positive control (*see* **Note 2**) supplied in sterile filtered (0.2 μm) PBS.

2. Human Perforin ELISpot^{PLUS} (Mabtech AB):

   Strip plates pre-coated with mAbs Pf-80/164 (anti-human Perforin mAb, cross-reactive with NHP) as capture antibody.

   Biotinylated detection mAb Pf-344 (anti-human Perforin mAb, cross-reactive with NHP) supplied in sterile filtered (0.2 μm) PBS with 0.02% sodium azide.

   Streptavidin-ALP supplied in 0.1 M Tris buffer with 0.002% Kathon CG.

   Peptide pools and individual peptides for epitope mapping.

3. BCIP/NBT-plus substrate: filtered (0.22 μM membrane) before use.

2.5 Reagents, Materials, and Equipment for Flow Cytometry-Based Assay (Peptide Stimulation to Evaluate the Antigen-Specific T-Cell Responses)

1. Round-bottom 96-well cell culture plates.
2. Peptide pools (15-mer overlapping by 11 a.a) (*see* **Note 3**).
3. Cell stimulation cocktail (500 ×): PMA (Phorbol 12-Myristate 13-Acetate) and calcium ionophore (Ionomycin).
4. BD GolgiStop working solution (contains monensin, a protein transport inhibitor).
5. FACS surface staining washing buffer: PBS supplemented (0.2%) with heat-inactivated AB human serum (*see* **Note 4**).

6. T-cell antibody panel. The combination of markers included in the antibody panel obviously depends on the technical specifications of the flow cytometer available for each researcher. One of the common panels used in our cytometer (BD LSRFortessa) includes anti-CD107a (clone: eBioH4A3), anti-CD3 (clone: SP34-2), anti-CD4 (clone: L200), anti-CD8 (clone: 3B5), anti-CD28 (clone: CD28.2), anti-CD95 (clone: DX2), anti-IFN-γ (clone: B27), anti-Granzyme B (GrzB) (clone: GB12) and anti-Ki-67 (clone: B56) (*see* **Note 5**).
7. UltraComp eBeads Compensation Beads (*see* **Note 6**).
8. Foxp3/Transcription Factor staining buffer set: Fixation/Permeabilization concentrate, Fixation/Permeabilization diluent, and Permeabilization buffer (10×). The Fixation/Permeabilization buffer (referred to as Foxp3 fixation buffer) is prepared freshly by mixing 1 part of concentrate with 3 parts of diluent. The Permeabilization buffer (referred to as Foxp3 Perm/Wash buffer) is diluted to 1× with distilled water and can be stored at 4 °C for up to 1 month (*see* **Note 7**).
9. Flow cytometer.

2.6 Reagents for Tetramer Staining

1. Fluorochrome conjugated Tetramer/ MamuA*01 SIV Gag CM9 (CTPYDINQM).
2. FACS fixation buffer: BD Fixation/Permeabilization solution.
3. BD Perm/Wash Buffer (the concentrate must be diluted tenfold with distilled water and stored at 4 °C).
4. Antibody panel for T-cell markers. The panel should include, at last, anti-CD3 (clone: SP34-2), anti-CD4 (clone: L200) and anti-CD8 (clone: 3B5) (*see* **Note 5**).
5. Other reagents and equipment described in Subheading 2.5.

3 Methods

3.1 Processing of Blood Samples and Freezing and Thawing of Peripheral Blood Mononuclear Cells (PBMC)

3.1.1 Plasma Separation

1. Spin the blood tubes at 1460 × *g* for 10 min at RT.
2. Collect the plasma and transfer to 15 mL conical tubes.
3. Spin the conical tubes containing plasma at 3739 × *g* for 10 min at RT.
4. Aliquot the plasma into cryogenic tubes and store at −80 °C (from 10 mL blood, expect 4–5 mL plasma).

3.1.2 PBMC Isolation Using Ficoll-Paque PLUS and Freezing Viable PBMC

1. After removing the plasma, mix the compacted blood cells with PBS increasing the volume to 10 mL (for a 15 mL conical tube) or 30 mL (for separation in 50 mL tubes) (*see* **Note 8**). If there

are several tubes from the same animal, they can be combined before the Ficoll separation.

2. Add 5 mL of Ficoll-Paque PLUS into a 15 mL conical tube (or 15 mL for a 50 mL conical tube).
3. Carefully, overlay the diluted blood on top of the Ficoll-Paque PLUS: place the pipette to the inner surface of the tube and let the blood slide down on top of the Ficoll-Paque PLUS using the "slow" position of the pipettor.
4. Spin at 757 × *g* for 30 min at RT with the centrifuge Brake OFF.
5. Collect the mononuclear cells (ring of cells from the interphase) with a pipette in a circular motion trying to avoid taking Ficoll as much as possible (collect the cells from the top of the ring). Transfer the cells into a new 15 mL or 50 mL conical tube.
6. Fill up the tube with 1 × PBS, mix, and spin at 526 × *g* for 10 min at RT with the Brake ON (*see* **Note 9**).
7. Discard the liquid.
8. If there is significant red blood contamination (the cell pellet is entirely red), resuspend the cells in 3 mL of Lonza BioWhittaker™ ACK Lysing Buffer using a plastic transfer pipette. Incubate the cells for 5 min at RT (remember, this step is needed only if the sample is significantly contaminated with red blood cells).
9. Fill up the tube with PBS, mix, and spin at 336 × *g* for 10 min at RT.
10. Remove supernatant and resuspend the pellet in 10–20 mL of PBS containing 0.5% FCS or R-10 medium by gently pipetting up and down using a plastic transfer pipette (make sure that you get a perfect single-cell suspension).
11. Count the cells using Acridine Orange/Ethidium Bromide dye (1:2 dilution) under the fluorescence microscope.
12. Resuspend the PBMC in freezing medium at a density of 5–ten million cells/mL. Aliquot the cells in cryovials and immediately transfer into the rate freezer (*see* **Note 1**) to complete the programmed freezing before moving the samples to the liquid nitrogen tank for long-term storage.

3.1.3 Thawing Procedure of PBMC

Retrieve the PBMC vials from the liquid nitrogen and transport them on dry ice to the BSL-2* facility. Handle 2–3 vials at a time.

1. To thaw the cells, place the vials in a floating cryotube rack inside a beaker filled with lukewarm water. Gently shake the vials after ~1 min incubation. The thawing takes less than 5 min.

2. Transfer the cells to a 15 mL conical tube.
3. Dropwise, add pre-warmed R-10 medium to a final volume of 10 mL.
4. Gently, invert the tubes several times (at least three times).
5. Spin at 336 × *g* for 10 min at RT.
6. Discard the supernatant and resuspend the cells in 3 mL pre-warmed R-10/DNase I medium.
7. Incubate at 37 °C for 1 h.
8. Spin the cells, discard the supernatant, and resuspend the cells in an appropriate volume of pre-warmed R-10 medium.
9. Count the cells (*see* **step 15** of Subheading 3.1.2) and then seed cells in the proper culture plates for the subsequent experiment.

3.2 Isolation of Lymphocytes from Tissues

The fresh tissues should be shipped to the lab in tubes filled with RPMI-1640 medium and placed on wet ice. Shipment should take place immediately after collecting the samples to improve the viability of the cells.

1. Carefully, remove the tissue from the tube and place it in a Petri dish along with RPMI-1640 medium.
2. Hold the tissue using sterile forceps and cut it into small pieces with sterile blunt-end scissors (this step is necessary only when we get large pieces of tissue).
3. Collect all the pieces and transfer them into a 50 mL conical tube containing 30 mL of pre-warmed digestion solution. If the size of the tissue is small, the digestion can be done with 10 mL of digestion solution in a 15 mL conical tube.
4. Incubate the samples at 37 °C on a lab shaker or rocker for 60 min.
5. After the incubation, pass the medium and digested tissue through a 100 μm cell strainer placed on top of a 50 mL conical tube. Use the plunger of a 3 mL syringe to crush the fragments of the tissue. Typically, two 100 μm cell strainers are used for each piece of digested tissue. Collect the medium and cells passing through the strainer in 50 mL conical tubes.
6. Give a brief spin at 58 × *g* (10 s) to pull down debris from the digestion.
7. Transfer the supernatant into a new 50 mL tube. Fill up to 50 mL by adding sterile PBS containing 1% FCS. Centrifuge at 336 × *g* for 10 min.
8. Discard supernatant and resuspend the pellet in 10 mL of R-10 medium. Transfer into 15 mL conical tubes.

9. Spin down at 336 × *g*, discard the supernatant. Then resuspend the pellet in R-10 medium to count the cells, and the cells are ready to be cultured or used for the subsequent tetramer staining.

3.3 ELISpot Assay to Enumerate the Antigen-Specific Cells Secreting IFN-γ or Perforin upon Peptide Stimulation

The ELISpot assay is a highly sensitive method to quantify the cells secreting cytokines upon peptide stimulation and particularly useful for high throughput mapping of the peptide responses at significant lower cost. Additionally, the ELISpot assay provides an advantage for the detection of some biomarkers, such as Perforin, that are actively released by cytotoxic cells after TCR recognition of the cognate peptide, resulting in a significant drop of the perforin content among the IFN-γ secreting cells [9]. The procedure can be performed using either cryopreserved or fresh lymphocyte samples. All the procedures described during day1 should be performed under sterile conditions.

Day 1: Assembling ELISpot plates in BSC

1. Assemble the required number of strips in the plate frame and mark the plates or strips with experiment date and other information according to the designed plate layout (see one example shown in Fig. 1, panel A) (*see* **Note 10**).
2. Wash the assembled plates five times with sterile PBS (200 μL/well) using a 12-well multichannel pipette.
3. To condition the plates, add 200 μL of R10 medium to each well. Incubate at RT for at least 30 min.

Day 1: Thawing of PBMC (fresh PBMC can be used as well)

4. Thaw the required PBMC by following the procedure of Subheading 3.1.3.
5. Spin down the cells at 336 × *g* for 10 min.
6. Resuspend the cells in 3 mL of R10 medium containing 30 U/mL DNase I, loosen the cap and incubate the cells at 37 °C and 5% CO_2 for 1 h.

Day 1: Preparation and addition of peptides

7. During the PBMC treatment with DNase I, dilute the peptides with R-10 medium to a concentration of 2 μg/mL for every single peptide or peptide pool (this is a 50-fold dilution for our standard 100 × peptide stocks).
8. Remove the R-10 medium of the plates (Ensure the plate conditioning has been done for at least 30 min).
9. Add 100 μL of diluted 2 × peptide pool (2 μg/mL) to each test well (peptide stimulation) using a 12-well multichannel pipette. An equal volume of plain R-10 medium and CD3-1 antibody diluted in R-10 medium (1000 × dilution) are added into the negative and positive control wells, respectively.

a

	Macaque-1			Macaque-2			Macaque-3			Macaque-4		
	1	2	3	4	5	6	7	8	9	10	11	12
A	p-82	p-82	Neg	p-82	p-82	Neg	p-82	p-82	Neg	p-82	p-82	Neg
B	p-83	p-83	Neg	p-83	p-83	Neg	p-83	p-83	Neg	p-83	p-83	Neg
C	p-84	p-84	Neg	p-84	p-84	Neg	p-84	p-84	Neg	p-84	p-84	Neg
D	p-85	p-85	Neg	p-85	p-85	Neg	p-85	p-85	Neg	p-85	p-85	Neg
E	p-86	p-86	**p-90**	p-86	p-86	p-90	p-86	p-86	**p-90**	p-86	p-86	p-90
F	p-87	p-87	**p-90**	p-87	p-87	p-90	p-87	p-87	**p-90**	p-87	p-87	p-90
G	p-88	p-88	Pos	p-88	p-88	Pos	p-88	p-88	Pos	p-88	p-88	Pos
H	p-89	p-89	Pos	p-89	p-89	Pos	p-89	p-89	Pos	p-89	p-89	Pos

b

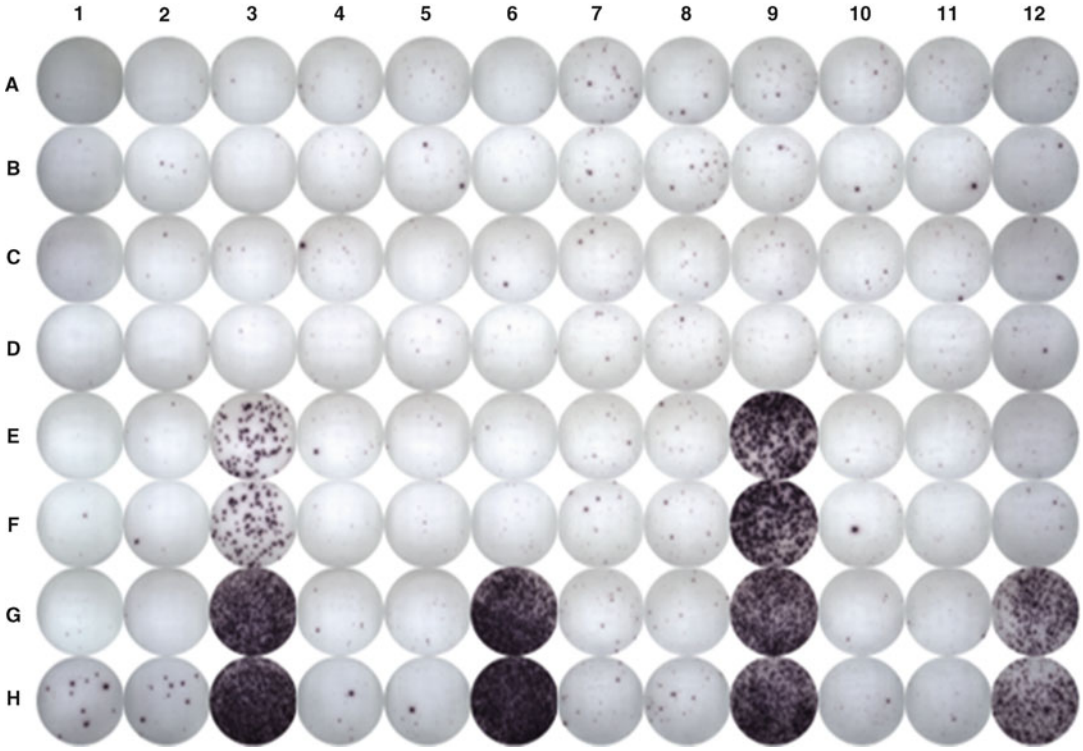

Fig. 1 Peptide mapping by IFN-γ ELISpot using PBMC from HIV $p55^{Gag}$ DNA immunized rhesus macaques. (**a**) Layout for mapping the responses within peptides 82–90 of HIV-1 $p55^{Gag}$ for 4 animals (coded as different colors) in a 96-well plate. PBMC collected 2 weeks after the second HIV $p55^{Gag}$ DNA vaccination were used in the IFN-γ ELISpot assay. Cells treated with medium only (labeled in the layout as "Neg") were run in quadruplicate wells and served as negative control. The anti-CD3 antibody (CD3-1, labeled in the layout as "Pos" in duplicate wells) was added as positive control. Equal amount of the single peptides (final concentration: 1 μg/mL) was added to the test wells (duplicates) to stimulate the antigen responses. (**b**) Image of the IFN-γ ELISpot plate (layout shown in **a**) read by the CTL-ImmunoSpot Plate Reader. The examples show that the positive controls are positive, the negative controls are negative and the wells incubated with peptide 90 are strongly positive in two of the animals (macaques 1 and 3) but negative for the other two (macaques 2 and 4)

Day 1: Counting and seeding the cells

10. After the DNase I treatment, count the cells according to **step 15** in Subheading 3.1.2. Resuspend the cells at a density of 1–2 × 10^6/mL in R-10 medium.
11. Put all the cells in the reagent reservoir. Gently mix and using a 12-well multichannel pipette add 100 μL of cell suspension into each well.
12. Wrap the plate with aluminum foil to avoid evaporation and incubate for 16 h at 37 °C in a humidified incubator with 5% CO_2 (*see* **Note 11**). Keep the incubation time constant for all the samples within the same study.

Day 2: Plate development

13. After 16 h incubation, discard the cells into the waste container inside the BSC and wash the plates five times with PBS (200 μL/well).
14. Dilute the detection antibody (for example, 7-B6-1-Biotin for IFN-γ detection, biotinylated mAb Pf-344 for Perforin detection) to 1 μg/mL in sterile PBS containing 0.5% FCS and add 100 μL/well. Incubate for 2 h at RT.
15. Wash the plate for five times as above (**step 13**).
16. Dilute the Strep-ALP 1:1000 in sterile PBS containing 0.5% FCS, and add 100 μL/well. Incubate for 1 h at RT.
17. Wash the plate for five times as above (**step 13**).
18. Add 100 μL of filtered BCIP/NBT-plus substrate solution and develop for about 15 min until spots emerge. Keep the development time constant for all the samples within the same study.
19. Stop the color development by washing five times with water (200 μL/well).
20. Leave the plates to dry inside the BSC (overnight).

Day 3: Spots detection

21. The spots are visualized and counted using the ImmunoSpot Imaging Analyzer system and ImmunoSpot software v7.0. (within 1 week).
22. All wells are counted with set parameters and then each count was verified to ensure the accuracy of the counting software. ELISpot results are expressed as the "number of spots per 10^6 cells" after subtracting the background spots obtained in wells containing cells without peptide stimulation (medium only). Figure 1 shows an example of a layout and ELISpot readout for a 96-well plate for IFN-γ measurement.

3.4 Peptide Stimulation to Evaluate the Antigen-Specific T-Cell Responses by ICS/Flow Cytometry

Flow cytometric analysis of peptide-stimulated lymphocytes is a powerful technique able to provide a large amount of information by combining intracellular and cell-surface staining of the antigen-specific T cells. The procedure can be performed using either cryopreserved or fresh lymphocyte samples.

Day 1: Peptide stimulation of primary lymphocytes

1. Resuspend the cells at a density of 7×10^6/mL in pre-warmed R-10 medium. Add 100 μL of the cell suspension to each well (96-well plates).
2. Dilute the peptide pools (100×) with R-10 medium to a concentration of 2 μg/mL of each peptide (corresponds to a 50-fold dilution). For each specimen, one well should be kept in plain R-10 medium without peptides as the negative control. Keep also one well for pharmacological stimulation as a positive control (only one or two wells for the experiment, there is no need of keeping a positive control for each specimen tested).
3. Add 100 μL of the 2× peptide pools (2 μg/mL) into each well (resulting in cell density of 3.5×10^6/mL with a final peptide concentration of 1 μg/mL).
4. Add 100 μL of 2× Cell Stimulation Cocktail solution (diluted in R-10 medium) to the positive control wells (final concentration should be 50 ng/mL and 250 ng/mL for PMA and calcium ionophore, respectively).
5. Add monensin (BD GolgiStop Protein Transport Inhibitor) to each well 30 min after adding the peptides (*see* **Note 12**).
6. Incubate the plate for 6–12 h at 37 °C (do not exceed 12 h because monensin is toxic beyond this time). If the staining is not going to be performed immediately after the incubation, the plate can be kept at 4 °C.

Day 2: Surface staining

7. Transfer the cells into 15 mL conical tubes. Add 10 mL of FACS surface staining buffer and centrifuge at 336 × *g* for 10 min at RT.
8. Discard the fluid and leave the tubes upside down on a paper towel (five tubes at a time).
9. Resuspend the cell pellet in the antibody cocktail (make sure to mix well the cells with the antibodies by pipetting several times) and incubate for 20 min at RT protecting the samples from light. The composition of the antibody mix depends on the experimental design and/or the type of flow cytometer available to the investigator. We typically include CD3, CD4, CD8, CD28, CD95, and CD107a to address the memory phenotype and degranulation ability of the $CD4^+$ and $CD8^+$ T-cell subsets. Surface staining Ab cocktail preparation as shown in Table 1 as one example.

10. After the incubation, fill the tubes with 10 mL of plain PBS and spin for 10 min at 336 × *g*.
11. Discard the supernatant and leave the tubes upside down on a paper towel.
12. To fix the cells, resuspend the cell pellet in 200 μL of Foxp3 fixation buffer and incubate for 30 min at 4 °C (*see* **Note 13**).

Day 2: Intracellular staining and data acquisition

The composition of the antibody mixture for the intracellular staining will depend on the scope of the experiment and the configuration of the flow cytometer. The most common antibody cocktail used in our lab for the analysis of antigen-specific T-cell responses includes GrzB, IFN-γ, and Ki67, which allows the monitoring of antigen-specificity, cytotoxic potential, and proliferative responses.

Intracellular staining Ab cocktail preparation as shown in Table 1 as one example.

1. Add 3 mL of FoxP3 Perm/Washing buffer and centrifuge at 336 × *g* for 10 min.

Table 1
Antibody cocktail for both surface staining and intracellular staining for one reaction upon peptide stimulation in PBMC

Antibody	Volume
Surface staining	
CD3-APC Cy7	2
CD4-V500	2.5
CD8-AF405	2
CD28-PerCP Cy5.5	2
CD95-FITC	10
CD107a-PE	2.5
Total volume (μL)	21
Antibody (buffer)	Volume
Intracellular staining	
IFN-γ-PE Cy7	2.5
GrzB-APC	0.5
KI67-AF700	2.5
1× FoxP3 perm/wash buffer	94.5
Total volume (μL)	100

2. Discard the fluid and add 100 μL of the antibody cocktail for intracellular staining (this cocktail should be prepared in 1× Foxp3 Perm/Washing buffer to make sure that the cells remain permeabilized during the incubation). Incubate for 20 min at RT.
3. Add 3 mL of 1× Foxp3 Perm/Washing buffer and centrifuge at 336 × *g* for 10 min.
4. Discard the supernatant, resuspend the cells in 300 μL of PBS, and transfer the cells into flow tubes to run the samples in the flow cytometer.
5. Analyze the data using any software suitable to read FCS data files. Figure 2 represents a gating strategy and analysis of antigen-specific cytotoxic T-cell responses in PBMC samples from a macaque immunized with SIV $p57^{Gag}$ DNA.

3.5 Tetramer Staining to Assess Mucosal Dissemination of Cellular Responses

Using MHC class I tetramers combined with cell phenotyping and flow cytometry is a sensitive approach to identify and measure antigen-specific $CD8^+$ T cells in different anatomical locations, especially mucosal sites, directly ex vivo.

3.5.1 Tetramer Staining

1. Take 10^6 cells (PBMC or single cells from digested tissues) and 10 mL of FACS surface staining buffer. Centrifuge at 336 × *g* for 10 min.
2. Decant the fluid and leave the tubes upside down on a paper towel.
3. Add 5 μL of CM9 tetramer, mix well and incubate for 5 min at RT (*see* **Note 14**).
4. Add the antibody cocktail to the tubes (at least CD3, CD8, and CD4) and gently mix. Incubate for 20 min at RT.
5. Add 10 mL of PBS and centrifuge at 336 × *g* for 10 min.
6. Discard the supernatant.
7. Resuspend the cells in 300 μL of PBS and transfer into flow tubes.
8. Run the samples in the flow cytometer.
9. Analyze the data. Figure 3 represents the analysis of $CM9^+$ $CD8^+$ T cells in PBMC and mucosal tissues.

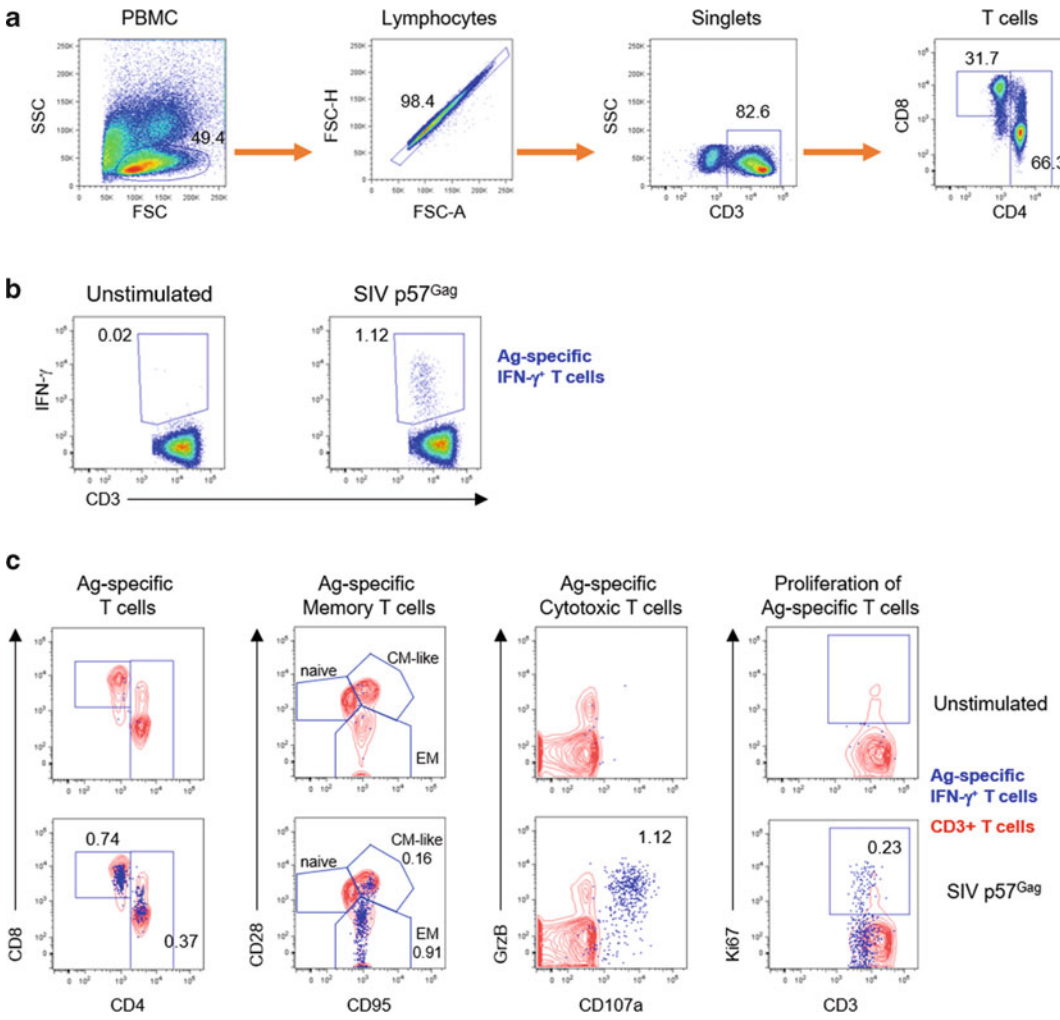

Fig. 2 Flow cytometric analysis of antigen-specific cytotoxic T cell in PBMC from a rhesus macaque vaccinated with SIV $p57^{Gag}$ DNA. (**a**) Gating Strategy to identify the $CD4^+$ and $CD8^+$ T lymphocytes. (**b**) Dot plots show IFN-γ^+ T cells upon stimulation with SIV $p57^{Gag}$ peptides (right panel) and the unstimulated control (medium only, left panel) in PBMC from a DNA vaccinated macaque. (**c**) Contour plots show the phenotype of the antigen-specific IFN-γ^+ T cell (overlayed in blue). The plots show $CD4^+$ and $CD8^+$ expression, memory phenotype ($CD28^+CD95^+$ as central memory and $CD28^-CD95^+$ as effector memory T cells), cytotoxic potential ($GrzB^+$ and/or $CD107a^+$) and proliferative responses ($Ki67^+$) of the antigen-specific T cells upon SIV $p57^{Gag}$ peptide stimulation. The data show that the DNA vaccination induced strong $CD4^+$ and $CD8^+$ antigen-specific memory T cells with cytotoxic potential ($GrzB^+$ and/or $CD107a^+$)

4 Notes

1. If the lab does not have a rate freezer, collect all the vials in Mr. Frosty and placed for at least 4 h in −80 °C freezer and then move vials to a liquid nitrogen freezer. Alternatively, place tubes in a Styrofoam box and store at −20 °C freezer for a

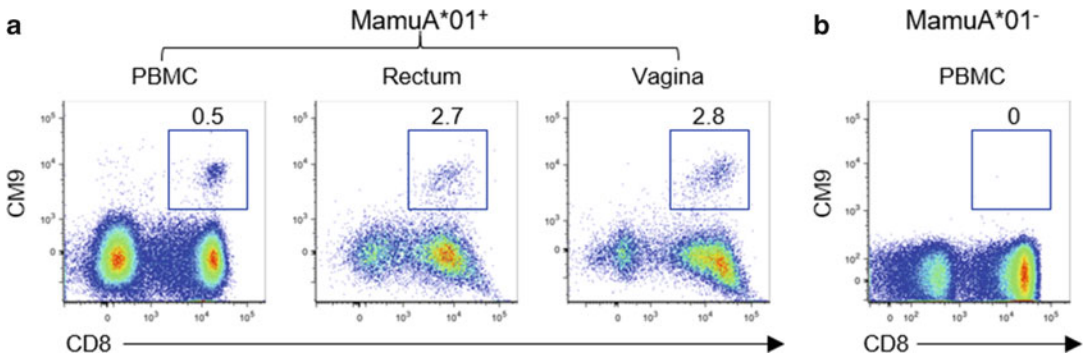

Fig. 3 Identification of antigen-specific $CD8^+$ T cells in different tissues by tetramer staining. (**a**) Dot plots show the frequency (numbers within the plots) of CM9 $tetramer^+$ $CD8^+$ T lymphocytes in blood (PBMC), rectum and vagina from $MamuA*01^+$ macaques immunized with plasmid DNA encoding SIV $p57^{Gag}$. (**b**) As negative control, the CM9 tetramer staining of blood $CD8^+$ T lymphocytes from a MamuA*01 negative macaque immunized with SIV $p57^{Gag}$ DNA is shown. The data show that $mamuA*01^+$ macaques immunized with plasmid DNA encoding SIV $p57^{Gag}$ generated strong CM9 responses in both blood and mucosal sites (**a**). No responses were found in the SIV $p57^{Gag}$ DNA vaccinated $MamuA*01^-$ macaque (**b**)

couple of hours, then move the whole box or boxes to −80 °C freezer overnight and the next day, place the tubes in dry ice and transfer immediately to the liquid nitrogen freezer for long-term storage.

2. As a positive control, it is possible to use cells stimulated with a broad range of reagents. The most commonly used are PMA/Ca^{2+} ionophore, mitogens such as PHA or ConA, or the use of anti-CD3 antibodies.
3. The composition of the peptide pools is determined by the investigator. Lyophilized individual peptides are dissolved in 10 μL of 100% DMSO per mg peptide overnight (100 mg/mL). The next day, the individual peptides are diluted to 10 mg/mL with RPMI and can be stored at −80 °C. Peptide pools are composed to contain for example peptides at 100 μg/mL of each peptide (100 × pool) and are stored in aliquots at −20 °C. Typically, 15-mer peptides overlapping by 11 a.a. are used to detect both CD4 and CD8 T-cell responses, but any other peptide length can be used depending on the experimental design. For instance, we have designed peptide pools that combine 15-mer peptides overlapping by 11 a.a. and 10-mer peptides overlapping by 9 a.a. to optimally cover both CD4 and CD8 T-cell epitopes [6, 8, 31].
4. Heat-inactivated AB human serum is used (it is possible to use serum from healthy macaques) to block the Fc receptors on the surface of the cells, preventing undesired antibody binding through the Fc portion of the immunoglobulins. This will decrease the unspecific fluorescent signal.

5. The antibody cross-reactivity with NHPs can be established by consulting the following NIH-sponsored website: https://www.nhpreagents.org/NHP/reagentlist.aspx. The composition of the antibody panels used in the experiment can be adjusted (both surface and intracellular markers) depending on the experimental design and the detectors in the available flow cytometer.
6. The singles for compensation are a fundamental part of the experiment assuring the reliability of the flow measurements. Remember, we do not compensate for the detectors, we compensate for the spillover of the specific fluorochromes included in our experiment in secondary detectors. For example, FITC and GFP can be measured in the same detector, but they are not interchangeable as compensation singles because of their emission spectra, and therefore the spillover in other fluorescent channels, are significantly different. It is possible to use either cells or beads for the compensation controls.
7. The fixation/permeabilization reagent of choice will depend on the panel being used for intracellular staining. Not all commercial reagents are able to permeabilize the nuclear membrane properly. Therefore for stainings, including nuclear proteins such as transcriptional factors or Ki67, we use the FoxP3 fixation/permeabilization reagent.
8. The density gradient separation of PBMC is optimally performed in a tube where the Ficoll is one-third of the volume and the mixture of blood and PBS accounts for the other two-third of the volume. The final volume and the tube of choice will depend on the original volume of the blood sample. After the initial centrifugation, the red blood cells and polynuclear leukocytes will be at the bottom, and the PBMC will form a visible ring between the liquid phases of the Ficoll (below) and the PBS (on the top).
9. This centrifugation step is critical if the transferred PBMC contains a significant amount of Ficoll, because carry-over Ficoll may significantly affect the density of the PBS used for washing resulting in a significant loss of the isolated PBMC.
10. The layout design for the ELISpot plate: a typical ELISpot plate should at least include the negative controls (usually quadruplicate wells added with R-10 medium), positive controls (duplicate wells for anti-CD3 antibody or other stimulation reagents described in the **Note 2**), and assayed samples (duplicate wells).
11. It is critical that the plate is not moved during this incubation. The movement will affect the location of the cells resulting in an image with blurred, not well-defined spots.

12. The reagent of choice to prevent protein secretion could be adjusted depending on the experiment. Monensin and Brefeldin are the two most commonly protein transport inhibitors used in cytokine detection by intracellular staining. The incubation time with either one of the two should never exceed 12 h; beyond that time the toxicity of the compounds will significantly affect the viability of the cells. At the time of adding the protein transport inhibitor, it is also possible to add an anti-CD107 antibody to monitor degranulation from the beginning of the stimulation. Adding anti-CD28 and anti-CD49d monoclonal antibodies to enhance the T-cell responses induced by the peptide stimulation [21] is an extended practice. Importantly, in our assay we never add co-stimulatory antibodies to increase the response mediated by TCR recognition of the cognate antigen; it should be noted that terminally differentiated effector memory T cells lack CD28 expression. Furthermore, adding anti-CD28 antibodies in the assay will prevent the identification of the T-cell memory subsets (combination of CD95 and CD28 antibodies for surface staining), which is an important component of the phenotyping performed in conjunction with the intracellular cytokine analysis.
13. It is very important that the tube does not contain any significant amount of washing buffer before adding the fixation/permeabilization reagents. Otherwise, the remaining fluid would dilute the permeabilization buffer resulting in suboptimal cells for efficient intracellular staining. If the procedure has to be interrupted, the cells can be kept in the fixative at 4 °C until the next day.
14. Tetramer staining benefits by exposing the cells to the tetramer a few minutes before adding the antibody mix containing the anti-CD8 antibody (the tetramer is a reagent combining the peptide specific for the TCR and four copies of the specific MHC class I molecule that will bind to CD8).

Acknowledgement

This work was funded by the Intramural Research Program of the National Cancer Institute to B.K.F.. The contents of this chapter does not necessarily reflect the views or policies of the Department of Health and Human Services, nor does mention of trade names, commercial products, or organizations imply endorsement by the US government. We thank T. Jones for editorial assistance.

References

1. Felber BK, Valentin A, Rosati M et al (2014) HIV DNA vaccine: stepwise improvements make a difference. Vaccines (Basel) 2:354–379
2. Hutnick NA, Myles DJ, Bian CB et al (2011) Selected approaches for increasing HIV DNA vaccine immunogenicity in vivo. Curr Opin Virol 1:233–240
3. Iyer SS, Amara RR (2014) DNA/MVA vaccines for HIV/AIDS. Vaccines (Basel) 2:160–178
4. Chen Y, Wang S, Lu S (2014) DNA immunization for HIV vaccine development. Vaccines (Basel) 2:138–159
5. Rosati M, Bergamaschi C, Valentin A et al (2009) DNA vaccination in rhesus macaques induces potent immune responses and decreases acute and chronic viremia after SIVmac251 challenge. Proc Natl Acad Sci U S A 106:15831–15836
6. Hu X, Valentin A, Dayton F et al (2016) DNA prime-boost vaccine regimen to increase breadth, magnitude, and cytotoxicity of the cellular immune responses to subdominant gag epitopes of simian immunodeficiency virus and HIV. J Immunol 197:3999–4013
7. Patel V, Valentin A, Kulkarni V et al (2010) Long-lasting humoral and cellular immune responses and mucosal dissemination after intramuscular DNA immunization. Vaccine 28:4827–4836
8. Hu X, Valentin A, Rosati M et al (2017) HIV Env conserved element DNA vaccine alters immunodominance in macaques. Hum Vaccin Immunother 13:2859–2871
9. Hu X, Valentin A, Cai Y et al (2018) DNA vaccine-induced long-lasting cytotoxic T cells targeting conserved elements of human immunodeficiency virus Gag are boosted upon DNA or recombinant modified vaccinia Ankara vaccination. Hum Gene Ther 29:1029–1043
10. Valentin A, McKinnon K, Li J et al (2014) Comparative analysis of SIV-specific cellular immune responses induced by different vaccine platforms in rhesus macaques. Clin Immunol 155:91–107
11. von Gegerfelt AS, Rosati M, Alicea C et al (2007) Long-lasting decrease in viremia in macaques chronically infected with simian immunodeficiency virus SIVmac251 after therapeutic DNA immunization. J Virol 81:1972–1979
12. Patel V, Jalah R, Kulkarni V et al (2013) DNA and virus particle vaccination protects against acquisition and confers control of viremia upon heterologous simian immunodeficiency virus challenge. Proc Natl Acad Sci U S A 110:2975–2980
13. Czerkinsky CC, Nilsson LA, Nygren H et al (1983) A solid-phase enzyme-linked immunospot (ELISPOT) assay for enumeration of specific antibody-secreting cells. J Immunol Methods 65:109–121
14. Autran B, Letvin NL (1991) HIV epitopes recognized by cytotoxic T-lymphocytes. AIDS 5(Suppl 2):S145–S150
15. Barouch DH, Santra S, Tenner-Racz K et al (2002) Potent CD4+ T cell responses elicited by a bicistronic HIV-1 DNA vaccine expressing gp120 and GM-CSF. J Immunol 168:562–568
16. Mascola JR, Lewis MG, VanCott TC et al (2003) Cellular immunity elicited by human immunodeficiency virus type 1/simian immunodeficiency virus DNA vaccination does not augment the sterile protection afforded by passive infusion of neutralizing antibodies. J Virol 77:10348–10356
17. Fulwyler MJ (1965) Electronic separation of biological cells by volume. Science 150:910–911
18. Jung T, Schauer U, Heusser C et al (1993) Detection of intracellular cytokines by flow cytometry. J Immunol Methods 159:197–207
19. Herzenberg LA, Parks D, Sahaf B et al (2002) The history and future of the fluorescence activated cell sorter and flow cytometry: a view from Stanford. Clin Chem 48:1819–1827
20. Roederer M, Brenchley JM, Betts MR et al (2004) Flow cytometric analysis of vaccine responses: how many colors are enough? Clin Immunol 110:199–205
21. Gauduin MC (2006) Cytokine staining for the characterization and quantitation of antigen-specific T lymphocyte responses. Methods 38:263–273
22. Tung JW, Heydari K, Tirouvanziam R et al (2007) Modern flow cytometry: a practical approach. Clin Lab Med 27:453–468
23. De Rosa SC, Lu FX, Yu J et al (2004) Vaccination in humans generates broad T cell cytokine responses. J Immunol 173:5372–5380
24. Makedonas G, Betts MR (2006) Polyfunctional analysis of human t cell responses: importance in vaccine immunogenicity and natural infection. Springer Semin Immunopathol 28:209–219
25. Almeida JR, Sauce D, Price DA et al (2009) Antigen sensitivity is a major determinant of CD8+ T-cell polyfunctionality and HIV-suppressive activity. Blood 113:6351–6360

26. Demberg T, Mohanram V, Venzon D et al (2014) Phenotypes and distribution of mucosal memory B-cell populations in the SIV/-SHIV rhesus macaque model. Clin Immunol 153:264–276
27. Demberg T, Robert-Guroff M (2015) B-cells and the use of non-human primates for evaluation of HIV vaccine candidates. Curr HIV Res 13:462–478
28. Mohanram V, Demberg T, Tuero I et al (2014) Improved flow-based method for HIV/SIV envelope-specific memory B-cell evaluation in rhesus macaques. J Immunol Methods 412:78–84
29. Altman JD, Moss PA, Goulder PJ et al (1996) Phenotypic analysis of antigen-specific T lymphocytes. Science 274:94–96
30. Melenhorst JJ, Scheinberg P, Chattopadhyay PK et al (2008) Detection of low avidity CD8 (+) T cell populations with coreceptor-enhanced peptide-major histocompatibility complex class I tetramers. J Immunol Methods 338:31–39
31. Kulkarni V, Valentin A, Rosati M et al (2014) Altered response hierarchy and increased T-cell breadth upon HIV-1 conserved element DNA vaccination in macaques. PLoS One 9:e86254

Part III

Biotechnological Processes to Obtain DNA Vaccines

Chapter 7

Enhanced Biosynthesis of Plasmid DNA from *Escherichia coli* Applying Experimental Design

Luís A. Passarinha

Abstract

Therapeutic applications of plasmid DNA (pDNA) have significantly advanced during the last years. Currently, several pDNA-based drugs are already in the market, whereas several others have entered phases 2 and 3 of clinical trials. The present and future demand for pDNA requires the development of efficient bioprocesses to produce it. Commonly, pDNA is produced by cultures of *Escherichia coli*. It has been previously demonstrated that specific strains of *E. coli* with a modified substrate transport system can be able to attain high cell densities in batch mode, due to the very low overflow metabolism displayed. However, the large amounts of oxygen demanded can lead to microaerobic conditions after some hours of cultivation, even at small scale. Typically, the inherent problems for these cultures are the high oxygen demand and the accumulation of acetate, a metabolic byproduct that is synthesized aerobically when the glucose rate exceeds the limits.

In recent years, several researches have been focused on the study of induction of plasmid DNA as well as strategies for fermentation using semi-defined mediums. These studies conceived relevant results that allow us to design a production platform for enhanced plasmid DNA. So, the main goal of this chapter is to show how the development of an experimental design directed to aromatic amino acids pathway can improve the yield of a therapeutic plasmid DNA by culture of a new strain of *Escherichia coli* VH33.

Key words Aromatic amino acids, Biosynthesis, Box–Behnken experimental design, *Escherichia coli* VH33, Plasmid DNA

1 Introduction

At the beginning of the present century, the optimism of the DNA-based therapy research community was encouraged by the first report of successful treatment of genetic diseases. The majority of the clinical trials (64.4%) in gene therapy have addressed cancer, monogenic, infectious, and cardiovascular diseases [1]. Also DNA vaccines have been extensively evaluated in humans, with a significant increase of products in clinical trials, from 94 in 2008 to 2597 in 2017 [1, 2]. This strong growth was mainly due to the improvement of the production step design, the development of new purification methods, and the progression of knowledge on new

Ângela Sousa (ed.), *DNA Vaccines: Methods and Protocols*, Methods in Molecular Biology, vol. 2197,
https://doi.org/10.1007/978-1-0716-0872-2_7,

delivery systems. For the choice and design of the therapeutic plasmid DNA (pDNA), it is crucial to achieve a final biologically active formulation. Typically, DNA vectors have to combine sequences for replication and selection in bacteria (bacterial region) with sequences necessary to express the encoded transgenes in vertebrate cells (eukaryotic region) after delivery and transfection of target cells [3, 4].

During the last decades, many strains of *Escherichia coli* (*E. coli*) such as DH5α [5], MG1655 [6], and VH32 [7] have been created through a series of mutations to facilitate cloning of heterologous genes and maintain the stability of pDNA. However, plasmid-bearing cells have an altered profile of central metabolic gene expression and a slower growth rate when compared to plasmid-free cells [8, 9]. So, cell line engineering efforts have sought to improve pDNA production by knockout or overexpression of rationally selected genes. One focus is the modification of central carbon metabolism genes to increase flux toward nucleotide and amino acid precursor synthesis and reduction of byproducts, such as acetate [10]. A molecular solution could be the replacement of the natural glucose uptake system in *E. coli* (phosphoenolpyruvate carbohydrate phosphotransferase system, PTS) by galactose permease (GalP) and glucokinase (GIk). Compared to the PTS system, the expression of GalP reduces the transport rate of glucose [11, 12]. This enables an increase of the initial glucose concentration and decreases the acetate accumulation during the fermentation process, which is a metabolic advantage that improves the availability of phosphoenolpyruvate (PEP) for pDNA biosynthesis [13]. However, as described in literature, the acetate accumulation has low effect in DNA replication, but a negative consequence in the final cell titers [14]. Nowadays, in order to avoid continuous changes of the genetic identity of the bacteria, it is possible to chemically control the metabolic pathways of interest. For instance, the metabolic production of aromatic amino acids is not necessary for pDNA production; however, these two paths use the same precursors [6, 15]. Thus, the inhibition of 3-deoxy-D-arabinoheptulosonate-7-phosphate DAHP synthases (initial aromatic pathway), which catalyzes DAHP production, is achieved through the use of aromatic amino acids, providing more nutrients to nucleotide biosynthesis [16].

Traditional optimizations were focused on the rate and in the physical parameters that control cell growth, and also substrate composition (Table 1). The purpose of these modifications is to increase cell density, stability, and the copy number of plasmid [17]. So, due to the wide range of process variables, experimental design procedures are often used to define the ideal operation conditions in the fermentation processes for pDNA biosynthesis. According to the factor number of factors to be investigated at a time, the experimental design can be classified into two categories:

Table 1
Relationship between cause–effect on an upstream optimization process

Optimization	Cause	Effect
Growth rate	Reduce growth rate	High-quality and high-yield plasmid production Less acetate production Less plasmid instability Control plasmid replication
Growth conditions	Oxygen Temperature pH Dissolve oxygen	Increase supercoiled plasmid Plasmid stability
Media	Minimal media	Higher plasmid copy numbers and highly reproducible
	Semi-defined and complex media	Higher cell densities and decrease in reproducibility

Adapted from [17]

one-factor-at-a-time design (single-factor design) and factorial design (multiple-factor design) [18]. The one-factor-at-a-time design is a traditional design, which investigates one-factor-at-a-time, while keeping the levels of other parameters constant. In contrast, factorial design is able to study the effects of more than one factor at two or more levels and enables to depict the interactions among different factors. This design can be classified into two categories: full factorial design and fractional factorial design (Taguchi, Central Composite, Plackett–Burman, and Box–Behnken) [19]. In a full factorial design, every combination of each factor level is tested. The most commonly used full factorial design is a two-level strategy [18, 20]. In contrast, the fractional factorial design is used when the number of runs is too large to be tested by experimental work. The Taguchi design using an orthogonal array allows the effects of many factors with two or more levels on a response to be studied in a relatively small number of runs. The central composite design is a five-level fractional factorial design that consists of 2^n full factorial design, $2 \times n$ axial designs, and m central designs [18].

Another approach to deal with a large number of factors is to use Plackett–Burman design. This strategy identifies the key factors of the respective production system, called as "Screening." Second, gradient method needs to be used to find the optimum variable ranges [21]. Plackett–Burman design allows testing of the largest number of factor effects with the least number of observations and allows random error variability estimation and testing of the statistical significance of the parameters [21, 22]. Besides analyzing the effects of the independent variables, this methodology generates a mathematical model, which can be used to describe the process for

better understanding. As an example of RSM, the Box–Behnken design is a three-level factorial design, which allows estimating and interpreting interactions between various variables at a time during the optimization process. It is suitable for the exploration of quadratic responses and constructs a second-order polynomial model with very few runs [23, 24]. Recently, a mathematical representation of the neurological functioning of a brain, called as neural network, which is able to describe the interactive effects of several factors has been applied successfully to construct bioprocess models [24]. A neural network does not need any model or screening before the development of a network, and it may be applied on designed data or on the data that is not statistically designed. This powerful tool uses all the data making the model more accurate and can perform tasks that cannot be performed by linear programming [18, 24].

To sum up, there is a huge potential of all tools described above to develop models (fermentation conditions, physical parameters) and achieved optimal range concentrations of medium components (carbon and nitrogen sources, mineral salts, trace elements, vitamins, and other growth factors) [21]. The combination of engineered strains and experimental design may be extremely advantageous by bringing new design resolutions for the biosynthesis of therapeutic pDNA [19, 23]. So, in this chapter, a laboratory protocol will be described to improve the yield of a therapeutic pDNA by culture of *E. coli* VH33, based on the variation of nutritional substrates. Additionally, an experimental design directed to aromatic amino acid pathway is established in order to understand the influence of these amino acids in nucleotide network.

2 Materials

2.1 Plasmid and Strain

1. 6.6 kbp pcDNA3–FLAG, ampicillin-resistant plasmid, with pcDNA3-based backbone (*see* **Note 1**)

2.2 Cell Banking

For the preparation of Master and Working Cell Bank, consider the following materials:

1. Luria-Bertani agar (LB/agar) plates and Luria-Bertani (LB) liquid medium.
2. 50 mg/mL ampicillin and glycerol stock solutions.
3. Falcon tubes and cryotubes (capacity of 50 and 1 mL, respectively).
4. Orbital shaker.
5. UV/visible spectrophotometer.
6. 10% glycerol.

7. Centrifuge.
8. Liquid nitrogen.
9. GYT medium: 10% glycerol, 0.125% yeast extract, 0.25% tryptone.
10. Electroporation cuvette and system.
11. Shake flasks of 500 mL and 1 L of capacity.

2.3 Pre-culture and Batch Fermentations

1. Resuspension buffer: 50 mM glucose, 25 mM Tris–HCl, 10 mM ethylenediamine tetraacetic acid (EDTA), pH 8.0.
2. Lysis buffer: 200 mM NaOH, 1% (w/v) sodium dodecylsulfate (SDS).
3. Neutralizing buffer: 3 M potassium acetate, pH 5.0 adjusted with glacial acetic acid.
4. Pre-cultures and batch fermentations salt media composition: 90 mM K_2HPO_4, 10 mM KH_2PO_4, 40 mM $(NH_4)_2SO_4$, 20 mM NaCl, 1.6 mM $MgSO_4{\cdot}2H_2O$, 0.05 mM $CaCl_2$, 0.072 mM $FeSO_4{\cdot}7H_2O$ (*see* **Notes 2** and **3**).
5. Test medium: glucose (5 or 10 g/L), 20 g/L of tryptone, 0.17 M KH_2PO_4, and 0.72 M K_2HPO_4. Specifically, yeast extract and glycerol may be absent or present on this medium at concentrations of 24 g/L, and 4 mL/L. respectively.
6. The Box–Behnken design is applied in a semi-defined medium: using 10 g/L glucose as the main carbon source, 24 g/L yeast extract as potent nitrogen source, salt solution (90 mM K_2HPO_4, 10 mM KH_2PO_4, 40 mM $(NH_4)_2SO_4$, 20 mM NaCl, 1.6 mM $MgSO_4{\cdot}2H_2O$, 0.05 mM $CaCl_2$, 0.072 mM $FeSO_4{\cdot}7H_2O$), and the three target amino acids (tyrosine, phenylalanine, and tryptophan).
7. According to the model levels, the amino acid concentration should vary respectively to 10, 50, and 100 μg/mL (*see* **Notes 4** and **5**).

2.4 Plasmid DNA Quantification

For the implementation of the analytical method, the following materials are necessary:

1. A 4.6/100 mm HIC source 15 PHE PE column.
2. An ÄKTA purifier system.
3. Equilibration buffer: 1.5 M $(NH_4)_2SO_4$ in 10 mM Tris–HCl buffer, pH 8.0.
4. Elution buffer: 10 mM Tris–HCl buffer, pH 8.0.
5. A loop of 20 μL sample injection with 1 mL/min of flow rate. The absorbance of samples is recorded at 260 nm.
6. Plasmid DNA standards (1–100 μg/mL) can be purified by a commercial kit for instance.

7. Agarose.
8. Green safe.
9. TAE buffer: 40 mM Tris, 20 mM acetic acid, 1 mM EDTA in Milli-Q filtered water, pH 8.0.
10. Vilber Lourmat system.

3 Methods

3.1 Preparation and Transformation of Competent Cells

1. Inoculate a single colony of *E. coli* into LB/agar plates overnight at 37 °C.
2. With these cells, inoculate an LB medium, previously autoclaved, and grow the cells in an orbital shaker at 37 °C, under 300 rpm. The growth should be suspended when the OD_{600} achieve 0.35–0.40.
3. Next, chill the falcon tubes and centrifuge the cells under 5445 × *g*, 20 min and 4 °C.
4. Subsequently, the supernatant should be discarded and the pellet should be resuspended with prechilled glycerol at 10%.
5. After glycerol addition, the cells should be centrifuged, the glycerol discarded, and the pellet resuspended with GYT medium. Typically, the cell concentration is approximately $2–3 \times 10^{10}$ cells per milliliter.
6. Rapidly, distribute the total volume by aliquots of 100 μL in cryotubes, freeze in liquid nitrogen, and transfer/store at −80 °C, until further handling.
7. For transformation, an aliquot of competent cells (obtained in **step 6**) should be thawed and the target plasmid be added to the cell suspension.
8. Transfer the mixture to the electroporation cuvette and incubate during 5 min in ice. The cuvette is placed on an electroporation system where a pulse of 2500 V is applied.
9. After this, 250 μL of LB medium should be added and the broth transferred to a sterile culture and incubated for 2 h.
10. Finally, the LB plates must be supplemented with ampicillin 50 μg/mL for further inoculation.

3.2 Master and Working Cell Bank

1. The master cell bank must be prepared from a single colony picked from an agar plate and inoculated in LB medium supplemented with 50 μg/mL ampicillin.
2. Grow the cultures to 0.6 OD_{600} at 250 rpm and 37 °C (*see* **Note 6**).

3. Place 14 mL of the cell culture into a falcon tube, followed by the addition of glycerol to achieve a final concentration of 30% (v/v).
4. Distribute the mixture above into 1 mL cryogenic vials and freeze at −80 °C (*see* **Note 7**).

3.3 Plasmid DNA Biosynthesis — Standard Culture Conditions

1. All fermentations should be carried out in 1 L shake flasks containing 250 mL of the test medium (*see* **Notes 2** and **3**). Typically for the preparation of 1 L, mix tryptone, yeast extract, and glycerol, add distilled water in appropriate volume taking into account the addition of glucose and potassium salts after sterilization. Autoclave (liquid cycle), allow liquid to cool to less than 60 °C, and finally add 100 mL of potassium phosphate solution, and correct volume of a glucose solution at 5 or 10 g/L.
2. Schedule the operation parameters in shaker rotation and temperature to 250 rpm and 37 °C, respectively.
3. All the batches should started with an OD_{600} of approximately 0.2 by inoculation with a pre-culture grown in 500 mL shake flasks, at 250 rpm and 37 °C, containing 125 mL of the test medium. All fermentation (including pre-culture) should be supplemented with 50 μg/mL ampicillin.
4. For further analysis of pDNA yield and purity, cells should be harvested in the final of exponential growth phase after 14 h of the upstream stage.

3.4 Alkaline Cell Lysis and pDNA Quantification

1. Centrifuge the cell broth at 3900 × *g* for 30 min at 4 °C to obtain bacterial pellets.
2. Thaw nearly 100 mL of bacterial pellet and dissolve in 10 mL resuspension buffer.
3. To perform the alkaline lysis, add 10 mL of lysis buffer.
4. After 5 min of incubation at room temperature, cellular debris, gDNA, and proteins should be precipitated by adding and mixing 8 mL of prechilled neutralizing buffer and incubate for 20 min on ice.
5. Remove the pellet by centrifuging twice at 20,000 × *g* (30 min, 4 °C) (*see* **Note 8**), to obtain the pDNA sample to be analyzed.
6. Construct a calibration curve with pDNA standards (1–100 μg/mL) purified by a commercial kit.
7. Monitor the Akta system at 260 nm.
8. Equilibrate a 4.6/100 mm HIC source 15 PHE PE column with the equilibration buffer, under a flow rate of 1 mL/min.

9. Inject the sample in a loop of 20 μL and after 4 min with the equilibrium buffer to elute the pDNA, change to elution buffer during 10 min.
10. Detect the supercoiled pDNA peak.
11. Quantify the pDNA concentration in each sample based on the calibration curve obtained from **step 6** (*see* **Note 9**).

3.5 Plasmid DNA Quality Analysis

The quality of the produced plasmid and isoforms proportion can be achieved by agarose gel electrophoresis, so:

1. Perform a 1% agarose gel supplemented with 0.5 μg/mL green safe.
2. Run the gel at 110 V for 30 min in TAE buffer.
3. Visualize the agarose gels under UV light, for instance, in a Vilber Lourmat system.

3.6 Construction of a Box–Behnken Design

1. Create a typical Box–Behnken design (BBD) applying the *Design-Expert 7.0.0* software and using three aromatic amino acids (tyrosine, phenylalanine, and tryptophan) as independent variables.
2. Set X_1, X_2, and X_3 as inputs corresponding to tyrosine, phenylalanine, and tryptophan medium concentration, respectively, including in the semi-defined medium.
3. To check if there is a nonlinear relationship between the variables and the responses, on the main schedule include a run of five replicates at the central point level.
4. According to the preestablished model levels, the amino acid concentration must vary between level −1, 0, and 1, which corresponds, respectively, to 10, 50, and 100 μg/mL.
5. The total number of trials should be set as 17 (Table 2) (*see* **Note 10**).
6. To complement the experimental design, all fermentation (runs) should be monitored. This control involves the calculation of specific growth rate, final mass of cells, specific pDNA yield, and purity (Table 3) (*see* **Notes 11** and **12**).
7. Generate and evaluate the statistical experimental design by ANOVA data (*see* **Note 13**).
8. Test the fit of the model, the regression equation and determination coefficient (R^2) (*see* **Note 13**).
9. For predicting the optimal point, a polynomial function should be fitted to correlate the relationship between independent variables and target response, pDNA-specific yield, and purity (Table 3).

Table 2
Runs of Box–Behnken design with codded factors (−1, 10 μg/mL; 0, 50 μg/mL; +1, 100 μg/mL)

Run	Factor 1 A: TYR (μg/mL)	Factor 2 B: PHE (μg/mL)	Factor 3 C: TRP (μg/mL)
1	1	−1	0
2	1	−1	0
3	**1**	**0**	**1**
4	0	−1	−1
5	0	0	0
6	**1**	**0**	**−1**
7	0	−1	1
8	−1	1	0
9	−1	0	−1
10	0	0	0
11	−1	−1	0
12	0	0	0
13	0	1	−1
14	**0**	**1**	**1**
15	0	0	0
16	0	0	0
17	−1	0	1

Note: Bold values represent the fermentation experiments for model validation

4 Notes

1. The strain VH33 is a derivative from *E. coli* W3110 in which the GalP promoter was substituted by the trc promoter, thus making constitutive the expression of GalP. The glucose import is dependent on GalP and glucose phosphorylation on glucokinase activity. This bacterial strain was transformed with the 6.6 kb plasmid.
2. The culture media to be tested should contain 50 μg/mL of ampicillin to maintain a selective growth and equal salt composition. The salt solution must be sterilized separately at 121 °C.
3. In order to understand the effect of glucose on a test medium for pDNA production and purity, *E. coli* strain VH33 can grow into different media composition. All contained glucose (5 or 10 g/L) and 20 g/L of tryptone. Yeast extract and glycerol can

Table 3
Fermentation run results of Box–Behnken design

Run	Specific growth rate (h^{-1})	Cell dry mass (g/L)	pDNA volumetric yield (μg/mL)	pDNA-specific yield (μg pDNA/mg CDM)	Purity
1	0.22	2.40	70.17	29.25	3.20
2	0.35	2.13	74.19	34.86	3.74
3	**0.30**	**1.46**	**78.72**	**53.83**	**4.36**
4	0.37	1.64	75.28	45.83	3.73
5	0.44	2.11	78.47	37.26	3.84
6	**0.33**	**1.63**	**85.88**	**52.72**	**4.18**
7	0.33	1.57	66.44	42.37	3.46
8	0.36	1.53	75.27	49.20	3.76
9	0.37	1.58	74.12	46.79	3.37
10	0.48	2.28	78.78	34.60	3.77
11	0.28	1.62	75.62	46.68	3.51
12	0.47	2.22	77.93	35.06	3.84
13	0.28	1.65	76.62	46.46	3.76
14	**0.37**	**1.53**	**82.59**	**54.06**	**4.15**
15	0.47	2.25	77.49	34.51	3.90
16	0.35	2.17	78.86	36.28	3.86
17	0.36	1.73	81.49	47.04	3.82

Note: Bold values represent the fermentation experiments for model validation

be present (or absent) at concentrations of 24 g/L and 4 mL/L, respectively. The nutrient composition of pre-culture should be the same as the mother culture. After these assays, the next step should be the selection of the ideal fermentation media. Based on the selected media, the carbon source type and its concentration, glucose, and/or glycerol can be varied. The glucose concentration can be screened from 5, 7.5, 20, and 30 g/L and glycerol from 4 m/L to 30 mL/L.

4. The aromatic amino acid solution stock can be prepared weighing 250 mg of each amino acid and dissolved in Milli-Q water at a final concentration of 1 mg/mL. Since amino acids cannot be autoclaved (thermolabile compounds), they must be sterilized by 0.22 μm syringe filter into sterile Falcon tubes and stored at 4 °C in the absence of light.
5. In the development of the model, the Box–Behnken factorial experimental design employs three independent variables of the aromatic amino acids: tyrosine, phenylalanine, and

tryptophan. Typically, several enzymes of aromatic amino acid biosynthetic pathway are subject to feedback regulation. As reported in literature, the range concentration of aromatic amino acids that is enough to perturb their pathway is approximately 15–500 μg/mL [16, 25]. In order to avoid the feedback inhibition caused by the introduction of three amino acids, lower aromatic amino acid concentrations of approximately 10, 50, and 100 μg/mL should be applied.

6. The master cell bank must be prepared from a single colony picked from an agar plate and inoculated in Luria-Bertani medium supplemented with 50 μg/mL ampicillin.
7. The working cell bank should be prepared by growing an aliquot of the master cell bank. The hands-on conditions applied must be the same as described for the master cell bank.
8. The pDNA quantification must be made from the extract of second centrifugation. In these clarified extracts, there are no further purification steps.
9. The HPLC method is based on hydrophobic interaction chromatography and performed to measure the pDNA concentration and purity [26]. The purity degree is defined as the percentage of the pDNA peak area related to the total area obtained from all peaks in the chromatogram.
10. All runs must be carried out in 500 mL shake flasks containing 125 mL of medium at 250 rpm under 37 °C and started with an OD_{600} of 0.2 by inoculation with a pre-culture containing 10 g/L of glucose, yeast extract, salts, and ampicillin. After 9 h of growth, the cells should be harvested.
11. A typical Box–Behnken design (BBD) was performed using the independent variables. In this study, three aromatic amino acids (tyrosine, phenylalanine, and tryptophan) were the independent variable. Five replicates at the central point level were also run to check if there was a nonlinear relationship between variables and responses, leading to a total number of 17 trials. For predicting the optimal point, polynomial function was fitted to correlate the relationship between independent variables and response. The X_1, X_2, and X_3 were the factors used in design that correspond to tyrosine, phenylalanine, and tryptophan medium concentration, respectively.
12. The values of volumetric pDNA yield must act as an output (response) to the BBD. The parameters related to specific pDNA yield and purity could be considered as responses to the model development. The choice will always be related to the achieved statistical significance.
13. An example of the model type obtained can be described in Eq. 1 [28]. The model *F* value of 3.70 implies that the model is significant, and there is only a 4.91% chance that a model *F*-

Source	Sum of Squares	df	Mean Square	F value	p-valu (Prob > F)	
Model	268.95	9	29.88	3.70	0.0491	significant
A-TYR	0.76	1	0.76	0.094	0.7678	
B-PHE	56.08	1	56.08	6.95	0.0336	
C-TRP	0.87	1	0.87	0.11	0.7518	
AB	4.78	1	4.78	0.59	0.4669	
AC	52.73	1	52.73	6.53	0.0378	
BC	54.87	1	54.87	6.80	0.0350	
A^2	0.11	1	0.11	0.014	0.9091	
B^2	91.29	1	91.29	11.31	0.0120	
C^2	10.56	1	10.56	1.31	0.2902	
Residual	56.49	7	8.07			
Lack of fit	55.14	3	18.38	54.21	0.0011	significant
Pure Error	1.36	4	0.34			
Cor Total	325.44	16				
St. Dev.	2.84					
Mean	76.94					
C.V.%	3.69					
R-Squared	0.8264					
Adj R-Squared	0.6032					

Fig. 1 ANOVA for the quadratic response surface model fitting to the plasmid DNA biosynthesis

value could occur due to noise. The analysis of variance (ANOVA) (Fig. 1) quadratic regression model demonstrates that the model is significant for pDNA production with the low probability ($P < 0.0491$) of the *F*-test. The fitted model is considered adequate if the *F*-test is significant ($P < 0.05$) [27]. Another important value is lack-of-fit test that is performed by comparing the variability of the current residual model to the variability between observations at replicate settings of factors. The lack of fit is designed to determine whether the selected model is adequate to describe the observed data or whether a reformulation of the model should be applied. Despite the lack-of-fit value was significant, a contribution of other values such as coefficient variation, standard deviation, and R^2 should support the validity of model.

Therefore, the determination coefficient ($R^2 = 0.83$) being a measure of goodness of fit to the model indicates an acceptable degree of correlation between the observed value and predicted values (Fig. 2). The coefficient of variation (CV), ratio of the standard error of estimate to the mean value of the observed response, is a measure of reproducibility of the

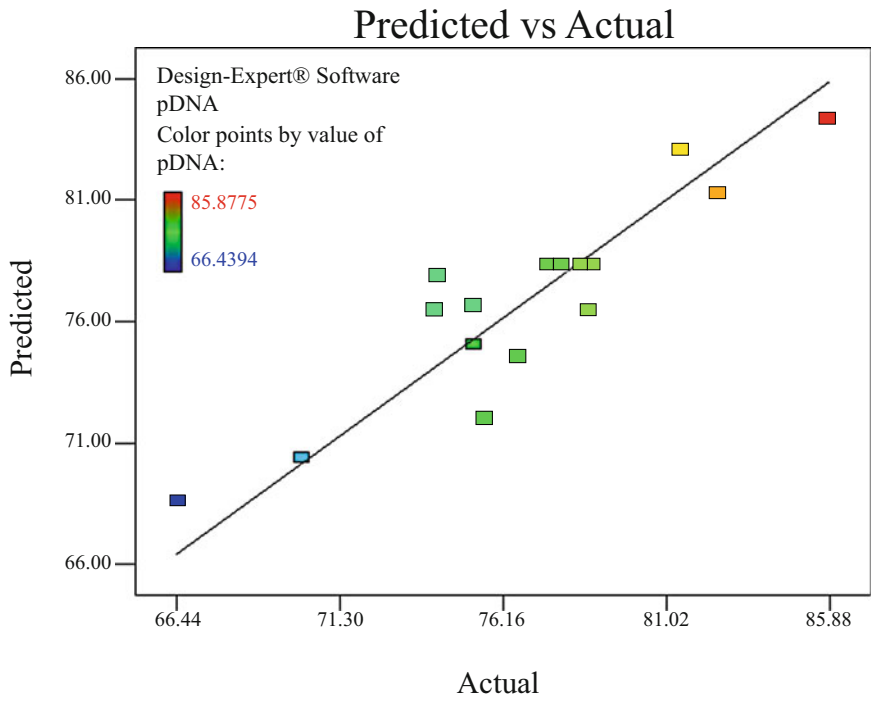

Fig. 2 An example for the plot representation of predicated values versus observed values

model; generally, a model can be considered reasonably reproducible if its CV is not greater than 10% [93]. Hence, the low variation coefficient value (CV = 3.69%) obtained indicates a high precision and reliability of the experiments (Fig. 1).

The significance of regression coefficients is considered at an impact level of 95%. The *p*-values of regression coefficients suggest that among the independent test variables, linear, quadratic, and interaction effects of tyrosine, phenylalanine, and tryptophan are highly significant (Fig. 1). In this example, B, AC, BC, and B^2 are significant model terms and had a potential effect on pDNA volumetric yield (Fig. 1 and Eq. 1) [28].

$$\begin{aligned}\text{pDNA} = {} & 78.304 + 0.308.\text{Tyr} + 2.647.\text{Phe} - 0.330.\text{Trp} \\ & + 1.093.\text{Tyr.Phe} - 3.631.\text{Tyr.Trp} \\ & + 3.704.\text{Phe.Trp} + 0.164.\text{Tyr}^2 - 4.656.\text{Phe}^2 \\ & + 1.584.\text{Trp}^2 \end{aligned} \quad (1)$$

Moreover, it can be observed that phenylalanine concentrations exerted more pronounced linear positive effect on pDNA production. The quadratic effect of tryptophan showed a good increment on plasmid production, unlike the phenylalanine.

For a multiple regression model, rather than plotting the observed and predicted values versus each of the independent variables in turn, it is simpler to generate a single plot of observed values versus the predicted values, in order to verify linearity (predicted vs. observed plot). Therefore, for continuous responses, the actual versus predicted plot (Fig. 2) shows how well the model fits the data. The diagonal line represents of where predicted and observed values are the same. For a perfect fit, all the points would be on this diagonal. As expected, the best points belong to central point because it is from these that the whole model is developed. The furthermost points of the line have higher residual value than those are closer to the line. Additionally, the observation value with large residual is called outlier. Specifically, it is an observation whose dependent-variable value is unusual, given its values on the predictor variables. An outlier may indicate a sample peculiarity or may indicate a data error or other problem. In this example and analyzing Fig. 2, it seems that a significant observed value that could be considered an outlier does not exist.

In order to provide an ideal case for this specific pDNA production with statistical significance, the goal can be set to maximized response (pDNA volumetric yield). The predicted optimum values of tyrosine, phenylalanine, and tryptophan corresponded to 10 μg/mL (−1 level), 78.5 μg/mL (0.57

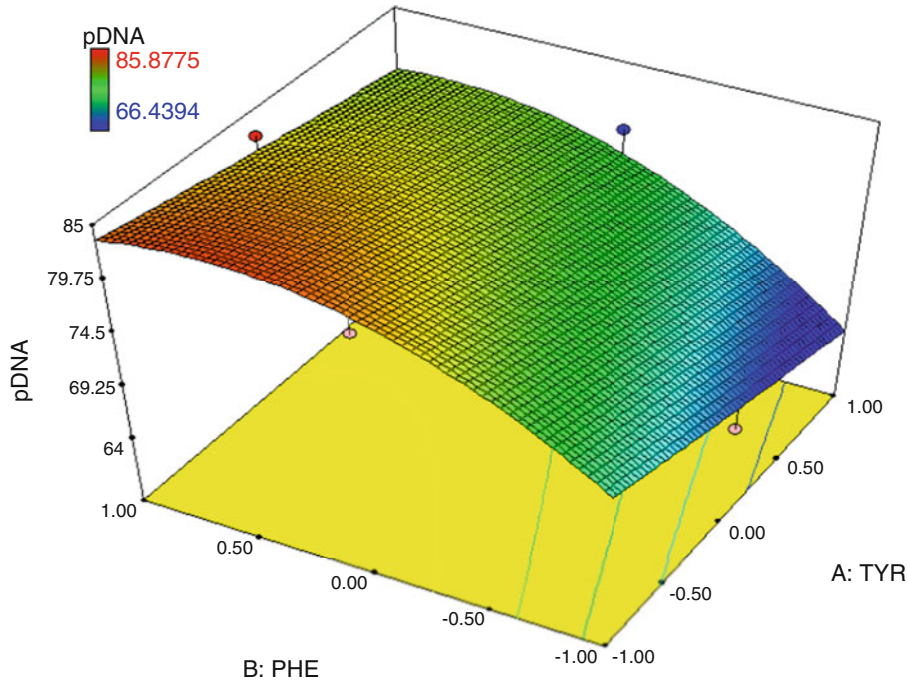

Fig. 3 Response surface plot of optimal conditions of pDNA volumetric yield

level), and 100 μg/mL (+1 level), respectively, to achieve 84.53 μg/mL of plasmid volumetric yield (Fig. 3). Analyzing the graph of the response surface, the levels of tyrosine and phenylalanine that reflect a reddish area are the conditions to achieve better response (pDNA production) with tryptophan at level +1. The optimal variable levels were achieved based on whole information provided by BBD and RSM [28].

Concerning these facts, this case study combines the potential of VH33, which uses a different glucose transport, allowing efficient growth and lower acetate production, for pDNA biosynthesis with a validated factorial design. The results revealed which combination should be applied in terms of nitrogen and carbon source requirements in order to obtain 36.69 μg pDNA/mg cell dry mass of specific yields and 6.01% of purity on lysates. Overall, the proposal model shown the influence of tyrosine, phenylalanine, and tryptophan on their pathway, providing necessary precursors to nucleotide network.

Acknowledgments

L.A. Passarinha acknowledges a sabattical fellowship (SFRH/BSAB/150376/2019) from the Portuguese Foundation for Science and Technology (FCT) within the scope of POCH—Advanced Formation programs co-funded by European Social Fund and MCTES. This work was also supported by the Applied Molecular Biosciences Unit—UCIBIO, which is financed by national funds from FCT/MCTES (UID/Multi/04378/2019). A special thanks to Professor Guillermo Gosset (Instituto de Biotecnología from Universidad Nacional Autónoma de México) for providing us the *E.coli* VH33 strain and to Dr. Thomas Roberts for providing the pcDNA3-FLAG construct through Addgene (reference 10838).

References

1. Ginn SL, Amaya AK, Alexander IE (2018) Gene therapy clinical trials worldwide to 2017—an update. J Gene Med 20:1–16
2. Kutzler MA, Weiner DB (2008) DNA vaccines: ready for prime time? Nat Rev Genet 9:776–788
3. Williams J (2013) Vector design for improved DNA vaccine efficacy, safety and production. Vaccine 1:225–249
4. Mairhofer J, Grabherr R (2008) Rational vector design for efficient non-viral gene delivery: challenges facing the use of plasmid DNA. Mol Biotechnol 39:97–104
5. Phue J, Lee SJ, Trinh L et al (2008) Modified *Escherichia coli* B (BL21), a superior producer of plasmid DNA compared with *Escherichia coli* K (DH5alpha). Biotechnol Bioeng 101:831–836
6. Gonçalves GAL, Prazeres DMF, Monteiro GA et al (2012) De novo creation of MG1655-derived *E. coli* strains specifically designed for plasmid DNA production. Appl Microbiol Biotechnol 97:611–620

7. Lara AR, Caspeta L, Gosset G et al (2008) Utility of an *Escherichia coli* strain engineered in the substrate uptake system for improved culture performance at high glucose and cell concentrations: an alternative to fed-batch cultures. Biotechnol Bioeng 99:893–901
8. Yau SY, Keshavarz-Moore E, Ward J (2008) Host strain influences on supercoiled plasmid DNA production in *Escherichia coli*: implications for efficient design of large-scale processes. Biotechnol Bioeng 101:529–544
9. Bower DM, Prather KLJ (2009) Engineering of bacterial strains and vectors for the production of plasmid DNA. Appl Microbiol Biotechnol 82:805–813
10. Gonçalves GAL, Bower DM, Prazeres DMF et al (2012) Rational engineering of *Escherichia coli* strains for plasmid biopharmaceutical manufacturing. Biotechnol J 7:251–261
11. Meza E, Becker J, Bolivar F et al (2012) Consequences of phosphoenolpyruvate:sugar phosphotranferase system and pyruvate kinase isozymes inactivation in central carbon metabolism flux distribution in *Escherichia coli*. Microb Cell Factories 11:127–140
12. Pablos TE, Soto R, Mora EM et al (2012) Enhanced production of plasmid DNA by engineered *Escherichia coli* strains. J Biotechnol 158:211–214
13. Soto R, Caspeta L, Barrón B et al (2011) High cell-density cultivation in batch mode for plasmid DNA production by a metabolically engineered *E. coli* strain with minimized overflow metabolism. Biochem Eng J 56:165–171
14. Carnes AE, Luke JM, Vincent JM (2011) Plasmid DNA fermentation strain and process-specific effects on vector yield, quality, and transgene expression. Biotechnol Bioeng 108:354–363
15. Losen M, Frölich B, Pohl M et al (2004) Effect of oxygen limitation and medium composition on *Escherichia coli* fermentation in shake-flask cultures. Biotechnol Prog 20:1062–1068
16. Polen T, Krämer M, Bongaerts J et al (2005) The global gene expression response of *Escherichia coli* to L-phenylalanine. J Biotechnol 115:221–237
17. Carnes AE (2005) Fermentation design for the manufacture of therapeutic plasmid DNA. Bioprocess Technol:36–42
18. Wang J, Wan W (2009) Experimental design methods for fermentative hydrogen production: a review. Int J Hydrog Energy 34:235–244
19. Bezerra MA, Santelli RE, Oliveira EP et al (2008) Response surface methodology (RSM) as a tool for optimization in analytical chemistry. Talanta 76:965–977
20. Cofré O, Ramirez M, Gomez JM et al (2012) Optimization of culture media for ethanol production from glycerol by *Escherichia coli*. Biomass Bioenergy 37:275–281
21. Bakonyi P, Nemestóthy N, Lövitusz É et al (2011) Application of Plackett–Burman experimental design to optimize biohydrogen fermentation by *E. coli* (XL1-BLUE). Int J Hydrog Energy 36:13949–13954
22. O'Kennedy RD, Ward JM, Keshavarz-Moore E (2003) Effects of fermentation strategy on the characteristics of plasmid DNA production. Biotechnol Appl Biochem 37:83–90
23. Ferreira SLC, Bruns RE, Ferreira HS et al (2007) Box-Behnken design: an alternative for the optimization of analytical methods. Anal Chim Acta 597:179–186
24. Nelofer R, Ramanan RN, Rahman R et al (2012) Comparison of the estimation capabilities of response surface methodology and artificial neural network for the optimization of recombinant lipase production by *E. coli* BL21. J Ind Microbiol Biotechnol 39:243–254
25. Sprenger GA (2007) From scratch to value: engineering *Escherichia coli* wild type cells to the production of L-phenylalanine and other fine chemicals derived from chorismate. Appl Microbiol Biotechnol 75:739–749
26. Diogo MM, Queiroz JA, Prazeres DMF (2003) Assessment of purity and quantification of plasmid DNA in process solutions using high-performance hydrophobic interaction chromatography. J Chromatogr A 998:109–117
27. Agarry SE, Ogunleye OO (2012) Box-Behnken design application to study enhanced bioremediation of soil artificially contaminated with spent engine oil using biostimulation strategy. Int J Energy Environ Eng 3:31
28. Martins LM, Pedro AQ, Oppolzer D et al (2015) Enhanced biosynthesis of plasmid DNA from *Escherichia coli* VH33 using Box-Behnken design associated to aromatic amino acids pathway. Biochem Eng J 98:117–126

Chapter 8

Primary Purification of Plasmid DNA Using Differential Isopropanol Precipitation

Alexandra Wagner, A. Rita Silva-Santos, Sara Sousa Rosa, Sophie Gierak, Ana M. Azevedo, and Duarte Miguel F. Prazeres

Abstract

A method for the intermediate recovery of plasmid DNA (pDNA) from alkaline lysates is described that comprises differential isopropanol precipitation steps. In a first low-cut precipitation, a smaller amount of isopropanol (20% v/v) is used so that only high molecular weight RNA precipitates. After solid liquid separation, a high-cut precipitation is performed by bringing isopropanol concentration to 70% v/v to precipitate pDNA. Tests made with lysates show that the differential precipitation increases purity threefold compared to the conventional one-step precipitation at 70% v/v without affecting pDNA recovery (>80%).

Key words Isopropanol, Plasmid DNA, Precipitation, Purity, RNA

1 Introduction

Plasmid DNA (pDNA) vectors are an attractive gene delivery option in gene-based therapy/vaccination due to their superior safety profile when compared with viral vectors [1, 2]. Manufacturing of plasmid vectors calls for replication in *Escherichia coli* (*E. coli*) and a train of unit operations to isolate pDNA and remove host impurities like RNA, genomic DNA, and proteins [3]. Alcohol precipitation is an inexpensive and simple method to separate DNA from RNA, which is often used as an intermediate step in the downstream processing of plasmid DNA [4]. In particular, isopropanol precipitation is often used to concentrate pDNA following the standard initial alkaline lysis step [4]. This method uses isopropanol (~70–80% v/v) to remove solvation water molecules and promote aggregation of pDNA molecules, taking advantage of the high salt content (~1 M potassium acetate) in alkaline lysates [4–6]. This aggregation results

Alexandra Wagner and A. Rita Silva-Santos contributed equally with all other contributors.

Ângela Sousa (ed.), *DNA Vaccines: Methods and Protocols*, Methods in Molecular Biology, vol. 2197,
https://doi.org/10.1007/978-1-0716-0872-2_8,

from the strong electrostatic interactions between cations and the negatively charged phosphate groups of the nucleic acids [5]. While some purification can be afforded by isopropanol precipitation, the vast majority of RNA coprecipitates with pDNA and is thus carried over to the subsequent unit operations [6]. This RNA usually impacts operations like chromatography, by reducing the binding capacity of resins for pDNA and decreasing resin lifetime [7]. In this work, we use a differential isopropanol precipitation strategy that overcomes the RNA coprecipitation problem by removing substantial amounts of RNA without compromising pDNA yield. As an alternative to the one-step precipitation, we reasoned that pDNA purity could be increased by adopting a two-step differential precipitation that explores the different patterns of precipitation of RNA and pDNA. The strategy designed combines a first, low-cut RNA precipitation step that removes high MW RNA and leaves pDNA in solution, with a second, high-cut precipitation of pDNA.

2 Materials

Prepare all solutions using Milli-Q water and analytical grade reagents, unless otherwise specified. All solutions are prepared and stored at room temperature, unless indicated otherwise.

2.1 Agarose Gel

1. Electrophoresis-grade agarose.
2. Running buffer (*see* **Note 1**): Tris–acetate–EDTA (TAE) buffer—40 mM Tris base, 20 mM acetic acid, and 1 mM EDTA, pH 8.0 (*see* **Note 2**). Prepare a 50× concentrated buffer and dilute to the desired final volume.
3. Loading buffer 6×: 40% (w/v) sucrose, 0.25% (w/v) bromophenol blue (*see* **Note 3**).
4. Molecular weight marker (*see* **Note 4**).
5. Staining solution: 0.4 μg/mL ethidium bromide (*see* **Note 5**).

2.2 Urea Denaturing Polyacrylamide Gel

1. 40% polyacrylamide/bisacrylamide stock solution (29:1).
2. 1× Tris–Borate–EDTA (TBE) buffer (*see* **Note 1**)—100 mM Tris base, 100 mM boric acid, 2 mM EDTA, pH 8.0. Prepare a 10× stock solution and dilute to the desired final volume. Store at 4 °C.
3. 6.5 M ultrapure urea.
4. 0.08% (v/v) ammonium persulfate solution (APS), prepared from a stock solution of 10% (w/v). Always prepare APS freshly before use.
5. *N*,*N*,*N*′,*N*′-Tetramethylethylenediamine (TEMED).

6. Denaturing loading buffer 2×: 95% formamide (v/v), 18 mM EDTA, 0.025% SDS (w/v), and 0.05% (w/v) bromophenol blue. Prepare stock solutions of 500 mM EDTA and 10% (w/v) SDS.
7. Molecular weight marker (*see* **Note 4**).
8. Staining solution: 0.4 μg/mL ethidium bromide (*see* **Note 5**).

2.3 Plasmid Quantification

1. Equilibration buffer: 1.5 M ammonium sulfate in 10 mM Tris–HCl buffer pH 8.0. First, prepare a 10 mM Tris–HCl solution by weighing the desired amount. Weigh the necessary amount of ammonium sulfate (*see* **Note 6**). Add water up to 70% of the desired volume. Mix well and adjust the pH to 8.0 with concentrated HCl (*see* **Note 7**). Add the appropriate amount of water to make up the desired volume of solution. Filter the buffer through a 0.22 μm membrane.
2. Elution buffer: 10 mM Tris–HCl buffer pH 8.0. Filter the buffer through a 0.22 μm membrane filter.

2.4 Culture Media

1. *E. coli* DH5α cells harboring plasmid pVAX1-GFP (~3.7 kb [8], *see* **Note 8**).
2. Luria-Bertani broth (LB) medium. Prepare the LB medium according to the manufacturer's indications. Adjust the pH to 7.2 by adding 1 M NaOH. Tightly cover the flask mouth with aluminum foil, similar plug or lose cap. Autoclave the LB broth at 121 °C for 20 min. Remove the media from the autoclave and leave to cool at room temperature prior to use.
3. Kanamycin (30 mg/mL). Filter the antibiotic through a 0.22 μm syringe membrane filter in a sterile environment.

2.5 Alkaline Lysis

1. Resuspension buffer (P1 buffer): 50 mM glucose, 25 mM Tris–HCl, and 10 mM EDTA, pH 8.0. Prepare stock solutions of 1 M Tris–HCl, pH 8.0, and 500 mM EDTA, pH 8.0. Dilute to the desired concentration. Store at 4 °C.
2. Lysis buffer (P2 buffer): 200 mM NaOH, 1% (w/v) SDS.
3. Neutralization buffer (P3 buffer): 3 M sodium acetate, pH 6.0. Store at 4 °C.

2.6 Isopropanol Precipitation

1. Analytical reagent grade isopropanol.
2. TE buffer: 10 mM Tris–HCl, 1 mM EDTA, pH 8.0. Prepare stock solutions of 1 M Tris–HCl, pH 8.0, and 500 mM EDTA, pH 8.0. Dilute to the desired final concentration.

3 Methods

Carry out all procedures at room temperature unless otherwise specified.

3.1 Agarose Gel Electrophoresis

1. Agarose gels are prepared using solutions with a w/v percentage which, depending on the size of the DNA fragments to be separated, ranges between 0.5% and 2%. For a 1% agarose gel, weigh 1.5 g of electrophoresis grade agarose into an Erlenmeyer flask.
2. Add 150 mL of running buffer to the flask, mixing thoroughly. Melt the agarose mixture in a microwave and swirl to ensure even mixing (*see* **Note 9**). Allow the solution to cool.
3. Pour the warm agarose solution onto the gel plate in the electrophoresis box and insert a comb. Make sure that no bubbles are trapped underneath the combs and that all bubbles on the surface of the agarose are removed (*see* **Note 10**). Allow the gel to completely set (between 30 and 45 min) and carefully withdraw the gel comb, so that the sample wells do not tear.
4. Place the gel casting plate with the gel in the electrophoresis tank. Add sufficient running buffer to cover the gel and top of the wells. Make sure no air pockets are formed inside the wells.
5. Prepare the samples. Add 0.2 volumes of loading buffer to each sample, e.g., 4 μL of loading buffer into a 20 μL sample. Load the marker and the samples, taking care not to puncture the bottom of wells. Also, if there are air bubbles in the tip of the pipette or in the wells, do not load the sample (*see* **Note 11**).
6. Attach the lid and set the voltage to the desired level (1–10 V/cm of gel) to begin electrophoresis. The progress of the separation can be monitored by visualizing the migration of the dye. Halt separation when the dye front has migrated around ¾ of the way down the gel.
7. Remove the gel from the casting tray and place it in the ethidium bromide staining solution for 10–30 min. De-stain gels in water to remove excess ethidium bromide.

3.2 Urea Denaturing Polyacrylamide Gel Electrophoresis

1. Assemble the gel plates with the desired thickness on a stable even surface.
2. Prepare the gel solution with the appropriate percentage of acrylamide. This will depend on the sizes of RNA molecules one wishes to resolve [9]. For a 5% acrylamide gel, the volumes of components added are summarized in Table 1. Add water to 100 mL.

Table 1
Recipe for a 5% urea denaturing polyacrylamide gel

Reagents	Volume added (mL)/100 mL	Final concentration
TBE	10	1×
Acrylamide/bisacrylamide (29:1)	12.5	5%
Urea	65	6.5 M
APS	0.8	0.08%

Table 2
Recipe for denaturing loading buffer

Reagents	Amount added	Final concentration
Formamide	9.5 mL	95%
EDTA	360 μL	500 mM
SDS	25 μL	10%
Bromophenol blue	5 mg	0.05%

Add water to make a final volume of 10 mL

3. Add 40 μL TEMED for a final volume of 100 mL gel mixture. Quickly mix the solution before it polymerizes. Pour the gel solution in the plates assembled with spacers, until it overflows.
4. Insert the comb, taking special care that no air bubbles are inside the wells or trapped in the gel. Allow the gel to polymerize at room temperature for about 20–30 min.
5. Remove the gel plates from the casting stand and mount them on the electrophoresis tank. Fill with 1× TBE making sure that the gel wells are covered with the buffer. Remove the comb and rinse the wells with the buffer to remove any residual urea.
6. Perform a pre-run at 90 V, for 30–60 min, in a controlled temperature of 60 °C using a water bath before sample loading.
7. Prepare the samples. Dilute the samples in water (1:10) and add the denaturing loading buffer (recipe is summarized in Table 2). Denature the samples at 95 °C for 5 min. Rinse the wells with the buffer and load the marker and the samples.
8. Run the gel at 60 mV at a controlled temperature of 60 °C using a water bath. Monitor the dye front to determine when to stop the electrophoresis.

9. Remove the gel from the holder, wash it with TBE 1× and place it in the ethidium bromide staining solution for 10–30 min. De-stain gels in water to remove excess ethidium bromide.

3.3 Plasmid Quantification and Determination of pDNA Purity

All the experiments were performed using an ÄKTA Purifier system with the Unicorn control system Version. The column used in this work was a SOURCE 15PHE 4.6/100 PE, with 1.7 mL bed volume (*see* **Note 12**).

1. Prepare plasmid standards with concentrations in the range 0–100 μg/mL by diluting a concentrated plasmid solution (*see* **Note 13**). Determine the pDNA concentration of this solution by spectrophotometry (here a Nanodrop UV spectrophotometer was used). Dilute the concentrated solution with 10 mM Tris–HCl buffer pH 8.0 in order to obtain pDNA standards with concentrations of 10, 20, 30, 40, 50, and 100 ng/μL.
2. Prepare the ÄKTA Purifier system by connecting 1.5 M ammonium sulfate in 10 mM Tris–HCl buffer, pH 8.0 to pump A and 10 mM Tris–HCl buffer, pH 8.0 to pump B.
3. Connect the column to the system and equilibrate with 1.5 M ammonium sulfate in 10 mM Tris–HCl, pH 8.0, at a flow rate of 1 mL/min.
4. Inject 50 μL of samples or standards and elute in a step mode, with 0.5 column volumes of 10 mM Tris–HCl buffer, pH 8.0, at a flow rate of 1 mL/min (*see* **Note 14**).
5. Re-equilibrate the column with 3.2 column volumes of the initial buffer.
6. Measure the absorbance and conductivity of the eluate at 260 nm.
7. Calculate the plasmid peak area and construct a calibration curve (linear correlation between peak area and plasmid concentration). Calculate the purity of the pDNA-containing sample by comparing the areas of the plasmid and impurity peaks in HPLC chromatograms using the following formula:

$$\text{Purity } (\%) = \frac{A_{\text{plasmid peak}}}{A_{\text{plasmid peak}} + A_{\text{impurities peak}}} \times 100\%$$

3.4 Bacterial Cell Growth

1. Prepare a 100 mL shake flask with 30 mL of LB medium supplemented with 30 μg/mL kanamycin (for a 100 mL shake flask add 30 μL of 30 mg/mL kanamycin stock solution). Inoculate the flask with a small amount of *E. coli* DH5α

harboring pVAX-GFP cells. Cover the culture with a cap that is not air tight. Incubate overnight at 37 °C and 250 rpm.

2. Measure the optical density at 600 nm (OD_{600nm}) and calculate the volume of this culture required to inoculate 250 mL of medium at an OD_{600nm} of approximately 0.1. Add this volume of culture to 250 mL of LB medium supplemented with 250 μL of 30 μg/mL kanamycin in 2 L shake flasks. Incubate the cells at 37 °C and 250 rpm for 8 h.
3. Harvest the cells by centrifuging at 6000 × *g* for 15 min. Store pellets at −20 °C until further experiments.

3.5 Alkaline Lysis

1. Resuspend the cell pellets in buffer P1 up to an OD_{600nm} of 60 (*see* **Note 15**). Vortex until cells are completely resuspended (*see* **Note 16**).
2. Add buffer P2 at a volume ratio of 1:1 and gently mix by inverting the tube (*see* **Note 17**). The solution should turn transparent and become viscous indicating that lysis has taken place. Leave to rest for 10 min.
3. Add buffer P3 at a volume ratio of 1:1 to neutralize the lysate. Gently mix and place the lysate on ice for 10 min.
4. Centrifuge the samples for 30 min, at 18,250 × *g* and 4 °C. Repeat until a pDNA clarified lysate is obtained.

3.6 Differential Precipitation

1. Incubate 1 mL of lysate with 20% v/v isopropanol for 15 min at 4 °C (*see* **Notes 18** and **19**).
2. Centrifuge the sample for 30 min, at 13,000 × *g* and 4 °C.
3. Carefully collect the supernatant. Save the pellet to have a control sample.
4. Incubate the pDNA-rich supernatants with 70% v/v isopropanol, relatively to the lysate volume, for 15 min at 4 °C.
5. Centrifuge the sample for 30 min, at 13,000 × *g* and 4 °C.
6. Resuspend the pellet in 1 mL TE buffer.
7. Analyze the samples by electrophoresis and HPLC (*see* **Notes 21–24**).

4 Notes

1. Other running buffers could be chosen. The most commonly used are Tris/acetate (TAE) and Tris/borate (TBE). Both have different effects on DNA mobility—longer fragments are better resolved when TAE is used, but TAE has a lower buffering capacity than TBE. This results in a faster exhaustion during

extended or high-voltage electrophoresis. Therefore, repeated use of this buffer should be avoided.

2. The free acid form of EDTA is insoluble in water. Therefore, a strong base must be used. Add the desired amount of EDTA to water and stir vigorously on a magnetic stirrer. Do not add the total volume of water, because, in most cases, solution volume increases when a large amount of solute dissolves in the solvent. Add NaOH solution or pellets to adjust the pH to 8.0. Adjust to the desired final volume.
3. Bromophenol blue migration rate is equivalent to 350–400 bp, which provides an index of the mobility of the fastest fragments. For larger fragments, a loading buffer with xylene cyanol, which migrates at approximately the same rate as a 4000 bp fragment, should be used. Other loading buffers can be used, but be sure to use the same for samples and ladders.
4. The choice of molecular weight marker is related to the size of the molecules to be separated and/or determined. Commercially available ladders come in a variety of different size ranges, so a good coverage of the size range should be chosen. For this work, molecular weight markers with a size range of 200–10,000 bp (for agarose gels) and 50–1500 bp (for urea page gels) were selected and used according to the manufacturer's instructions.
5. Ethidium bromide is mutagenic and should be handled with caution. It is a DNA intercalator, inserting itself between the base pairs in the double helix. Therefore, use gloves and dispose of any contaminated material into a dedicated ethidium bromide waste container.
6. Ammonium sulfate can expand in solution, due to the high concentration needed for this buffer. Therefore, start stirring the solution and add salt to it in small portions, allowing it to dissolve before adding the next portion.
7. Adding concentrated HCl to the Tris buffer will increase the temperature of the solution, which affects the pH. Allow the solution to cool to room temperature before making final adjustments to the pH.
8. Many *E. coli* strains can be used to produce and isolate plasmid DNA, but the strain used can have a substantial influence on the final quality [10]. The most used high-density strains of *E. coli* for DNA production are DH5α, DH5, DH1, JM108, SCS1-L, and DH10B. The recA1 and endA1 mutations in the DH5α strain improve plasmid stability and yield.
9. You should not see any bubbles in the solution. An agarose solution with trapped bubbles will originate distorted bands. For a 150 mL solution, agarose will melt in about 3 min at maximum microwave power. Pause the heating and swirl every

minute and then continue toward a boil. Be careful not to overboil the solution, since some of the buffer could evaporate, changing the concentration of agarose in the final gel.

10. To avoid bubbles, pour the solution slowly. To remove bubbles, use a pipette tip to push them away from the wells or toward the sides.
11. To prevent bubbles or buffer from entering the tip, maintain positive pressure when loading the sample. Slowly push the sample filling the well, carefully raising the pipette straight of the buffer.
12. The choice of column and/or media is related to the hydrophobicity of the molecules. When applied to the purification of pDNA, the higher hydrophobicity of the impurities results in a stronger interaction with the hydrophobic matrix. Although pDNA is naturally a hydrophilic molecule due to the shielding of hydrophobic bases inside the double helix and exposure of sugar phosphate chains that are available to establish hydrogen bonds with surrounding water molecules, this character can be to some extent modified by an increase of the ionic strength of a kosmotropic salt (such as ammonium sulfate) on the mobile phase [4]. Although the column SOURCE 15PHE 4.6/100 PE is designed for preparative purposes, it can also be used for the quantification of pDNA.
13. The plasmid standard stock solution was prepared using a commercially available plasmid purification kit (HiSpeed plasmid Maxi Kit). The majority of the available kits are able to deliver highly concentrated and pure plasmid DNA from bacteria, e.g., by combining modified versions of the classic alkaline lysis method and a silica-based membrane in a spin column format.
14. In this method, the plasmid DNA elutes in the flowthrough, while the majority of impurities are retained due to a higher hydrophobic character and lower molecular mass [11]. The decrease in the ionic strength of the mobile phase causes the impurities to elute.
15. The volume of buffer P1 (V_{P1}) is calculated to produce a concentrated suspension with an $OD_{600nm} = 60$, by taking into account the final OD_{600nm} and the volume of the respective cell culture (V_{cg}), i.e.:

$$V_{P1} = \frac{OD_{600nm} \times V_{cg}}{60}$$

16. Ensure that the pellets are completely resuspended, leaving no clumps, in order to maximize the number of cells that will be exposed to the lysis buffer.

17. Do not vortex or stir vigorously the lysate. Invert the container 4–6 times in order to mix the solution and allow a rapid homogenization while avoiding the fragmentation of the released genomic DNA.
18. The isopropanol concentration value indicated here refers to the percentage of isopropanol volume added relatively to the volume of lysate, e.g., 20% v/v refers to the addition of 20 mL isopropanol to 100 mL of lysate.
19. To determine the optimal condition for the first step of the isopropanol precipitation, 1 mL of lysate was incubated with increasing volumes of isopropanol (10–100% relatively to the volume of lysate). The results show that RNA precipitation (Fig. 1a) is already significant with lower amounts of isopropanol (10–20% v/v). Also, the urea-PAGE analysis further supports the idea that low isopropanol (<40% v/v) essentially promotes the precipitation of high MW RNA, leaving low MW RNA in solution (data not shown). A HPLC analysis of the resuspended pellet solutions shows that isopropanol amounts of 60% v/v are sufficient to obtain pDNA recoveries close to 100% (Fig. 1b).
20. Results indicate that the amount of pDNA lost in the first precipitation with 20% v/v is negligible (lane 20, Fig. 2). Furthermore, pDNA solutions obtained after the second precipitation (lanes 30–100, Fig. 2a) have substantially less RNA when compared with solutions obtained with a one-step precipitation.
21. The HPLC analysis further shows that by introducing the second precipitation step, pDNA recoveries higher than 80% can be obtained as long as the total amount of isopropanol used is at least 70% v/v (Fig. 2b).
22. The urea-PAGE analysis supports the idea that low isopropanol (<40% v/v) essentially promotes the precipitation of high MW RNA, leaving low MW RNA in solution (Fig. 3a). Furthermore, pDNA solutions obtained after the second precipitation (lanes 30–100, Fig. 2a) have substantially less RNA (Figs. 2a and 3) when compared with solutions obtained with a one-step precipitation (Fig. 1a).
23. The purification afforded by one-step isopropanol precipitation can be judged by comparing the analytical HPLC chromatograms of the initial lysate and of the pDNA solutions obtained after precipitation (Fig. 4a, b). While there is clear evidence of a reduction of the impurity load, essentially due to a reduction of low MW RNA species, the purity of pDNA solutions obtained when using the standard amounts of isopropanol (>60% v/v) does not exceed 4% due to the

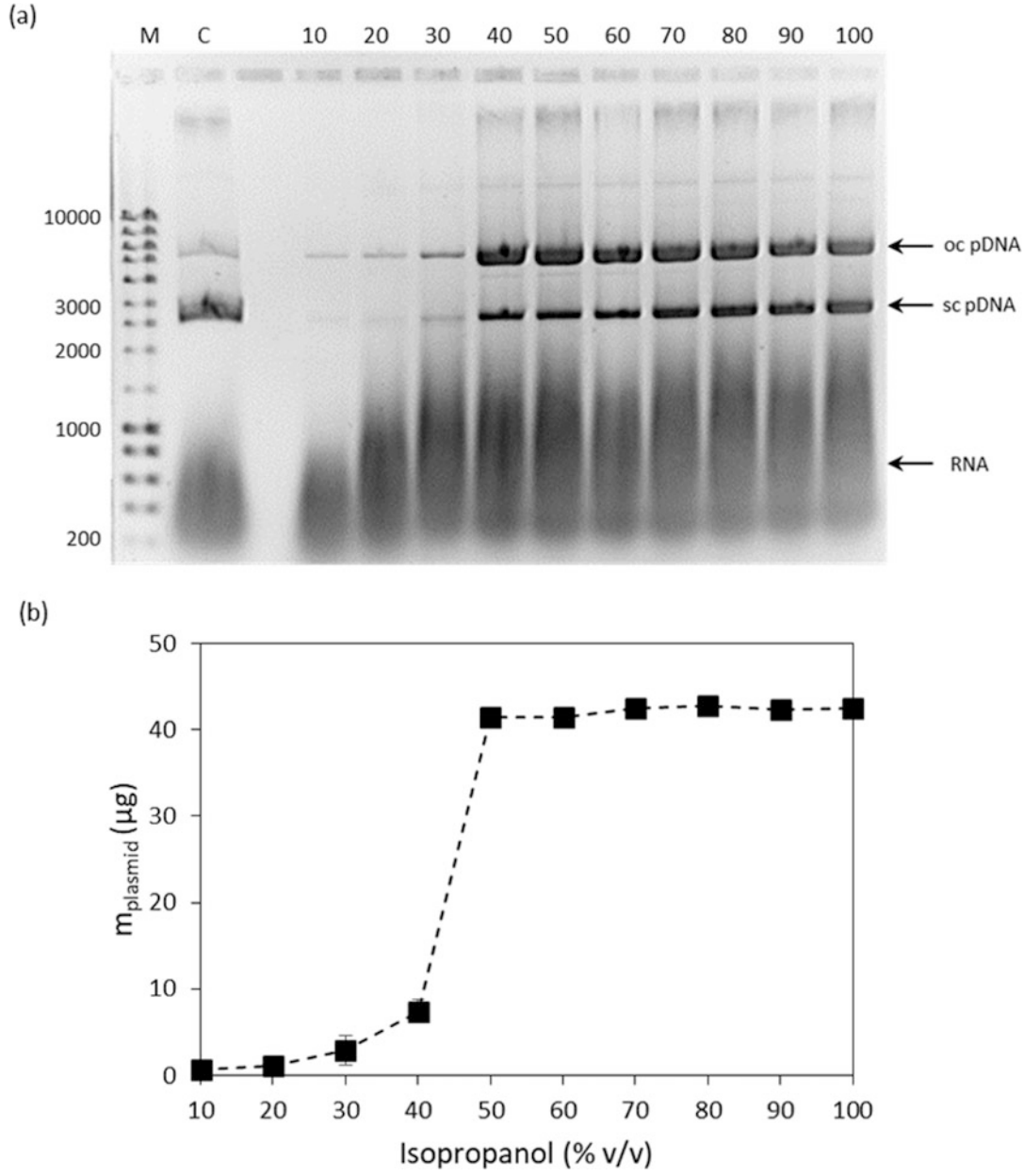

Fig. 1 Intermediate recovery of pDNA from alkaline lysates of *E. coli* cells using a one-step isopropanol precipitation. Lysates (1 mL) were incubated with increasing volumes of isopropanol (10–100% relatively to the volume of lysate) and centrifuged. Pellets were resuspended in 1 mL TE buffer and analyzed by gel electrophoresis and supernatants by HPLC. (**a**) Agarose gel electrophoresis analysis of pDNA containing samples. Lane M—molecular weight marker. Numbers of lanes 10–100 match with the amount of isopropanol (% of lysate volume) used. *oc* open circle, *sc* supercoiled. (**b**) Plasmid mass recovered in pellets as measured by HPLC

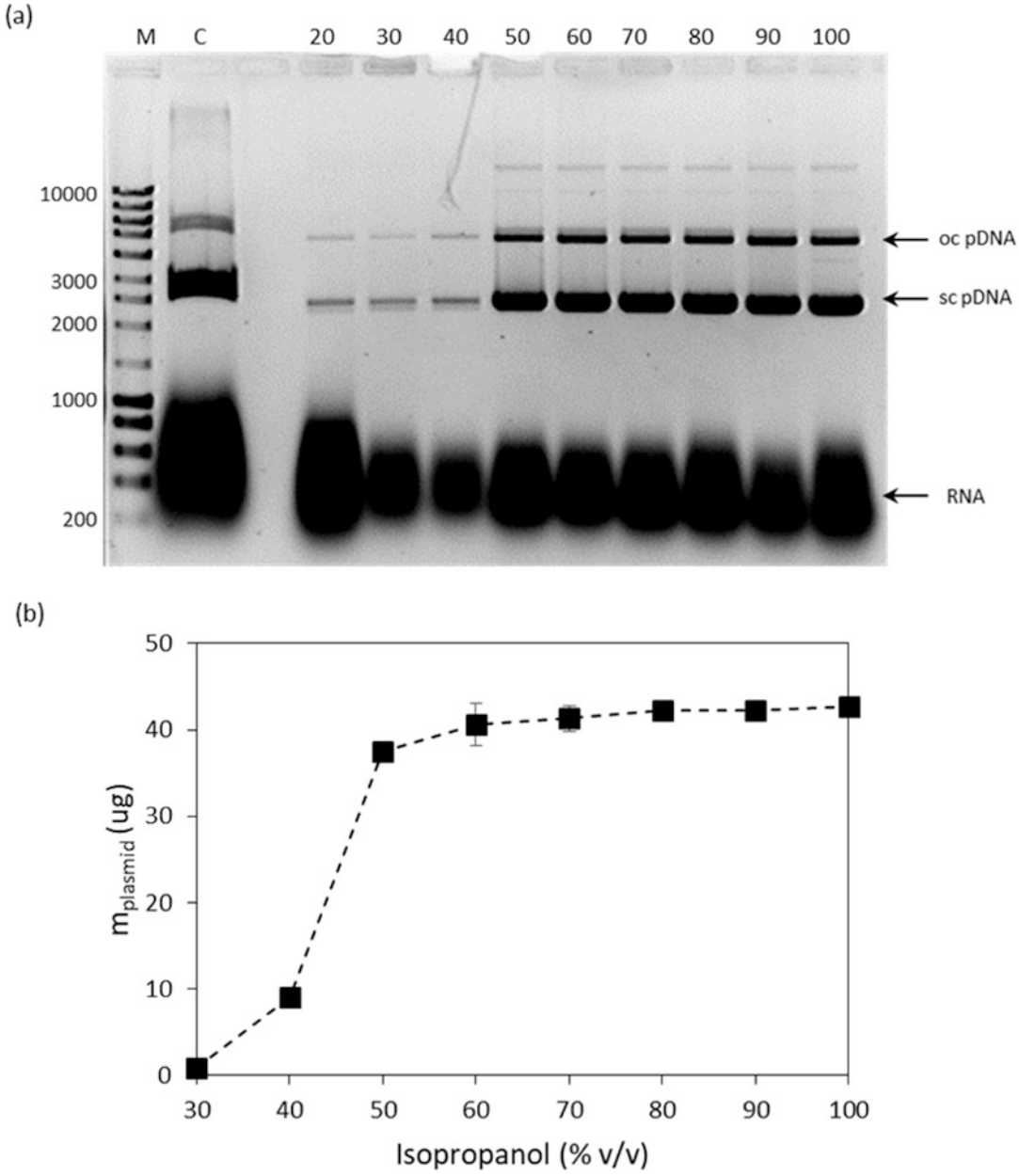

Fig. 2 Intermediate recovery of pDNA from alkaline lysates of *E. coli* cells using differential isopropanol precipitation. The first precipitation was performed with 20% v/v isopropanol. After removal of precipitates, additional amounts of isopropanol were added to the pDNA-rich supernatant, bringing total isopropanol volume up to 30–100% v/v relatively to the lysate volume. The pellets were resuspended in TE buffer and analyzed by agarose gel electrophoresis, and supernatants by HPLC. (**a**) Agarose gel electrophoresis analysis of pDNA containing samples. Lane M—molecular weight marker, lane C—clarified lysate. Numbers of lanes 20–100 match with the total amount of isopropanol (% of lysate volume) used. *oc* open circle, *sc* supercoiled. (**b**) Plasmid recovery yield as measured by HPLC

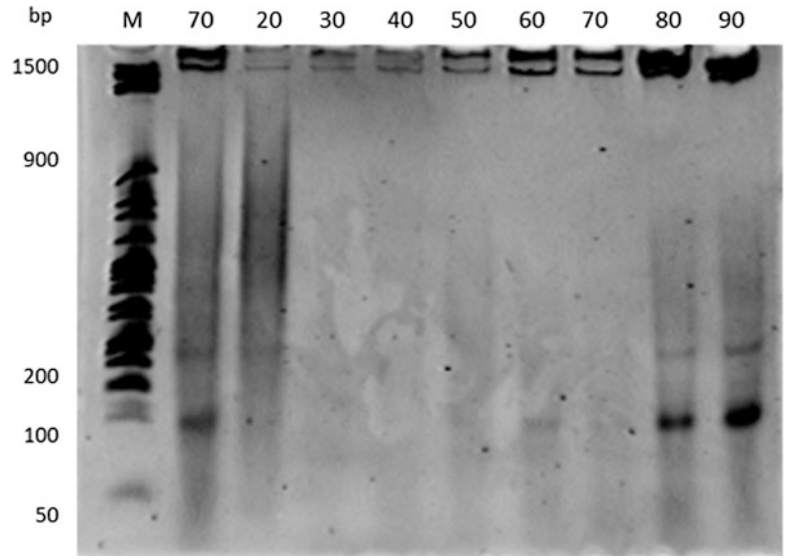

Fig. 3 Denaturing urea PAGE (5%) analysis of RNA in samples obtained after a differential isopropanol precipitation of alkaline lysates. Differential precipitation: the first precipitation was performed with 20% v/v isopropanol (lane 20). After removal of precipitates, additional amounts of isopropanol were added to the pDNA-rich supernatant, bringing total isopropanol volume up to 30–90% v/v relatively to the lysate volume. The pellets were resuspended in TE buffer and analyzed by urea PAGE. Numbers of lanes 20–100 match with the total amount of isopropanol (% of lysate volume) used. Lane S70 corresponds to a one-step precipitation with 70% v/v isopropanol

coprecipitation of high MW RNA [6]. The different patterns of precipitation of RNA and pDNA can be explained by the fact that the higher exposure of the hydrophobic bases in RNA facilitates aggregation upon alcohol-induced removal of solvation water molecules [6]. This is favored even further by the fact that the concentration of RNA in lysates is much higher when compared to pDNA.

24. The obtained HPLC chromatograms demonstrate very clearly that clearance of RNA by differential precipitation (Fig. 4c) is superior than the one obtained with one-step precipitation (Fig. 4b). The higher effectiveness of differential precipitation in impurity clearance is confirmed by the purity data shown in Fig. 4d. For example, when a total amount of 70% v/v isopropanol was used, a purity of 11.2% was obtained by differential precipitation versus the 3.8% obtained with a one-step precipitation.

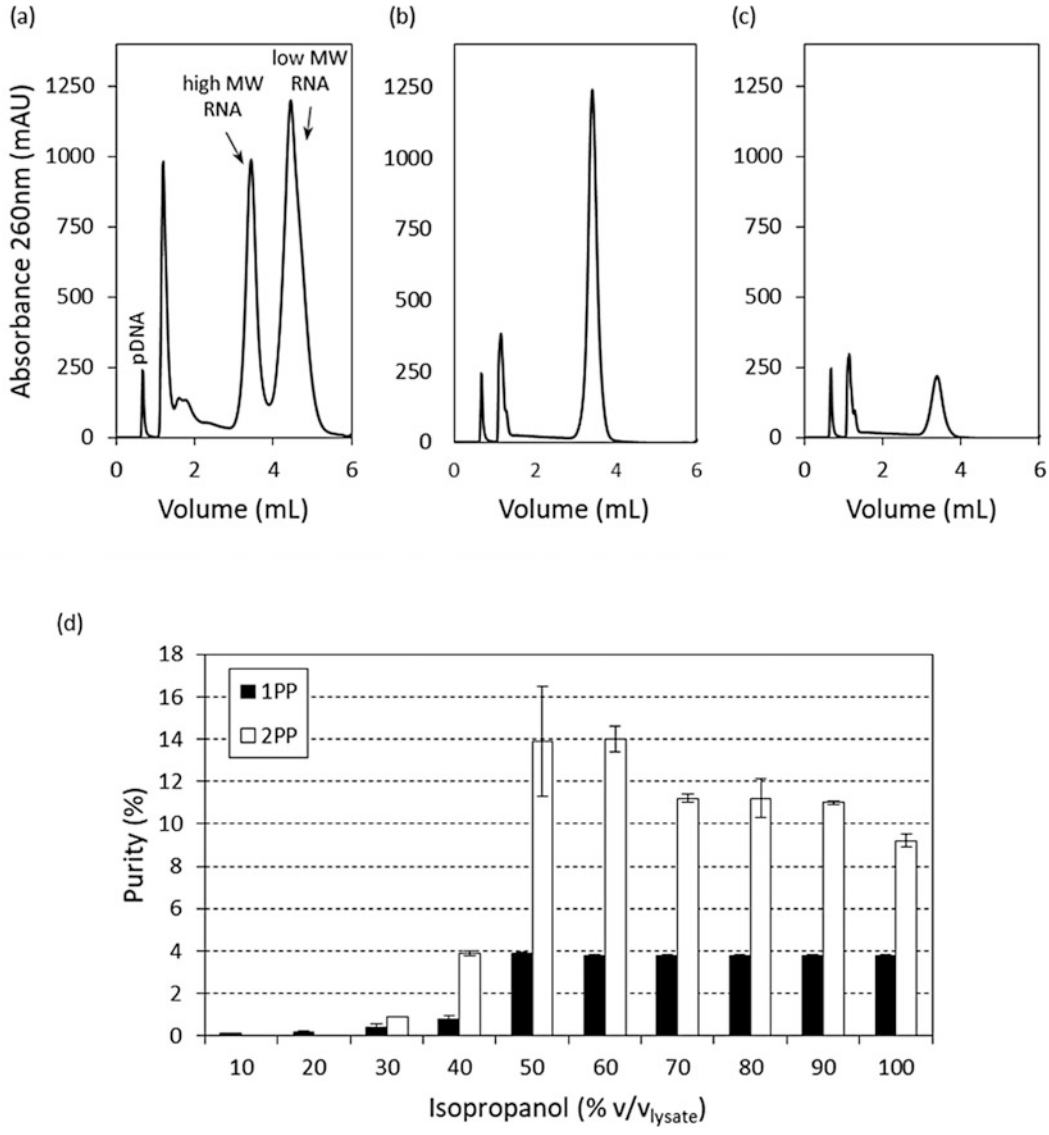

Fig. 4 HPLC analysis of pDNA-containing solutions obtained after isopropanol precipitation. Chromatograms are shown for (**a**) a clarified *E. coli* lysate, (**b**) a solution obtained after one-step precipitation with 70% v/v isopropanol, and (**c**) a solution obtained after differential precipitation with 20% and 70% v/v isopropanol. Peaks corresponding to pDNA, low and high molecular weight RNA are identified in the chromatograms. (**d**) Analysis of the pDNA purity of the resuspended precipitates obtained after a one-step precipitation (1PP) and a differential precipitation (2PP) that combines a first precipitation at 20% v/v with the second precipitation. The isopropanol percentage indicated in the *x*-axis refers to the total amount of isopropanol used (relatively to the lysate volume)

Acknowledgments

Funding received by iBB-Institute for Bioengineering and Biosciences from FCT-Portuguese Foundation for Science and Technology, Portugal (grant UID/BIO/04565/2019), the research project PureMab (PTDC/QEQ-PRS/0286/2014), and from Programa Operacional Regional de Lisboa 2020, Portugal (Project N. 007317) is acknowledged. A. Rita Silva-Santos acknowledges FCT for the PhD grant PD/BD/135138/2017 (BIOTECnico program).

References

1. Prather KJ, Sagar S, Murphy J et al (2003) Industrial scale production of plasmid DNA for vaccine and gene therapy: plasmid design, production, and purification. Enzym Microb Technol 33:865–883
2. Mairhofer J, Grabherr R (2008) Rational vector design for efficient non-viral gene delivery: challenges facing the use of plasmid DNA. Mol Biotechnol 39:97–104
3. Prazeres DMF, Monteiro GA (2014) Plasmid biopharmaceuticals. Microbiol Spectr 2. https://doi.org/10.1128/microbiolspec.PLAS-0022-2014
4. Prazeres DMF (2011) Plasmid biopharmaceuticals: basics, applications and manufacturing. John Wiley & Sons, Hoboken, NJ. https://doi.org/10.1002/9780470939918.ch12
5. Flock S, Labarbe R, Houssier C (1996) Dielectric constant and ionic strength effects on DNA precipitation. Biophys J 70:1456–1465
6. Freitas SS, Santos JAL, Prazeres DMF (2006) Optimization of isopropanol and ammonium sulfate precipitation steps in the purification of plasmid DNA. Biotechnol Prog 22:1179–1186
7. Silva-Santos AR, Alves CPA, Prazeres DMF et al (2017) A process for supercoiled plasmid DNA purification based on multimodal chromatography. Sep Purif Technol 182:94–100
8. Azzoni AR, Ribeiro SC, Monteiro GA et al (2007) The impact of polyadenylation signals on plasmid nuclease-resistance and transgene expression. J Gene Med 9:392–402
9. Sambrook J, Russell DW (2006) Neutral polyacrylamide gel electrophoresis. CSH Protoc 2006. https://doi.org/10.1101/pdb.prot4028
10. Singer A, Eiteman MA, Altman E (2009) DNA plasmid production in different host strains of *Escherichia coli*. J Ind Microbiol Biotechnol 36:521–530
11. Diogo MM, Queiroz JA, Prazeres DMF (2003) Assessment of purity and quantification of plasmid DNA in process solutions using high-performance hydrophobic interaction chromatography. J Chromatogr A 998:109–117

Chapter 9

Scale-Up of Plasmid DNA Downstream Process Based on Chromatographic Monoliths

Urh Černigoj and Aleš Štrancar

Abstract

Purification of high-quality plasmid DNA in large quantities is a crucial step in its production for therapeutic use and is usually conducted by different chromatographic techniques. Large-scale preparations require the optimization of yield and homogeneity, while maximizing removal of contaminants and preserving molecular integrity. The advantages of Convective Interaction Media® (CIM®) monolith stationary phases, including low backpressure, fast separation of macromolecules, and flow-rate-independent resolution qualified them to be used effectively in separation of plasmid DNA on laboratory as well as on large scale. A development and scale-up of plasmid DNA downstream process based on chromatographic monoliths is described and discussed below. Special emphasis is put on the introduction of process analytical technology principles and tools for optimization and control of a downstream process.

Key words Chromatography, Column, Downstream process, Large-scale, Monolith, Pharmaceutical grade, Plasmid DNA manufacturing, Plasmid DNA purification, Process analytical control, Scale-up

1 Introduction

1.1 Downstream Processing of Plasmid DNA

Plasmid DNA (pDNA) used in vaccination and gene therapy has to be highly pure and homogenous, thus it requires efficient, reproducible, and scalable manufacturing processes [1]. Additionally, pDNA vaccination usually requires milligram amounts per individual to become effective. Therefore, large-scale manufacturing (more than 1 g or even more than 1 kg of pDNA) must meet the need of producing gram to kilogram amounts of these molecules in order to satisfy requirements.

The typical biopharmaceutical manufacturing scheme is traditionally divided into fermentation/cell culture (e.g., bioreactor-based or upstream operations) and the so-called downstream processing (DSP) operations [2]. The latter deal with everything related to product purification and concentration, including primary recovery, further (high-resolution) polishing and final formulation of the product.

Ângela Sousa (ed.), *DNA Vaccines: Methods and Protocols*, Methods in Molecular Biology, vol. 2197,
https://doi.org/10.1007/978-1-0716-0872-2_9,

A challenge that modern downstream bioprocessing practice faces today is the need for targeting new classes of (bio) products like viruses, virus-like particles, messenger RNA, extracellular vesicles, and pDNA. The purification of such entities is a complicate process and DSP normally includes several steps, such as cell alkaline lysis, multiple solid-liquid separations, multiple precipitation steps, chromatography, and membrane operations [1]. Due to stringent regulatory requests and due to process economics, the majority of pDNA DSPs are partially based on chromatography, which enables the highest quality levels of product of interest [1]. Chromatographic adsorbent systems with very low dynamic capacity require a large volume of adsorbent (e.g., a very large column) to process modest amounts of mentioned supramolecular complexes. This, in turn, involves an excessive consumption of resources, particularly large volume of buffers and water. Traditional porous adsorbent beads for column chromatography were designed to accommodate separation of proteins of moderate molecular weight. Their ability to bind bigger entities is severely reduced due to increased mass transfer limitations or binding site accessibility [3]. Convective chromatographic supports, such as chromatographic monoliths, often bypass this limitation by providing large capacity and superior resolution power for bigger entities, including pDNA [4]. The channels of a monolithic column allow convective mass transfer between the mobile phase and the resin. This property of monoliths simplifies the scale-up process as residence time does not affect the resolution and dynamic binding capacity of the column [3]. Convective Interaction Media® (CIM®) monolithic chromatographic columns were designed with unique operating properties that make them ideally suited to the challenging requirements of purification of very large biomolecules such as virus particles, vesicles, proteins, RNAs, plasmids, and other forms of DNA [5]. CIMmultus™, the preparative line of CIM® monolithic chromatographic columns, starts with a bed volume of 1 mL (bench scale purification) and enables easy scaling up to the large-scale production employing 800 mL, 4 L, 8 L, or 40 L [6], because:

(a) Monoliths come prepacked and qualified regardless the scale—you never need to pack them yourself.

(b) Flow-rate-independent binding capacity and resolution enable flexibility of varying the flow rate during scale-up.

(c) The columns are compliant with Current Good Manufacturing Practice (cGMP), enabling the product production for direct clinical applications.

There are a variety of existing methods to purify plasmids, but not many are suitable for large-scale preparations [1]. Laboratory-scale purification techniques simply cannot be scaled up for the volumes involved in large-scale pDNA preparation. Many of these

purification methods rely on the use of potentially dangerous, toxic, expensive substances, which are not desirable for large-scale purification.

Multiple challenges must be overcome when developing a large-scale purification approach. Optimization of yield, processing time, and molecular integrity, while maximizing the removal of contaminants, represents several hurdles in the process. BIA Separations offers a pDNA DSP with these challenges in mind, applicable for laboratory-scale purification and scalable for manufacturing of pDNA as raw material or drug substance [7]. The following needs are fulfilled:

(a) Minimal, highly efficient process steps.
(b) No enzymes, no dangerous and toxic chemicals.
(c) High-yield and high final concentration of pDNA.
(d) Minimal degradation of pDNA.
(e) Clinical-grade purity of the product.
(f) Straightforward scale-up.

DSP train (*see* Fig. 1) based on CIM® monoliths starts with alkaline lysis followed by a selective precipitation of impurities using calcium chloride ($CaCl_2$) that removes cell debris, organelles, most of proteins, and bacterial genomic DNA (gDNA). This step leaves part of the RNA as the main contaminant of the target pDNA together with some proteins, endotoxins, and gDNA [7]. Then, after (a) a primary, secondary, and optionally tertiary filtration and (b) a conductivity adjustment with deionized water, the capture of pDNA is achieved by passing the lysate through CIMmultus™ DEAE weak anion exchanging monolithic column [7]. In the second chromatography step performed on CIMmultus™ C4 HLD chromatographic monolith, the supercoiled pDNA (sc pDNA) is separated from other isoforms and from remains of other impurities using hydrophobic interaction chromatography in step-gradient elution mode [7–9]. Finally, concentration and buffer exchange are done using ultrafiltration or tangential flow filtration and are followed by sterile filtration.

1.2 Process Analytical Technology for pDNA

Process analytical technology (PAT) is a system for designing, analyzing, and controlling manufacturing through timely measurements (i.e., during processing) of critical quality and performance attributes of raw and in-process materials and processes, with the goal of ensuring final product quality. PAT is primarily focused on reducing process variability, achieved by the integration of quality control closer to the line (at-line) or even better in real time (on-line, in-line) with automated feedback [10]. Implementation of PAT in biotechnological industry and designing the process following a systematic manufacturing design should, despite the

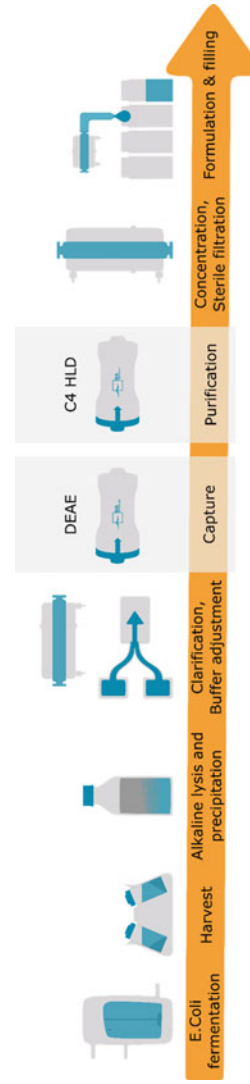

Fig. 1 General scheme of DSP for pDNA based on chromatographic monoliths

initial investment, result in the reduction of the process development times, reduction of the production costs, and increased productivity.

Chromatographic analysis approach, such as HPLC, offers high resolution for characterization of different components of the sample and their easy quantification with high precision, high reproducibility, high sample throughput, and high robustness. Traditionally, a HPLC method duration is an average of 30 min. This makes them unsuitable for high-throughput analysis. With efficient analytical monolithic columns, analysis time is reduced which allows implementation of HPLC as PAT tool. Such method improves process understanding in both upstream production and

downstream purification and ensures consistent product quality [11]. HPLC analysis using dedicated CIMac™ pDNA Analytical Column allows fast quantification of sc pDNA as well as determination of chromatographic pDNA purity [12, 13]. Additionally, when used in parallel with the pDNA DSP, it ensures that each production step is yielding the amount of sc pDNA anticipated [14].

2 Materials

Prepare all solutions using deionized water and, when needed, cGMP compliant reagents. Prepare and store all reagents at room temperature for up to a week (unless indicated otherwise). For analytical chromatography, prepare all solutions using ultrapure water (a sensitivity of 18 MΩ/cm at 25 °C) and analytical-grade reagents. Diligently follow all waste disposal regulations when disposing waste materials.

2.1 pDNA Lysis

1. Resuspension buffer: 50 mM Tris–HCl, 10 mM EDTA, pH 8.0 (1 L). Weigh 6.06 g Tris–HCl and 3.72 g Na_2EDTA and transfer them to the 1 L glass beaker. Add about 800 mL water and while mixing with magnetic stirrer adjust the pH with HCl solution to 8.0 (*see* **Note 1**). Transfer the solution to a 1 L graduated cylinder and make up to 1 L with water (*see* **Note 2**). Mix again and recheck the pH of the buffer. Filter the buffer through a 0.22 μm PES filter.
2. Cell lysis buffer: 0.2 M NaOH, 1% sodium dodecyl sulfate (SDS) (1 L). Weigh 8 g NaOH and transfer it to the 1 L glass beaker. Add about 100 mL water and dissolve NaOH by mixing with magnetic stirrer. Add water to approximately 800 mL. Weigh 10 g SDS, transfer it to the NaOH solution and dissolve it by mixing. Transfer the solution to a 1 L graduated cylinder and make up to 1 L with water (*see* **Note 2**). Use the solution freshly prepared, do not store.
3. Neutralization buffer: 3 M potassium acetate, pH 5.5 (1 L). Weigh 294.5 g potassium acetate and transfer to a 1 L glass beaker. Add about 800 mL water, and while mixing with magnetic stirrer, adjust the pH with HCl solution to 5.5 (*see* **Note 1**). Transfer the solution to a 1 L graduated cylinder and make up to 1 L with water (*see* **Note 2**). Mix again and recheck the pH of the buffer. Filter the buffer through a 0.22 μm PES filter and keep it at 4 °C until use.
4. Stock $CaCl_2$ solution: 5 M $CaCl_2$ (1 L). Weigh 554.8 g anhydrous $CaCl_2$ and transfer it to a 1 L glass beaker. Add about 800 mL water and dissolve the salt by mixing with magnetic stirrer. While dissolving, there is extensive heat release. After cooling the solution back to room temperature (*see* **Note 3**),

transfer it to a 1 L graduated cylinder and make up to 1 L with water (*see* **Note 2**). Filter the buffer through a 0.22 μm PES filter. Use the solution freshly prepared, do not store.

5. Primary filter: A filter with filtration range between 50 and 100 μm. Laboratory scale—centrifugation or cotton filtration can be used (*see* **Note 4**). Large scale—bag filtration or cartridge filtration (pleated filters) fitted in appropriate filter vessel, equipped with pumping system.
6. Secondary filter: A filter with filtration range between 1 and 25 μm. Laboratory scale—depth filter or membrane filter. Large scale—depth filtration or pleated cartridge filter fitted in appropriate filter vessel, equipped with pumping system.
7. Final filtration: A filter with filtration range between 0.2 and 0.8 μm. Laboratory scale—membrane filter, for example, Sartopore 2 capsules. Large scale—membrane or depth filter fitted in appropriate filter vessel, equipped with pumping system.
8. Conductivity meter with measuring range between 1 and 300 mSi/cm.

2.2 pDNA Capture Using Anion-Exchange Chromatography

1. CIMmultus™ DEAE weak anion-exchanging column. Laboratory scale—1, 4, or 8 mL bed volume, large scale—40, 80, 400, 800 mL, 4, 8 L, or 40 L bed volume.
2. Appropriate pumping system equipped with pressure sensors. Laboratory scale—peristaltic pump or FPLC system equipped with conductivity meter.
3. Equilibration buffer A1: 50 mM Tris, 10 mM EDTA, pH 7.2 (1 L). Weigh 6.06 g Tris–HCl and 3.72 g Na_2EDTA and transfer them to a 1 L glass beaker. Add about 800 mL water, and while mixing with magnetic stirrer, adjust the pH with HCl solution to 7.2 (*see* **Note 1**). Transfer the solution to the 1 L graduated cylinder and make up to 1 L with water (*see* **Note 2**). Mix again and recheck the pH of the buffer. Filter the buffer through a 0.22 μm PES filter.
4. Elution buffer A3: 50 mM Tris, 10 mM EDTA, 1.0 M NaCl, pH 7.2 (1 L). Weigh 6.06 g Tris–HCl, 58.44 g NaCl and 3.72 g Na_2EDTA and transfer them to a 1 L glass beaker. Add about 800 mL water, and while mixing with magnetic stirrer, adjust the pH with HCl solution to 7.2 (*see* **Note 1**). Transfer the solution to a 1 L graduated cylinder and make up to 1 L with water (*see* **Note 2**). Mix again and recheck the pH of the buffer. Filter the buffer through a 0.22 μm PES filter.
5. Storage solution: 20% (v/v) ethanol (1 L). Measure 200 mL of 96% ethanol in a 1 L graduated cylinder and make up to 1 L with water. Mix well and filter the solution through 0.22 PES filter.

2.3 pDNA Polishing Using Hydrophobic Interaction Chromatography (HIC)

1. Equilibration buffer B1: 50 mM Tris, 10 mM EDTA, 3 M ammonium sulfate (AS), pH 7.2 (1 L). Weigh 6.06 g Tris–HCl, 396.4 g AS, and 3.72 g Na_2EDTA and transfer them to a 1 L glass beaker. Add about 800 mL water and while mixing with magnetic stirrer adjust the pH with HCl solution to 7.2 (*see* **Note 1**). Transfer the solution to a 1 L graduated cylinder and make up to 1 L with water (*see* **Note 2**). Mix again and recheck the pH of the buffer. Filter the buffer through a 0.22 μm PES filter.
2. Elution buffer A1: 50 mM Tris, 10 mM EDTA, pH 7.2 (1 L): The same procedure as for equilibration buffer A1.
3. Adjustment solution A4: 4 M AS (1 L): Weigh 528.56 g AS and transfer it to a 1 L glass beaker. Add about 900 mL water and dissolve it by mixing with magnetic stirrer (*see* **Note 5**). Transfer the solution to a 1 L graduated cylinder and make up to 1 L with water (*see* **Note 2**). Mix well again. Filter the solution through a 0.22 μm PES filter. Store the solution at room temperature up to 1 month.
4. Storage solution: 10 mM NaOH (1 L). Weigh 0.40 g NaOH and transfer it to a 1 L glass beaker. Add about 100 mL water and dissolve NaOH by mixing with magnetic stirrer. Transfer the solution to a 1 L graduated cylinder and make up to 1 L with water. Mix well and filter the solution through 0.22 PES filter.
5. CIMmultus™ C4 HLD column. Laboratory scale—1, 4, or 8 mL bed volume, large scale—40, 80, 400, 800 mL, 4, 8, or 40 L bed volume.
6. Chromatographic system equipped with UV, conductivity, and pH detectors. Laboratory scale—FPLC or HPLC system; Large scale—industrial HPLC system.

2.4 pDNA Analytics Using CIMac™ pDNA Column

1. CIMac™ pDNA column.
2. Analytical HPLC system, equipped with UV detector at 260 nm and conductivity detector.
3. Mobile phase A (MPA): 100 mM Tris, pH 8.0 (1 L). Weigh 12.11 g Tris–HCl and transfer it to a 1 L glass beaker. Add about 800 mL water and while mixing with magnetic stirrer adjust the pH with HCl solution to 8.0 (*see* **Note 1**). Transfer the solution to a 1 L graduated cylinder and make up to 1 L with water (*see* **Note 2**). Mix again and recheck the pH of the buffer. Filter the buffer through a 0.22 μm PES filter.
4. Mobile phase B (MPB): 100 mM Tris, 1 M NaCl, pH 8.0 (1 L). Weigh 12.11 g Tris–HCl, 58.44 g NaCl and transfer them to a 1 L glass beaker. Add about 800 mL water and while mixing with magnetic stirrer adjust the pH with HCl solution

to 8.0 (*see* **Note 1**). Transfer the solution to a 1 L graduated cylinder and make up to 1 L with water (*see* **Note 2**). Mix again and recheck the pH of the buffer. Filter the buffer through a 0.22 μm PES filter.

3 Methods

The methods described below present all the steps of pDNA DSP from the process optimization on laboratory scale to the final process scale up. Carry out all procedures at room temperature unless otherwise specified.

3.1 Optimization of Cell Lysis and Clarification Step

1. Weigh 1–2 g of frozen biomass containing pDNA into a 25 mL beaker or reagent flask. Add the resuspension buffer (ratio is 10 mL of buffer per g of frozen biomass). Add a small magnetic stirrer bar, cover the beaker and stir on a magnetic stirrer plate. Wait until the biomass is completely homogeneously suspended, which usually takes around 60 min.
2. Divide the resuspended biomass into three parts (use 50 mL centrifuge tubes) using a pipette.

*3.1.1 Optimization of Cell Lysis Time (See **Note 6**)*

1. Follow the flowchart in Fig. 2, enter and calculate the needed volumes, and perform the optimization experiments as instructed below.
2. Prepare 20 mL of fresh cell lysis buffer in 50 mL centrifugal tube (*see* **Note 7**).
3. Chill the neutralization buffer (3 M potassium acetate, pH 5.5), in the fridge at 4–8 °C.
4. Add cell lysis buffer (volume added is equal to the volume of suspended cells) to the dissolved biomass to lyse the cells. Mix gently and carefully. Incubate the sample for exactly the time specified in the Fig. 2.
5. To lower the pH of the sample add chilled neutralization buffer (volume added is equal to the volume of suspended biomass) while gently mixing the suspension. Some precipitation of detergent can be observed in this step. Proceed directly to clarification phase to avoid any decomposition of pDNA.
6. Add the calculated (*see* Fig. 2) amount of 5 M $CaCl_2$ into the sample solution, mix and incubate at room temperature for 10 min.
7. Pipette liquid fraction (at least 3 mL) and filter it through disk filter with filtration range between 0.45 and 0.8 μm, into a clean container (*see* **Note 8**).

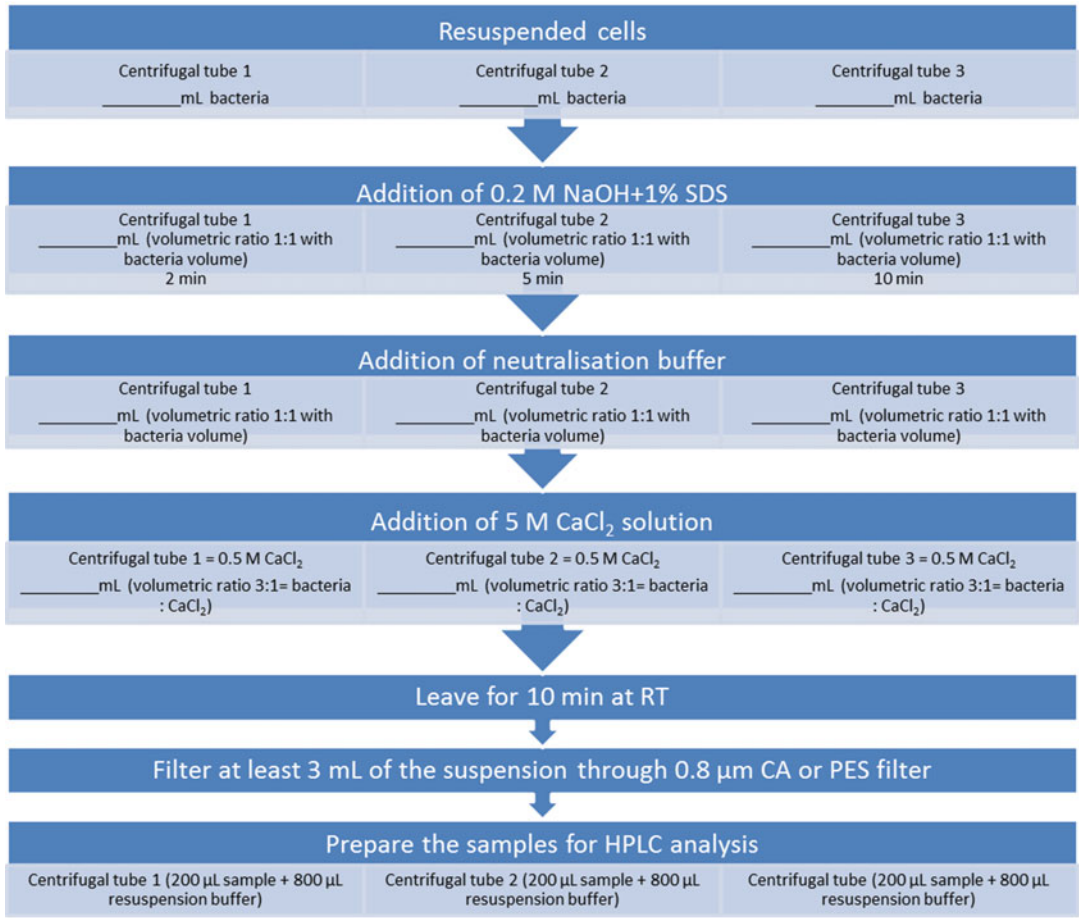

Fig. 2 Lysis and clarification workflow—optimization of lysis time

8. Take 200 µL aliquot, transfer it to an HPLC vial, and dilute it five times with MPA (100 mM Tris, pH 8.0). Label the HPLC samples as LYSATE-2-min, LYSATE-5-min, and LYSATE-10-min.
9. To analyze the fractions, follow instructions in Subheading 3.1.3. The optimal lysis time will be determined from the analytical results.

3.1.2 Optimization of Clarification Step (See ***Note 9***)

1. Follow the flowchart in Fig. 3, enter and calculate the needed volumes, and perform the optimization experiments as instructed below.
2. Prepare 20 mL of fresh cell lysis buffer in 50 mL centrifuge tube.
3. Chill the 3 M potassium acetate, pH 5.5, in the fridge at 4–8 °C.

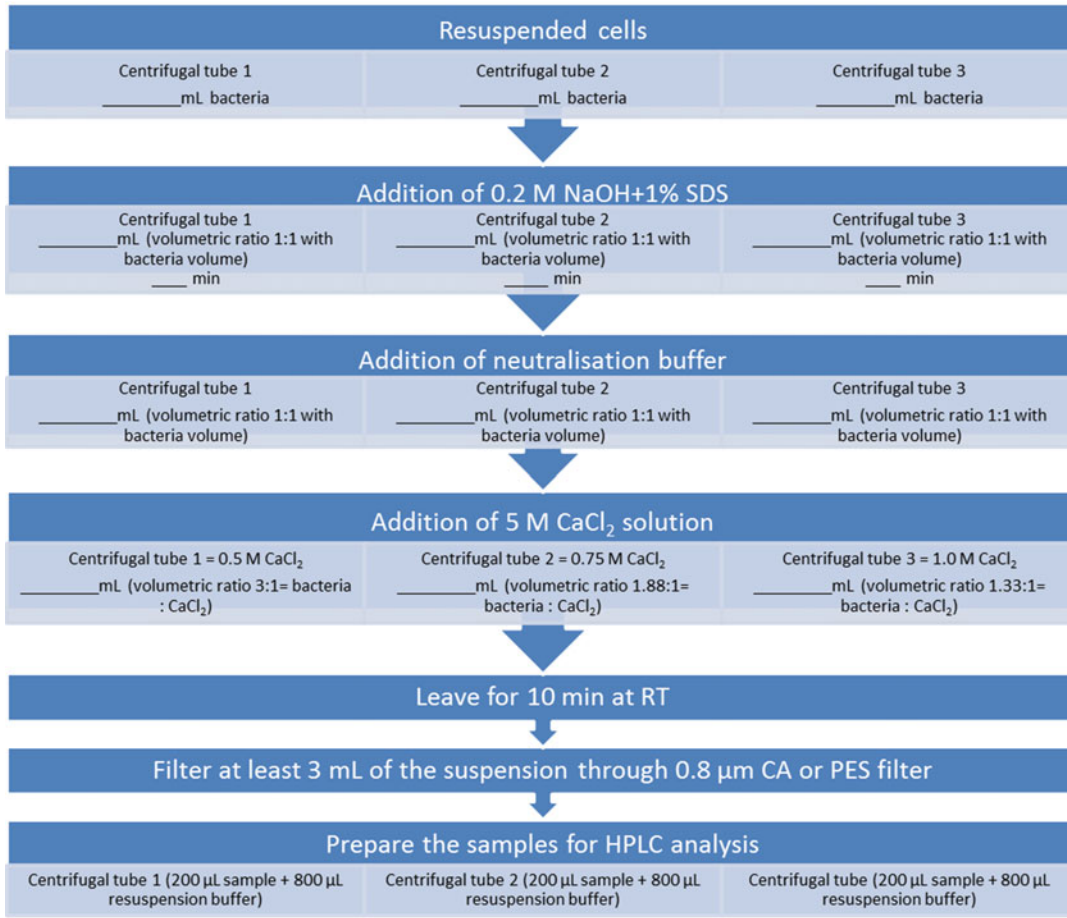

Fig. 3 Lysis and clarification workflow—optimization of $CaCl_2$ concentration

4. Add cell lysis buffer (volume added is equal to the volume of suspended cells) to suspended biomass to lyse the cells. Mix gently and carefully. Incubate the sample for exactly the time, specified as optimal in the previous experiment.
5. To lower the pH of the sample, add chilled neutralization buffer (volume added is equal to the volume of suspended cells) while gently mixing the suspension. Some precipitation of detergent can be observed in this step. Proceed directly to clarification phase to avoid any decomposition of pDNA.
6. Add the calculated amount of 5 M $CaCl_2$ into the sample solution in order to reach final $CaCl_2$ concentration of 0.5, 0.75, and 1.0 M. Mix and incubate at room temperature for 10 min.
7. Pipette liquid fraction (at least 3 mL) and filter it through disk filter with filtration range between 0.45 and 0.8 µm into a clean container (*see* **Note 8**).

8. Take 200 µL aliquot, transfer it to a HPLC vial, and dilute it five times with MPA (100 mM Tris, pH 8.0). Label the HPLC samples as $CaCl_2$—0.5, $CaCl_2$—0.75, and $CaCl_2$—1.
9. To analyze the fractions, follow instructions in Subheading 3.1.3. The optimal $CaCl_2$ concentration will be determined from the analytical results.

*3.1.3 pDNA Analytics (See **Note 10**)*

Chromatographic runs are performed using analytical chromatographic system equipped with 10 mL pump heads. It is advisable to perform the analyses at constant temperature due to high temperature sensibility of the pDNA separation (*see* **Note 11**). CIMac™ pDNA column is used as an analytical column for pDNA analysis. Injection volume is between 10 and 100 µL, depending on the pDNA concentration in the sample. The flow rate applied is 1.0 mL/min, the UV signals at 260 nm and optionally at 280 nm are followed. The chromatographic separation is performed in NaCl linear gradient (Fig. 4), for more info regarding establishing the optimal linear gradient, *see* **Note 12**.

1. Equilibrate the CIMac pDNA column by applying 6 mL of buffer MPA, followed by 6 mL MPB, followed by 6 mL MPA.
2. Inject a pDNA standard and perform the chromatographic run. *See* the chromatogram in Fig. 4 as an example of chromatographic profile. The peak areas from the chromatogram (s) will be used for single- or multi-point calibration curve formation for oc and sc pDNA (*see* **Note 13**).

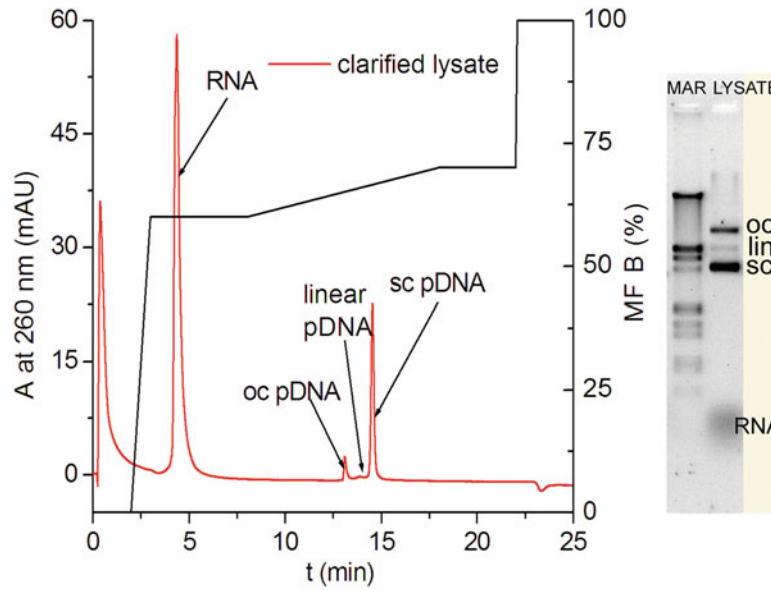

Fig. 4 (Left) A typical chromatogram obtained with CIMac™ pDNA column with indicated resolved analytes. (Right) Agarose gel obtained from the same sample

Table 1
Chromatographic method used for pDNA capture step optimization

Fraction	*t* (min)	Flow rate (mL/min) (*see* Note 24)	% of A1	Purpose
	0–4	5	100	
WASH-CAPTURE 1	4.05–6	5	45	RNA wash
WASH-CAPTURE 2	6.05–8	5	40	RNA wash
WASH-CAPTURE 3	8.05–10	5	35	RNA wash
ELUTION-CAPTURE	10.05–14	2	0	pDNA elution
	14.05–16	5	100	

3. Inject samples from lysis optimization and analyze the data (peak areas) and calculate the pDNA concentrations for pDNA using the equation from calibration curve (*see* **Note 14**).
4. Column sanitization should be done at minimum after every 30th pDNA injection or as soon a resolution decrease is observed. This is performed with washing the column with 1 M NaOH for at least 1 h at room temperature in reverse direction, followed by thorough conditioning of the column, especially with MPB.
5. Collect the experimental results from lysis optimization (an example of results collection is shown in Table 1), calculate the parameters, which are γ_{total} (pDNA) in mg/mL; m_{total} (pDNA) in mg; sc pDNA homogeneity defined as area of sc pDNA divided by sum of sc and oc pDNA area; RNA/pDNA ratio, defined as RNA peak area divided by sum of sc and oc pDNA area. From the data analysis decide for the optimal lysis conditions (*see* **Note 15**).

3.2 Chromatographic Capture Optimization

CIMmultus™ DEAE monolithic column with 1 mL bed volume is used for the chromatographic optimization (*see* **Note 16**).

1. Prepare an appropriate amount of lysate using the optimal conditions defined above. The amount of plasmid DNA present in the sample before chromatographic loading should be at least 5 mg. More than that can be prepared to allow additional subsequent experiments (*see* **Note 17**).
2. After $CaCl_2$ precipitation perform a coarse filtration. The simplest way is to pass the lysate through an approximately 1 cm thick cotton sheets, held in a strainer. More sophisticated procedure involves a filtration through 40–80 μm depth filters.

3. Measure the conductivity of your sample and add deionized H_2O to a final conductivity of 35 mS/cm (measured at reference temperature of 25 °C) (*see* **Note 18**). Be careful: mix the solution constantly, add purified H_2O in step-by-step manner, and wait until conductivity settles before adding additional H_2O.
4. Perform a 0.45 μm filtration of adjusted sample using an appropriate membrane or depth filter. Not filtering the material would clog the column in the subsequent step. In-line filtration during chromatographic loading can also be performed (*see* **Note 19**).
5. Take 100 μL aliquot of the sample before loading on the column, and label it as LOAD-CAPTURE.
6. Equilibrate CIMmultus DEAE-1 mL column by applying 20 column volumes (CV) of equilibration buffer A1 (*see* **Note 20**).
7. Load-clarified diluted bacterial lysate containing approximately 5 mg of pDNA to the column at 5 mL/min (*see* **Notes 21** and **22**). Collect at least three fractions (for pDNA analytics) at the outlet of the column after loading a third, two thirds, and at the end of loading sample. Label the fractions collected as: FT-CAPTURE 1, 2, and 3.
8. Use the following chromatographic method (*see* Table 1) to selectively wash and elute the sample (*see* **Note 23**). Collect the samples into 15 mL centrifugal tubes and label them WASH-CAPTURE 1, 2, and 3 and ELUTION-CAPTURE.
9. pDNA analytics: inject diluted samples from capture step on CIMac™ pDNA column. Calculate the following parameters: sc pDNA recovery calculated as the amount of sc pDNA in elution fractions divided by sc pDNA in loading fraction; RNA/pDNA ratio in elution fractions. Analyze the data and decide for the optimal pDNA loading amount, washing, and elution conditions (*see* **Note 25**).
10. Before the next pDNA chromatographic capture using the same column, it is recommended to thoroughly wash the column with 1 M NaOH for at least 2 h at room temperature (*see* **Note 26**), followed by a thorough conditioning of the column.

3.3 Polishing Step Optimization

CIMmultus™ C4 HLD monolithic column with 1 mL bed volume is used for the chromatographic optimization (*see* **Note 27**). It is recommended to perform polishing step on HPLC or FPLC system enabling step gradients employed at least with UV and conductivity detectors.

Table 2
Chromatographic method used for pDNA polishing step optimization

Fraction	*t* (min)	Flow rate (mL/min)	% of B1 buffer	AS concentration according to B1 percentage (M)
	0–4	5	100	3
POLISHING 1	4.05–7	5	65	1.95
POLISHING 2	7.05–10	5	60	1.8
POLISHING 3	10.05–13	5	55	1.65
POLISHING 4	13.05–16	5	50	1.5
POLISHING 5	16.05–19	5	45	1.35
POLISHING 6	19.05–22	5	35	1.05
POLISHING 7	22.05–25	5	30	0.9
POLISHING 8	25.05–28	5	25	0.75
POLISHING 9	28.05–32	5	0	0

1. Adjust the pDNA-containing eluate from the DEAE column by adding three volumes of A4 per one volume of collected eluate (*see* **Note 28**). Take 100 μL aliquot of the sample and label it as LOAD-POLISHING.
2. Connect the 1 mL C4 HLD column on an appropriate chromatographic system. The flow rate applied is 5 mL/min, and the UV signals at 260 nm and 280 nm are followed. Equilibrate the column by applying 20 CV of buffer B1.
3. Load exact amount of adjusted pDNA fraction eluted from the DEAE column, containing 1.8 ± 0.3 mg pDNA per mL chromatographic support (*see* **Notes 29** and **30**).
4. Perform a descending step gradient method from B1 to A1 (*see* the gradient in Table 2). Collect the peaks in each step into 15 mL centrifugal tubes and label them POLISHING 1–9 (*see* **Note 31**). Instead of using a step gradient method a linear gradient elution could be employed as well (*see* **Note 32**).
5. Before the new pDNA chromatographic polishing using the same column, it is recommended to thoroughly wash the column with 1 M NaOH for at least 2 h at room temperature, followed by a thorough conditioning of the column (*see* **Note 26**).
6. pDNA analytics: inject diluted samples from capture step on CIMac™ pDNA column. Determine the following parameters: ratio between oc pDNA and sc pDNA isoform in each collected fraction; sc pDNA/RNA ratio in collected fractions; ratio

between sc pDNA and pDNA multimers in each collected fraction.

7. Define the optimal AS concentration in the washing buffer (oc pDNA removal) and in pDNA elution buffer (RNA removal) (*see* **Note 33**).

3.4 pDNA Quality Control (See Note 34)

Sample containing the product (sc pDNA) has to be analyzed for the following parameters. The specifications for each impurity depend on the quality level of pDNA needed; therefore, they are not specified in the text.

1. Concentration of pDNA in aqueous solution. This can be done spectrophotometrically or by chromatographic analysis, such as described above.
2. RNA presence: visual checking for RNA on agarose gel. The absence of RNA is proven on gel, if there is no smeared band below 500 bp.
3. pDNA homogeneity (oc pDNA and linear pDNA presence): can be proven by chromatographic analysis as described above or by visual checking for oc pDNA on agarose gel.
4. Quantification of genomic (bacterial) DNA: Quantitative real-time PCR analysis is used for this purpose, so that the number of gene copies of the ribosomal operons can be determined.
5. Quantification of endotoxins: Usually the endotoxins released from bacteria are determined in final pDNA solution by the limulus amebocyte lysate (LAL)-based test.
6. Determination of proteins: Chromogenic BCA or micro-BCA™ tests are used to determine the protein concentration in the sample.

3.5 Scaling-up the DSP—Intermediate Step

1. After finishing the optimization steps the following parameters are fixed: lysis time, NaOH concentration, $CaCl_2$ concentration, conductivity and volume of loading sample in DEAE capture step, the concentration of NaCl in capture washing step, the amount of pDNA sample loaded in C4 HLD polishing step, the concentration of AS in washing, and elution steps.
2. Perform a whole process using fixed parameters on laboratory-scale level (up to 50 mg of purified pDNA) (*see* **Note 35**). The quality and the amount of produced pDNA should correspond to the values predicted from the process optimization.
3. After the polishing step, the purified pDNA sample is dissolved in a TE buffer containing AS. The pDNA concentration should be between 100 and 300 μg/mL. Thus, the buffer exchange to a buffer of choice together with plasmid DNA concentration (usually above 1 mg/mL) needs to be performed (*see* Subheading 3.6).

3.6 Scaling-up the DSP—Large-Scale Purification

1. At this point a scale-up to large-scale production starts. But up-scaling from laboratory to industrial scale is not just multiplying relevant parameters and factors, but each step to be performed has to be carefully evaluated regarding reproducibility and product quality [15, 16]. When large-scale production of pDNA must be performed in pharmaceutical-grade purity, usually a process is done under cGMP conditions. GMP ensures that manufacturing, formulation, packaging, quality controls, etc., result in a product suitable for intended application with respect to product safety, quality, and efficiency. One of the most important aspects of GMP production is a dedicated GMP facility, equipped with clean rooms.
2. Employ PAT principles and tools throughout all the steps of large-scale DSP in order to keep control over the process and ensure the highest possible productivity together with the highest possible impurity removal efficiency.
3. Cell lysis: While it is relatively easy to conduct a fast lysis at stable temperature on laboratory scale by just mixing the suspension and controlling the temperature, this is not straightforward on large scale. In order to perform reproducible and efficient large-scale lysis, in-line lysis employing "Y" connector together with mixing device, such as in-line mixer, is a prerequisite. pDNA lysate after the in-line mixer enters the holding coil (the length and the diameter have to be optimized), which provides a sufficient contact time (but not too long, *see* the optimization step above) between the cells and the lysis agent [15]. The neutralization is usually done in conjunction with a bubble column mixer. Lysate suspension enters the bubble mixer from one side, while neutralizing buffer from the other side. Neutralized lysate solution flows vertically up the column and exits the mixer near the top. The passage of gas bubbles (nitrogen, argon, CO_2) through the vertical column serves to mix the lysate with neutralizing buffer, gently and with low shear in order to prevent pDNA degradation and to prevent contamination with degraded genomic (bacterial) DNA and endotoxins [15]. Similar principle as used for neutralization is employed afterwards for precipitation with $CaCl_2$. After lysis is complete, the neutralized lysate is kept in a holding tank at 2–8 °C for a specified time period.
4. Clarification: Batch filtration or continuous centrifugation is impractical at large scale, but bag or cartridge filter (50–100 μm particle size limit) in continuous mode can be employed due to their high dirt holding capacities. The filter material should be cGMP compliant and have low non-specific pDNA adsorption. Depending on the process, the pumping of the lysate from holding tank is processed in a way that precipitate or floated flocculent is not pumped together with a liquid

lysate to the clarification step. In this way, no primary filtration (bag or cartridge) is needed afterwards, and the lysate goes directly to secondary filtration. A secondary filter could be a depth or membrane filter (10–60 μm particle size limit, depending on the process). The third membrane filter with 0.2–0.80 μm particle size limit is used to remove the smallest particles, and in such way, a lysate for a subsequent chromatographic step is prepared.

5. Chromatographic capture: After filtration train, the lysate is stored in a holding tank. The dilution with purified water is achieved employing "Y" connector and a low shear mixer, before the solution enters the first chromatographic column. The column size and the flow rate depend on the amount of processed pDNA (*see* **Note 36**). For example, approximately 40 g of pDNA could be processed in a single run using an 8 L monolithic column. The washing and elution steps are defined from small-scale experiments. The eluate containing the product is kept in another holding tank.
6. Chromatographic polishing: The ion exchange eluate recovered from the capture step enters a polishing chromatographic step employing hydrophobic interaction principle. The conditioning of the eluate is achieved by an addition of 4 M AS solution in a similar way as a dilution is done in chromatographic capture. If a linear gradient elution is used instead of step gradient, refer to **Note 37** to get the information of scaling-up the linear gradients on CIM monoliths. The binding capacity of HIC monolithic column for pDNA is approximately three times lower compared to an anion exchanger, thus a larger column or more polishing cycles are needed to process one unit of eluate from a capture step.
7. Ultrafiltration/diafiltration: Ultrafiltration concentrates the biologically active material and removes excess salts. This could be done employing an ultrafiltration unit with hollow fiber cartridges or tangential flow filtration unit with membranes (e.g., 300 kDa cut-off). In such way, low molecular weight material passes the membrane. Final concentration of pDNA in the buffer could be even higher than 10 mg/mL.
8. Membrane sterile filtration through 0.22 μm pores is typically the last operation in the production of pharmaceutical-grade pDNA. Especially for larger pDNA molecules, it is necessary to optimize this step as well, because the recovery of the pDNA together with its integrity depends on the type of membrane and on the buffer used in filtration [17].

4 Notes

1. Concentrated HCl (12 M) can be used at first to rapidly approach the required pH. For fine tuning, a series of HCl solutions with lower ionic strengths (e.g., 6 and 1 M) should be used to avoid a sudden drop in pH below the required pH.
2. For laboratory-scale experiments, it is easier to prepare buffers "by volume," using graduated cylinders. When scaling-up, the buffer preparation should be prepared "by mass." The easiest way is to define the exact amount of added water and acid/base on 1 L scale and then recalculate the amounts of the reagents for larger volumes.
3. While cooling/storing the $CaCl_2$ solution, seal the flask to prevent contact with atmosphere. Calcium cations and carbon dioxide react, forming a calcium carbonate precipitate.
4. For laboratory-scale pDNA preparation, the coarse filtration could be performed very efficiently using approximately 1 cm thick cotton sheets, held in a strainer. The neutralized lysate is simply poured over the cotton, and the filtrate is collected in a vessel below. In such way, no external pump is needed.
5. 4 M AS is close to its solubility point at room temperature; therefore, it is necessary to add water close to the final solution volume to achieve complete AS dissolution.
6. pDNA is usually extracted from *Escherichia coli* (*E. coli*) cells through classical approaches such as alkaline lysis first presented by Birnboim and Doly [18]. Since then, alternative approaches have been tested, but with little success at large scale. An alkaline cell lysis phase consists of two steps: lysis step and neutralization step. In lysis step, the bacterial cell walls are disrupted with high pH in lysis buffer which results in a release of pDNA in the solution. The aim of neutralization step is to stop degradation of biological material.
7. Two parameters could be optimized in lysis—concentration of NaOH and lysis time. In the protocol described, only lysis time optimization is performed, but a similar approach could be used to optimize NaOH concentration (e.g., testing the concentration range between 0.05 and 0.2 M NaOH in final lysis solution).
8. After $CaCl_2$ precipitation, most of the cell debris floats at the top of the neutralized lysate as flocculent precipitate. In order to simplify the "mini-lysis" procedure and to skip the coarse filtration/centrifugation, a sample collection before final filtration is done by careful pipetting of the liquid phase below the flocculent precipitate.

9. Clarification phase consists of two steps: precipitation and filtration train. Precipitation is done by $CaCl_2$, which is an ionic compound that precipitates large molecules of RNA, genomic DNA and endotoxins, but it does not precipitate pDNA. This is the basis for its usage for the removal of large amount of nucleic acid impurities from pDNA samples. The working concentration of $CaCl_2$ must be optimized for each pDNA sample. For example, a 1 M $CaCl_2$ solution is often optimal for small plasmids, while causing partial precipitation, and loss, of pDNA for larger plasmids (above 10 kbp).
10. CIMac™ pDNA Analytical Column allows the quantification of sc pDNA as well as monitoring of degradation products (oc, linear, dimeric pDNA), the removal of impurities (RNA) and gDNA. Due to its high precision, high reproducibility, and easy quantification, it can be efficiently used in lysis optimization (monitoring the pDNA concentration as well as calculating RNA–pDNA ratio and sc–oc pDNA ratio etc.). If underestimation of oc pDNA concentration is observed, consider evaluation of CIMac pDNA column with larger monolith channel size.
11. Retention times of pDNA molecules on CIMac™ pDNA analytical columns are extremely sensitive to the temperature of the chromatographic system. It is therefore of great importance to keep temperature fluctuations within 1 °C. Fortunately, temperature change affects only retention times of pDNA, while the resolution between the isoforms is retained.
12. The chromatographic separation is performed in NaCl linear gradient where proteins elute below 0.3 M NaCl, RNA elutes somewhere between 0.3 and 0.6 M NaCl, and pDNA isoforms between 0.6 and 0.8 M NaCl. The exact gradient method should be optimized by the user, an example of the typical analysis together with linear gradient used is presented in Fig. 4. If needed, NaCl could be replaced with other salts, which may favorably affect separation of different plasmid conformations. Chaotropic salts like guanidine are of particular interest because they are strong hydrogen donor-acceptors.
13. Depending on the needs, different types of calibration curves could be constructed. For screening purposes, single-point calibration with one standard of known concentration could be done. With 10 mm detector cell at 260 nm, a limit of quantification for pDNA using CIMac pDNA column is around 1 μg/mL and the linear response range is up to 100 μg/mL.
14. pDNA standard is often available, while this is not true for RNA. However useful information is obtained from analytics

even without knowing absolute numbers. For example, peak area ratio between RNA and pDNA peaks gives you an info on RNA removal efficiency in lysis step.

15. The crucial parameters for the decision regarding optimal conditions in lysis optimization:
    - As high as possible amount of pDNA per gram of biomass.
    - As high as possible sc pDNA homogeneity.
    - As low as possible RNA/pDNA area ratio.
16. Partial purification and concentration of pDNA is performed using weak anion exchanging monolithic chromatographic column. Especially RNA and remains of proteins are removed in this step, while pDNA concentration factor could be higher than 100. If pressure problems are observed on CIM anion exchange columns during pDNA loading or column regeneration, consider evaluation of larger monolith channel size. A rough estimation is that 2 μm monolith channels are optimal for purification of pDNA sizes below 10 kbp.
17. The amount of biomass needed has to be calculated from the pDNA concentration found in the samples from clarification optimization. For high copy number pDNA, more than 0.5 mg of pDNA per gram of biomass should be achieved.
18. The optimal conductivity could be defined as a value where the dynamic binding capacity for pDNA is higher than 4 mg/mL of support for CIM DEAE columns with 2 μm channel size, while keeping most of the RNA in the unbound fraction. Although not described in the procedure, the optimal conductivity is not always 35 mS/cm and is subject to optimization. As a rule of thumb, it especially depends on the $CaCl_2$ concentration added in the precipitation step. Higher concentration of added $CaCl_2$ results in a decrease of optimal conductivity and vice versa. However, always try to find the optimal concentration in the range between 30 and 40 mS/cm. Instead of diluting the sample with water to achieve the appropriate binding conditions onto DEAE column a buffer exchange and pDNA concentration could be done by tangential flow filtration with 300 kDa cut-off membranes or hollow fibres. If TFF is used, the optimal conductivity for loading on DEAE column changes compared to dilution-based process.
19. The last filtration step should be performed just before the sample loading onto a chromatographic column, otherwise a precipitation of some impurities reappears. If the filtrated lysate is kept overnight at 4–8 °C, it has to be filtered again before the column application.
20. The chromatographic capture could be performed on FPLC system, but to keep the procedure simpler and faster, a

peristaltic or membrane pump without a detector could be used instead.

21. One of the advantages of monolithic columns is flow-rate-independent chromatographic characteristics. Thus, to accelerate the time-consuming loading of pDNA lysate, a flow rate could be increased to the highest possible flow rates (or to the maximum pressure drop), recommended by the column producer [6].
22. It is very important to load the same amount of pDNA per milliliter of monolith in this screening experiment and in the subsequent large-scale run [8].
23. Fraction volumes are collected according to UV signal. When the absorbance of the eluting peak decreases below 100 milli-absorbance units, the collection is stopped. If working without UV detector (not recommended), collect approximately 10 CV of each fraction.
24. Especially in the elution step, the flow rate has to be decreased to counter-act the increase in pressure drop. The increased pressure drop is a consequence of a sudden desorption of large amount of pDNA from the column, increasing the viscosity of the mobile phase considerably [19].
25. The crucial parameters for the decision regarding optimal chromatographic capture conditions:
    - No pDNA in FT fractions.
    - As high as possible RNA removal in washing fractions together with as low as possible loss of pDNA in washing fractions.
    - As high as possible pDNA amount in the elution fraction.
26. Do not reverse the flow rate on CIMmultus columns, because there is a high risk of irreversible damage of the chromatographic support.
27. High ligand density butyl-modified (CIMmultus™ C4 HLD) monolithic support is used in a polishing step of a pDNA purification process and is mainly focused to sc pDNA isoform separation from the oc, linear, and dimeric pDNA isoform as well as for the removal of the remaining genomic DNA and RNA [7, 8]. The binding of pDNA on butyl-modified column is achieved with the addition of high concentration of kosmotropic salt, such as AS. Decreasing the AS concentration enables selective desorption of molecules with different hydrophobicities.
28. After buffer adjustment with 4 M AS, a colloidal precipitation sometimes occurs due to RNA precipitation. In such cases, a

filtration through 0.45 μm filter is recommended before loading the sample onto the chromatographic column.

29. The capacity of the column for pDNA at these conditions is approximately 3 mg pDNA per mL of support. It is usual to load approximately two thirds of the full capacity, this is 2 mg of pDNA in total [8]. It is important to load the same amount of pDNA per milliliter of monolith in the large-scale experiment, because the final pDNA yield and purity depend on the amount of loaded pDNA. However, although not described in the procedure, it is recommended to test different loading amounts between 1 and 2 mg pDNA per milliliter support in order to find the optimal conditions.
30. If any pDNA is observed in FT fraction (constant absorbance increase in the second half of loading), this is a sign of overloading. In the following experiment, reduce the volume of sample loaded.
31. Especially in case of small elution peaks, it is recommended to collect the peak of the fraction separately from the tail to obtain high enough pDNA concentration for further analysis.
32. Linear gradient elution is sometimes preferential over the step gradient, because the elution profile helps with appropriate fraction collection. For optimization of a polishing step on 1 mL CIMmultus C4 HLD column a suggested linear gradient would be 10 min long gradient from B1 to A1 buffer at 5 mL/min. An efficient, low volume mixing chamber is needed to thoroughly mix mobile phases B1 and A1 in front of the column. It is recommended to collect the fractions automatically by a fraction collector.
33. Use of higher AS concentration results in higher sc pDNA yield, but homogeneity of sc pDNA could be lower. Usually the concentration of AS in the washing buffer is between 1.5 and 1.9 M AS, depending on the pDNA molecule and sc/oc ratio in the loading material. Instead of loading the pDNA in 3 M AS, it can be loaded in washing buffer (1.5 to 1.9 M AS), where sample displacement mechanism is used. In such case oc pDNA is removed in flow through fraction and the pDNA loading is stopped immediately after the beginning of sc pDNA breakthrough. Such conditions results in higher robustness and usually higher purity and recovery of sc pDNA [9]. Usually the concentration of AS in the elution buffer is between 0.6 and 1.2 M AS, depending on the pDNA molecular structure and pDNA/RNA separation capability. Use of higher AS concentration in elution buffer results in purer sc pDNA, but with lower yield.

    The crucial parameters to define optimal chromatographic polishing conditions:

- As high as possible oc pDNA removal in washing fractions together with as low as possible loss of pDNA in washing fractions.
- As high as possible RNA, gDNA and multimers removal in elution fractions together with as high as possible pDNA recovery in elution fractions.

34. The final sample containing the product (sc pDNA) has to be analyzed for all known impurities. These methods are not thoroughly described below, but instead they are just mentioned for the reader to be aware of necessary analyses, which need to be performed [20].
35. When confirming the process using the fixed parameters chosen from optimization, use 1, 4, 8 or 80 mL column size.
36. Scaling-up the flow rate on monoliths could in theory be done by keeping the flow rate constant in CV/min. For example—use 1 mL/min (1 CV/min) on 1 mL scale and 8 L/min (1 CV/min) on 8 L column. But be careful, because the pressure drop over the column is not the same on 8 or 1 mL column at same flow rate expressed in CV/min. In practice it is therefore not possible on 8 L chromatographic units with 2 μm channel size to use 5 CV/min, because the pressure limit of the column would already be exceeded.
37. Scaling-up the linear gradient could be done by two different approaches—"isoresolution" or "isoconductivity" approach. Isoresolution transfer is valid only for steep gradient slopes [21] (approximately less than 15 CV, but this value depends on the monolith bed height) and results in a separation between two compounds with the same resolution on different scales. Milavec Zmak et al. derived a very simple equation for scaling-up/down an isoresolution gradient [22]. For starting (lab-scale) column 1 and target (large-scale) column 2, the equation is:

$$t_{g,2} = t_{g,1} \times \left(\frac{V_{v,2}}{V_{v,1}}\right) \times \left(\frac{F_1}{F_2}\right) \times \left(\frac{L_1}{L_2}\right) \quad (1)$$

where t_g is the gradient time, V_v is the column volume, F is the flow rate, and L is the bed height, calculated as half the difference between the outer and inner radii of the column.

Isoconductivity gradient transfer is based on the theory that peak salt concentration (elution concentration) is a function of gradient slope [23]. In the approximation, a normalized gradient slope (GH) is expressed with Eq. 2, where t_g is the gradient time, V_v is the column volume, F is the flow rate, and c_F and c_0 are the final and initial salt concentrations, respectively.

$$\mathrm{GH} = \frac{(c_\mathrm{F} - c_0) \times V_v}{F \times t_\mathrm{g}} \quad (2)$$

Keeping GH the same on different column scales result in the elution of the solute at the same conductivity value, but this does not guarantee the same resolution between two separated analytes. Simultaneous resolution and peak salt concentrations could be achieved if only the bed height is the same on different scales. Both the approaches allow the flexibility of varying the flow rate during scale-up, which is enabled by diffusion-free mass transfer in monoliths. It is important to note that some fine tuning of the gradient may be required after the method is transferred.

5 Future Aspects

The advantages of Convective Interaction Media® (CIM®) monolith stationary phases, including low backpressure and quick separation of macromolecules, qualified them to be used effectively in separation of pDNA with outstanding productivity. Due to the uniform structure at research and large scale, investigators can explore the column's industrial behavior in laboratory setting. This enables scale-down experiments to troubleshoot or evaluate new samples and conditions. Moreover, small monoliths packed as analytical columns serve as an excellent tool in Process Analytical Technology (PAT) for at-line monitoring and final quality control of industrial DSP.

While the downstream process thoroughly described above was developed for conventional pDNA typically derived from *E. coli* cells, it could be applied with some changes to minicircle DNA (mcDNA), which at the moment presents the ultimate non-viral DNA vector, presenting higher biosafety and therapeutic effect [24].

From another perspective, CIM® chromatographic monoliths can be successfully applied for the purification of large plasmids, ranging above 10 kbp [19]. For such processes, monoliths with larger channel size and consequently higher permeability have been developed. These avoid large pressure drops over the chromatographic column caused by the extremely large pDNA molecules [25, 26].

While the current DSP process meets the needs of the biopharmaceutical community, a new, third-generation pDNA purification based on monolithic columns is under development. The main emphasis of the novel process will be on additional product purity improvements, while increasing the process productivity. There is room for improvement especially within the precipitation and capture steps.

Acknowledgments

We thank the research and application team of BIA Separations, Ajdovščina, Slovenia, for contributing work and discussions, especially Franci Smrekar, Boštjan Gabor, Nika Lendero Krajnc, Miloš Barut, and Aleš Podgornik for their crucial roles in pDNA DSP development; Tomas Kostelec for his support with figures and text revision.

References

1. Abdulrahman A, Ghanem A (2018) Recent advances in chromatographic purification of plasmid DNA for gene therapy and DNA vaccines: a review. Anal Chim Acta 1025:41–57
2. Jungbauer A (2013) Continuous downstream processing of biopharmaceuticals. Trends Biotechnol 31:479–492
3. Podgornik A, Yamamoto S, Peterka M et al (2013) Fast separation of large biomolecules using short monolithic columns. J Chromatogr B 927:80–89
4. Urthaler J, Schlegl R, Podgornik A et al (2005) Application of monoliths for plasmid DNA purification development and transfer to production. J Chromatogr A 1065:93–106
5. Podgornik A, Barut M, Peterka M et al (2012) Monoliths in bioprocessing. In: Biopharmaceutical production technology. Wiley-VCH Verlag GmbH & Co. KGaA, Weinheim, Germany, pp 333–375
6. Home—BIA Separations. https://www.biaseparations.com/
7. Smrekar F, Podgornik A, Ciringer M et al (2010) Preparation of pharmaceutical-grade plasmid DNA using methacrylate monolithic columns. Vaccine 28:2039–2045
8. Cardoso S, Černigoj U, Lendero Krajnc N et al (2015) Chromatographic purification of plasmid DNA on hydrophobic methacrylate monolithic supports. Sep Purif Technol 147:139
9. Černigoj U, Martinuč U, Cardoso S et al (2015) Sample displacement chromatography of plasmid DNA isoforms. J Chromatogr A 1414:103
10. Rathore AS, Bhambure R, Ghare V (2010) Process analytical technology (PAT) for biopharmaceutical products. Anal Bioanal Chem 398:137–154
11. Peljhan S, Jakop T, Šček D et al (2017) HPLC fingerprinting approach for raw material assessment and unit operation tracking for IVIG production from Cohn I+II+III fraction. Electrophoresis 38:2880–2885
12. Mota É, Sousa Â, Černigoj U et al (2013) Rapid quantification of supercoiled plasmid deoxyribonucleic acid using a monolithic ion exchanger. J Chromatogr A 1291:114–121
13. Gabor B, Černigoj U, Barut M et al (2013) Reversible entrapment of plasmid deoxyribonucleic acid on different chromatographic supports. J Chromatogr A 1311:106
14. Gabor B, Černigoj U, Smrekar F (2010) In-process control of pDNA production on CIMac pDNA analytical column. Bioprocess Int 8
15. Hebel H, Attra H, Khan A et al (2006) Successful parallel development and integration of a plasmid-based biologic, container/closure system and electrokinetic delivery device. Vaccine 24:4607–4614
16. Cai Y, Rodriguez S, Rameswaran R et al (2010) Production of pharmaceutical-grade plasmids at high concentration and high supercoiled percentage. Vaccine 28:2046–2052
17. Kong S, Titchener-Hooker N, Levy MS (2006) Plasmid DNA processing for gene therapy and vaccination: studies on the membrane sterilisation filtration step. J Membrane Sci 280:824–831
18. Birnboim HC, Doly J (1979) A rapid alkaline extraction procedure for screening recombinant plasmid DNA. Nucleic Acids Res 7:1513–1523
19. Krajnc NL, Smrekar F, Štrancar A et al (2011) Adsorption behavior of large plasmids on the anion-exchange methacrylate monolithic columns. J Chromatogr A 1218:2413–2424
20. Schmeer M, Buchholz T, Schleef M (2017) Plasmid DNA manufacturing for indirect and direct clinical applications. Hum Gene Ther 28:856–861
21. Dubinina NI, Kurenbin OI, Tennikova TB (1996) Peculiarities of gradient ion-exchange

high-performance liquid chromatography of proteins. J Chromatogr A 753:217–225

22. Milavec Zmak P, Podgornik H, Jancar J et al (2003) Transfer of gradient chromatographic methods for protein separation to convective interaction media monolithic columns. J Chromatogr A 1006:195–205
23. Yamamoto S, Kita A (2005) Theoretical background of short chromatographic layers. J Chromatogr A 1065:45–50
24. Diamantino T, Pereira P, Queiroz JA et al (2016) Minicircle DNA purification using a CIM® DEAE-1 monolithic support. J Sep Sci 39:3544–3549
25. Podgornik A, Hamachi M, Isakari Y et al (2017) Effect of pore size on performance of monolithic tube chromatography of large biomolecules. Electrophoresis 38:2892–2899
26. Mao Y, Kulozik U (2018) Selective hydrolysis of whey proteins using a flow-through monolithic reactor with large pore size and immobilised trypsin. Int Dairy J 85:96–104

Chapter 10

Purification of Plasmid DNA by Multimodal Chromatography

A. Rita Silva-Santos, Sara Sousa Rosa, Duarte Miguel F. Prazeres, and Ana M. Azevedo

Abstract

Multimodal (MM) chromatography can be described as a chromatographic method that uses more than one mode of interaction between the target molecule and the ligand to achieve a particular separation. Owing to its advantages over traditional chromatography, such as higher selectivity and capacity, its application for the purification of biomolecules with therapeutic interest has been widely studied. The potential of MM chromatography for the purification of plasmid DNA has been demonstrated. In this chapter, a downstream process for the purification of supercoiled plasmid DNA using MM chromatography with two different ligands—Capto™ adhere and PPA HyperCell™—is described. In both the cases, the purification process yields a high purity and highly homogeneous sc plasmid product.

Key words Downstream processing, Multimodal chromatography, Plasmid DNA, Purification, Supercoiling

1 Introduction

The mainstream use of chromatography as the core purification step in the downstream processing is widely accepted in the biopharmaceutical industry. Its selectivity, scalability, robustness, and cost-effectiveness make chromatography the method of choice for purification in many downstream processing schemes. Most of the well-established chromatographic techniques separate the molecules according to their charge (ion exchange chromatography), hydrophobicity (hydrophobic interaction chromatography), size (size-exclusion chromatography), or ability to participate in specific biological interactions (affinity chromatography). Although the use of these techniques is well implemented, the separation is limited, and to achieve a high degree of purification, multiple steps of different types of chromatography in a single process are used [1]. The need for a high throughput purification that uses more

A. Rita Silva-Santos and Sara Sousa Rosa contributed equally with all other contributors.

Ângela Sousa (ed.), *DNA Vaccines: Methods and Protocols*, Methods in Molecular Biology, vol. 2197,
https://doi.org/10.1007/978-1-0716-0872-2_10,

than one interaction to achieve a higher purity [2] made the industry look for alternatives.

Multimodal (MM) chromatography explores more than one mode of interaction between the molecule and the ligands to achieve separation. The different modes of interaction can work in combination or individually. The mode of action and the strength of the interaction will depend on different parameters, such as resin chemistry, target molecule, and the experimental conditions [3]. The control of the experimental conditions determines the separation behavior [4]. The use of MM chromatography can bring multiple advantages over single-mode chromatography, such as better separation resolution, higher binding capacity, and salt tolerance [5, 6]. In production, it can be a time-saving and cost-effective alternative to a multistep chromatography purification process.

Owing to its advantages, the use of MM chromatography has been studied for the purification of therapeutic biomolecules, namely plasmid DNA (pDNA) [7–11]. Plasmid DNA is a large, covalently closed and negatively charged double-stranded DNA biomolecule. The core of the double helix is essentially hydrophobic, whereas the external sugar-phosphate backbone is highly hydrophilic. The pDNA structural conformation—linear, open circular (oc), and supercoiled (sc)—is an important aspect that is important to consider in pDNA purification. Since sc is the most physiologically active conformation [12], other isoforms must be addressed as impurities. The MMligand Capto™ adhere was already successfully applied for the purification sc pDNA [7, 9]. This multimodal anion exchanger (*N*-benzyl-*N*-methyl ethanolamine) engages in electrostatic interactions, hydrogen bonding, and hydrophobic interactions to achieve separation. Capto adhere presents a high capacity and productivity and a wide operational window of pH and conductivity. PPA HyperCell™ is a novel MM media, where the amine of the diethylethanolamine was substituted by an aromatic anime (phenylpropylamine). This configuration promotes binding involving hydrophobic and electrostatic interactions and an elution based on charge repulsion [13]. It promotes purification at higher yield under a low to moderate salt concentrations when compared with hydrophobic interaction chromatography [6].

This chapter presents a downstream processing scheme for sc pDNA purification that relies on precipitation steps and MM chromatography. The methods for the use of Capto™ adhere and PPA HyperCell™ ligands and the preceding purification operations are described. Using Capto™ adhere, it is possible to recover 100% of the sc pDNA with a homogeneity of 93% from a maximum load of 15 μg total pDNA per mL of resin. In the case of PPA HyperCell™, 97% of homogeneity and a 100% recovery of sc pDNA was achieved loading a maximum of 20 μg total pDNA per mL of resin. The

purification processes using both ligands deliver a high-purity, high-quality product with the recommended minimum homogeneity of 80% in sc pDNA [14] conformation.

2 Materials

Prepare all solutions using Milli-Q water and analytical-grade reagents, unless otherwise specified. All solutions are prepared and stored at room temperature, unless indicated otherwise.

2.1 Culture Media

1. *E. coli* GALG20 cells harboring plasmid pVAX1-GFP (≈3.7 kb) (*see* **Note 1**).
2. Luria-Bertani broth (LB) medium. Prepare the LB medium according to the manufacturer's instructions.
3. Basal medium: 10 g/L bacto peptone, 10 g/L yeast extract, 3 g/L ammonium sulfate, 3.5 g/L potassium hydrogen phosphate, and 3.5 g/L potassium dihydrogen phosphate. Adjust the pH to 7.1. Tightly cover the baffled flask mouth with a loose cap and aluminum foil. Autoclave the medium at 121 °C for 20 min. Remove the media from the autoclave and leave to cool at room temperature prior to use.
4. 500 g/L glucose. Autoclave at 121 °C for 20 min and store at 4 °C.
5. Medium supplement solution: 240 g/L magnesium sulfate, 24 g/L thiamine. Filter through a 0.22 μm syringe filter and store at −20 °C.
6. Trace element solution: 27 g/L $FeCl_3 \cdot 6H_2O$, 2 g/L $ZnCl_2$, 2 g/L $CoCl_2 \cdot 6H_2O$, 2 g/L $Na_2MoO_4 \cdot 2H_2O$, 1 g/L $CaCl_2 \cdot 2H_2O$, 1.3 g/L $CuCl_2 \cdot 2H_2O$, 0.5 g/L H_3BO_3, 1.2 M HCl. Filter-sterilize through a 0.22 μm syringe filter and store at 4 °C protected from light.
7. Kanamycin (30 mg/mL). Filter through a 0.22 μm syringe filter and store at −20 °C.

2.2 Primary Purification and Intermediate Recovery

1. Stock solutions: 1 M Tris–HCl, pH 8.0, and 500 mM EDTA, pH 8.0.
2. Resuspension buffer (P1 buffer): 50 mM glucose, 25 mM Tris–HCl, and 10 mM EDTA, pH 8.0. Dilute from the stock solutions to the desired volume. Store at 4 °C.
3. Lysis buffer (P2 buffer): 200 mM NaOH, 1% (w/v) SDS.
4. Neutralization buffer (P3 buffer): 3 M sodium acetate, pH 6.0. Store at 4 °C.
5. Isopropanol.

6. TE buffer: 10 mM Tris–HCl, 1 mM EDTA, pH 8.0. Prepare from the stock solutions. Dilute to the desired final volume.
7. Ammonium acetate salt.
8. 30% (w/v) PEG-8000 1.6 M NaCl. First, prepare a solution of 1.6 M NaCl by weighing the desired amount of salt. Weigh the necessary amount of PEG-8000 and add the desired volume of salt solution.

2.3 Multimodal Chromatography

1. Tricorn 10/50 column (*see* **Note 2**).
2. Capto™ adhere MM chromatography resin.

2.3.1 Capto™ Adhere MM Chromatography

3. Packing buffer: 10 mM NaCl.
4. Acetone.
5. Buffer A: 10 mM Tris–HCl buffer pH 8.0. Filter the buffer through a 0.22 μm membrane filter.
6. Buffer B: 2 M NaCl in 10 mM Tris–HCl buffer pH 8.0. First, prepare 10 mM Tris–HCl by weighing the desired amount. Weigh the necessary amount of NaCl. Add water up to 70% of the desired volume, mix well, and adjust the pH to 8.0 with concentrated HCl. Fill the solution with water to the desired volume. Filter the buffer through a 0.22 μm membrane.

2.3.2 PPA HyperCell™ MM Chromatography

1. Tricorn 10/50 column.
2. PPA Hypercell™ MM chromatography resin.
3. Packing buffer: PBS, pH 7.4.
4. Acetone.
5. Buffer A1: 10 mM Tris–HCl buffer pH 8.0. Filter the buffer through a 0.22 μm membrane filter.
6. Buffer B: 1 M NaCl in 10 mM Tris–HCl buffer pH 8.0. First, prepare 10 mM Tris–HCl by weighing the desired amount. Weigh the necessary amount of NaCl. Add water up to 70% of the desired volume, mix well, and adjust the pH to 8.0 with concentrated HCl. Fill the solution with water to the desired volume. Filter the buffer through a 0.22 μm membrane.
7. Buffer C: 1 M NaOH. Weigh the required amount of NaOH and add water up to 70% of the desired volume. Mix well and adjust to the final volume. Filter the buffer through a 0.22 μm membrane.

2.4 Gel Electrophoresis and Densitometry Analysis

1. Electrophoresis-grade agarose.
2. Running buffer: Tris–acetate–EDTA (TAE) buffer—40 mM Tris base, 20 mM acetic acid, and 1 mM EDTA, pH 8.0. Prepare a 50× concentrated buffer and dilute to the desired final volume.

3. Loading buffer 6×: 40% (w/v) sucrose, 0.25% (w/v) bromophenol blue.
4. Molecular weight marker ranging from 200 to 10,000 bp.
5. Staining solution: 0.4 μg/mL ethidium bromide.
6. ImageJ software.

2.5 Micro-Dialysis

1. Dialysis membrane with 23 μm thickness and 12–14 kDa molecular weight cut-off.
2. TE buffer.
3. Rubber bands.

2.6 Plasmid Quantification

1. SOURCE 15PHE 4.6/100 PE column.
2. Buffer A: 1.5 M Ammonium sulfate in 10 mM Tris–HCl buffer pH 8.0. First, prepare 10 mM Tris–HCl by weighing the desired amount. Weigh the necessary amount of ammonium sulfate. Add water up to 70% of the desired volume. Mix well and adjust the pH to 8.0 with concentrated HCl. Fill in the solution with water to the desired volume. Filter the buffer through a 0.22 μm membrane.
3. Buffer B: 10 mM Tris–HCl buffer pH 8.0. Filter the buffer through a 0.22 μm membrane filter.

3 Methods

3.1 Bacterial Cell Growth

The procedure for the production of pVAX1-GFP using *E. coli* GALG20 described is based on the method described in [15].

1. Inoculate *E. coli* GALG20 cells harboring pVAX1-GFP cells in a 5 mL conical centrifuge tube, containing 5 mL LB supplemented with 30 μg/mL kanamycin. Incubate overnight at 37 °C and 250 rpm.
2. Prepare 250 mL baffled shake flasks containing 48 mL basal medium, 2 mL glucose, 415 μL medium supplement solution, 50 μL trace element solution and 50 μL kanamycin. Measure the optical density at 600 nm (OD_{600nm}) and calculate culture volume necessary to inoculate the 250 mL baffled shake flasks at an OD_{600nm} of approximately 0.1, using the relationship $OD_{initial} \times V_{initial} = OD_{final} \times V_{final}$. Transfer the calculated volume and incubate the cells at 37 °C and 250 rpm for 8 h.
3. Harvest the cells by centrifuging at 6000 × *g* for 15 min. The pellets can be stored at −20 °C until further experiments.

3.2 Primary Purification and Intermediate Recovery

1. Resuspend the cell pellets in buffer P1 up to an OD_{600nm} of 60 (*see* **Note 3**). Vortex until completely resuspended (*see* **Note 4**).

2. Add buffer P2 at a volume ratio of 1:1 and gently mix by inverting the tube (*see* **Note 5**). The solution should turn transparent and become viscous indicating that lysis has taken place. Leave to rest for 10 min.
3. Add buffer P3 at a volume ratio of 1:1 to neutralize the lysate. Gently mix and place the lysate on ice for 10 min.
4. Centrifuge the samples for 30 min, at 18,250 × *g* and 4 °C. Repeat until a pDNA clarified lysate is obtained.
5. Take a sample for electrophoresis and HPLC analysis.
6. Add 0.7% (v/v) isopropanol (*see* **Note 6**). Gently mix and incubate 2 h at −20 °C.
7. Centrifuge the samples for 30 min, at 18,250 × *g* and 4 °C.
8. Discard the supernatant and leave the pellet to dry overnight at room temperature.
9. Resuspend the pellet in the lowest possible amount of TE buffer (*see* **Note 7**).
10. Take a sample for electrophoresis and HPLC analysis.
11. Add 2.5 M ammonium acetate by dissolution of the appropriate amount of salt. Place the solution on ice for 15 min (*see* **Note 8**).
12. Centrifuge for 30 min at 15,000 × *g* and 4 °C.
13. Recover the supernatant and take a sample for electrophoresis and HPLC analysis.
14. Add an equal volume of 30% (w/v) PEG-8000 in 1.6 M NaCl (*see* **Notes 8–10**). Incubate overnight at 4 °C.
15. Centrifuge for 30 min, 15,000 × *g* and 4 °C. Discard the supernatant and resuspend the pellet in TE buffer (*see* **Note 11**).
16. Take a sample for electrophoresis and HPLC analysis.

3.3 Multimodal Chromatography

3.3.1 Capto™ Adhere Multimodal Chromatography

1. Pack a Tricorn 10/50 column with 5 mL Capto™ adhere multimodal chromatography resin according to the manufacturer's instructions using the packing buffer.
2. Evaluate the column performance by assessing the height equivalent to a theoretical plate (HETP) and asymmetry factor by injecting 25 μL of a 5% acetone solution. The column should be pre-equilibrated with packing buffer, the flow should be set to 76 cm/h and the absorbance at 280 nm (*see* **Note 12**).
3. Set the run parameters: constant flow of 76 cm/h and continuous monitoring of conductivity and absorbance at 254 or 260 nm.
4. Condition the sample by dilution (up to 15 μg total pDNA per mL of resin) with 830 mM NaCl in 10 mM TE (*see* **Note 13**).

5. Equilibrate the column with three column volumes (CV) of 41.5% buffer B, or until the conductivity reads remain stable at 69 mS/cm.
6. Inject 1 mL of previously conditioned sample by washing the loop with 3 mL of 41.5% buffer B.
7. Washout the unbound material with two CV of 41.5% buffer B.
8. Elute the sc pDNA by increasing buffer B concentration to 46% (75 mS/cm) for three CVs.
9. A peak in absorbance is expected. As soon as the absorbance signal starts to increase, collect 1.5 mL fractions. When the signal stabilizes close to the baseline, stop the collection of fractions (*see* **Note 14**).
10. Elute the remaining impurities by increasing buffer B to 100% (140 mS/cm) for three CVs.

3.3.2 PPA HyperCell™ Multimodal Chromatography

1. Pack a Tricorn 10/50 column with 5 mL Capto™ adhere multimodal chromatography resin according to the manufacturer's instructions using the packing buffer.
2. Evaluate the column performance by assessing the height equivalent to a theoretical plate (HETP) and asymmetry factor by injecting 25 μL of a 5% acetone solution. The column should be pre-equilibrated with packing buffer, the flow should be set to 76 cm/h and the absorbance at 280 nm (*see* **Note 15**).
3. Set up run parameters: constant flow rate of 76 cm/h and continuous monitoring of the conductivity and absorbance at 254 or 260 nm.
4. Condition the sample by dilution (up to 20 μg total pDNA per mL of resin) with 650 mM NaCl in 10 mM TE (*see* **Note 16**).
5. Equilibrate the column with three CVs with 56.3% of buffer B in buffer A1, buffer B, or until the conductivity reads remain stable at 51.4 mS/cm (*see* **Note 17**).
6. Wash the unbound material with 56.3% of buffer B in buffer A1 for one CV.
7. Elute the sc pDNA by increasing buffer B concentration to 100% (85 mS/cm) for two CVs.
8. A peak in absorbance is expected. As soon as the absorbance signal starts to increase, collect 1.5 mL fractions. When the signal stabilizes close to the baseline stop the collection of fractions.
9. Elute the remaining impurities by flowing two CVs of A2 buffer (1 M NaOH).

3.4 Micro-Dialysis

1. Remove the tube caps of the Eppendorfs.
2. Insert the desired volume of peak fractions into the Eppendorfs and cover them with the dialysis membrane.
3. Fix the membrane tightly with a rubber band. Make sure there are no leaks.
4. Invert the tubes assuring that all the solution is in contact with the membrane.
5. Place the tubes floating on a beaker containing at least 50 times more volume of TE buffer than the volume of samples (*see* **Note 18**).
6. Mix overnight at 4 °C.

3.5 Agarose Gel Electrophoresis

1. Prepare 1% agarose gels by weighing the appropriate amount of electrophoresis-grade agarose into an Erlenmeyer flask.
2. Add the desired volume of running buffer to the agarose flask, mixing thoroughly. Melt the agarose mixture in a microwave and swirl to ensure even mixing (*see* **Note 19**). Allow to cool.
3. Pour the warm agarose solution onto the gel plate in the electrophoresis box and insert the comb. Make sure that no bubbles are trapped underneath the combs, and all bubbles on the surface of the agarose are removed (*see* **Note 20**). Allow the gel to completely set (between 30 and 45 min). Carefully withdraw the gel comb, so that the sample wells do not tear.
4. Place the gel casting plate containing the gel in the electrophoresis tank. Add sufficient running buffer to cover the gel, so that the top of the wells are covered. Make sure no air pockets are formed inside the wells.
5. Prepare the samples. Add 0.2 volumes of loading buffer to each desalted sample, e.g., 4 μL of loading buffer into 20 μL sample. Load the marker and the samples, taking care not to puncture the well bottoms. Also, if there are air bubbles in the tip of the pipette or in the wells, do not attempt to load the sample.
6. Attach the lid and set the voltage to the desired level (1–10 V/cm of gel) to begin electrophoresis. The progress of the separation can be monitored by the migration of the dyes (dye line has run around ¾ of the gel).
7. Remove the gel from the casting tray and place it in the ethidium bromide staining solution for 10–30 min. Gels can be detained in water to remove excess ethidium bromide.

3.6 Plasmid Quantification

1. Prepare the calibration curve with standards of the model pDNA in a concentration range from 0 to 100 μg/mL (*see* **Note 21**). Determine the pDNA concentration of the stock (in this work, the concentration of pDNA was estimated using nanodrop UV spectrophotometry). Dilute the standard sample

in 10 mM Tris–HCl buffer pH 8 in order to obtain pDNA standards with concentrations of 10, 20, 30, 40, 50, and 100 ng/μL.

2. Connect the SOURCE 15PHE 4.6/100 PE column to the system and operate at 1 mL/min.
3. Continuously measure the absorbance of the eluate at 260 nm and the conductivity.
4. Equilibrate the column with buffer A.
5. Inject sample volumes of 50 μL and wash the column with buffer A for 0.6 CVs (*see* **Note 22**).
6. Elute the impurities with buffer B for 0.5 CVs.
7. Re-equilibrate the column for 3.2 CVs with the initial buffer.
8. Calculate the plasmid peak area and construct a calibration curve (linear correlation between peak area and plasmid concentration).

4 Notes

1. The cell culture method described is applicable to the growth of *E. coli* GALG20 strain harboring pVAX-GFP1. pUC18 and pCEP4 were also successfully purified from *E. coli* DH5α cell cultures produced using LB media [9].
2. The column Tricorn™ 10/50 was chosen to pack 5 mL of the resin. For a different resin volume, choose a column according to the manufacturer's instructions.
3. The volume of buffers P1, P2, and P3 (V_P) is calculated to concentrate the solution to an $OD_{600nm} = 60$, taking into account the final OD_{600nm} and the volume of the respective cellular growth (V_{cg}), using the following formula:

$$V_{P1} = V_{P2} = V_{P3} = \frac{V_{cg} \times OD_{600nm}}{60}$$

4. Ensure that the pellets are completely resuspended in order to maximize the number of cells exposed to the lysis buffer.
5. Do not vortex or stir vigorously the lysate. Mix the solution by inverting the tube several times. Make sure to allow a rapid homogenization, while avoiding the fragmentation of genomic DNA.
6. 70% (v/v) refers to the percentage of isopropanol volume added relative to the volume of lysate. For example, for 100 mL of lysate, add 70 mL isopropanol.
7. For better results, the volume added should be at least 20 times less than the culture volume.

8. Ammonium acetate will promote the precipitation of proteins and RNA. The bypass of both ammonium acetate and PEG-8000 precipitation will lead to significantly increase in the impurity content of the sc pDNA fractions collected from MM chromatography, namely proteins and RNA. Furthermore, the higher RNA and protein load in the column feed is expected to compromise some of the capacity of the resin to bind sc pDNA and have an impact in resin lifetime.
9. PEG-8000/0.53 M NaCl precipitation is performed to (1) concentrate pDNA, (2) reduce the RNA load, and (3) remove the ammonium acetate salt.
10. To achieve higher yields, it is strongly recommended to use 50 mL conical centrifuge tubes to perform this final precipitation.
11. The volume of TE used for the resuspension should be calculated considering reducing 160 times the cell culture volume. For a 50 mL cell culture production, the TE volume used should be 0.312 mL.
12. The reduced plate height is calculated as follows: $\frac{\mathrm{HETP}}{d}$, where d corresponds to the resin bead diameter, and the HETP corresponds to the height equivalent to one theoretical plate. HETP can be calculated by: $\frac{d^2 \times L}{5.54 \times t^2}$, where t is the acetone retention time, and L is the column length. Both HETP and asymmetry values can be calculated using UNICORN systems. The acceptable HETP value for a well-packed column should be <3, whereas the peak asymmetry factor should be between 0.8 and 1.5.
13. Loading studies indicated that the column capacity for total pDNA is 15 μg per mL of resin. The chromatographic profile is shown in Fig. 1. It is possible to recover 8 μg per mL of resin of sc pDNA, corresponding to 100% of recovery yield. The recovered pDNA fractions present a composition of 93% of sc pDNA.
14. The difference in retention between the oc pDNA, sc pDNA, and RNA can be explained based on their charge density and hydrophobic character. At the working pH of 8, all nucleic acids are negatively charged and, thus, will bind to the strong anion-exchanger group present in the Capto adhere ligand. Due to its more compact structure, supercoil pDNA presents a higher charge density than oc pDNA and is eluted at a higher salt concentration. Furthermore, stronger hydrophobic interactions of sc pDNA molecules with the phenyl group of the ligand can also favor the retention of this isoform. RNA binds strongly to the resin due to its hydrophobic nature (single-stranded nucleic acid: bases directly exposed to the solvent).

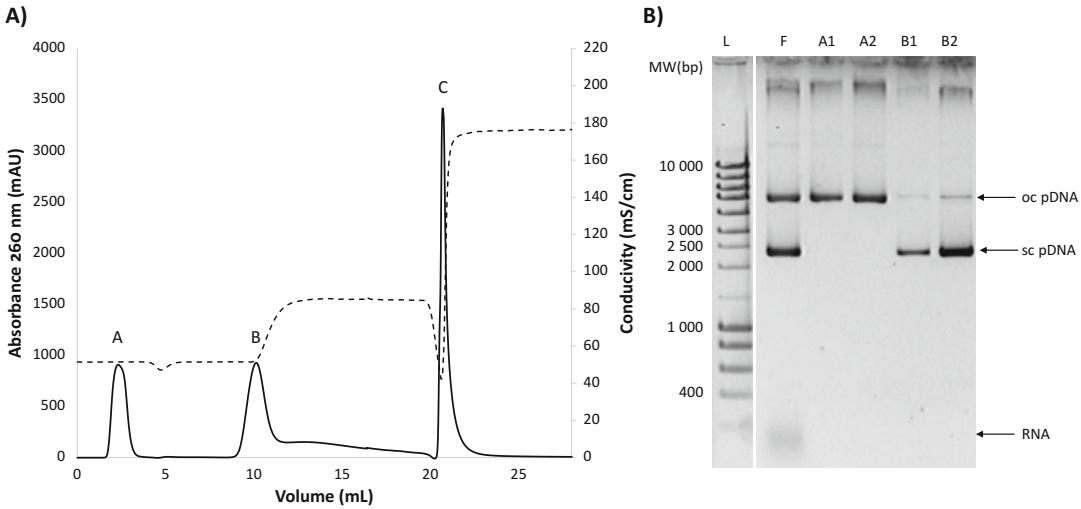

Fig. 1 Capto™ adhere MM chromatography purification of sc pDNA from a clarified feed containing oc pDNA, sc pDNA, and RNA. (**a**) Chromatogram illustrative of sc pDNA purification. 1 mL of pDNA solution (90 μg) preconditioned to set NaCl at 830 mM, was injected into a 5 mL Capto adhere column, pre-equilibrated with 41.5% buffer B (69 mS/cm). Unbound material was washed out with two CV of 41.5% buffer B, and stepwise elution was performed with three CV of 46% buffer B (75 mS/cm) and three CV of 100% buffer B (140 mS/cm). Letters over peaks correspond to collected fractions. Continuous line: absorbance at 254 nm; dashed line: conductivity (mS/cm); dotted line: percentage of buffer B (% B). (**b**) Agarose gel electrophoresis analysis of fractions collected during the chromatographic run. Lane L corresponds to the molecular weight marker and lane F (2 μL) to the column feed. A, B, and C correspond to the fractions collected during the chromatographic run (10 μL of sample for lanes A and B; 30 μL of sample for lane C)

15. The number of the plates/meter (N/m) is calculated as follows: $\frac{5.54\times t^2}{d^2\times L}$, where t corresponds to the retention value of acetone, d to the peak width at half height, and L to the column length. The acceptable value for a well-packed column should be N/m between 1500 and 3000 plates/meter. The peak asymmetry factor should be between 0.8 and 1.4.
16. Loading studies indicated that the column capacity for total pDNA is 20 μg per mL of resin. The chromatographic profile is shown in Fig. 2. It is possible to recover 7 μg per mL of resin of sc pDNA, corresponding to 100% of recovery yield. The recovered pDNA fractions present a composition of 96% of sc pDNA.
17. The oc pDNA, sc pDNA, and RNA retention profile difference is explained due to its differences in charge and hydrophobic character. At the working pH of 8, all nucleic acids are negatively charged and, thus, will bind to the anion-exchanger. In this case, since it is a weak anion-exchanger, a lower amount of salt is necessary. As previously described, supercoil pDNA presents a higher charge density than oc pDNA, and it will elute at a higher salt concentration. Furthermore, the presence of the

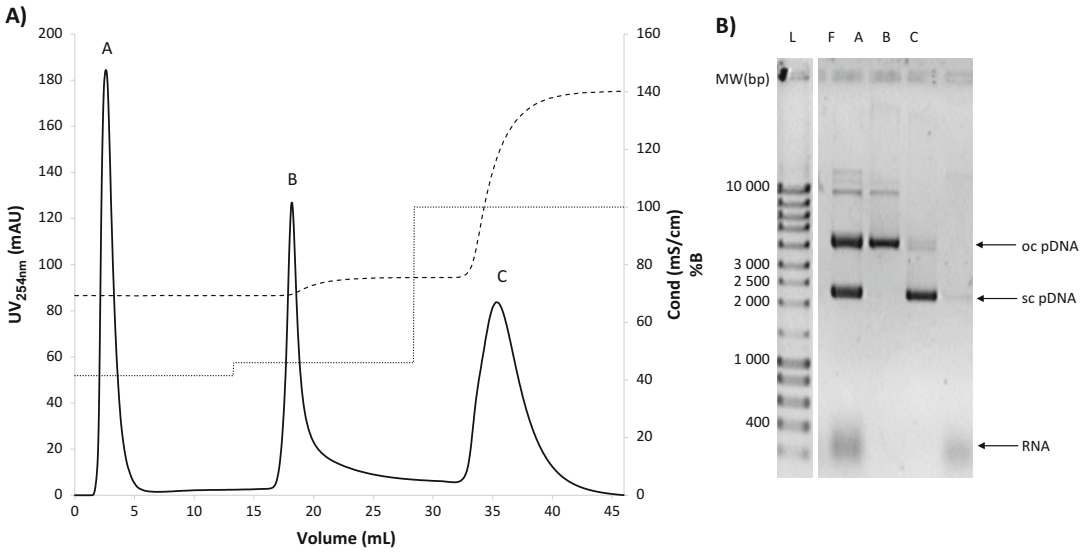

Fig. 2 PPA HyperCell™ MM chromatography purification of sc pDNA from a clarified feed containing oc pDNA, sc pDNA, and RNA. (**a**) Chromatogram illustrative of sc pDNA purification. 1 mL of pDNA solution (103 μg) preconditioned to set NaCl at 650 mM was injected into a PA HyperCell™ column, pre-equilibrated with 56.3% buffer B (51.4 mS/cm). Unbound material was washed out with one CV of 56.3% buffer B, and stepwise elution was performed with two CV of 100% buffer B (85 mS/cm) and two CV of 100% buffer A2 (178 mS/cm). Letters over peaks correspond to collected fractions. Continuous line: absorbance at 254 nm; dashed line: conductivity (mS/cm). (**b**) Agarose gel electrophoresis analysis of fractions collected during the chromatographic run. Lane L corresponds to the molecular weight marker and lane F (2 μL) to the column feed. A (1, 2) and B (1, 2) correspond to the fractions collected during the chromatographic run (10 μL of sample)

phenyl group favors the retention of sc pDNA isoform. RNA binds strongly to the resin due to its hydrophobic nature.

18. Make sure that all the Eppendorfs are moving around the beaker and that the dialysis membrane is submerged. However, a swirl should not be visible.
19. For 150 mL solution, it should take about 3 min at maximum power. For every minute, pause the heating and stir, and then continue toward a boil. Be careful not to overboil the solution, since some of the buffer could spill, changing the concentration of agarose in the gel.
20. Make sure to remove any air bubbles with a pipette tip. Push them away from the wells toward the sides.
21. The pDNA standard stock solution was prepared using a commercially available pDNA purification kit (HiSpeed plasmid Maxi Kit from Qiagen). This kit is able to separate and purify high concentrated and pure pDNA from bacteria, combining an alkaline lysis method and a silica-based membrane in a spin column format.

22. pDNA elutes in the flowthrough (at a retention time of 0.69 min), while the impurities are retained due to its higher hydrophobicity and lower molecular mass. Elution of impurities is accomplished by decreasing the ionic strength of the mobile phase.

Acknowledgments

Funding received by iBB—Institute for Bioengineering and Biosciences from FCT–Portuguese Foundation for Science and Technology, Portugal (grant UID/BIO/04565/2019) and from Programa Operacional Regional de Lisboa 2020, Portugal (Project N. 007317) is acknowledged. A. Rita Silva-Santos acknowledges FCT for the PhD grant PD/BD/135138/2017 (BIOTECnico program). This work was supported by National Funds by FCT—Fundação para a Ciência e Tecnologia—through the research contract IF/00048/2014/CP1214/CT0010.

References

1. Sun B, Yu X, Yin Y et al (2013) Large-scale purification of pharmaceutical-grade plasmid DNA using tangential flow filtration and multi-step chromatography. J Biosci Bioeng 116:281–286
2. Halan V, Maity S, Bhambure R et al (2019) Multimodal chromatography for purification of biotherapeutics – a review. Curr Protein Pept Sci 20:4–13
3. Yang Y, Geng X (2011) Mixed-mode chromatography and its applications to biopolymers. J Chromatogr A 1218:8813–8825
4. Kallberg K, Johansson H-O, Bulow L (2012) Multimodal chromatography: an efficient tool in downstream processing of proteins. Biotechnol J 7:1485–1495
5. Pinto IF, Aires-Barros MR, Azevedo AM (2015) Multimodal chromatography: debottlenecking the downstream processing of monoclonal antibodies. Pharm Bioprocess 3:263–279
6. Zhao G, Dong X-Y, Sun Y (2009) Ligands for mixed-mode protein chromatography: principles, characteristics and design. J Biotechnol 144:3–11
7. Silva-Santos AR, Alves CPA, Prazeres DMF et al (2016) Separation of plasmid DNA topoisomers by multimodal chromatography. Anal Biochem 503:68–70
8. Sousa A, Pereira P, Sousa F et al (2014) Binding mechanisms for histamine and agmatine ligands in plasmid deoxyribonucleic acid purifications. J Chromatogr A 1366:110–119
9. Silva-Santos AR, Alves CP, Prazeres DMF et al (2017) A process for supercoiled plasmid DNA purification based on multimodal chromatography. Sep Purif Technol 182:94–100
10. Matos T, Queiroz JA, Bülow L (2014) Plasmid DNA purification using a multimodal chromatography resin. J Mol Recognit 27:184–189
11. Černigoj U, Vidic U, Barut M et al (2013) A multimodal histamine ligand for chromatographic purification of plasmid DNA. J Chromatogr A 1281:87–93
12. Prazeres DMF (2011) Plasmid biopharmaceuticals: basics, applications, and manufacturing. John Wiley & Sons, Hoboken, NJ. , 615p. https://doi.org/10.1002/9780470939918.ch12
13. Brenac BV, Schapman A, Santambien P et al (2008) Fast purification process optimization using mixed-mode chromatography sorbents in pre-packed mini-columns. J Chromatogr A 1177:226–233
14. Ghanem A, Healey R, Adly FG (2013) Current trends in separation of plasmid DNA vaccines: a review. Anal Chim Acta 760:1–15
15. Gonçalves GAL, Prather KLJ, Monteiro GA et al (2014) Plasmid DNA production with *Escherichia coli* GALG20, a pgi-gene knockout strain: fermentation strategies and impact on downstream processing. J Biotechnol 186:119–127

Chapter 11

Minicircle DNA Vaccine Purification and E7 Antigen Expression Assessment

Ana M. Almeida, Dalinda Eusébio, João A. Queiroz, Fani Sousa, and Ângela Sousa

Abstract

Human papillomavirus (HPV) has been extensively associated with the development of cervical cancer due to the expression of oncoproteins like E7. This protein can interfere with pRB tumor suppressor activity, enabling the uncontrolled proliferation of abnormal cells. DNA vaccines are known as the third-generation vaccines, providing the ability of targeting viral infections such as HPV in a preventive and therapeutic way. Although current strategies make use of plasmid DNA (pDNA) as the vector of choice to be used as a DNA vaccine, minicircle DNA (mcDNA) has been proving its added value as a non-viral DNA vector by demonstrating higher expression efficiency and increased biosafety than the pDNA. However, due to its innovative profile, few methodologies have been explored and implemented for the manufacture of this molecule. This chapter describes the detailed procedures for the production, extraction, and purification of supercoiled E7-mcDNA vaccine, by using size-exclusion chromatography to obtain mcDNA with a purity degree which meets the regulatory agency criteria. Then, the assessment of E7 antigen expression through immunocytochemistry is also described.

Key words Alkaline lysis, Antigen expression, Cervical cancer, DNA vaccine, Fermentation, Human papillomavirus, Immunocytochemistry, Minicircle DNA, Size-exclusion chromatography

1 Introduction

Human papillomavirus (HPV) oncoproteins action in the development of cervical cancer has led researchers to focus in establishing therapeutic approaches directed toward this virus. In fact, it was found that the main prompters of such events are HPV E6 and E7 oncoproteins, widely known to interfere with the regulation of cell proliferation and repair commonly mediated by tumor suppressors p53 and pRB, respectively. E6 protein is known to form a complex by binding to E6AP. Such complex is then able to bind to p53 tumor suppressor protein and lead to its degradation, therefore interfering with p53 DNA repair mechanisms. In turn, this leads to the survival of abnormal cells with severe DNA damage, which,

Ângela Sousa (ed.), *DNA Vaccines: Methods and Protocols*, Methods in Molecular Biology, vol. 2197,
https://doi.org/10.1007/978-1-0716-0872-2_11,

in usual circumstances, would be eliminated by apoptosis induction through p53 regulation [1]. On the other hand, E7 protein is able to bind to pRB, releasing E2F transcription factor. The lack of E2F regulation leads to uncontrolled cell proliferation, favoring the propagation of abnormal cells [2]. DNA vaccines appear as the next vaccine generation, allowing humoral and cellular immunological responses and presenting a lower-cost manufacture with easier distribution than conventional peptide vaccines. While the transfection of cells with the DNA vaccine may lead to direct antigen presentation to cytotoxic T lymphocytes, triggering cell death by cellular immune response, antigen production by transfected cells can also lead to its uptake by antigen presenting cells, triggering the production of memory B cells by humoral immune response [3]. The fact that both immune responses are covered by this approach gives this vaccine the ability to act simultaneously as a preventive and therapeutic approach. Considering this, the study of DNA vaccines encoding HPV antigens has been explored as a pathway to confer immunization, while also allowing treatment, against the HPV infection. In fact, the use of E7 antigen has proven to be more fruitful than E6, allowing better tumor inhibition outcomes [4]. Thus, the use of E7 gene, especially modified to avoid its harmful interaction with tumor suppressor pRB but preserving its antigenicity, presents high potential for the development of a DNA vaccine for the prevention and treatment of cervical cancer induced by HPV infection.

Minicircle DNA (mcDNA) is an innovative vector, which has currently been placed under intense study by many scientists, due to its remarkable features comparatively to other conventional non-viral vectors, such as plasmid DNA (pDNA) [5, 6]. Such technology offers the possibility of excising the prokaryotic sequences, necessary for bacterial amplification, conferring an increased therapeutic efficiency to mcDNA due to higher and prolonged target gene expression. These structural properties of mcDNA also make this molecule more safe, since it avoids the possible triggering of immune responses commonly associated with the recognition of foreign prokaryotic sequences by the immune system [7]. Moreover, pDNA can also carry the selection marker gene that confers to the host resistance against a given antibiotic. Thus, the elimination of such sequences also prevents the patient from acquiring antibiotic resistance. Through the use of a parental plasmid (PP), which contains two sites recognizable by a specific recombinase, bacterial amplification can be carried out to increase vector production before in vivo induction of PP recombination into smaller and safer mcDNA molecule [8]. As portrayed in Fig. 1, amplification of PP is first carried out in a suitable prokaryotic host. Once bacterial growth has stagnated, induction with L-arabinose must be performed to allow the expression of a recombinase that will recognize two sites carried by PP molecule. Thus, mcDNA,

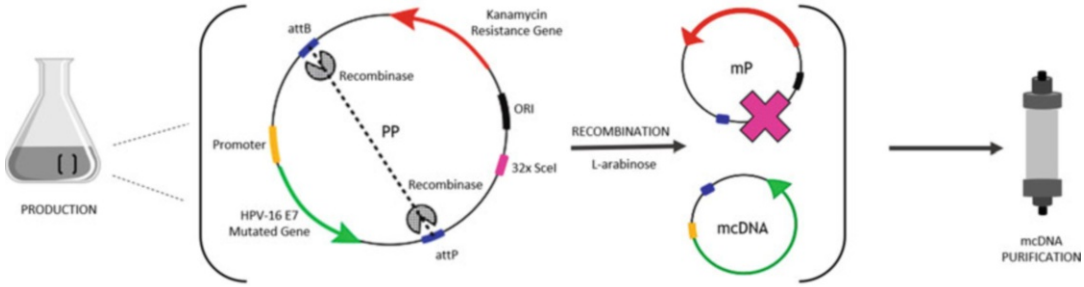

Fig. 1 Schematic representation of mcDNA manufacturing process

containing only the eukaryotic sequences responsible for the therapeutic effect, is retrieved from the recombination process. Also resultant from this process is miniplasmid (mP), a small molecule containing all the prokaryotic sequences which were originally excised from PP.

Given that the recombination process might not occur at its full extension, one may find the presence of unrecombined PP molecules concomitantly with mcDNA and mP molecules in the final sample. To reduce the contamination of mcDNA sample with pDNA-like molecules containing prokaryotic sequences, Chen and coworkers developed a recombination system, within genetically modified *E. coli* ZYCY10P3S2T strain, which allows the degradation of such molecules through the inclusion of site-specific sequences recognizable by endonuclease I-SceI in the prokaryotic region [9]. Thus, operating under the regulation of a pBAD/AraC promoter, PhiC31-integrase and I-Sce endonuclease are expressed upon L-arabinose addition. Although contamination is found to be reduced, PP and mP residual content may still be present in mcDNA final sample. Taking into account that regulatory agencies, such as Food and Drug Administration, strongly recommend the sample to be free from host impurities (such as genomic DNA (gDNA), RNA, proteins, and endotoxins) and to present more than 97% of the target DNA vector in its supercoiled (sc) isoform, it is crucial the use of suitable strategies to reduce the presence of molecules without therapeutic interest [10].

Considering the structural and chemical similarity displayed by PP and mcDNA molecules, the purification task can be found increasingly difficult [11–16]. However, size-exclusion chromatography has been found to be a suitable strategy to isolate mcDNA in its biologically active form, the sc isoform, from a complex sample containing host contaminants and PP residual content [17]. This strategy has proven to retrieve 66.7% of the injected sc mcDNA with 98.1% purity, while eliminating host impurities, respecting the specifications imposed by regulatory agencies. Figure 1 summarizes the process to obtain pure sc mcDNA. However, besides ensuring a rapid and cost-effective mcDNA manufacturing process, it is also

necessary to guarantee its efficacy. Antigen detection must be performed to confirm the ability of the vector to transfect cells and express the target antigen. To accomplish this, different methodologies can be used according to the final aim. Immunocytochemistry, for instance, is a technique widely used to detect and locate the expression of proteins within cells [18]. Thus, in this chapter, optimized protocols for E7-mcDNA vaccine production and purification resorting to Sephacryl SF-1000 matrix, followed by antigen expression assessment through immunocytochemistry, will be described.

2 Materials

2.1 Bacterial Growth for PP Amplification and Recombination for mcDNA Production

1. *E. coli* ZYCY10P3S2T strain transformed with 7.4 kbp PP encoding E7mut gene and bearing selection marker for kanamycin.
2. Antibiotic solution 1000×: 50 mg/mL of kanamycin in distilled water (*see* **Note 1**). Store at −20 °C.
3. Solid Luria Broth (LB) medium: 35 g/L of LB agar in distilled water, autoclaved and supplemented with 1 mL/L of the previously prepared antibiotic solution (*see* **Note 1**).
4. Liquid Terrific Broth (TB) medium: 20 g/L tryptone, 24 g/L yeast extract, 4 mL/L glycerol, 17 mM KH_2PO_4, 72 mM K_2HPO_4 (*see* **Notes 2** and **3**) in distilled water, autoclaved and supplemented with 1 mL/L of the previously prepared antibiotic solution (*see* **Note 1**).
5. L-Arabinose solution: 20% L-arabinose (w/v) in distilled water (*see* **Note 1**).
6. LB induction medium: 25 g/L of LB, 0.04 M NaOH (*see* **Notes 4** and **5**) in distilled water, autoclaved and supplemented with 1 mL/L of the previously prepared antibiotic solution and 2 mL/L of the previously prepared L-arabinose solution (*see* **Note 1**).
7. Visible spectrophotometer.
8. Erlenmeyers, suitable corks, and refrigerated shaker flask.

2.2 mcDNA Extraction by Alkaline Lysis

1. P1 buffer: 50 mM glucose, 25 mM of tris-hydroxymethyl aminomethane (Tris), 10 mM of ethylene-diamine tetraacetic acid (EDTA) in Milli-Q filtered water, pH adjusted to 8.0. Store at room temperature.
2. P2 buffer: 200 mM NaOH; 1% sodium dodecylsulfate (SDS) (w/v) in Milli-Q filtered water, pH adjusted to 12.0. Store at room temperature (*see* **Note 6**).

3. P3 buffer: 3 M potassium acetate, pH adjusted to 5.0 (*see* **Note 7**). Store at 4 °C (*see* **Note 8**).
4. Resuspension buffer: 10 mM Tris, 10 mM EDTA, pH adjusted to 7.0 (*see* **Note 9**).
5. Centrifuge tubes and a centrifuge, both able to endure 20,000 × *g*.

2.3 mcDNA Purification

1. Sephacryl SF-1000 matrix (GE Healthcare, Buckinghamshire, UK) (*see* **Note 10**).
2. Equilibration buffer: 10 mM Tris, 10 mM EDTA, 150 mM NaCl in Milli-Q filtered water, pH adjusted to 7.0 (*see* **Notes 9** and **11**).
3. 1.6 cm diameter chromatographic column with 60 cm bed height.
4. ÄKTA Pure system (GE Healthcare, Buckinghamshire, UK), consisting of a compact separation unit and a personal computer with UNICORN™ 6.3 software, or similar.
5. 10,000 MW centrifugal concentrators (*see* **Note 12**).

2.4 Agarose Gel Electrophoresis

1. TAE buffer: 40 mM Tris, 20 mM acetic acid, 1 mM EDTA in Milli-Q filtered water, pH adjusted to 8.0.
2. 0.016 μL/mL Greensafe premium (NZYTech, Lda.—Genes and Enzymes, Lisbon, Portugal) (*see* **Note 13**), or similar.
3. Loading buffer: 30% glycerol, 2% blue bromophenol (w/v) in filtered Milli-Q water.
4. Horizontal electrophoresis system and power supply.
5. Imaging equipment with UV light detector.

2.5 Cell Culture and Transfection

1. Cell line suitable for transfection, such as CHO-1.
2. Growth medium: Dulbecco's Modified Eagle Medium (DMEM)-F12 High Glucose Medium (Sigma-Aldrich, St. Louis, MO, USA) in Milli-Q filtered water, pH adjusted to 7.0, supplemented with sterile 10% (v:v) of fetal bovine serum (FBS) and 1% of a sterile mixture of penicillin (100 μg/mL) and streptomycin (100 μg/mL) (*see* **Note 14**).
3. Transfection medium: Dulbecco's Modified Eagle Medium (DMEM)-F12 High Glucose Medium (Sigma-Aldrich, St. Louis, MO, USA) (*see* **Note 14**) supplemented with sterile 10% (v:v) of fetal bovine serum (FBS) (*see* **Notes 14** and **15**).
4. Transfection reagent: Lipofectamine 2000 (Invitrogen, Life Technology, USA), or similar.
5. Twelve-well plates and sterilized glass coverslips.

2.6 Immunocytochemistry

1. PBS: 137 mM NaCl, 10 mM Na_2HPO_4, 1.8 KH_2PO_4, 2.7 mM KCl, in Milli-Q filtered water, pH adjusted to 7.4.
2. Fixation solution: 4% paraformaldehyde in PBS solution, pH adjusted to 6.9 (*see* **Note 16**). Store at −20 °C for long-term storage. Once it has been thawed, store at 4 °C up to 1 month.
3. Permeabilization solution: 1% Triton X-100 in PBS buffer (*see* **Note 17**).
4. PBS-T: PBS solution supplemented with 0.1% Tween-20 (*see* **Note 18**).
5. Blocking medium: 20% FBS in PBS-T (*see* **Note 19**).
6. Staining materials: mouse anti-E7 IgG primary monoclonal antibody (Santa Cruz Biotechnology, Heidelberg, Germany), Alexa 546 goat anti-mouse (Life Technologies, CA, USA), and Hoescht 33342 (*see* **Notes 20** and **21**).
7. Glass slides and mounting medium.
8. Laser scanning confocal microscope, or similar.

3 Methods

Carry out all procedures at room temperature unless otherwise specified. When necessary, the material, solutions, or culture media should be adequately sterilized by heat or filtration. All procedures to bacterial and eukaryotic growth are performed under aseptic conditions.

3.1 PP Amplification by Bacterial Growth and PP Recombination

1. Inoculate the recombinant *E. coli* ZYCY10P3S2T transformed with PP-E7mut in petri dishes, previously prepared with LB agar, and incubate overnight at 37 °C.
2. Transfer an isolate *E. coli* colony from solid culture medium to liquid TB medium and carry out the fermentation at 42 °C, under 250 rpm shaking (*see* **Note 22**). Cell growth is controlled, each hour, by measuring the optical density (OD) of the culture at 600 nm.
3. Once an OD_{600nm} of 5 is reached, recombination of PP into mcDNA should be carried out by induction with L-arabinose. Add the fermentation medium in a proportion of 1:1 to the LB induction medium (*see* **Note 23**). Incubate for 3 h at 32 °C, under 250 rpm shaking [8].
4. Recover cells by centrifugation at 4500 × *g* for 10 min at 4 °C and discard the supernatant. Cell pellets can be stored at −20 °C or readily be used in the next procedure.

3.2 Alkaline Lysis for mcDNA Extraction

1. If using frozen cell pellets, thaw them at room temperature. Otherwise, ignore this step.
2. Add 20 mL of P1 buffer to a cell pellet corresponding to 250 mL fermentation volume and shake vigorously (a vortex might be used) until the cells are entirely resuspended (*see* **Notes 24** and **25**). Then, transfer the resuspended cell pellet to a suitable centrifuge tube (*see* **Note 26**).
3. Add 20 mL of P2 buffer, carefully homogenize the solution and incubate for 5 min at room temperature (*see* **Note 27**).
4. Immediately add 20 mL of P3 buffer, carefully homogenize, and leave on ice for 20 min (*see* **Note 28**).
5. Centrifuge the tubes at 20,000 × *g*, 4 °C, for 30 min twice, discarding the cell debris pellet in between.
6. Measure the lysate volume remaining in the tube and add 0.7 volumes of isopropanol (*see* **Note 29**). Homogenize and incubate in ice for a minimum of 30 min (*see* **Note 30**).
7. Centrifuge the tubes at 16,000 × *g*, 4 °C and for 30 min. Discard the supernatant.
8. Resuspend the resulting pellet (1 mL for a 250 mL cell pellet) in resuspension buffer. If working with multiple tubes, transfer the resuspended pellets to a single tube and homogenize.
9. Add ammonium sulfate up to a final concentration of 2.5 M and homogenize carefully (*see* **Note 31**). Incubate for 15 min on ice.
10. Centrifuge the tubes at 16,000 × *g*, 4 °C and for 20 min. Discard the pellet and store the supernatant at −80 °C or readily use it in the next procedure.

3.3 mcDNA Purification

1. Prepare a packed column containing Sephacryl SF-1000 matrix with a bed height of 60 cm (*see* **Note 32**) by gradually and homogeneously adding the matrix to the chromatographic column, leaving it to settle down evenly until a volume of 121 mL has been added.
2. After connecting the column to the AKTA equipment, wash the column with filtered Milli-Q water. Then, equilibrate the column, in an isocratic gradient, with the equilibration buffer at a flow rate of 0.3 mL/min (*see* **Note 33**), for three column volumes (CV).
3. Directly add 2 mL of mcDNA clarified extract (*see* **Note 34**), obtained in the previous procedure, to the matrix surface, and wait until all the samples are loaded onto the matrix by gravity flow. Close the column and start the assay.

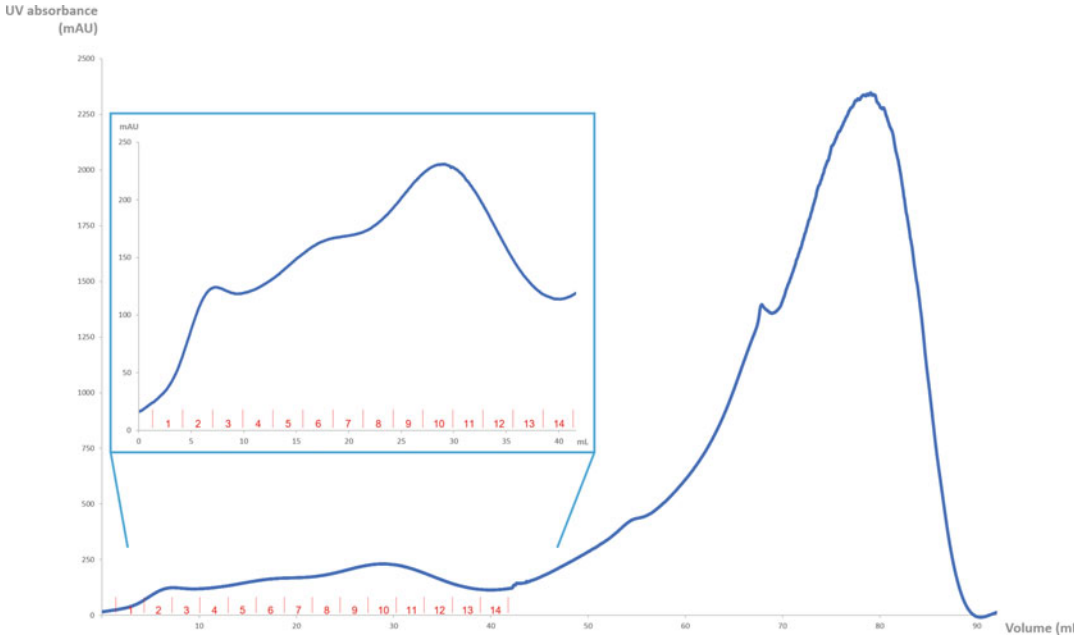

Fig. 2 Chromatographic profile obtained with Sephacryl SF-1000 in the separation of a clarified mcDNA complex extract, alongside fractions recovered for further electrophoretic analysis. Isocratic elution with 150 mM NaCl, 10 mM Tris, 10 mM EDTA buffer at pH 7.0

4. Monitor the UV light detector for changes in absorbance at 260 nm. Once the UV light begins to increase, start to collect the first chromatographic peaks by initiating the fraction collector (Fig. 2) (*see* **Note 35**).
5. After collecting the peaks, wash the salt present in the sample by using concentrators at 800 × *g*, 4 °C until the minimum volume is reached. Add resuspension buffer and concentrate again to the appropriate final volume intended.
6. Store the obtained samples at −80 °C or readily use them in the next procedure.
7. Wash the column and the system with 1 CV of filtered Milli-Q water.

3.4 Horizontal Electrophoresis

1. Prepare a 0.8% agarose gel by dissolving agarose in TAE buffer in a glass container (*see* **Note 36**).
2. Decrease the temperature of the agarose solution by leaving it still for several minutes at room temperature or by passing the flask under running water (*see* **Note 37**).
3. Add Greensafe to the agarose solution (*see* **Note 38**), mix it, and pour it down to a tray before placing the comb (*see* **Note 39**). Leave it at room temperature for some minutes (about 15–20 min) for gel polymerization.

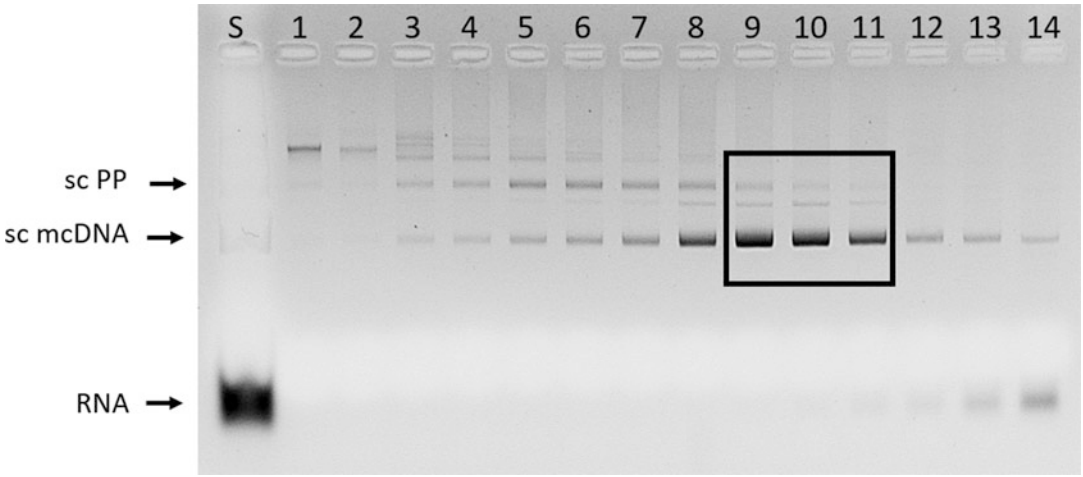

Fig. 3 Electrophoresis of fractions recovered in the chromatographic run

4. Add loading buffer (1:10) to the samples, homogenize, and inject them in the agarose gel wells (*see* **Note 40**). Run the gel at 150 V, for 30 min, before visualizing it in the imaging equipment (Fig. 3).
5. Choose the samples mainly containing isolated sc mcDNA (*see* **Note 41**) before proceeding to transfection.

3.5 Cell Culture and Transfection

1. Place sterile glass coverslips in the bottom of 12-well plates.
2. Seed 2×10^5 CHO-1 cells per well in the growth medium, homogenize, and incubate at 37 °C, 5% CO_2.
3. Once 80–90% confluence is reached, substitute growth medium for transfection medium nearly 12 h before transfection.
4. Prepare lipofectamine 2000–mcDNA complexes accordingly to the manufacturer's protocol and add them to the wells.
5. After 6 h, replace the transfection medium for growth medium and incubate for 72 h.

3.6 Immunocytochemistry for E7 Antigen Expression Detection

1. Discard medium from the 12-well plates and carefully rinse the wells with pre-blocking washing buffer (PBS) three times (*see* **Note 42**).
2. Add fixation solution and incubate for 15 min at room temperature (*see* **Note 43**).
3. Remove the fixation solution, discard it, and rinse carefully the wells with washing buffer three times.
4. Add permeabilization solution and incubate for 5 min at room temperature (*see* **Note 44**).

5. Discard the permeabilization solution and rinse carefully the wells with washing buffer (PBS) three times.
6. Add blocking solution and incubate for 2 h at room temperature (*see* **Note 45**).
7. Discard the blocking solution and, with the aid of a pair of thin tweezers, remove the coverslips from the wells and place them in a flat container, which can be placed at 4 °C without creating humidity (*see* **Note 46**).
8. Rinse the coverslips carefully with post-blocking washing buffer (PBS-T) three times.
9. Add a few drops of freshly prepared 1:50 dilution of primary E7 antibody solution (*see* **Note 47**) and incubate it overnight at 4 °C (*see* **Note 48**).
10. Rinse the coverslips carefully with post-blocking washing buffer for six times.
11. Add a few drops of freshly prepared 1:1000 dilution of secondary Alexa 546 antibody solution and incubate it 1 h at room temperature.
12. Repeat **step 8**.
13. Add a few drops of freshly prepared 1:1000 dilution of Hoescht and incubate it 10 min at room temperature.
14. Repeat **step 8**.
15. Add a drop of mounting medium to a glass slide and, after carefully removing the washing buffer, place the coverslip side containing the stained cells in contact with the mounting medium, without moving it any further and avoiding bubbles formation (*see* **Note 49**).
16. Visualize the slides in a laser scanning confocal microscope (Fig. 4) and check for differences between transfected and non-transfected cell samples.

4 Notes

1. Thermodegradable solutions must be filtered (0.2 μm pore membrane) to sterile tubes, in close proximity to a flame or in a flow cabinet, to guarantee its sterility before its addition to autoclaved microbiology media.
2. A stock solution containing 10× the potassium salts concentration should be prepared (170 mM KH_2PO_4, 720 mM K_2HPO_4). Add 100 mL/L of potassium salt stock solution to the TB medium, before adjusting water volume accordingly.
3. Liquid culture media should be first prepared in bulk and then distributed to Erlenmeyers with a proportion of 1:4 oxygen, before autoclaving. For example, if you intend to use 1 L

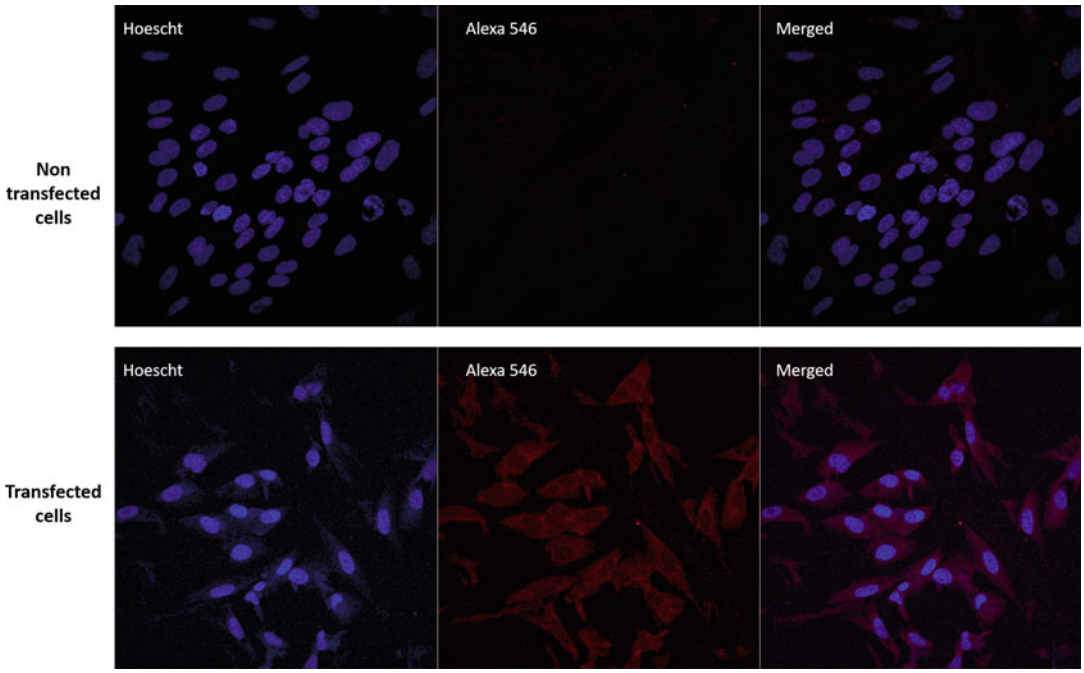

Fig. 4 Immunocytochemistry images for antigen E7 staining. Blue—cell nuclei; red—E7 protein

Erlenmeyer, then 250 mL of medium should be placed in it. This will guarantee that cells have enough oxygen and space to suitably exchange other gases inside the Erlenmeyer.

4. 1 M of NaOH stock solution should be prepared to reduce pH variation. Add 40 mL/L to the LB induction medium, before adjusting water volume accordingly. This will confer higher pH to the induction medium, allowing to neutralize the acidic and consumed fermentation medium that will be added later.
5. LB induction medium volume should be prepared according to the fermentation volume intended (1:1). When dividing the induction medium into the Erlenmeyers, keep in mind that 1:8 of the Erlenmeyer's volume should be placed. This will guarantee that, once the fermentation medium is added to the induction medium, the final volume will respect the 1:4 oxygen proportion rule, since fermentation volume will be added 1:1 in the induction medium Erlenmeyers.
6. Avoid low temperatures when storing this buffer since it might lead to SDS precipitation.
7. Before adjusting the pH, add approximately 30% of the final volume in water. Then, use glacial acetic acid to adjust buffer pH. Once pH has been suitably adjusted, add the remaining water to reach the intended final volume.
8. Storing this buffer at low temperatures will facilitate the precipitation of cell debris.

9. Chromatographic buffers used in mcDNA purification should be freshly prepared and filtered to avoid contamination and clogging of chromatographic system.
10. This matrix was specifically selected due to its broad fractionation range (5×10^5 to 10^8 molecular weight), which allows better resolution for a sample containing plasmid molecules or derivatives with similar sizes such as PP and sc mcDNA. With this matrix, it is expected that first elute the larger molecules and finally the smaller ones due to their higher retardation when entering onto the particle pores [17].
11. All buffers used within the chromatographic system must be sonicated to prevent air bubbles that might compromise UV detection.
12. The 10,000 MW pore size was chosen accordingly with sc mcDNA size (4.1 kbp). This step is crucial to desalt the sample, which is diluted in the equilibration buffer. The presence of salt can have severe consequences that can end up in cell death, thereby compromising the safety of this potential therapy.
13. Greensafe is a light-sensitive product and must be protected from light to maximize its effect.
14. Cell culture solutions must be filtered inside a flow cabinet by using sterilized filtration units.
15. Transfection medium should not contain antibiotic. Throughout transfection, the cells are more sensitive to antibiotic intake, which can lead to its death even in the presence of antibiotic levels lower than usual.
16. Paraformaldehyde is toxic and can release fumes; hence, dissolve it inside a ventilated hood. Also, heat PBS solution, while stirring paraformaldehyde to dissolve it, to 60 °C. Avoid boiling.
17. Triton X-100 might be found difficult to dissolve. Slightly heat PBS solution and gradually add Triton X-100 in small amounts to correctly dissolve it.
18. Tween-20 addition to PBS solution will allow to prevent unspecific binding between the antibodies used and non-target proteins.
19. Blocking medium should be filtered to avoid the presence of impurities and to guarantee clean images.
20. Fluorescent reagents should be carefully used away from light. All dilutions should be performed in PBS-T.
21. Hoechst will be used to stain cell's nuclei.
22. Before actually proceeding with the fermentation, a pre-fermentation in a smaller Erlenmeyer should be carried out to allow cell adaptation to the medium and to reach

exponential growth. Once the latter is achieved, by controlling OD_{600nm} (OD_{600} pre-fermentation) and assuring it reached 2.6, a pre-fermentation volume (vi) should be transferred to the fermentation Erlenmeyers, according to its fermentation volume. Assuming the Erlenmeyers used present a capacity of 1 L, then its fermentation volume ($v_{fermentation}$) will be assumed to be 250 mL. The starting fermentation OD_{600nm} must be normalized to 0.2 to avoid discrepancies between fermentations. The inoculation volume should be determined by the following equation: OD_{600} pre-fermentation $\times$ vi $= 0.2 \times (v_{fermentation} + vi)$.

23. To avoid contamination by repeatedly transferring fermentation medium to induction medium, autoclave a glass beaker to measure the amount of volume that will be necessary to transfer to the induction medium (e.g., if fermentation volume used is 250 mL then glass beaker should be able to measure 125 mL). Then, proceed the fermentation transfer to induction medium inside a flow cabinet to guarantee aseptic conditions.
24. P1 buffer will be used to resuspend cells and chelate divalent ions that can serve as substrate to DNases, to prevent later damage to target mcDNA. Also, it helps maintaining osmotic pressure and destabilize the cell wall.
25. When experiencing low recovery yields, increase, proportionally, the P1, P2, and P3 volumes added to the cell pellet. This will allow to increase the efficiency of the lysis process.
26. Calculate the maximum volume the centrifuge tube can take. If necessary, divide the 20 mL between two tubes to guarantee the maximum volume is not surpassed. Adjust the following P2 and P3 volumes, accordingly.
27. P2 buffer will solubilize the lipids of cell membrane, allowing cell content release and DNA and protein denaturation. Since only smaller DNA molecules will be able to later renature in this process, homogenization should be carried out carefully to prevent genomic DNA contamination due to its degradation in smaller pieces.
28. P3 buffer will neutralize the basic pH, resultant from the previous step, and renature small DNA molecules such as mcDNA. The incubation on ice will allow to facilitate cell debris precipitation.
29. Isopropanol will mainly allow the precipitation of nucleic acids, to separate them from the lysis solution. If necessary, divide the lysis solution containing the nucleic acids between two tubes to guarantee the maximum volume is not surpassed, before adding isopropanol.

30. Long exposure to cold will allow better precipitation of nucleic acids.
31. Ammonium sulfate will allow the precipitation of some RNA and proteins, clarifying the final sample.
32. Column size might be modified according to PP/mcDNA sizes. If working with larger molecules, larger column sizes will help to increase chromatographic resolution [17].
33. Flow rate might be adjusted to increase chromatographic resolution. If resolution is found to be poor, decrease the flow rate to allow differently sized molecules to have a different distribution along the matrix and favor its separation [17].
34. In size-exclusion chromatography sample volume should not be superior to 5% of the matrix volume to guarantee the separation of the target molecules [19].
35. High weight molecules such as PP and gDNA molecules will be expected to elute first, due to the lack of access to the matrix pores. However, mcDNA is only expected to elute approximately after 25 mL elution of equilibration buffer, followed by RNA after 45 mL (Fig. 2).
36. Gel percentage might be adjusted according to the size of the molecules expected to be visualized in the gel. If working with smaller molecules, higher agarose percentages should be used to tighten the gel pores and provide better separation. On the other hand, lower agarose percentages should be used when working with larger molecules, to stretch the pore size of the gel and increase its resolution. To correctly dissolve agarose in TAE buffer, heat it in an appropriate heat device (like a microwave). Make sure no agarose residues are found undissolved to guarantee a clean image, devoid of artifacts.
37. Lowering the gel temperature will prevent Greensafe from degrading. Once a bearable temperature is reached, stop lowering the temperature. If temperature is too low, it might polymerize before adding Greensafe.
38. Greensafe will bind to the nucleic acids present in the gel and allow its detection under UV light exposure.
39. Burst any air bubbles that might be enclosed in the gel to guarantee the sample will pass it uniformly.
40. Adding loading buffer to the sample will allow to increase its density, settling it down in the well, and to keep track of the migration front.
41. Horizontal electrophoresis, through the appliance of a suitable voltage, will result in the migration of negatively charged nucleic acids from the negative pole to the positive pole. Such migration will be affected by size and conformation of the nucleic acids. Thus, smaller and more compact molecules will

be found to migrate further, due to faster passage between the agarose pore net, while high weight and more relaxed molecules will be found to migrate little below the well. Thus, as it is visible in Fig. 3, the distribution of nucleic acids starts with gDNA, followed by PP isoforms (oc, linear and sc), mcDNA, and RNA (ordered from the well to the migration front). While oc isoform presents a more relaxed structure, sc is very compact, thus migrating further than oc and linear isoforms.

42. Make sure that every solution addition or withdrawal from the coverslip is performed gently to avoid cell detachment. Never leave a coverslip without medium, as it will dry and interfere with cell imaging.
43. Fixing cells will allow to maintain cell architecture and immobilize all molecules inside the cell.
44. Permeabilizing cells will allow antibody entry in cells, for specific antigen staining.
45. Blocking solution will allow to block nonspecific binding between primary antibody and non-target molecules. The proteins present in this solution will bind nonspecifically instead.
46. To avoid humidity, surround the inside of the container with paper towel.
47. Some fluorescence controls must be performed for the adjustment of laser conditions. Thus, coverslips without taking any antibody, only taking primary antibody, and only taking secondary antibody must be prepared. For each control, substitute the excluded antibody solutions accordingly by washing solution instead.
48. Antibody incubation can be performed either at room or cold temperatures. However, the higher the temperature is, the higher unspecific binding might occur. Thus, to guarantee that only specific binding between primary antibody and target antigen is occurring, incubation should take place at 4 °C for a prolonged time.
49. If many air bubbles are detected, try pressing the coverslip against the slide with the tweezers, without moving the coverslip in any direction. This pressure should direct the air outside the mounting medium.

References

1. Vande Pol SB, Klingelhutz AJ (2013) Papillomavirus E6 oncoproteins. Virology 445:115–137
2. Roman A, Munger K (2013) The papillomavirus E7 proteins. Virology 445:138–168
3. Almeida AM, Queiroz JA, Sousa F et al (2019) Cervical cancer and HPV infection: ongoing therapeutic research to counteract the action of E6 and E7 oncoproteins. Drug Discov Today 24:2044–2057

4. Peng S, Tomson TT, Trimble C et al (2006) A combination of DNA vaccines targeting human papillomavirus type 16 E6 and E7 generates potent antitumor effects. Gene Ther 13:257–265
5. Gaspar V, de Melo-Diogo D, Costa E et al (2015) Minicircle DNA vectors for gene therapy: advances and applications. Expert Opin Biol Ther 15:353–379
6. Mayrhofer P, Schleef M, Jechlinger W (2009) Use of minicircle plasmids for gene therapy. Methods Mol Biol 542:87–104
7. Dietz WM, Skinner NEB, Hamilton SE et al (2013) Minicircle DNA is superior to plasmid DNA in eliciting antigen-specific CD8+ T-cell responses. Mol Ther 21:1526–1535
8. Gaspar VM, Maia CJ, Queiroz JA et al (2014) Improved minicircle DNA biosynthesis for gene therapy applications. Hum Gene Ther Methods 25:93–105
9. Chen Z-Y, He C-Y, Kay MA (2005) Improved production and purification of minicircle DNA vector free of plasmid bacterial sequences and capable of persistent transgene expression *in vivo*. Hum Gene Ther 16:126–131
10. (2008) Guidance for Industry: Considerations for plasmid DNA vaccines for infectious disease indications. Biotechnol Law Rep 26:641–647
11. Mayrhofer P, Blaesen M, Schleef M et al (2008) Minicircle-DNA production by site specific recombination and protein-DNA interaction chromatography. J Gene Med 10:1253–1269
12. Hou XH, Guo XY, Chen Y et al (2015) Increasing the minicircle DNA purity using an enhanced triplex DNA technology to eliminate DNA contaminants. Mol Ther Methods Clin Dev 1:14062
13. Alves CPA, Šimčíková M, Brito L et al (2016) Development of a nicking endonuclease-assisted method for the purification of minicircles. J Chromatogr A 1443:136–144
14. Almeida AM, Queiroz JA, Sousa F et al (2019) Minicircle DNA purification: performance of chromatographic monoliths bearing lysine and cadaverine ligands. J Chromatogr B Anal Technol Biomed Life Sci 1118–1119:7–16
15. Silva-Santos AR, Alves CPA, Monteiro G et al (2019) Multimodal chromatography of supercoiled minicircles: a closer look into DNA-ligand interactions. Sep Purif Technol 212:161–170
16. Almeida AM, Černigoj U, Queiroz JA et al (2020) Quality assessment of supercoiled minicircle DNA by cadaverine-modified analytical chromatographic monolith. J Pharm Biomed Anal 180:113037
17. Almeida AM, Eusébio D, Queiroz JA et al (2020) The use of size-exclusion chromatography in the isolation of supercoiled minicircle DNA from *Escherichia coli* lysate. J Chromatogr A 1609:460444
18. Almeida AM, Tomás J, Pereira P et al (2018) HPV-16 targeted DNA vaccine expression: the role of purification. Biotechnol Prog 34:546–551
19. Grove A, Kushwaha AK, Nguyen KH (2015) Determining the role of metal binding in protein cage assembly. Methods Mol Biol 1252:91–100

Part IV

DNA Vaccine Delivery

Chapter 12

Tumor-Specific CD8$^+$ T-Cell Responses Induced by DNA Vaccination

Pablo Cáceres-Morgado and Alvaro Lladser

Abstract

DNA vaccines assisted by electroporation efficiently trigger antitumor cytotoxic CD8$^+$ T cell responses in preclinical cancer models and hold potential for human use. They can be easily engineered to express either tumor-associated self-antigens, which are broadly expressed among tumor patients but also in healthy tissue, or tumor-specific neoantigens, which are uniquely expressed in tumors and differ among patients. Recently, it has been demonstrated that DNA vaccination generates both circulating and tissue-resident compartments of CD8$^+$ T cells, which act concertedly against tumors. Here we describe the steps to obtain and test DNA vaccines against models of self-antigens and neoantigens in mice. It includes the evaluation of effector and memory CD8$^+$ T cell responses, as well as assessing the antitumor potential in vivo using transplantable syngeneic tumor models.

Key words Antitumor immunity, CD8$^+$ T cells, Circulating memory T cells, DNA vaccine, Flow cytometry, Immunization, Resident memory T cells, Tumor model

1 Introduction

DNA vaccines induce the activation of different branches of the immune response, in particular CD8$^+$ T cells, which are key for the eradication of viruses and tumors. To this end, DNA vaccination triggers maturation of dendritic cells (DC) through the activation of DNA-sensing immune receptors [1, 2], resulting in the subsequent presentation of DNA-encoded antigens on MHC class I molecules by directly transfected DCs or by type 1 conventional DCs (cDC1), which are specialized in cross-presentation [3]. This results in the efficient expansion of CD8$^+$ T cell responses against DNA-encoded antigens [4]. It has been recently demonstrated that efficient antitumor immunity requires the contribution of both circulating and tissue-resident CD8$^+$ T cell compartments [5]. Interestingly, DNA vaccination assisted by electroporation efficiently generates both circulating and resident memory CD8$^+$ T cell responses [6].

Ângela Sousa (ed.), *DNA Vaccines: Methods and Protocols*, Methods in Molecular Biology, vol. 2197,
https://doi.org/10.1007/978-1-0716-0872-2_12,

The choice of tumor-associated antigens is critical to achieve effective and specific antitumor immunity. DNA vaccines can be easily engineered to express tumor-associated self-antigens, which are overexpressed in tumors from different patients but are also expressed in healthy non-malignant tissues. As a result of immune self-tolerance, $CD8^+$ T cells bearing T-cell receptors (TCR) with high affinity against peptides derived from tumor-associated self-antigens are deleted [7]. Still, $CD8^+$ T cells against tumor-associated self-antigens have been demonstrated to mediate clinically relevant antitumor responses [8]. Emerging evidence derived from immunotherapy studies involving blockade of the PD-1/PD-L1 axis indicates that T-cell responses that mediate tumor regression are largely directed against tumor neoantigens, which arise from somatic mutations rendering new peptide sequences or neoepitopes [9, 10]. Since neoepitope-specific $CD8^+$ T cells are not subject to central tolerance, they carry high-affinity TCRs and therefore mediate strong and highly specific antitumor activity [11]. Given their high variability among individuals, personalized vaccination strategies are required to target neoepitopes [12, 13]. The comparative advantages of DNA vaccines, including safety, stability, and relative ease of production, make them a promising strategy for targeting both self-antigens and neoantigens in different types of cancer. Moreover, the ability of DNA vaccines to generate both circulating and resident memory $CD8^+$ T cells against tumor neoantigens is anticipated to foster antitumor efficacy. Here we describe the necessary steps to obtain and test DNA vaccines in preclinical mouse models.

2 Materials

These protocols are developed for immunization of C57BL/6 mice.

2.1 DNA Vaccine

2.1.1 Obtaining the DNA

1. Agarose for analysis of nucleic acids.
2. Autoclaved 25 g/L LB Broth Miller's formulation media (LB).
3. DNA ladder (1 kb).
4. DNA dye, such as SYBR® Safe DNA Gel Stain.
5. Electrophoresis equipment.
6. Endotoxin-free plasmid purification kit, such as NucleoBond® Xtra Midi EF.
7. Kanamycin (50 mg/mL) or ampicillin (100 mg/mL) resuspended in distilled water 0.2 μm filtered. Indicated concentrations to dissolve 1 mL of antibiotic in 1 L of LB media.
8. Nuclease-free distilled water.

Table 1
Restriction enzyme assays

	pVAX-OVA (μL)			dpcDNA-GP100 (μL)		
Nuclease-free distilled water	17.7	16.7	15.7	17.7	16.7	15.7
FastDigest Green Buffer	2.0	2.0	2.0	2.0	2.0	2.0
1 μg/μL DNA vaccine	0.3	0.3	0.3	0.3	0.3	0.3
FastDigest EcoRI	–	1.0	1.0	–	–	–
FastDigest XbaI	–	–	1.0	–	–	–
FastDigest HindIII	–	–	–	–	1.0	1.0
FastDigest XhoI	–	–	–	–	–	1.0
Total	*20*	*20*	*20*	*20*	*20*	*20*

Designed to work with FastDigest reagents (ThermoFisher)

9. Orbital shaker, 37 ° C.
10. Restriction enzymes and required buffer (as shown in Table 1), such as FastDigest enzymes and buffer.
11. Sterile phosphate-buffered saline (PBS) solution, pH 7.4.
12. Transformed *Escherichia coli* (*E. coli*) DH5α with pVax-OVA or pcDNA-hGP100 vector (as shown in Table 1).
13. Tris–acetate–EDTA buffer (TAE): 40 mM Tris, 20 mM acetic acid, 1 mM EDTA in Milli-Q filtered water, pH adjusted to 8.0.
14. Ultraviolet (UV) transilluminator.
15. UV/visible spectrophotometer (*see* **Note 1**).

2.1.2 $CD8^+$ T-Cell Transfer

1. 15 and 50 mL conical centrifuge tubes.
2. 1 mL tuberculin syringe with 25 G detachable needle (*see* **Note 2**).
3. 60 mm × 15 mm cell culture dishes.
4. 70 μm cell strainer.
5. 70% ethanol.
6. CO_2 chamber.
7. $CD8^+$ T-cell isolation kit using immunomagnetic negative selection, such as EasySep™ Mouse $CD8^+$ T-Cell Enrichment Kit.
8. Flow cytometry antibodies (as shown in Table 2).
9. Heat lamp.
10. Mouse restrainer.

Table 2
Antibody panel

	FITC	PE	PerCP	PeCy7	APC	APC/Cy7	BV421	ZA
OTI cells	CD3	Vα2	–	CD45.1	Vβ5	–	CD8α	ZA
PMEL1 cells	CD3	Vβ13	–	CD90.1	–	–	CD8α	ZA
Blood	CD8α	–	–	CD90.1[a]	CD127	CD3	KLRG-1	ZA
Spleen	CD8α	CD62L	CD44	CD90.1[a]	CD3	–	CD45	ZA
Skin	CD8α	CD103	CD45	CD90.1[a]	CD69	–	CD3	ZA

[a]OVA-specific CD8+ T cells (OT-I cells) can be identified using αCD45.1 and to identify GP100-specific CD8+ T cells (PMEL1 cells) using αCD90.1

11. Microscope slides with ground edge.
12. Neubauer chamber.
13. PBS.
14. PBS-FBS-EDTA: PBS, 2% (v/v) FBS and 1 mM EDTA.
15. Refrigerated centrifuge.
16. Surgical material.
17. TCR-transgenic mice, such as PMEL1 or OTI, expressing congenic markers CD90.1 or CD45.1.
18. Trypan blue.

2.1.3 Immunization

1. 0.5 mL insulin syringe with 30 G needle.
2. 1 μg/μL DNA vaccine (*see* Subheading 2.1.1).
3. 70% ethanol.
4. Electroporator system for the delivery of DNA vaccines, such as the AgilePulse In Vivo System, complemented with a parallel needle array electrode (two rows of four 2 mm pins, 1.5 × 4 mm gaps; 47-0040, BTX electroporation systems).
5. Razors.
6. Sevoflurane and required inhalation systems (*see* **Note 3**).

2.2 Test CD8⁺ T-Cell Response

Effector $CD8^+$ T-cell responses will be measured in blood, whereas circulating and resident memory responses will be determined in spleen and skin, respectively, by flow cytometry. For this, the following materials are necessary:

1. 15 mL conical centrifuge tubes.
2. 96-Well plate with curved bottom.
3. Anti-mouse CD16/32 diluted 1:100 in PBS.
4. Calibrated suspension of microspheres (optional), such as CountBright™ absolute counting beads.

5. Cytometer, such as BD FACSCanto™ II.
6. Cytometry antibodies diluted in PBS-FBS (as shown in Table 2).
7. FACS tubes.
8. Fixable Viability, such as Zombie Aqua™, diluted 1:125 in PBS.
9. Fixation and permeabilization solution, such as Cytofix/Cytoperm™.
10. PBS-FBS: PBS, 2% (v/v) FBS.
11. Refrigerated centrifuge.

2.2.1 Effector Phase

1. 1.5 mL Eppendorf tubes.
2. 70% ethanol.
3. Heat lamp.
4. Red blood cell (RBC) lysis buffer, such as RBC Lysis Buffer.
5. Mouse restrainer.
6. Scalpel.
7. Sodium heparin solution of 500 IU/mL diluted in sterile PBS.

2.2.2 Memory Phase

1. First digestion solution: 100 μL collagenase type IV 10,000 U/mL and 5 μL DNase I grade II 4000 U/mL. Both enzymes prepared in Hank's buffer saline solution with Ca^{+2} and Mg^{+2}.
2. Second digestion solution: 10 μL DNase I grade II 4000 U/mL in 1 mL R10 media.
3. 6- and 24-well plates.
4. 70 μm cell strainer.
5. 70% ethanol.
6. CO_2 chamber.
7. Microscope slides with ground edge.
8. R10 media 5 mM EDTA (at 4 °C).
9. R10 media: RPMI 1640 media supplemented with 10% FBS, 2 mM L-alanyl-L-glutamine, 1 mM sodium pyruvate, 1% MEM non-essential amino acids solution, 100 U/mL penicillin, and 100 μg/mL streptomycin.
10. RBC buffer.
11. RPMI 1640 media.
12. Scissors (to cut the skin in the wells).
13. Surgical material.

Table 3
Cell lines and transgenic CD8+ T cells

	B16F10	B16F10-OVA	B16F10-OTI	EL4	EL4-hPMEL1	EL4-mPMEL1
OVA full antigen	–	Yes	–	–	–	–
GP100 full antigen	Yes (murine)	Yes (murine)	Yes (murine)	–	–	–
H-2 Kb-restricted peptide[a]	–	$OVA_{257–264}$	$OVA_{257–264}$	–	–	–
H-2 Db-restricted peptide[a]	$mGP100_{25–33}$	$mGP100_{25–33}$	$mGP100_{25–33}$	–	$hGP100_{25–33}$	$mGP100_{25–33}$
OVA-specific CD8+ T cells (OT-I cells) recognition	–	Yes	Yes	–	–	–
GP100-specific CD8+ T cells (PMEL cells)	Yes	Yes	Yes	–	Yes	Yes

m murine, *h* human
[a]Other peptides can be loaded, but here are mentioned peptides related to the examples discussed in the chapter

2.3 Evaluate Antitumor Immune Response

1. 1 mL tuberculin syringe with 25 G detachable needle.
2. 100 mm × 15 mm cell culture dishes or 75 cm^2 culture flasks.
3. 50 mL conical centrifuge tubes.
4. 70 μm cell strainer.
5. 70% ethanol.
6. Caliper.
7. Cell line (as shown in Table 3).
8. PBS.
9. R10 media.
10. Razors.

3 Methods

Carry out all procedures at room temperature unless otherwise specified.

3.1 DNA Vaccine

3.1.1 Obtaining the DNA

The vector that will be used as a vaccine must be transformed into bacteria that allow it to amplify. As an example, for immunization against the OVA or GP100 antigen, the pVAX-OVA or pcDNA-hGP100 vector is respectively transformed into *E. coli* DH5α.

1. Incubate an inoculum of transformed bacteria in 1 L of LB media at 37 °C and 230 rpm in orbital shaker. Incubate for ~16 h to achieve a satisfactory OD_{600}. For pVAX-OVA or

pcDNA-GP100 vectors, the LB media must contain 50 μg/mL kanamycin or 100 μg/mL ampicillin, respectively.

2. Purify the plasmid according to the manufacturer's instructions of the endotoxin-free DNA purification kit. This kit is based on alkaline lysis.
3. Quantify your purified DNA and verify its purity by spectrophotometry (*see* **Note 4**).
4. Bring plasmid to a concentration of 1 μg/μL with PBS.
5. Verify plasmid integrity and identity by restriction enzyme test (as shown in Table 1). Digest 300 ng of plasmid samples with the appropriate restriction enzymes, according to the manufacturer's protocol.
6. Prepare 1% agarose gel adding 1 g of agarose in 100 mL of TAE.
7. Melt the agarose, add and mix 5 mL of SYBR® Safe DNA Gel Stain and place the mixture in the tray of electrophoresis equipment.
8. Once the agarose solidifies, add TAE until gel is covered and load 20 μL digested samples and 10 μL DNA ladder (1 kb) into each gel wells.
9. Run the digest product in 1% agarose gel at 90 V for 45 min. Evaluate the gel in the transilluminator (Fig. 1).

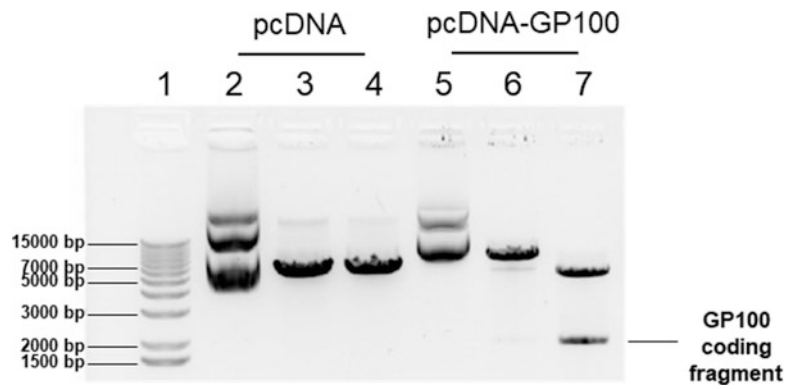

Fig. 1 Evaluation of integrity and identity of vaccine plasmids. Electrophoresis using 1% (w/v) agarose gel. (1) Molecular weight marker used was 1 kb Plus DNA Ladder. (2–4) Digestion products of pcDNA plasmid. (5–7) Digestion products of pcDNA-GP100 plasmid, this pcDNA vector contains the coding sequence for GP100 in the multiple cloning region, this sequence can be identified by being cleaved by restriction enzymes. (2 and 5) undigested samples. (3 and 6) Vector linearization by single digestion with HindIII. (4 and 7) Fragment release by double digestion with HindIII/XhoI

3.1.2 $CD8^+$ T-Cell Transfer

One day prior to immunization, 2×10^5 TCR-transgenic $CD8^+$ T cells are intravenously transferred into recipient C57BL/6. To facilitate the detection of $CD8^+$ T cells reactive against models of tumor-associated antigens or neoantigens (*see* **Note 5**):

1. Euthanize the transgenic mouse in a CO_2 chamber.
2. Spray the mouse with 70% ethanol and remove the spleen and inguinal lymph nodes with surgical material. To maximize the numbers of $CD8^+$ T cells, you can also process axillary, popliteus, brachial, and mesenteric lymph nodes.
3. Place the spleen and lymph nodes in 60 mm × 15 mm cell culture dishes with 5 mL of PBS-FBS EDTA. Disaggregate it by rubbing the spleen between microscope slides.
4. Pass the cell suspension through a 70 μm cell strainer into a coated 15 mL tube. Rinse the slides, dish, and cell strainer with 5 mL of PBS-FBS-EDTA.
5. Centrifuge at 400 × *g* for 5 min at 4 °C and flip the tube to discard the supernatant.
6. Purify $CD8^+$ T cells according to the manufacturer's instructions by using for example the EasySep™ Mouse $CD8^+$ T-Cell Enrichment Kit. This kit is based on immunomagnetic negative selection. Then, place the purified product in 15 mL tube, add PBS until 10 mL.
7. Centrifuge at 400 × *g* for 5 min at 4 °C and flip the tube to discard the supernatant. Resuspend the cells in 5 mL of PBS to wash the FBS and EDTA (Wash 1).
8. Repeat **step 7** (Wash 2), pass the cells through cell strainer and take an aliquot (10 μL), stain it with trypan blue, and bring to the Neubauer chamber to count twice.
9. Take an aliquot (1×10^5 cells) to check the purity of the product by flow cytometry. The protocol for flow cytometry staining is in Subheading 3.2.1.
10. Resuspend cells in the required PBS volume to achieve 2×10^6 $CD8^+$ T cells/mL in 50 mL tube.
11. Before starting the transfer, put a heat lamp close to the mouse cage for 2 min to increase irrigation and make the mouse tail vein more visible. Immobilize the mouse carefully in restrainer, keeping the tail free to transfer $CD8^+$ T cells.
12. Clean the mouse tail with 70% ethanol and using 1 mL tuberculin syringe with 25 G detachable needle transfer 2×10^5 cells in 100 μL by intravenous way in the mouse tail vein (*see* **Note 6**).

3.1.3 Immunization

1. Shave the lower back of the mouse with the razor and clean the shaved skin with 70% ethanol.
2. Anesthetize mice, in a chamber with a flow of 3% sevoflurane.
3. Accommodate mice for immunization and place the head inside a mask with continuous flow of sevoflurane to maintain anesthesia.
4. Intradermally inoculate 20 μg (20 μL) of the DNA vaccine using 0.5 mL insulin syringe with 30 G needle in two spots at the lower back.
5. Immediately place the electrode needles around the blebs and administer two electrical pulses of 0.05 ms and 1.125 V/cm followed by eight pulses of 10 ms and 275 V/cm on the vaccinated site.
6. Repeat **steps 4** and **5** at the opposite site of the previous vaccination. In total, 40 μg (40 μL) of the DNA vaccine is administered in two spots of 20 μg (20 μL) each one.

3.2 Test $CD8^+$ T-Cell Response

The $CD8^+$ T-cell response can be evaluated by flow cytometry (Fig. 2).

3.2.1 Effector Phase

The effector responses of $CD8^+$ T cells is evaluated in peripheral blood samples. The peak of these responses are found at day 10–12 after immunization.

1. Immobilize the mouse carefully in restrainer, keeping the tail free to obtain the blood sample. Before starting to obtain the blood samples, put a heat lamp close to the mouse cage for 2 min to increase irrigation and facilitate bleeding.
2. Clean the mouse tail with 70% ethanol and make a small cut in the lateral tail vein with a sterile scalpel (*see* **Note 7**).
3. Extract ~200 μL of blood from the mouse tail vein. Collect the *samples* in 1.5 mL Eppendorf tubes coated with 70 μL of sodium heparin. Mix quickly to avoid coagulation and place it on ice.
4. Transfer the blood sample to 15 mL tube with 2 mL of RBC buffer and incubate 5 min at room temperature. To stop the lysis reaction, add PBS up to 15 mL and centrifuge at 400 × *g* for 5 min at 4 °C, flip the tube to discard the supernatant.
5. Resuspend the cells of PBS in rest and transfer cell suspension to 96-well plate. Once all your samples are loaded on the plate, centrifuge at 900 × *g* for 2 min at 4 °C and flip plate to remove supernatant.

*Hereinafter these steps (**6–12**) are common for flow cytometry staining.*

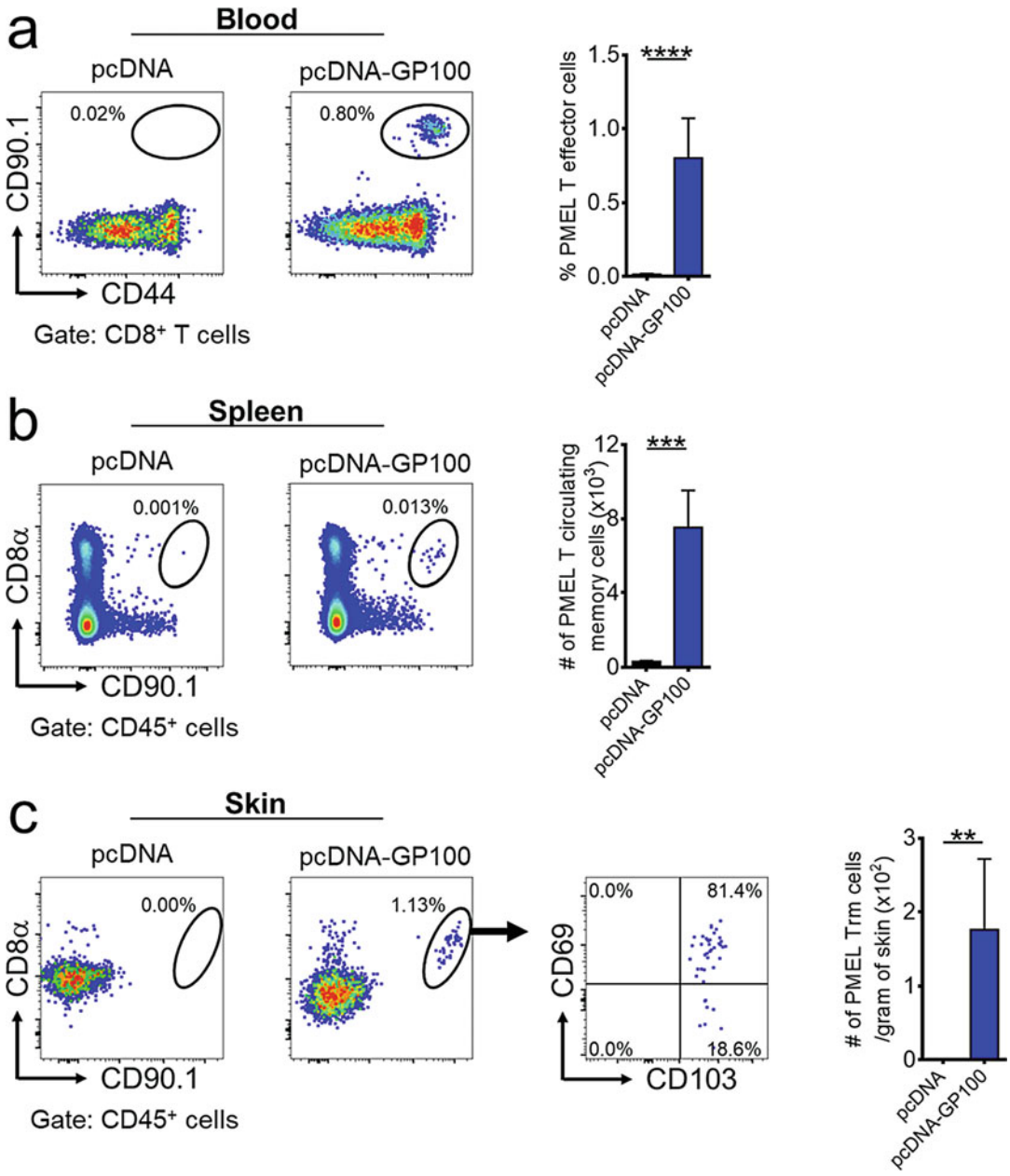

Fig. 2 DNA intradermal vaccination generates effector and memory CD8$^+$ T-cell responses. C57 BL/6 mice were intravenously transferred with PMEL cells (CD90.1$^+$ CD8$^+$ T cells) and, a day later, intradermally vaccinated with pcDNA-GP100. The analysis was performed 2 or 4 weeks after immunization to evaluate effector (blood) and memory (spleen and skin) responses, respectively. Control mice were vaccinated with empty plasmid as control. (**a**) Representative dot-plot showing the expression of CD44 and CD90.1 in CD8$^+$ T-cell population in blood. Graph showing % PMEL CD8$^+$ T-cell population, in blood after pcDNA-GP100 vaccination. PMEL T-effector cells were defined as CD90.1$^+$ CD44$^+$. (**b**) Representative dot-plot showing the expression of CD90.1 and CD8α in total CD45 cell population of spleen. Quantification of CD90.1$^+$ PMEL circulating memory CD8$^+$ T cells generated in spleen after pcDNA-GP100 vaccination. (**c**) Representative

6. Wash the cells with 150 μL of PBS-FBS, centrifuge at 900 × *g* for 2 min at 4 °C and flip plate to remove supernatant (going forward, *wash the cells*).
7. Resuspend the cells in 30 μL of anti-mouse CD16/32 dilution and incubate for 5 min at 4 °C. Add 150 μL of PBS-FBS, centrifuge at 900 × *g* for 2 min at 4 °C and flip plate to remove supernatant.
8. Resuspend the cells in 30 μL of Zombie Aqua™ dilution and incubate for 20 min at 4 °C in dark. Add 150 μL of PBS-FBS, centrifuge at 900 × *g* for 2 min at 4 °C and flip plate to remove supernatant.
9. Resuspend the cells in 30 μL of antibodies dilution and incubate for 20 min at 4 °C in dark. Add 150 μL of PBS-FBS, centrifuge at 900 × *g* for 2 min at 4 °C and flip plate to remove supernatant.
10. Wash the cells.
11. Resuspend the cells in 100 μL of Cytofix/Cytoperm™ and incubate for 20 min at 4 °C in dark. Centrifuge at 900 × *g* for 2 min at 4 °C and flip plate to remove supernatant.
12. Wash the cells twice.
13. Resuspend cells in 150 μL PBS-FBS and transfer suspension into FACS tubes. Acquire the samples in the flow cytometer.

3.2.2 Memory Phase

The memory responses of $CD8^+$ T cells is evaluated in skin (T resident memory) and secondary lymphoid organs such spleen (T circulating memory). Memory responses can be evaluated from week 4 after initial immunization.

1. Euthanize the mouse in a CO_2 chamber.
2. Use the shaver to remove the hair from the area of skin that you will get with (*see* **Note 8**).
3. Spray 70% ethanol on the mouse and with surgical material remove the spleen and 1 cm^2 of skin from the lower back of the mouse (*see* **Note 9**). Clean the fat carefully.
4. Place the spleens in a well (six-well plate) with 5 mL of R10 media. Disaggregate it by rubbing the spleen between microscope slides.

Fig. 2 (continued) dot-plot showing the expression of CD90.1 and CD8α in total CD45 cell population of vaccinated skin (left panel), and expression of CD103 and CD69 in PMEL cell population (right). Quantification showing $CD90.1^+$ PMEL Trm cells (defined as $CD103^+$ $CD69^+$) in vaccinated skin. Pooled data of two independent experiments, $n = 4$–6 mice per group for (**a**), $n = 3$–4 mice per group for (**b**, **c**). Bars are the mean ± SEM. $^{**}p < 0.01$; $^{***}p < 0.001$ by Mann–Whitney unpaired *t*-test

5. Filter the cell suspension through a 70 μm cell strainer into a coated 15 mL tube. Wash the slides, the well, and cell strainer with 5 mL of R10 media.
6. Centrifuge at 400 × *g* for 5 min at 4 °C and flip the tube to discard the supernatant.
7. Resuspend the cell in 1 mL of RBC and incubate 5 min at room temperature. To stop the lysis reaction add PBS up to 10 mL and centrifuge at 400 × *g* for 5 min at 4 °C, flip the tube to discard the supernatant (*see* **Note 10**).
8. Resuspend the cells in 5 mL of PBS-FBS and take 20 μL. Count the cells by flow cytometry by using the CountBright™ absolute counting beads following the manufacturer's instructions. Optional step (*see* **Note 11**).
9. Centrifuge at 400 × *g* for 5 min at 4 °C and flip the tube to discard the supernatant. Resuspend the cells in 1 mL of R10 media.
10. Place 50 μL aliquot in a well (96-well plate) according to the amount of samples needed (*see* **Note 12**).
11. Once all your samples are loaded on the plate, add 100 μL of PBS centrifuge at 900 × *g* for 2 min at 4 °C and flip plate to remove supernatant.

*Hereinafter, staining for flow cytometry is continued as described in the Subheading 3.2.1 (**steps 6–12**).*

12. For skin, weight skin sample (work with less than 200 μg) and place it in the well (24-well plate) with 895 μL RPMI media. With a scissors cut the skin into small pieces.
13. Add 105 μL of pre-warmed first digestion solution and incubate for 30 min at 37 °C. Stop the digestion by adding 1 mL of R10 media 5 mM EDTA at 4 °C.
14. Pass the skin sample to a 60 mm × 15 mm cell culture dishes, disaggregate the tissue by pipetting and rubbing the pieces of skin between microscope slides (*see* **Note 13**).
15. Filter the cell suspension through a 70 μm cell strainer into a coated 15 mL tube. Wash the slides, the well, the dish, and cell strainer with 5 mL of R10 media.
16. Centrifuge at 400 × *g* for 5 min at 4 °C and flip the tube to discard the supernatant.
17. Resuspend the cells in 1 mL of second digestion buffer and incubate 5 min at 4 °C. Centrifuge at 400 × *g* for 5 min at 4 °C and flip the tube to discard the supernatant.
18. Resuspend the cells in 2 mL of PBS-FBS and take 20 μL. Count the cells by flow cytometry by using the CountBright™ absolute counting beads following the manufacturer's instructions. Optional step (*see* **Note 11**).

19. Centrifuge at 400 × *g* for 5 min at 4 °C and flip the tube to discard the supernatant. Resuspend the cells of PBS in rest and transfer cell suspension to a well (96-well plate).
20. Once all your samples are loaded on the plate, centrifuge at 900 × *g* for 2 min at 4 °C and flip plate to remove supernatant.

*Hereinafter, staining for flow cytometry is continued as described in the Subheading 3.2.1 (**steps 6–12**).*

3.3 Evaluate Antitumor Immune Response

The antitumor response can be measured by comparing the tumor growth between vaccinated and unvaccinated groups. By vaccinating with a DNA vaccine encoding an immunogenic protein, different branches of the immune response can be activated. To evaluate the response of $CD8^+$ T cells, which are key in the antitumor immune response, challenges can be performed with tumor cells expressing MHC class I-restricted epitopes for $CD8^+$ T cells, such as H2-K^b-$OVA_{(257–264)}$ or H2-D^b-$GP100_{(25–33)}$ (as shown in Table 3) (Fig. 3).

3.3.1 Adherent Cells

Culture the B16F10 (B16F10-OVA or B16F10-OTI) cells in 100 mm × 15 mm cell culture dishes. The cells are harvested during the exponential phase (~70% confluence), by treatment with 0.25% trypsin 0.1% EDTA for 3 min at 37 °C, and subsequent addition of 5 mL of R10 media.

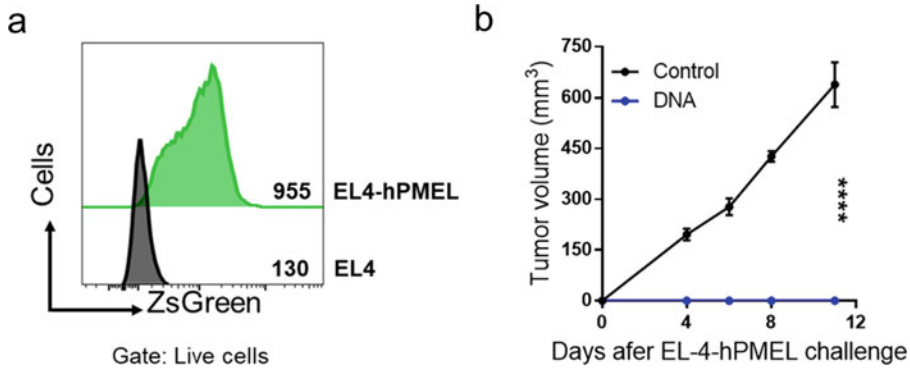

Fig. 3 DNA vaccination-induced $CD8^+$ T-cell response mediate protection against tumor challenge. C57BL/6 mice were intradermally vaccinated with pcDNA-GP100. Control mice were not vaccinated. After 12 days, mice were intradermally challenged with EL4-hPMEL cells, which were engineered to express the H-2 Db-restricted $GP100_{(25–33)}$ peptide fused to the ZsGreen fluorescent protein to specifically assess the contribution of $CD8^+$ T cells to the anti-tumor response. (**a**) Representative histograms showing the expression of ZsGreen (black histogram: EL4 cells; green histogram: EL4 cells-hPMEL). (**b**) Tumor growth curves of mice challenged EL-4-hPMEL. Data from independent experiment, $n = 5$. Bars are the mean ± SEM. $^{****}p < 0.0001$ by two-way ANOVA and Bonferroni post hoc test

3.3.2 Non-adherent Cells Culture the EL4-hPMEL1 (or EL4-mPMEL1) cells in 75 cm^2 culture flask. The cells in suspension are collected during the exponential growth phase (~7 × 10^5 cells/mL).

1. Bring the cells in suspension to a 50 mL tube. Centrifuge at 400 × *g* for 5 min at 4 °C and flip the tube to discard the supernatant. Resuspend the cells in 5 mL of PBS to wash the R10 media (Wash 1).
2. Repeat **step 1** (Wash 2).
3. Repeat **step 1** (Wash 3), pass the cells through cell strainer and take an aliquot (10 μL), stain it with trypan blue and bring to the Neubauer chamber to count twice.
4. Resuspend cells in the required PBS volume to achieve 2 × 10^7 cells/mL (*see* **Note 14**).
5. Following **steps 1–3** of Subheading 3.1.3, intradermally inoculate each mouse lower back with 50 μL of the cell suspension (1 × 10^6 cells) using 1 mL tuberculin syringe with 25 G detachable needle (*see* **Note 6**).
6. In the next few days, record tumor growth with caliper. In accordance with bioethical standards if required, sacrifice mice when the main diameter of the tumor reached ≥15 mm, when the mouse showed physical discomfort or when the tumor presents ulcers.

4 Notes

1. The UV/visible spectrophotometer is used for checking bacteria density in culture at 600 nm (OD_{600}). Additionally, it is used for measuring both the DNA concentration and purity by 260/280 nm ratio.
2. It is recommended to take the cells with the syringe without the needle to avoid cell death.
3. It could also be anesthetized with ketamine/xylazine, but sevoflurane is simpler and safer for mice.
4. When used correctly, each column of the kit allows to obtain ~1 mg of DNA with a ratio 260/280 ~1.9.
5. If you want to evaluate the effects of the vaccine on the endogenous repertoire of T cells you can use MHC class I tetramer staining or intracellular cytokine stains.
6. Resuspend the cells every three injections, to ensure inoculate the correct amount.
7. Let the ethanol dry before making the cut, or the blood will not fall from the tail, but will spread through it.

8. Do not apply ethanol before passing the shaver or you will have difficulty cutting the mouse hair.
9. Even if immunization was performed in the lower back of the mouse, skin Trm cells can also be found in other sites such as the upper back.
10. If the lysis of red blood cells worked well, the splenocytes pellet should be white, and the supernatant should become red. If it does not work, try again, with a new RBC buffer.
11. This stage is optional, you can also analyze the frequencies of the populations of interest, but the absolute numbers can help you obtain better conclusions.
12. Spleen cells are useful for compensation samples.
13. If the microscope slide has a rough area, use it to disaggregate the skin.
14. Consider that pellet volume is close to 200 μL.

References

1. Ligtenberg M, Rojas-Colonelli N, Kiessling R et al (2013) NF-κB activation during intradermal DNA vaccination is essential for eliciting tumor protective antigen-specific CTL responses. Hum Vaccin Immunother 9:2189–2195
2. Ishikawa H, Ma Z, Barger G (2009) STING regulates intracellular DNA-mediated, type I interferon-dependent innate immunity. Nature 461:788–792
3. Roberts E, Broz M, Binnewies M et al (2016) Critical role for $CD103^+$ /$CD141^+$ dendritic cells bearing CCR7 for tumor antigen trafficking and priming of T cell immunity in melanoma. Cancer Cell 30:324–336
4. Tondini E, Arakelian T, Oosterhuis K et al (2019) A poly-neoantigen DNA vaccine synergizes with PD-1 blockade to induce T cell-mediated tumor control. Onco Targets Ther 8:1652539
5. Enamorado M, Iborra S, Priego E et al (2017) Enhanced anti-tumour immunity requires the interplay between resident and circulating memory $CD8^+$ T cells. Nat Commun 8:16073
6. Gálvez-Cancino F, López E, Menares E et al (2018) Vaccination-induced skin-resident memory CD8+T cells mediate strong protection against cutaneous melanoma. Onco Targets Ther 7:e1442163
7. Vrisekoop N, Monteiro J, Mandl J et al (2014) Revisiting thymic positive selection and the mature T cell repertoire for antigen. Immunity 41:181–190
8. Schwartzentruber D, Lawson D, Richards J et al (2011) gp100 peptide vaccine and interleukin-2 in patients with advanced melanoma. N Engl J Med 364:2119–2127
9. Burrack A, Spartz E, Raynor J et al (2019) Combination PD-1 and PD-L1 blockade promotes durable neoantigen-specific T cell-mediated immunity in pancreatic ductal adenocarcinoma. Cell Rep 28:2140–2155.e6
10. Yost K, Satpathy A, Wells D et al (2019) Clonal replacement of tumor-specific T cells following PD-1 blockade. Nat Med 25:1251–1259
11. Fritsch E, Rajasagi M, Ott P et al (2014) HLA-binding properties of tumor neoepitopes in humans. Cancer Immunol Res 2:522–529
12. Sahin U, Derhovanessian E, Miller M et al (2017) Personalized RNA mutanome vaccines mobilize poly-specific therapeutic immunity against cancer. Nature 547:222–226
13. Aurisicchio L, Pallocca M, Ciliberto G et al (2018) The perfect personalized cancer therapy: cancer vaccines against neoantigens. J Exp Clin Cancer Res 37:86

Chapter 13

Therapeutic DNA Vaccine Against HPV16-Associated Cancer

Meihua Yu and Janin Chandra

Abstract

Human papillomavirus (HPV) is a contagious cause of anogenital and oropharyngeal cancers developing from persistently infected and subsequently transformed basal keratinocytes of mucosal epithelium. DNA-based immunotherapy offers great potential for the treatment of persisting HPV infections and associated cancers. Preclinical testing of therapeutic DNA-based HPV-targeted immunotherapy requires robust animal models which mimic HPV-associated cancer disease in humans. Here we describe a detailed protocol of intradermal delivery of a therapeutic DNA vaccine and a grafting model of neoantigen expressing skin to evaluate vaccine efficacy against HPV16 mediated hyperproliferative epithelium in mice.

Key words Cancer, DNA vaccine, Human papillomavirus, Immunotherapy, Intradermal immunization, K14E7, Skin grafting

1 Introduction

Human papillomavirus (HPV) infects epidermal cells of skin and mucosa and, if persistent, can induce benign (low-risk HPV types) or malignant (high-risk HPV types) cell growth [1, 2]. High-risk HPV types can cause a range of anogenital (e.g., cervical, vulvar, penile) and oropharyngeal cancers, of which HPV16-associated cancer is the most prevalent. While prophylactic vaccines are available and effectively prevent HPV infection, a global annual death burden of >300,000 remains and is associated with insufficient global vaccine uptake [3]. Hence, the development of HPV-targeted immunotherapy remains a high priority. DNA vaccines combine flexibility to target a variety of viral antigens of different HPV strains and immune-modulation, capable to prime antigen-specific cellular immunity and to kill HPV-infected and transformed cells. Furthermore, custom synthesis of DNA sequences is fast, and large-scale production is cost-effective, making this vaccine technology globally highly desired. Currently, five therapeutic HPV-targeting DNA vaccines have progressed from preclinical development to clinical evaluation: pNGVL4a-

Ângela Sousa (ed.), *DNA Vaccines: Methods and Protocols*, Methods in Molecular Biology, vol. 2197,
https://doi.org/10.1007/978-1-0716-0872-2_13,

Sig/E7(detox)-HSP70 (NCT00788164), VGX-3100 (NCT00685412), pNGVL4a-CRT/E7(detox) (NCT00988559), GX-188E (NCT02139267), and AMV002 (ACTRN12618000140257). These DNA vaccines are either delivered intramuscularly with or without electroporation [4–7] or intradermally [8].

The successful development of an efficient therapeutic HPV vaccine requires a robust preclinical animal model which closely mimics HPV-associated disease in humans. Routinely, therapeutic HPV vaccines are preclinically tested in mice using subcutaneously growing HPV16 E7-expressing TC-1 tumor cells [9]. However, TC-1 cells were derived from HPV16 E7 transformed primary lung epithelial cells, which are not a natural target for HPV infection [10]. Hence, the TC-1 model does not resemble persistent HPV infection and subsequent transformation of epithelial cells as occurring in humans.

Transgenic K14E7 mice express the high-risk HPV16 E7 oncoprotein under the control of the K14 promotor in keratinocytes, leading to epithelial hyperplasia, immune cell infiltration, and immune modulation similar to HPV-associated neoplasia in humans [11]. Furthermore, the K14E7 skin shares a common gene signature with cervical intraepithelial neoplasia stage 3 in humans [12]. While transplanted skin expressing a neoantigen such as ovalbumin is rejected from immunocompetent mice, K14E7 skin is tolerated when transplanted to wild-type or T-cell receptor transgenic E7TCR269 mice with increased E7-specific cytotoxic T cells [13]. Tolerance of HPV16 E7-expressing skin grafts is mediated by a variety of factors such as interferon gamma, natural killer T cells, and mast cells [14–16]. The therapeutic HPV DNA vaccine AMV002 was shown to overcome immune suppression mediated by K14E7 skin grafts [8].

Exemplary to testing therapeutic vaccines specific to skin-derived viral or tumor neoantigens, we here describe a detailed methodology of intradermal immunization using a DNA vaccine and transplantation of skin expressing a viral antigen often expressed in cervical cancer.

2 Materials

We use sterile solutions for injections and graft preparation. Maintain sterility of surgical tools and materials throughout the surgical procedure. Mice are preferably females to reduce the possibility of aggression and kept under specific pathogen-free conditions in a biological research facility. Animal ethics approval from research institutes on all animal procedures and treatments is required.

2.1 Animals

1. C57BL6/J mice (Animal Resources Center).
2. K14E7 mice transgenic for the HPV16 E7 oncoprotein driven by the K14E7 promotor were originally provided by Paul Lambert [11] and were cross-bred to C57BL6/J for 12 generations [17].
3. E7TCR269 mice were obtained from Graham Leggatt [18] and were bred in house at the Biological Research Facility of Translational Research Institute Brisbane.

2.2 Intradermal Immunization

1. Syringes and needles: ultra-fine insulin syringe 0.5 mL 30 G needle × 8 mm thin wall in individual packaging for intradermal injection, and 1 mL syringe with a 26 G needle for intraperitoneal injection.
2. Ketamine/xylazine anesthetic cocktail: Dilute 0.5 mL of Ceva Ketamine Injection (100 mg/mL ketamine) and 0.25 mL of Ilium Xylazil-20 (20 mg/mL xylazine) into 4.25 mL sterile water for injection to make a stock solution containing 10 mg/mL ketamine and 1 mg/mL xylazine. Administrate ketamine/xylazine anesthetic cocktail intraperitoneal at a dose of 100 μL/10 g body weight.
3. Blue tack.
4. HPV16 E7 encoding DNA vaccine.
5. Saline solution: 0.9% sodium chloride solution for injection.
6. Sterile Eppendorf tubes.
7. Eppendorf tube racks.
8. Isoflurane vaporizer.

2.3 Skin Grafting Surgery and Monitoring

1. Sterile 1× phosphate-buffered saline (PBS).
2. Sterile polystyrene plastic petri dishes plate with lids.
3. Donor mice: C57BL/6J or K14E7 mice aged 6–13 weeks as donors to provide ear skin grafts.
4. Recipient mice: C57BL/6J or E7TCR269 mice aged 8–12 weeks as recipients to receive single or double grafts (*see* **Note 1**).
5. Surgical tools: curved fine forceps, straight scissors, sharp/blunt dressing scissors, surgical knife handles, and scalpel blades.
6. Surgical bandages: Bactigras, micropore tape and Flex-wrap, and sensitive dressing lengths.
7. Wound-Gard antiseptic bitterant spray.
8. Ketamine/xylazine anesthetic cocktail (*see* **item 2** of Subheading 2.2).
9. Electrical clippers (clip skip blade #4–8 mm extra coarse).

10. Isoflurane vaporizer.
11. 70% (w/v) ethanol.
12. Ear notchers.
13. Tattoo ink paste.
14. Disposable stainless steel lancets.
15. Lacrilube lubricant eye ointment.
16. Povidone iodine wipes.
17. Heatpads at ~30 °C.
18. Recovery cabinets (29 °C).
19. Temgesic solution: Dilute 0.1 mL of Temgesic Injection (buprenorphine 300 μg/mL) into 5.9 mL of Hartmann's solution (sodium lactate solution containing 102 mmol/L sodium chloride, 2 mmol/L calcium chloride, 5 mmol/L potassium chloride and 29 mmol/L sodium lactate). Administrate diluted Temgesic subcutaneously at a dose of 100 μL/10 g body weight.
20. Ruler.
21. Camera.

3 Methods

Animal procedures were performed in compliance with ethical guidelines of the National health and Medical Research Council of Australia, with approval from the University of Queensland Animal Ethics committee.

3.1 Intradermal Immunization

1. Anesthetize female mice (C57BL/6J background) by intraperitoneal injection of pre-mixed ketamine–xylazine cocktail at a dose of 100 μL/10 g body weight (*see* **Note 2**).
2. Draw up 40 μL of DNA (30 μg) saline solution using an ultrafine insulin syringe (30 G needle) without air trapped inside (*see* **Note 3**).
3. Intradermal injection at the ear skin: Forming a cone of blue tack on index finger, place ear pinnae around blue tack and hold taut, until the ear skin is flat (Fig. 1a). Insert the needle at approximately 3° angle at the center of the ear skin intradermally and inject 20 μL solution per ear slowly (Fig. 1b, *see* **Note 4**).
4. Intradermal injection at other parts of the mouse (e.g., flank, back, or neck): Shave the hair on the skin with an electrical clipper. Hold the shaved skin taut with thumb and index fingers, and then insert the needle at approximately 3° angle intradermally followed by slow injection of vaccine solution.

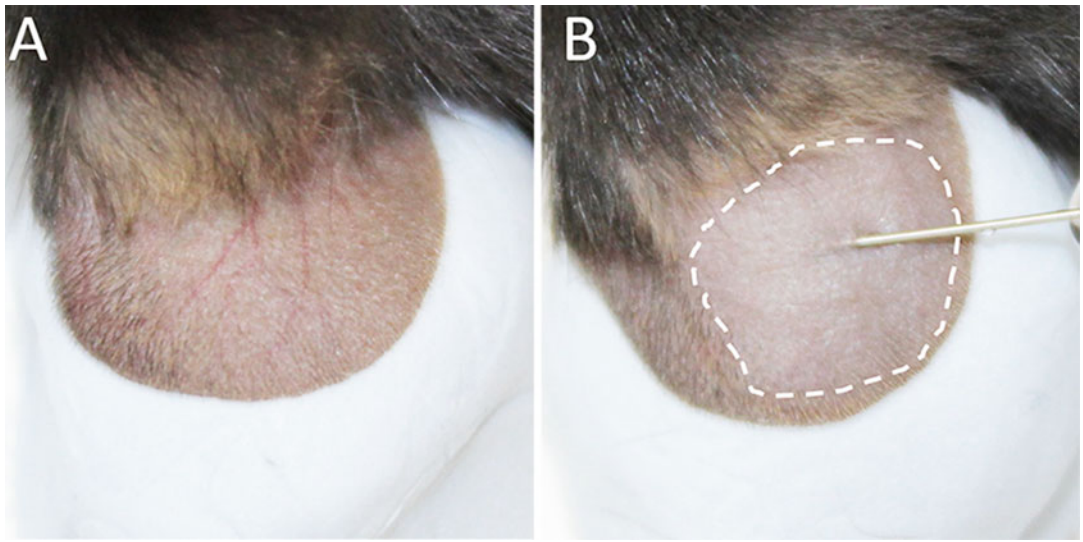

Fig. 1 Intradermal delivery of DNA vaccine. (**a**) Place ventral side of ear pinnae onto blue tack-formed cone on top of index finger and hold skin taut. (**b**) Insert the needle at a 3° angle into skin surface and inject DNA vaccine slowly. Injection will result in the formation of a raised wheal (indicated by circled area)

5. Place mice back to the cage in 29 °C recovery cabinet or on a heat pad for recovery.

3.2 Preparation of Ear Skin Grafts

1. Sacrifice donor mice by cervical dislocation or CO_2 asphyxiation.
2. Thoroughly sterilize gloves, working bench, and surgical instruments with 70% ethanol.
3. Sterilize mouse ears from dorsal and ventral side using 70% ethanol spray.
4. Cut ears close to base using large scissors (*see* **Note 5**).
5. Wash ears in PBS in a petri dish.
6. Separate dorsal and ventral layers by carefully entering the curved fine forceps into the space at ear base (Fig. 2a).
7. Place separated ear hair-side down onto Bactigras backing paper (Fig. 2b).
8. Spread ear tissue uniformly flat and remove cartilage by scraping tissue surface with flat end of curved forceps (Fig. 2c).
9. Cut paper around the skin outline.
10. Float skin-paper (paper-side up) in a petri dish containing sterile PBS (Fig. 2d).

3.3 Recipient Surgery Preparations

1. Change gloves and thoroughly sterilize gloves, working bench, and surgical instruments with 70% ethanol. Wear face mask. Resterilize gloves and surgical instruments between every mouse.

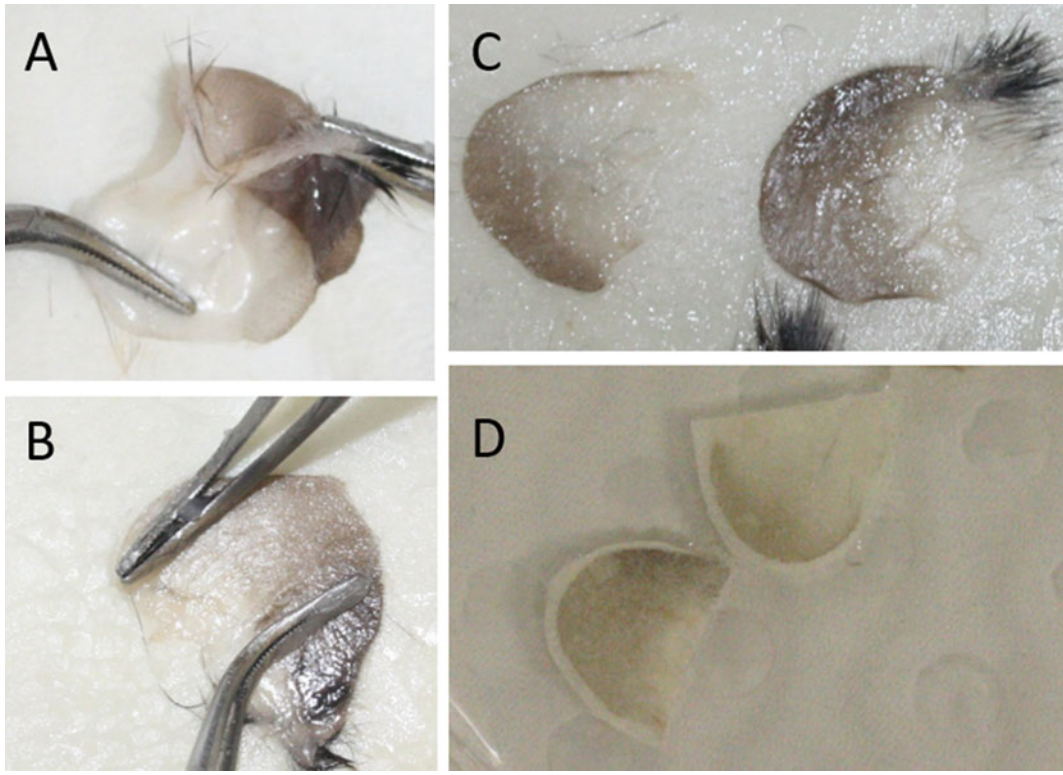

Fig. 2 Preparation of skin grafts. (**a**) Ears are cut close to the base. Dorsal and ventral layers are separated. (**b**) Ear layers are placed and spread onto Bactigras backing paper facing hairy site down. (**c**) Cartilage is removed by careful scraping using curved forceps. (**d**) Skin layers on paper are cut to shape and placed paper side up into petri-dish containing sterile PBS

2. Anesthetize graft recipient mice depending on weight (e.g., intraperitoneal injection of pre-mixed ketamine–xylazine at 100 μL/10 g body weight).
3. Confirm successful anesthesia by testing muscle reflexes (e.g., foot pinch). If mouse flinches or wakes up during surgery, immediately apply isoflurane through a nose cone (*see* **Note 2**). Monitor respiration throughout surgery.
4. Remove hair from grafting site (e.g., right flank) and toward abdomen and spine using electrical clippers.
5. Apply mouse identifiers (if graft recipients will receive intradermal immunization to ear, a tattooing method is preferred).
6. Apply lacrilube to eyes.
7. Wipe grafting site with 70% ethanol, followed by iodine.
8. Place mouse on a heatpad covered with absorbent low lint paper towel.

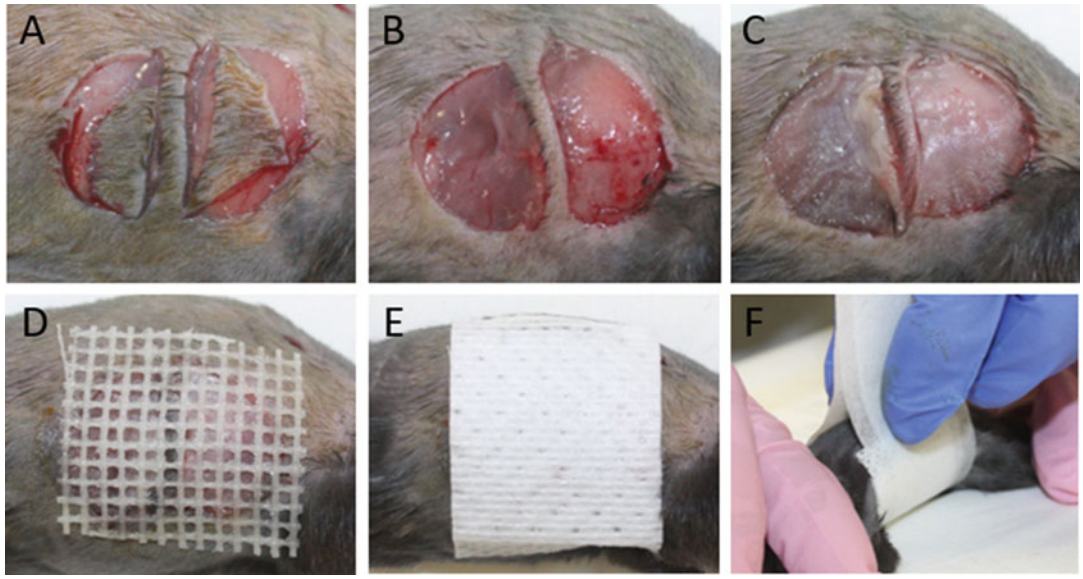

Fig. 3 Skin grafting procedure. (**a**) Flank skin is incised down to panniculus carnosus using scalpel in shape and size of ear grafts. (**b**) Flank skin is carefully removed, leaving panniculus carnosus intact. (**c**) Ear skin grafts on backing paper are placed paper-side up onto graft bed. Backing paper is removed. Grafts are spread to fit graft bed. (**d**) Bactigras is applied to grafting site. (**e**) Band aid with non-adherent pad is applied to grafting site. (**f**) First layer of micropore tape is applied around thorax of mouse

3.4 Grafting Procedure

1. Single or double grafts will be placed on the flank between front and hind limbs (*see* **Note 6**).
2. Pull skin of flank taut. Using a scalpel, incise skin down to panniculus carnosus in size and shape corresponding to ear graft tissue (approximately 1 cm^2) (*see* **Note 7**). The panniculus carnosus appears frosty white. When placing double grafts, leave 2 mm recipient skin between grafts (Fig. 3a).
3. Blot bleeding to sterile gauze.
4. Prepare the graft bed by firmly holding the edge of excised skin using forceps and teasing apart skin from panniculus carnosus until completely separated (Fig. 3b).
5. Choose appropriate-sized skin graft from petri dish and tap dry on sterile filter paper.
6. Place graft (paper-side up) onto graft bed. Carefully remove paper and spread graft using fine forceps, removing air bubbles from underneath the graft by stroking outwards (Fig. 3c).
7. Trim any excess overlapping graft skin using fine scissors. The graft should cover 90–100% of the graft bed.
8. Place Bactigras (approximately 2.5 (w) × 2 (h) cm) onto grafts (Fig. 3d) (*see* **Note 8**).

3.5 Bandaging Procedure

1. Cut fabric dressing length with non-adherent pad to approximately 4 (h) × 2.5 (w) cm. Place non-adherent pad onto graft site and stick adherent dressing above and underneath grafts (Fig. 3e) (*see* **Note 9**).
2. Prepare and overlap two pieces of micropore tape (approximately 15 cm long) to create strip of approximately 4.5 cm width.
3. Place micropore tape on bench (adherent site up) and hold taut on both ends, while the assistant lifts the mouse on front and hind limbs and places the mouse spine down onto micropore at 90° angle. Carefully roll mouse onto graft side on micropore tape.
4. The assistant gently stretches mouse while the operator firmly wraps micropore around the body, allowing mouse to breathe and walk (Fig. 3f). Trim excess micropore (Fig. 4a).
5. When mice regain consciousness but are not yet fully awake, overlay micropore with Vetflex bandage (approximately 4.5 cm wide) by overlapping both ends (Fig. 4b) (*see* **Notes 10** and **11**).
6. Administer Temgesic subcutaneously via neck skin at a dose of 100 μL/10 g of diluted Temgesic (i.e., 0.05 μg/g buprenorphine body weight) per day for pain relief (*see* **Note 12**).
7. Apply a second layer of micropore tape (Fig. 4c) (*see* **Note 13**).
8. Place mouse into fresh cage into 29 °C recovery cabinet (alternatively onto heat pad) until fully awake.

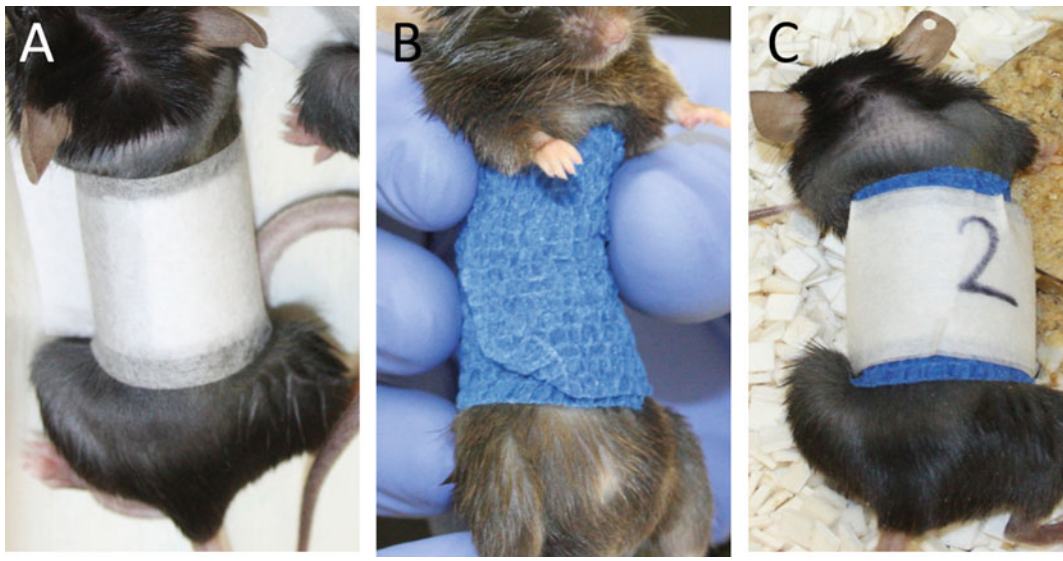

Fig. 4 Bandaging. (**a**) Micropore tape runs between front and hind limbs, allowing limb movement. (**b**) Vetflex is applied as second dressing layer. (**c**) Micropore tape is applied as third dressing layer

3.6 Post-Surgery Care

1. Repeat administration of Temgesic to the recipients for 3 consecutive days post-surgery.
2. Provide water bottle, food pellets, and moistened mashed pellets or nectar to cage for easy access (*see* **Note 14**).
3. Monitor mice twice daily after surgery for general well-being, weight loss, movement, and slippage of dressing (*see* **Note 15**). Anogenital discharge should be wiped with 0.9% saline. Mice might require redressing when substantial slippage occurs and can be performed under isoflurane anesthesia.
4. At signs of dehydration, animals can be injected subcutaneously via neck skin with 250 μL of 0.9% saline.
5. Remove bandages 7 days after grafting. Anesthetize mice using isoflurane delivered by nose cone (*see* **Note 2**). At the abdominal side, pass closed blunt/curved large surgical scissors under the dressing from tail end towards head end to dislodge micropore tape from body. Insert open scissors into created space and cut dressing (*see* **Note 16**).
6. Peel dressing carefully from the mouse, dislodging the dressing from the graft site last (*see* **Note 17**).
7. Allow mice 1 day to groom before graft measurement.

3.7 Monitoring and Measurement of Graft Rejection

1. Graft rejection should be monitored twice to three times weekly, and photographs including a ruler taken weekly under temporary isoflurane anesthesia.
2. Accepted grafts display clear margins. Rejected grafts may display redness and inflammation, produce scar tissue or show loss of clear margins.
3. Depending on the immunization model (prophylactic immunization before grafting, or therapeutic immunization after grafting), the baseline graft size will be determined on day 8 or 21 after grafting, respectively.
4. Graft sizes are calculated from photographs including a ruler using imaging software (e.g., Fiji imaging software) and recorded as mm^2, and the percentage of graft shrinkage is calculated from the baseline graft size.
5. Graft rejection is defined as >70% shrinkage of the graft size (Fig. 5a, b).
6. At end point, euthanize mice.

4 Notes

1. If transplanting double grafts, recipient mice should be aged 8 weeks or older to ensure sufficient flank space to accommodate two ear skin grafts. Mice weighing >22 g will maintain

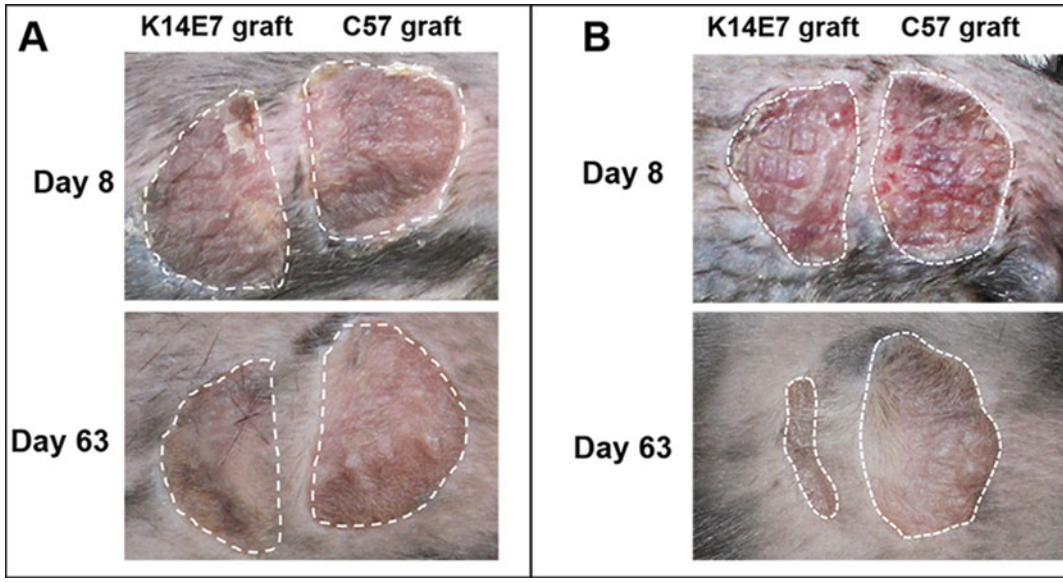

Fig. 5 Skin graft tolerance and rejection. Recipient mice received skin grafts of K14E7 and C57BL/6J donors. Digital images were taken including a ruler. (**a**) K14E7 grafts are tolerated on unimmunized recipients. (**b**) K14E7 grafts are rejected from immunized recipients 63 days after grafting

dressing better and experience less slippage of dressing and associated loss of grafts.

2. Alternatively, the intradermal injection can be performed under isoflurane anesthesia. Place mice in an anesthetic administration chamber with an induction flow rate of 1–2 L/min at 4–5% isoflurane. Once unconscious, apply a maintenance rate at 1–2 L/min at 1–3% isoflurane to mice via a nose cone. Monitor respiration throughout immunization process.
3. Each researcher should experiment other DNA amounts in order to determine the optimal immunogenic dose of their DNA vaccine.
4. It is important to flatten the ear skin on the blue tack before injection. Slow injection of vaccine solution will ensure even distribution of the solution in the ear, reducing skin damage. A resistance force will be felt during the vaccine injection process. A successful intradermal immunization will result in the formation of a raised wheal (indicated in Fig. 1b).
5. Ears should be cut close to the base, where an opening to separate dorsal and ventral layers can be identified.
6. Bandage should run between limbs and fully cover the skin grafts.
7. Bleeding indicates that incision is too deep, which should be avoided.

8. Bactigras is an antiseptic, reduces wound infection and inflammation, and prevents grafts from dehydration and adhering to dressing.
9. The band aid with non-adherent pad facilitates absorption of wound juice and prevents grafts from sticking to micropore dressing.
10. Second and third layer of dressing should be applied only when mouse is awake. If applied under anesthesia, mouse can suffocate after muscle tone and deep breathing functions are regained.
11. Vetflex bandages should be pretreated with Wound-Gard bitterant spray to prevent mice chewing bandages. To avoid stringent fumes, bitterant spray should dry completely before Vetflex is applied to mice.
12. Xylazine has analgesic properties. To reduce respiratory depression, the first administration of Temgesic is given post-surgery when the mice are awake.
13. The second layer of micropore tape prevents mouse from removing the dressing and dislodging the grafts.
14. Mice are restricted in movement while wearing dressing. Ensure the recipient mice have easy access to food and water until bandage removal.
15. Limbs and teeth likely get trapped in dressing and need to be freed during daily monitoring.
16. Avoid poking the mouse or cutting the skin.
17. If graft has not healed and excessive wounds present, mouse has to be sacrificed immediately.

Acknowledgments

This work was supported by the National Health and Medical Research Council (NHMRC) Early Career Fellowship (APP1124265) to M. Yu. We acknowledge TRI for providing the excellent research environment and core facilities that enabled this work. We particularly thank the Biological Resources Core Facility for excellent animal care and technical support.

References

1. Graham SV (2017) The human papillomavirus replication cycle, and its links to cancer progression: a comprehensive review. Clin Sci 131(17):2201–2221
2. Walboomers JMM, Jacobs MV, Manos MM et al (1999) Human papillomavirus is a necessary cause of invasive cervical cancer worldwide. J Pathol 189:12–19
3. Frazer IH (2014) Development and implementation of papillomavirus prophylactic vaccines. J Immunol 192:4007–4011

4. Trimble CL, Peng S, Kos F et al (2009) A phase I trial of a human papillomavirus DNA vaccine for HPV16+ cervical intraepithelial neoplasia 2/3. Clin Cancer Res 15:361–367
5. Trimble CL, Morrow MP, Kraynyak KA et al (2015) Safety, efficacy, and immunogenicity of VGX-3100, a therapeutic synthetic DNA vaccine targeting human papillomavirus 16 and 18 E6 and E7 proteins for cervical intraepithelial neoplasia 2/3: a randomised, double-blind, placebo-controlled phase 2b trial. Lancet 386 (10008):2078–2088
6. Alvarez RD, Huh WK, Bae S et al (2016) A pilot study of pNGVL4a-CRT/E7(detox) for the treatment of patients with HPV16+cervical intraepithelial neoplasia 2/3 (CIN2/3). Gynecol Oncol 140:245–252
7. Kim TJ, Jin HT, Hur SY et al (2014) Clearance of persistent HPV infection and cervical lesion by therapeutic DNA vaccine in CIN3 patients. Nat Commun 5:5317
8. Chandra J, Dutton JL, Li B et al (2017) DNA vaccine encoding HPV16 oncogenes E6 and E7 induces potent cell-mediated and humoral immunity which protects in tumor challenge and drives E7-expressing skin graft rejection. J Immunother 40:62–70
9. Lin KY, Guarnieri FG, StaveleyOCarroll KF et al (1996) Treatment of established tumors with a novel vaccine that enhances major histocompatibility class II presentation of tumor antigen. Cancer Res 56:21–26
10. Hung CF, Wu TC, Monie A et al (2008) Antigen-specific immunotherapy of cervical and ovarian cancer. Immunol Rev 222:43–69
11. Herber R, Liem A, Pitot H et al (1996) Squamous epithelial hyperplasia and carcinoma in mice transgenic for the human papillomavirus type 16 E7 oncogene. J Virol 70:1873–1881
12. Tuong ZK, Noske K, Kuo P et al (2018) Murine HPV16 E7-expressing transgenic skin effectively emulates the cellular and molecular features of human high-grade squamous intraepithelial lesions. Papillomavirus Res 5:6–20
13. Jazayeri SD, Kuo PT, Leggatt GR et al (2017) HPV16-E7-specific activated CD8 T cells in E7 transgenic skin and skin grafts. Front Immunol 8:524
14. Bergot AS, Ford N, Leggatt GR et al (2014) HPV16-E7 expression in squamous epithelium creates a local immune suppressive environment via CCL2-and CCL5-mediated recruitment of mast cells. PLoS Pathog 10(10): e1004466
15. Mattarollo SR, Frazer IH (2012) Response to comment on "Invariant NKT cells in hyperplastic skin induced a local immune suppressive environment by IFN-gamma production". J Immunol 188(3):931–932
16. Gosmann C, Mattarollo SR, Bridge JA et al (2014) IL-17 suppresses immune effector functions in human papillomavirus-associated epithelial hyperplasia. J Immunol 193:2248–2257
17. Matsumoto K, Leggatt GR, Zhong J et al (2004) Impaired antigen presentation and effectiveness of combined active/passive immunotherapy for epithelial tumors. J Natl Cancer Inst 96:1611–1619
18. Narayan S, Choyce A, Linedale R et al (2009) Epithelial expression of human papillomavirus type 16 E7 protein results in peripheral CD8 T-cell suppression mediated by CD4+CD25+ T cells. Eur J Immunol 39:481–490

Chapter 14

Bulk and Microfluidic Synthesis of Stealth and Cationic Liposomes for Gene Delivery Applications

Lucimara Gaziola de la Torre, Amanda Costa Silva Noronha Pessoa, Bruna Gregatti de Carvalho, Thiago Bezerra Taketa, Ismail Eş, and Gabriel Perli

Abstract

This chapter describes the synthesis of stealth and cationic liposomes and their complexation with plasmid DNA to generate lipoplexes for gene delivery applications. Two techniques are presented: a top-down approach which requires a second step of processing for downsizing the liposomes (i.e., ethanol injection method) and a microfluidic technique that explores the diffusion of ethanol in water to allow the proper lipid self-assembly. The synthesis of stealth liposomes is also a challenge since the use of poly(ethylene glycol) favors the formation of oblate micelles. In this protocol, the stealth cationic liposome synthesis by exploring the high ionic strength to overcome the formation of secondary structures like micelles is described. Finally, the electrostatic complexation between cationic liposomes and DNA is described, indicating important aspects that guarantee the formation of uniform lipoplexes.

Key words Cationic liposomes, Gene delivery, Microfluidics, Plasmid DNA complexation, Stealth liposomes

1 Introduction

Gene therapy is now regarded as a viable therapeutic tool to treat diseases [1], being also applied in vaccination approaches [2]. The therapy relies on efficacious delivery of genetic materials, DNA and RNAs nucleic acids, into target cells. However, the delivery of genetic materials is often impaired by several factors, as their susceptibility to nuclease enzymatic digestion through intracellular trafficking, in addition to their physicochemical characteristics, size, and anionic charge surface [3, 4].

The development of specific non-viral nanocarriers and their respective production methods have gained attention [3], since they may improve the delivery efficiency of nucleic acid into specific cells. One approach is the use of liposomes. These nanostructures are known due to their resemblance to cell membranes, which are

Ângela Sousa (ed.), *DNA Vaccines: Methods and Protocols*, Methods in Molecular Biology, vol. 2197,
https://doi.org/10.1007/978-1-0716-0872-2_14,

formed from their amphiphilic lipids self-aggregation, forming vesicles with an inner aqueous compartment. Among the developed non-viral vectors, cationic liposomes (CL) have stood out as an alternative to nucleic acid transport [5].

The electrostatic complexation of CL with nucleic acids is only possible due to the presence of cationic synthetic lipids [6, 7]. This electrostatic association may generate a variety of nanostructures, called lipoplexes (LPXs), which depend on the liposome composition (lipid types) and also production processes.

Specifically, CL have been developed using three specific phospholipids: (1) egg phosphatidylcholine (EPC), which helps to form the lipid bilayer and also to reduce cytotoxicity, (2) 1,2-dioleoyl-sn-glycero-3-phosphoethanolamine (DOPE), a helper lipid which promotes lipid bilayer disruption aiding DNA delivery [8], and (3) the monocationic synthetic lipid, 1,2- dioleoyl-3-trimethylammonium-propane (DOTAP) [9].

Another challenge in this research field is to eliminate the easy recognition of nanocarriers as exogenous molecules by the phagocyte system when administered systemically [10]. Alternatively, surface modifications have been investigated to blind these nano-vehicles from phagocytic cells. In this context, poly(ethylene glycol) (PEG) is one of the most commonly used polymers as surface binders of stabilized nanostructures in drug and gene delivery field [11].

Currently, most of the techniques used for liposome production require two operation steps, namely particle homogenization and size reduction. This is the case of the conventional ethanol injection process, which consists of the controlled addition of ethanol/lipid dispersion into an aqueous batch reactor under controlled stirring [12]. However, typically top-down methods require post-processing steps to decrease vesicle sizes, such as sonication [13], extrusion [14], and high-pressure homogenization [15].

In order to decrease the time consumption and costs of different processes, researchers have investigated techniques that simplify and optimize current production protocols [16]. To overcome these disadvantages, bottom-up methods have emerged as alternative processes. In this context, microfluidic processes have appeared as an option to directly produce discrete liposomes with controlled size, polydispersity, and shape, manipulating minute volumes of fluids inside microchannels [17, 18].

In this chapter, the top-down (ethanol injection) and bottom-up (microfluidics) methods to produce EPC/DOTAP/DOPE cationic liposomes, stealth cationic liposomes, and LPXs will be described.

2 Materials

2.1 Bulk and Microfluidic Production of Cationic Liposomes (CLs)

Cationic liposome (CL) synthesis is described using two different methodologies. Both conventional (bulk) and microfluidic methodologies are derived from ethanol injection method, using ethanol as an organic solvent. CLs are composed of:

1. Egg phosphatidylcholine (EPC, MW: 760 g/mol, purity: 96%).
2. 1,2-Dioleoyl-3-trimethylammonium-propane (DOTAP, MW: 698 g/mol, purity: 98%).
3. 1,2-Dioleoyl-*sn*-glycero-3-phosphoethanolamine (DOPE, MW: 744 g/mol, purity: 99.8%).
4. 99.5% ethanol: prepared using 4 Å molecular sieves overnight and subsequently filtered by a nylon syringe filter (0.22 μm), prior to use.
5. Prior to preparation, all glassware and lab materials should be autoclaved (three 20-mL glass flasks and ten 2-mL glass vials with proper caps, two beakers, four metallic spatulas, and disposable plastic tips for micropipettes (preferably, volumes of 1000, 5 or 10 mL)).
6. Ultrasonic bath with frequency of 40 kHz.
7. 1 and 20 mL glass syringes.
8. PTFE tubes of 0.56 mm ID × 1.07 mm OD and luer stubs (blunt needles) of 0.5 mm OD.
9. Cylindrical tank reactor (150 mL) with 8 × 6 cm (H × ID) and four baffles.
10. Syringe pump (PHD2000).
11. Ultra-Turrax® disperser, T25 digital model, with dispersing tool (S 25N—8 G) polycarbonate membranes (100 nm nominal diameter).
12. 2 mm ultrasound probe model SXB30.
13. Inverted microscope or a stereo microscope.
14. Microfluidic chip as described in Subheading 3.4.

2.2 Stealth Cationic Liposomes Synthesis

Stealth liposomes present improved steric stability and extended systemic circulation due to the presence of protective surface ligands, such as PEG. However, the synthesis of stealth cationic liposomes (SCLs) involve a series of challenging aspects, like the simultaneous formation of oblate micelles. In this way, the development of a microfluidic synthesis exploiting high ionic strength conditions in order to modulate the liposome self-assembly into SCL production only is important. For this purpose, phosphate-buffered saline (PBS) will minimize hydration forces between

lipids, aqueous side streams, and surface and also will favor the interactions between the phospholipid hydrophobic tails. In this section, the microfluidic synthesis of monomodal SCL with 1% of DSPE-PEG will be described [18].

Stealth cationic liposomes (SCLs) are prepared similarly to CLs described in Subheading 2.1. The SCLs are comprised of:

1. Egg phosphatidylcholine (EPC), 1,2-dioleoyl-3-trimethylammonium-propane (DOTAP).
2. 1,2-Dioleoyl-*sn*-glycero-3-phosphoethanolamine (DOPE), including 1,2-distearoyl-sn-glycero-3-phosphoethanolamine (DSPE, MW = 2805.497 g/mol, purity: >99%) conjugated with methoxy(polyethylene glycol) of MW = 2000 (PEG 2000)).
3. PBS and ethanol (99.5%).
4. Same as described in **items 4–14** in Subheading 2.1.

2.3 Synthesis of Lipoplexes for DNA Delivery

Cationic liposomes are used to complex with plasmid DNA to form LPXs. The complexation occurs in terms of electrostatic interaction between positively charged liposomes and negatively charged genetic material. Formed LPXs will effectively allow the cellular uptake of pDNA through internalization process as the delivery of pDNA in naked form is highly challenging. However, the aspects such as molar charge ratio between phospholipids and pDNA as well as complexation methods may directly influence the final physico-chemical properties of the lipid-based delivery systems. Hence, these parameters should be well-studied to synthesize LPXs with excellent characteristics.

Cationic liposomes were synthesized using the same phospholipid composition as shown in Subheading 2.1.

1. The plasmid pEGFP-N1 (4.7 kbp) is amplified in *Escherichia coli*, purified using for example the PureLink™ HiPure Plasmid DNA Purification Kit-Maxiprep and used for further complexation with cationic liposomes.
2. ND-1000 NanoDrop UV-vis spectrophotometer is used to quantify the pDNA. Please note that this plasmid is used as a gene reporter (model), but plasmid DNA or other genetic materials such as siRNA with known therapeutic outcomes can be used as well [19].
3. The same items from **items 4–14** of Subheading 2.1.

2.4 Microfabrication Technique

The microfluidic devices used for liposome synthesis are fabricated through microfabrication techniques, usually using soft lithography. In this protocol, all the steps needed for microfluidic chip fabrication is described.

1. Microchips are made with polydimethylsiloxane (PDMS) (Sylgard 184 elastomer kit).
2. For soft lithography, SU-8 photoresist.
3. Glass slides.
4. Aquapel® and Perfluorodecyltrichlorosilane (FDTS) for surface modification.
5. For general purposes, 4 Å molecular sieves, toluene, acetone, and isopropyl alcohol are employed.
6. Spin-coater.
7. UV light (250 mJ/cm^2, 365 nm).
8. Punch with 1 mm of diameter.
9. Scotch® MagicTM Invisible from 3M.
10. Plasma cleaner.
11. Ultrasonic bath.
12. 0.45 μm PTFE membranes.

3 Methods

3.1 Bulk and Microfluidic Production of Cationic Liposomes (CL)

3.1.1 Lipid Solution (Stock Solution)

1. The lipid dispersion should be prepared under a laminar flow hood.
2. The cationic liposomes (CL) are composed of EPC/DOTAP/DOPE phospholipids at molar proportions of 2:1:1, respectively (*see* **Note 1**).
3. Prepare at least 20 mL of solution with a total lipid concentration of 25 mM. This corresponds to a total number of moles of 0.000510 moles.
4. Use anhydrous ethanol to disperse the lipids.
5. In flask 1, weigh 0.0932 g of DOPE in a 20 mL flask. Add 10 mL of anhydrous ethanol, properly close the flask, and sonicate it for 15 min at 35 °C using an ultrasonic bath.
6. In flask 2 (20 mL flask), weigh 0.089 g of DOTAP and add 5 mL of anhydrous ethanol. One may use two spatulas to assist in the weighing of this phospholipid.
7. Using a micropipette, transfer the DOPE dispersion from flask 1 into flask 2, containing DOTAP. Close flask 2 and sonicate it for 15 min at 35 °C using an ultrasonic bath with frequency of 40 kHz.
8. In flask 3, weigh 0.198 g of EPC in the third 20 mL flask. Add 5 mL of anhydrous ethanol.
9. Transfer the lipid dispersion from flask 2, containing DOPE and DOTAP, into flask 3, with EPC.

10. Sonicate flask 3 for 20 min at 35 °C using an ultrasonic bath.
11. The solution is divided into ten glass vials of 2 mL, properly sealed and subsequently stored at −20 °C freezer.
12. Prior to all experiments, the lipid solution is sonicated in an ultrasonic water bath for 15 min at 35 °C.
13. All procedure described above can be done for more concentrated stock solution.

3.1.2 Bulk Synthesis (Ethanol Injection)

1. Sonicate the lipid solution stored at −20 °C freezer in an ultrasonic water bath for 15 min at 35 °C.
2. To prepare CL at the final lipid concentration of 2 mM, 8 mL of EPC/DOPE/DOTAP stock solution (25 mM) is loaded in a 20 mL glass syringe (*see* **Note 2**).
3. A tubing (PTFE tubes of 0.56 mm ID × 1.07 mm OD) and Luer stubs (blunt needles) of 0.5 mm OD are used to connect the PTFE tubing to the syringes.
4. Immerge the tubing inside a cylindrical tank reactor (150 mL) with 8 × 6 cm (H × ID) and four baffles containing 92 mL of PBS buffer (pH = 7.41 and ionic strength 0.1 M).
5. A syringe pump is used to feed the phospholipidic solution into the reactor at an injection flow rate of 44.4 mL/min. Keep all the procedure steps at room temperature.
6. Phospholipid solution is dispersed using an Ultra-Turrax® disperser, T25 digital model, with a dispersing tool (S 25N—8 G), at a continuous mechanical stirring rate of 750 × *g* for 15 min after completed feeding. In this step, an impeller can also be adopted to homogenize the phospholipid solution.
7. CL need to be stored at 8 °C.
8. CL size reduction and homogenization can be achieved using extrusion or ultrasonic treatments. For extrusion, use two stacked polycarbonate membranes (100 nm nominal diameter) to extrude the CL 15 times under nitrogen (12 kgf/cm^2) [20, 21]. Store at 8 °C.
9. Size reduction can also be performed using a 2 mm ultrasound probe, pulse mode (30% active cycle) for 1 min 30 s. Every 30 s, power is increased and achieve 60, 90, and 120 W. Store at 8 °C [22] (*see* **Notes 3–5**).

3.1.3 Microfluidic Synthesis

1. Prior to all experiments, the lipid solution stored at −20 °C freezer is sonicated in an ultrasonic water bath for 15 min at 35 °C [17].
2. Use polydimethylsiloxane (PDMS)/glass microfluidic chips based on hydrodynamic focusing fabricated using soft lithography technique (*see* Subheading 3.4).

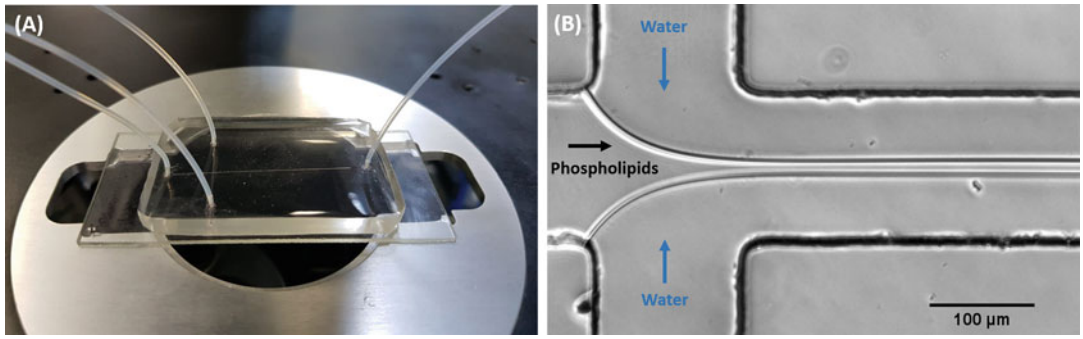

Fig. 1 (**a**) Image of the PDMS/glass microfluidic device based on hydrodynamic focusing with PTFE tubing connections. (**b**) Micrograph of typical experimental set-up for CL synthesis using FRR of 10

3. The phospholipid solution is loaded into a 1 mL glass syringe. Load two different 2.5 mL glass syringes with ultrapure water. Make sure that there are no gas bubbles trapped inside the syringe.
4. Use PTFE tubes of 0.56 mm ID × 1.07 mm OD and Luer stubs (blunt needles) of 0.5 mm OD to connect the PTFE tubing to the syringes. Cut pieces of the tubing taking into account the length between the syringe pumps and the microfluidic set-up. Fill the tubes with the respective solutions.
5. Connect the tubes to the inlet holes (Fig. 1a) of the microfluidic chip. The central stream is composed of the ethanolic lipid solution and the side streams are composed of ultrapure water. Place a tube at the outlet hole, for collection purposes (*see* **Note 6**).
6. Adapt the glass syringes connected to the tubes to the syringe pumps. Program the syringe pump by loading the correct syringe diameter, infuse mode, and flow rate unit. Make sure the syringes are well fixed to the syringe pumps.
7. The microfluidic synthesis of CL is carried out under the flow rate ratio (FRR) of 10, which is defined as the ratio of the sum of the side stream volumetric flow rates related to the flow rate of the central stream.
8. The total volumetric flow rate is 120.12 µL/min. Adjust the flow rates to 10.92 µL/min for the lipidic stream and 54.60 µL/min for each side streams composed of ultrapure water. Start pumping the fluids, just until there are no air bubbles trapped inside the tubes.
9. The microfluidic process is monitored in real-time with an inverted microscope or using a stereo microscope.
10. A typical hydrodynamic focusing pattern between the fluids is formed in the main outlet channel (Fig. 1b).

11. After flow stabilization (around 2–5 min, to avoid air bubbles inside the microchannels), start collecting the synthesized monodisperse unilamellar CL using a collection tube (*see* **Notes** 7 and **8**).

3.2 Stealth Cationic Liposomes Synthesis

Carry out the same procedures presented for microfluidic synthesis of CLs, unless otherwise specified.

1. The stealth cationic liposomes (SCLs) are comprised EPC/DOTAP/DOPE/DSPE-PEG_{2000} lipids at a molar proportion of 2:1:0.96:0.04, respectively.
2. The stock solution should be prepared according to the lipid solution protocol (*see* Subheading 3.1.1). For that, follow the process from **steps 1**–**5** of Subheading 3.1.1.
3. Change **step 6** to the following: weigh 0.8947 g of DOPE in a 20 mL flask. Add 10 mL of anhydrous ethanol, properly close the flask, and sonicate it for 15 min at 35 °C using an ultrasonic bath.
4. Follow the subsequent steps until **step 11**.
5. In flask 4, weigh 0.0141 g of DSPE-PEG_{2000} in the fourth 20 mL flask.
6. Transfer the lipid dispersion from flask 3, containing EPC, DOTAP, and DOPE, into flask 4 with DSPE-PEG_{2000}.
7. Sonicate flask 4 for 20 min at 35 °C using an ultrasonic bath.
8. The solution is also divided into ten glass vials of 2 mL, properly sealed, and stored at −20 °C freezer.
9. Prior to all experiments, the lipid solution is sonicated in a water bath for 15 min at 35 °C.
10. Subsequently, for the synthesis of SCL, microfluidic chips based on hydrodynamic focusing fabricated using soft lithography technique is applied (*see* Subheading 3.4). The microfluidic experiment should be executed similarly as reported in CL microfluidic synthesis (*see* Subheading 3.1.3).
11. Load the phospholipid solution into a 1 mL glass syringe. PBS at a concentration of 50 mM is loaded into two different 2.5 mL glass syringes. Make sure to avoid the formation of gas bubbles inside the syringes.
12. The microfluidic synthesis of SCL is carried out under the flow rate ratio (FRR) of 10, which is defined as the ratio of the sum of the side stream volumetric flow rates related to the flow rate of the central stream.
13. The total volumetric flow rate is 120.12 μL/min. Adjust the flow rates to 10.92 μL/min for the lipidic stream and 54.60 μL/min for side streams composed of PBS. At first, start pumping the PBS 50 mM for 10 min, then start pumping the phospholipid dispersion.

14. The microfluidic process is real-time monitored with an inverted microscope or using a stereo microscope. Make sure that there is no microaggregate formation on the microchannel glass surface.
15. After flow stabilization (around 2–5 min, to avoid air bubbles inside the microchannels), start collecting the synthesized monodisperse SCL using a collection tube (*see* **Notes 9–11**).

3.3 Synthesis of Lipoplexes for DNA Delivery

3.3.1 Molar Charge Ratio Between pDNA and Phospholipids for Lipoplex Synthesis

1. Molar charge ratio ($R_{\pm}$) is expressed as the ratio between the number of moles of positive charge and the negative charge (mol of positive charges/mol of negative charges). The optimum $R_{\pm}$ between the cationic liposomes composed of EPC/-DOTAP/DOPE and pDNA to transfect human epithelial carcinoma cells (HeLa cells) should be 3.
2. DOTAP is used as a cationic phospholipid to provide a positive charge to the cationic liposomes. DOTAP is a monocationic phospholipid as it possesses one positive charge in nitrogen atom at pH 7.4.
3. Plasmid DNA is negatively charged due to the phosphate atom in its backbone. Mixing DNA and phospholipids at varying concentrations leads to different molar charge ratios which will influence the efficiency of the transfection. To determine this ratio, it must be taken into consideration that 1 μg of pDNA contains 3 nmoles of negative charge in the backbone of the pDNA [23]. Also, it must be taken into consideration that the amount of phospholipids and pDNA varies depending on the complexation technique. In this section, conventional bulk mixing and complexation in microchannels will be addressed (*see* **Notes 12** and **13**).

3.3.2 Conventional Bulk Mixing

1. Conventional bulk production of LPXs is performed in an ice bath.
2. CL is synthesized in the microfluidic device, as shown in Subheading 3.1.3, prior to complexation with pDNA. Note that the percentage of cationic phospholipid (25%, DOTAP) used in the composition of liposome should be taken into consideration to calculate the molar charge ratio.
3. The optimum pDNA concentration is calculated based on the previously established in vitro transfection studies [20].
4. The proper amount of pDNA solution is added into the same amount of CL solution at such a phospholipid concentration that the molar charge ratio could be 3. The final concentration of pDNA in LPX formulation is defined as 0.01 μg/μL so it could seed at least 1 μg of pDNA into each well (100 μL) for transfection (*see* **Notes 12** and **13**).

5. Afterward, the Eppendorf tube containing pDNA and CL is vortexed for at least 40 s in an ice bath to form LPX and stored at 4 °C for further analysis.

3.3.3 Microfluidic Synthesis

1. Microfluidic synthesis of LPXs is performed in the microfluidic device shown in Fig. 1a and in Subheading 3.1.3 with the same syringe and tubing system. The syringes containing the pDNA and the CL solutions are placed in two separate infusion syringe pumps. The pDNA solution is injected in the central stream and hydrodynamically compressed by two liposomal streams from lateral channels [24].
2. The average fluid flow velocity of the stream is set to 140 mm/s. The flow rate ratio between the lateral flows and central flow should be experimentally defined as 5. The process temperature is set to 4 °C. According to these parameters, the fluid flow velocity of the pDNA solution should be 20 mm/s, whereas the CL solution from each lateral channel is fed at the velocity of 60 mm/s. The flow rate of lateral channels is the same to provoke a more uniform diffusion process along the main channel.
3. The sample collection started after establishing the flow through the main channel, as shown in Fig. 1b.
4. The duration of microfluidic synthesis of LPXs is determined according to the necessity of further experiments such as transfection studies and physico-chemical, structural, and morphological characterization (*see* **Note 14**).

3.4 Microfabrication Technique

This protocol should be performed inside a clean room and under laminar hoods. The chips are constructed using PDMS (polydimethylsiloxane) fixed on a glass slide, by means of standard soft lithography.

3.4.1 Chip Design

1. The microchannels are designed using computer-aided design software. The microfluidic design is printed as a negative plastic photomask (photolith film), with the dimensions specified in Fig. 2.
2. The soft lithography protocol for mold preparation is based on the process guidelines provided by SU-8 photoresist manufacturer [25].
3. For coating and soft-bake, SU-8 photoresist is spin-coated on a silicon wafer and soft-baked using 65 and 95 °C hot plates. Prepare the silicon wafers with a height between 50 and 100 μm. The rotation speed and baking times depend on the photoresist used and the desired thickness, following manufacturer recommendations.

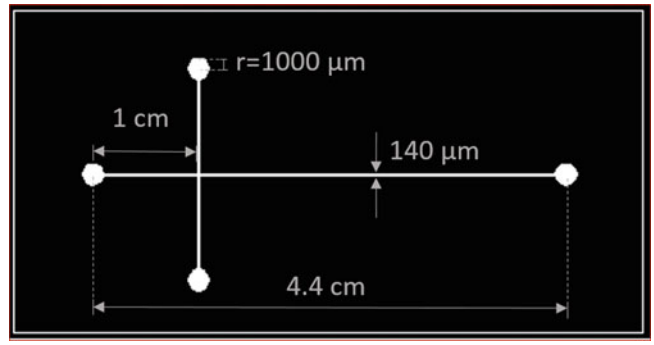

Fig. 2 Photomask containing the microfluidic chip design based on hydrodynamic focusing. The microchannels are 140 μm wide, 50–100 μm deep and have a full length of 4.4 cm. The inlet and outlet holes are designed with a radius of 1000 μm, which fits with the punch diameter and the width of the connecting tubes

4. For exposure and hard-bake, the wafer is UV-exposed (250 mJ/cm^2, 365 nm) through the negative photomask that contains the microchannel patterns. The wafer is then baked using 65 °C and 95 °C hot plates. The exposure and baking time are described by the manufacturer.
5. Submerge the wafer in a bath containing the SU-8 developer. Follow instructions to establish the time of development.
6. Use isopropyl alcohol to rinse the wafer and dry using an air gun. The mold is ready for the next steps.
7. For PDMS molding, the silicon wafer with the microchannel patterns is then used as a mold for the production of microfluidic devices. The mold is replicated using PDMS from Sylgard 184 elastomer kit.
8. The silicon wafer is placed into a petri dish (9.5 cm diameter).
9. Prepare PDMS at 1:10 (w/w) cross-linker/polymer ratio. Mix it well, gently transfer into the mold, and place it under vacuum for 30 min using a desiccator to remove air bubbles and ensure polymer homogeneity.
10. After degassing, the mold is cured on a hot plate at 100 °C for at least 50 min. The curing can also be performed using a 65 °C oven for 2 h.
11. Cut the chips into the desired shape. After demolding, use a punch with 1 mm of diameter to form the inlet and outlet holes of the patterned PDMS layer. Use a scotch tape (Scotch® MagicTM Invisible from 3 M) to clean the surface. Repeat this procedure for at least three times to ensure that dust and PDMS splinters are removed. For storage, cover the surface with a layer of Scotch® tape to protect the channels and holes.

3.4.2 Plasma Treatment

The PDMS/glass chips are irreversibly bonded using oxygen plasma. The plasma treatment alters the PDMS surface with silanol groups (SiOH), resulting in a temporarily hydrophilic character of the polymer surface.

1. For glass slide cleaning, submerge glass slides into a beaker containing detergent solution. Sonicate into an ultrasonic bath for 20 min. Wash the glass slides with distilled water, acetone, followed by isopropyl alcohol. Dry abundantly using an air gun. Repeat these steps as many times as needed. Alternatively, a piranha solution may be used to aggressively clean the glass before washing steps.
2. Remove the scotch tape from the PDMS mold and put the mold and the glass slide inside the plasma chamber. The side that has the patterned channels should be facing up when submitted to plasma treatment.
3. For plasma treatment, fill the plasma chamber with O_2. One can purge the air inside the chamber to ensure a maximum concentration of the desired gas. Plasma equipment may operate at 8 sccm of O_2, 25 W for 50 s. The parameters may change accordingly to plasma equipment.
4. After plasma, put the exposed surfaces in contact with (facing) each other. Ensure that there are no air bubbles within the channels. If needed, one may carefully press the borders of the device to remove the trapped air.
5. If hydrophilic conditions are required, one can use the chips within the first 1 h after plasma treatment, to ensure the hydrophilicity character of the channel walls.
6. Otherwise, wait at least 24 h to ensure the reestablishment of the hydrophobicity of the PDMS walls. An additional treatment may be done to enhance the hydrophobic character of the channels as described next.

3.4.3 Surface Treatments: Hydrophobic Conditions

Following, two surface modification strategies to enhance the hydrophobic character of glass slides are presented by using: (1) Aquapel®, a commercial water repellent, and (2) perfluorodecyltrichlorosilane (FDTS). This modification aims to prevent SCL deposition due to electrostatic interactions with glass onto the microfluidic device walls and further clogging or flow instability (*see* **Notes 15** and **16**).

1. Filter 2 mL of Aquapel® using 0.45 μm PTFE membranes.
2. Select the desired glass/PDMS devices to treat.
3. Fill the microchannels with filtered Aquapel®. Leave it for 5 min.

4. Use an empty syringe to slowly insert air to remove the excess of Aquapel® from inside the chips. Repeat this procedure twice.
5. For salinization using perfluorodecyltrichlorosilane (FDTS), the following procedure should be performed under a laminar flow hood appropriate for exhaustion of toxic chemicals.
6. Under a laminar flow hood, prepare anhydrous toluene using 4 Å molecular sieves overnight. Prior to use, filter it with 0.22 μm PTFE membranes.
7. Weigh 45 mg of FDTS and dissolve in 3 mL of dried toluene to prepare a 1.5% (m/v) FDTS solution.

For FDTS treatment, one may follow the protocol described in Subheading 3.4.4 or 3.4.5.

3.4.4 Glass Slide Treatment

1. Immerse the glass slides into a beaker containing detergent and sonicate for 30 min using an ultrasonic bath. Wash the glass slides with ultrapure water, followed by acetone and by isopropyl alcohol. Dry abundantly using an air gun. Repeat these steps as many times as needed.
2. Under a laminar flow hood, pour the FDTS solution on top of a clean glass slide. Leave it for 15 min. One can use a glass plate as a support to avoid leakage of the solution inside the hood.
3. Rinse the glass slide with isopropyl alcohol, dry with an air gun and place the treated glass slides into an oven (75 °C) overnight.
4. Follow waste regulations for disposing of waste materials and solutions.

3.4.5 Microfluidic Device Treatment

1. Follow the oxygen plasma protocol (*see* Subheading 3.4.2) to bond the glass/PDMS devices.
2. A few minutes after bonding, fill the microchannels with the solution of 1.5% FDTS in dried toluene (*see* **step 3** from Subheading 3.4.4) at room temperature. Repeat thrice every 5 min.
3. Clean the channels using isopropyl alcohol and dry with air.
4. Place the microchips in an oven at 90 °C overnight.

4 Notes

1. The order of phospholipid addition cited in this protocol is developed based on thermodynamic analysis for the adequate mixing between DOPE, DOTAP, and EPC phospholipids [26].

2. Due to the elevated hygroscopic feature of the lipids, make sure to properly seal the stock solution flasks with parafilm. Additionally, restrain their exposure to the atmospheric humidity. These procedures would prevent hydration and a previous random formation of self-assembled lipid aggregates.
3. Physicochemical properties such as size, polydispersity index (PDI), and zeta potential of CL and LPXs may be analyzed using for example a Malvern Zetasizer Nano ZS. Hydrodynamic diameter and PDI can be determined by dynamic light scattering (DLS) using CONTIN algorithm as the autocorrelation function. Zeta potential is obtained by applying an electric field across samples to estimate the electrophoretic mobility. Morphology, unilamellarity, and structural characterization of CL and LPXs should be analyzed with transmission electron microscopy (TEM), cryo-transmission electron microscopy (Cryo-TEM), and small-angle X-ray scattering (SAXS).
4. Using both the procedures described in Subheading 3.1.2, the injection method followed by extrusion or ultrasonic treatment, it is possible to synthesize CL with mean hydrodynamic diameter of 110 nm, polydispersity index (PDI) nearly 0.17, and zeta potential of +20 mV. Ethanol residue is kept constant at 3.08% v/v after liposome formation [27].
5. Through the described microfluidic protocol (Subheading 3.1.3), it is possible to produce CL in the range of 128–140 nm of mean diameter, PDI between 0.17–0.3 and zeta potential from +57 to +64 mV.
6. Be careful not to rip the microfluidic chip holes while connecting the tubing to the PDMS.
7. The PDMS/glass chips may be reused after synthesis. Wash the microfluidic devices using isopropyl alcohol, distilled water, and bath sonication for at least 15 min. Repeat this procedure as many times as needed.
8. The prepared CL present interesting features for further complexation with genetic material for gene delivery applications.
9. Bulk synthesis is performed by mixing the lipid dispersion with PBS 50 mM in a 2 mL tube, maintaining the volumetric proportions of 1:10 for lipid dispersion and solvent, respectively. This tube is further submitted to an ultrasonication bath for 15 min at room temperature using an ultrasonic bath with frequency of 40 kHz [18].
10. The SCL synthesized via bulk presented 100 nm in size and PDI of 0.22, but also bimodal size distribution. In comparison, microfluidic synthesis resulted in liposomes with 140 nm in

size, PDI of 0.17, +10 mV of zeta potential, and monomodal size distribution. This outcome showed that diffusion plays an important role in modulating lipid self-assembly.

11. If biological applications are needed, one may dialyze the synthesized stealth CL using a membrane of 3.5 kDa MWCO overnight in distilled water. The final dialyzed nanocarriers keep the size and PDI features and present increased zeta potential of approximately +40 mV. The high ionic strength of the medium helps to prevent undesired macromolecular aggregation. Additionally, surface modification may be employed to minimize CL deposition on the microchannel walls and the formation of PEG clusters. *See* Subheading 3.4.3 to check the alternatives to enhance glass hydrophobicity and then prevent clogging or flow instabilities in the device channels.
12. According to the experimental data, 1 μg of pDNA is required to transfect 50,000 HeLa cells at 80% confluency in each well of 24-well plate containing high glucose medium with 10% (v/v) fetal bovine serum (FBS) supplemented with nonessential amino acids, gentamicin, sodium pyruvate, and an antibiotic–antimycotic solution completed with lipoplex solution to obtain a final volume of 100 μL [28]. The final concentration of pDNA in the LPX is highly important to determine the therapeutic efficiency of the nanoparticle formulation. Low pDNA concentrations in the drug formulation most likely to fail to achieve the desired therapeutic effect while higher concentrations of pDNA may cause toxicity to the organism. Thus, the amount of genetic material must be carefully calculated prior to transfection studies.
13. Most of the drug formulation developed as a controlled release system is cell-specific, and their efficiency may vary depending on the cell type. Hence, cellular uptake and consequent therapeutic effect of the LPXs can be different for each cell type. Our group has tested a similar formulation on two different cell lines (HeLa and human prostatic tumor cell line, PC3) and the transfection efficiency of each formulation presented significant differences [20, 29].
14. The synthesized LPXs must present certain characteristics to be effective as a therapeutic agent. Therefore, their characterization plays an important role in such production for gene delivery purposes. The size and polydispersity of the produced LPXs were shown to greatly affect their transfection efficiency. Dynamic light scattering technique should be employed to determine the size, polydispersity index and zeta potential of the LPXs. The controlled release system should be highly monodisperse and with appropriate size to be applicable as a

gene delivery system. At molar charge ratio of 3, LPXs synthesized in the microfluidic system were as small as 100 nm (number-weighted mean diameter) with polydispersity index of 0.1 and zeta potential of +60 mV. For structural characterization, LPXs were structurally characterized using Synchrotron SAXS. The empty liposome presented a typical scattering profile for a unilamellar vesicle system. As it is increased DNA concentration in the LPX (molar charge ratio of 3), the scattering curve of LPX presented more intense correlation peaks, confirming that the system exhibited multilamellar order. For morphological characterization, LPXs may be analyzed using transmission electron microscopy to confirm the approximate size and lamellarity.

15. The Aquapel® coating should be performed prior to the use of the microfluidic chip. It is a surface physical coating, so it is not a permanent chemical surface treatment.
16. The measurement of static contact angle of water on glass slide surfaces after the hydrophobic salinization treatment [18] can result in 106.6 ± 7.7° for water-FDTS, in comparison to 21.3 ± 2.9° for water-untreated glass.

References

1. Kaleko M, Garcia JV, Miller AD (1991) Persistent gene expression after retroviral gene transfer into liver cells in vivo. Hum Gene Ther 32:27–32
2. de la Torre LG, Rosada RS, Trombone APF et al (2009) The synergy between structural stability and DNA-binding controls the antibody production in EPC/DOTAP/DOPE liposomes and DOTAP/DOPE lipoplexes. Colloids Surf B Biointerfaces 73:175–184
3. Verma IM, Weitzman MD (2005) Gene therapy: twenty-first century medicine. Annu Rev Biochem 74:711–738
4. Naldini L (2015) Gene therapy returns to centre stage. Nature 526:351–360
5. Zylberberg C, Gaskill K, Pasley S et al (2017) Engineering liposomal nanoparticles for targeted gene therapy. Gene Ther 24:441–452
6. Audouy S a L, de Leij LFMH, Hoekstra D et al (2002) In vivo characteristics of cationic liposomes as delivery vectors for gene therapy. Pharm Res 19:1599–1605
7. Sternberg B, Sorgi FL, Huang L (1994) New structures in complex formation between DNA and cationic liposomes visualized by freeze-fracture electron microscopy. FEBS Lett 356:361–366
8. Mönkkönen J, Urtti A (1998) Lipid fusion in oligonucleotide and gene delivery with cationic lipids. Adv Drug Deliv Rev 34:37–49
9. Parker AL, Newman C, Briggs S et al (2003) Nonviral gene delivery: techniques and implications for molecular medicine. Expert Rev Mol Med 5:1–15
10. Allen TM, Hansen C (1991) Pharmacokinetics of stealth versus conventional liposomes: effect of dose. BBA-Biomembranes 1068:133–141
11. Suk JS, Xu Q, Kim N et al (2016) PEGylation as a strategy for improving nanoparticle-based drug and gene delivery. Adv Drug Deliv Rev 99:28–51
12. Trevisan JE, Cavalcanti LP, Oliveira CL et al (2011) Technological aspects of scalable processes for the production of functional liposomes for gene therapy. In: Non-viral gene therapy. IntechOpen, Crotia. https://doi.org/10.5772/17869
13. Maulucci G, De Spirito M, Arcovito G et al (2005) Particle distribution in DMPC vesicles solutions undergoing different sonication times. Biophys J 88:3545–3550
14. De Paula Rigoletto T, Silva CL, Santana MHA et al (2012) Effects of extrusion, lipid concentration and purity on physico-chemical and biological properties of cationic liposomes for gene vaccine applications. J Microencapsul 29:759–769
15. Pupo E, Padrón A, Santana E et al (2005) Preparation of plasmid DNA-containing liposomes using a high-pressure homogenization-

extrusion technique. J Control Release 104:379–396

16. Meure LA, Foster NR, Dehghani F (2008) Conventional and dense gas techniques for the production of liposomes: a review. AAPS PharmSciTech 9:798–809
17. Balbino TA, Aoki NT, Gasperini AAM et al (2013) Continuous flow production of cationic liposomes at high lipid concentration in microfluidic devices for gene delivery applications. Chem Eng J 226:423–433
18. Perli G, Pessoa ACSN, Balbino TA et al (2019) Ionic strength for tailoring the synthesis of monomodal stealth cationic liposomes in microfluidic devices. Colloids Surf B Biointerfaces 179:233–241
19. Eş I, Ok MT, Puentes-Martinez XE et al (2018) Evaluation of siRNA and cationic liposomes complexes as a model for in vitro siRNA delivery to cancer cells. Colloids Surf A Physicochem Eng Asp 555:280–289
20. Balbino TA, Gasperini AAM, Oliveira CLP et al (2012) Correlation of the physicochemical and structural properties of pDNA/cationic liposome complexes with their in vitro transfection. Langmuir 28:11535–11545
21. Vitor MT, Bergami-Santos PC, Piedade Cruz KS et al (2016) Dendritic cells stimulated by cationic liposomes. J Nanosci Nanotechnol 16:270–279
22. Gómez-Mascaraque LG, Casagrande Sipoli C, de La Torre LG et al (2017) Microencapsulation structures based on protein-coated liposomes obtained through electrospraying for the stabilization and improved bioaccessibility of curcumin. Food Chem 233:343–350
23. Wetzer B, Gerardo BYK, Frederic M et al (2001) Reducible cationic lipids for gene transfer. Biochem J 356:747–756
24. Balbino TA, Azzoni AR, de La Torre LG (2013) Microfluidic devices for continuous production of pDNA/cationic liposome complexes for gene delivery and vaccine therapy. Colloids Surf B Biointerfaces 111:203–210
25. Moreira NH, de Almeida AL d J, de Oliveira Piazzeta MH et al (2009) Fabrication of a multichannel PDMS/glass analytical microsystem with integrated electrodes for amperometric detection. Lab Chip 9:115–121
26. de Paula Rigoletto T, Zaniquelli MED, Santana MHA et al (2011) Surface miscibility of EPC/-DOTAP/DOPE in binary and ternary mixed monolayers. Colloids Surf B Biointerfaces 83:260–269
27. Vitor MT, Bergami-Santos PC, Zômpero RHF et al (2017) Cationic liposomes produced via ethanol injection method for dendritic cell therapy. J Liposome Res 27:249–263
28. Toledo MAS, Janissen R, Favaro MTP et al (2012) Development of a recombinant fusion protein based on the dynein light chain LC8 for non-viral gene delivery. J Control Release 159:222–231
29. Eş I, Montebugnoli LJ, Filippi MFP et al (2020) High-throughput conventional and stealth cationic liposome synthesis using a chaotic advection-based microfluidic device combined with a centrifugal vacuum concentrator. Chem Eng J 382:122821

Chapter 15

Conception of Plasmid DNA and Polyethylenimine Delivery Systems with Potential Application in DNA Vaccines Field

Diana Costa, Ângela Sousa, Rúben Faria, Ana Raquel Neves, and João A. Queiroz

Abstract

In DNA-based therapy research, the conception of a suitable vector to promote the target gene carriage, protection, and delivery to the cell is imperative. Exploring the interactions between polyethylenimine (PEI) and a plasmid DNA can give rise to the formation of suitable complexes for gene release and concomitant protein production. The nanosystems formulation method, based on coprecipitation, seems to be adequate for the conception of nanoparticles with suitable properties (morphology, size, surface charge, and pDNA complexation capacity) for intracellular applications. The developed systems are able of cell uptake, intracellular trafficking, and gene expression, in an extent depending on the ratio of nitrogen to phosphate groups (N/P). It comes that the transfection process can be tailored by this parameter and, therefore, also the therapeutic outcomes. This knowledge contributes for progresses in the development of suitable delivery systems with potential application in DNA vaccines field.

Key words Cationic polymers, Co-precipitation, Gene delivery, Nanoparticles, N/P ratio, Plasmid DNA, Polyplexes

1 Introduction

DNA-based therapy attracts great and widespread interest due to its technological challenging characteristics and its promising therapeutic role [1, 2]. For DNA-based therapy to be feasible and effective in a clinical setting, the development of a convenient and efficient gene delivery system is mandatory. Although viral vectors offer the highest transfection rates, they present significant drawbacks such as the given antigenicity, potential oncogenic effects, and possible virus recombination [3]. Alternatively, synthetic vectors can be produced in a fast, easy, and tailored way, present lack of immune response, are biocompatible, and have unlimited genome carrying capacity, being considered incredible platforms for the controlled intracellular delivery of genetic cargos [4, 5]. Additionally, nonviral carriers can be chemically or physically engineered

Ângela Sousa (ed.), *DNA Vaccines: Methods and Protocols*, Methods in Molecular Biology, vol. 2197,
https://doi.org/10.1007/978-1-0716-0872-2_15,

and/or functionalized for specific cell targeting or cell recognition enhancing in vitro gene transfection process [6, 7]. Polyplexes, formed by the electrostatic interaction between a polycation and an oligonucleotide-based compound, are a class of nonviral vectors widely used for gene delivery applications [8–10]. PEI contains primary, secondary, and tertiary amine groups, which contribute to its high positive charge at physiological pH. As PEI can change its ionization degree with pH, it exhibits an impressive endosomolytic activity. In particular, the potentialities of PEI polymer have been explored in the conception of DNA-based complexes to be applied in a variety of biotechnological applications [8, 11, 12]. The high cationic charge density of PEI promotes its strong electrostatic interaction with the negatively charged phosphate groups of DNA molecule. From a simple experimental protocol of addition of PEI to pDNA, particles at the nanoscale and exhibiting appropriate characteristics concerning morphology, size, and surface charge can be formulated [8, 13, 14]. The properties of PEI, namely the molecular weight, the chain architecture, or the degree of branching are relevant parameters in determining the physico-chemical behavior of DNA-PEI polyplexes, as well as their transfection efficiency and cytotoxicity [13, 15, 16]. The high cationic charge density of PEI confers it significant cytotoxicity, which can limit its application. To overcome this drawback, PEI has been conjugated to a variety of ligands, aiming not only to reduce its cytotoxicity but also to improve its transfection ability [17, 18]. The characteristics exhibited by PEI/pDNA complexes can deeply be tailored by the nitrogen to phosphate groups ratio, defined at nanoparticle formulation step [8, 14]. A higher N/P ratio leads to a strong polymer amine density that can condense pDNA molecule more efficiently and confers to form nanosystems with a higher positive charge [14]. Vectors displaying positive surface charges strongly enable the interaction with the negatively charged proteoglycans present in the cellular membrane, which facilitates their entry into the cell [19, 20]. This process is then followed by vector transportation, possibly mediated by an endocytosis mechanism, into the organelle of interest. Experimental techniques such as scanning electron microscopy (SEM), dynamic light scattering (DLS), Fourier-transform infrared spectroscopy (FTIR), and electrophoretic mobility allow for a deep characterization of formulated PEI/pDNA polyplexes.

The methodology of PEI/pDNA-based vectors formulation is fully described in this chapter, along with the several experimental procedures for a convenient characterization of complexes properties. Furthermore, confocal microscopy experiments demonstrate cellular uptake, intracellular trafficking, and nucleus localization of the delivery systems.

2 Materials

All solutions should be prepared using deionized ultrapure-grade water and analytical-grade reagents, unless indicated otherwise.

2.1 PEI/pDNA Complexes

1. 6.07 kbp plasmid pcDNA3-FLAG, endotoxin-free at a concentration of 10 μg/mL.
2. PEI solution: 10% PEI in water (w/v), pH 7.9. Weigh 10 g of branched PEI (molecular weight of 25 kDa) and dissolve in 50 mL of H_2O. Adjust pH to 7.9 with concentrated HCL and add water to a volume of 100 mL. Filter the PEI solution through a 0.22 μm nitrocellulose filter. Store the solution at 4 °C (*see* **Note 1**).
3. Sodium acetate buffer (0.1 mM sodium acetate/0.1 M acetic acid, pH 4.5).
4. Centrifuge.
5. Vortex.
6. UV/visible NanoPhotometer.
7. Tungsten (*see* **Note 2**).
8. Sputter coater.
9. Scanning electron microscope.
10. Zetasizer nano ZS.

2.2 Agarose Gel Electrophoresis

1. TAE buffer 1×: 40 mM Tris base, 20 mM acetic acid, and 1 mM EDTA, pH 8.0 (*see* **Note 3**).
2. Agarose gel: 1% agarose, 40 mL TAE 1×, and 1 μg/mL GreenSafe Premium. Fill a graduated cylinder with 40 mL of TAE 1×, pour the solution into a small glass bottle, mix 0.4 g of agarose, heat until complete dissolution of agarose, and then add 40 μL of GreenSafe (*see* **Note 4**).
3. Horizontal electrophoretic system.
4. Loading buffer: 0.25% bromophenol blue and 30% glycerol (*see* **Note 5**). Weigh 25 mg of bromophenol blue, measure 3 mL of glycerol in a graduated flask, and complete 10 mL with water.
5. Molecular weight DNA standard (*see* **Note 6**).
6. Electrophoresis chamber.
7. Gel casting trays and combs.
8. UV transilluminator.

2.3 Fourier-Transform Infrared Spectroscopy

1. Nicolet iS10 FTIR spectrophotometer equipped with a deuterated triglycine sulfate detector (DTGS/KBr) (*see* **Note 7**).

2.4 Confocal Microscopy

1. Dulbecco's modified Eagle's medium with high glucose (DMEM-HG), supplemented with 10% heat-inactivated fetal bovine serum (FBS), 0.5 g/L sodium bicarbonate, 1.10 g/L HEPES, and 100 μg/mL of streptomycin-penicillin (*see* **Note 8**).
2. Cancer HeLa cells.
3. Cells were grown in DMEM-HG, at 37 °C, in a humidified atmosphere with 5% CO_2.
4. Phosphate-buffered saline (PBS) 10×: 1.37 M NaCl, 27 mM KCl, 100 mM Na_2HPO_4, and 20 mM KH_2PO_4, pH 7.4 (*see* **Note 9**).
5. Fluorescein isothiocyanate (FITC) (*see* **Note 10**).
6. For pDNA staining, 75 μL of labeling buffer (0.1 M sodium tetraborate, pH 8.5) and 2 μL of FITC (in sterile anhydrous dimethyl sulfoxide, 500 mg/mL) were considered. 3 M NaCl (85 μL) and 2.5 volumes of 100% ethanol (212.5 μL).
7. μ-Slide with eight wells.
8. DAPI (diamidino-2-phenylindole) fluorescent dye (*see* **Note 11**).
9. LSM 710 confocal laser scanning microscope and laser scanning confocal microscope.

3 Methods

3.1 Formation of PEI/pDNA Vectors

1. Prepare PEI and pDNA stock solutions in sodium acetate buffer (0.1 mM sodium acetate/0.1 M acetic acid, pH 4.5).
2. Prepare PEI-pDNA complexes at various nitrogen/phosphate (N/P) ratios, considering the mass per charge ratio of DNA and PEI and the pK_a value of the polymer (*see* **Note 12**).
3. To prepare vectors at a certain N/P ratio, add the correspondent amount of PEI (100 μL) to a fixed volume of pDNA (400 μL), vortex mixed for 15 s and left for equilibration for 30 min at 4 °C before use (*see* **Note 13**).
4. Centrifuge the formed polyplexes at 10,000 × *g* for 15 min and recover the pellet that contains the pDNA-based nanoparticles.
5. Determine the amount of non-bound pDNA by measuring spectrophotometrically the absorbance of the supernatant at 260 nm using a NanoPhotometer™.
6. Calculate the pDNA complexation capacity (CC) from the equation:

$$\mathrm{CC}\ (\%) = [(\text{total amount of pDNA} - \text{non} - \text{bound pDNA})/\text{total amount of pDNA}] \times 100 \quad (1)$$

3.2 Characterization of Developed Polyplexes

3.2.1 Nanoparticles Morphology

1. Information concerning the morphology of nanoparticles was obtained by SEM. Centrifuge the different formulations at 10,000 × *g*, for 15 min at 25 °C, recover the pellet, and suspend it in an aqueous solution containing 40 μL of tungsten.
2. Place the solution in round-shaped cover slip and dry overnight at room temperature.
3. Sputter coat the samples with gold by using a sputter coater (*see* **Note 14**).
4. Visualize the developed systems in a scanning electron microscope (accelerating voltage of 20 kV at various magnifications).

An example of morphology of developed PEI/pDNA delivery systems under SEM can be observed in Fig. 1.

3.2.2 pDNA Complexation

1. The pDNA binding ability of PEI/pDNA complexes can be monitored by agarose gel electrophoresis. The vectors were formed at various N/P ratios.

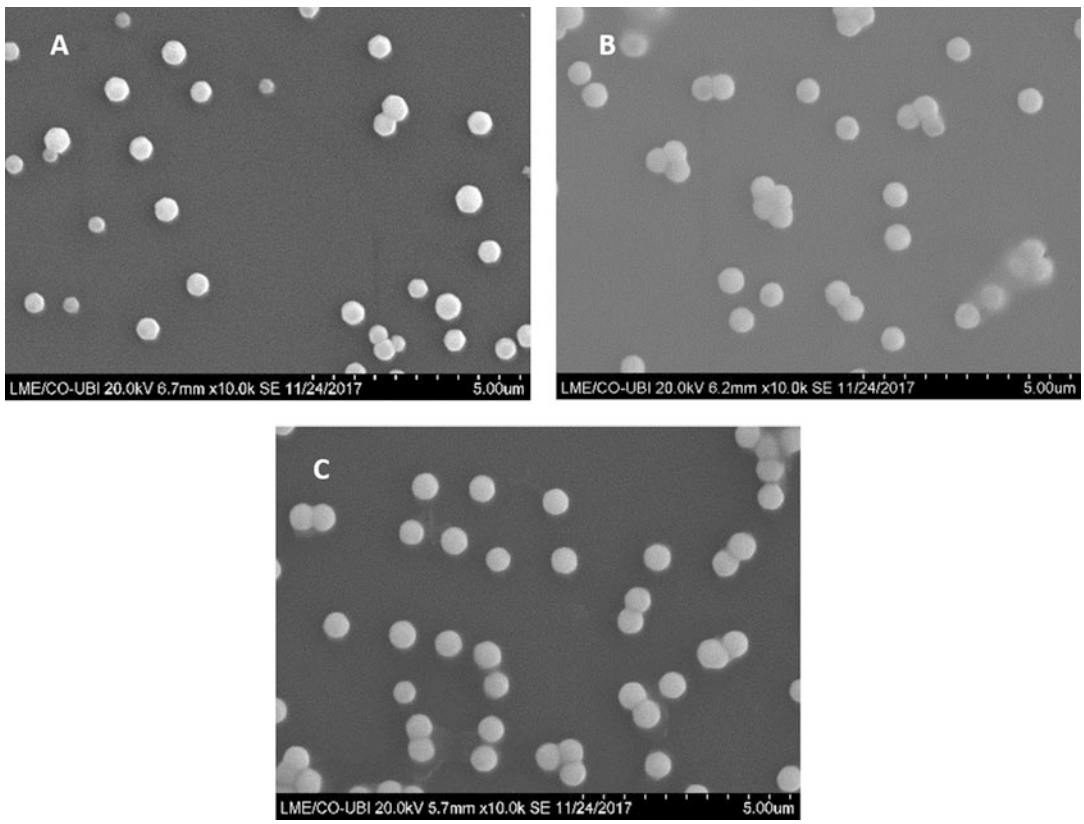

Fig. 1 Scanning electron micrographs of PEI/pDNA-based polyplexes formulated at N/P of 1.5 (**a**), N/P ratio of 2 (**b**), and N/P ratio of 5 (**c**)

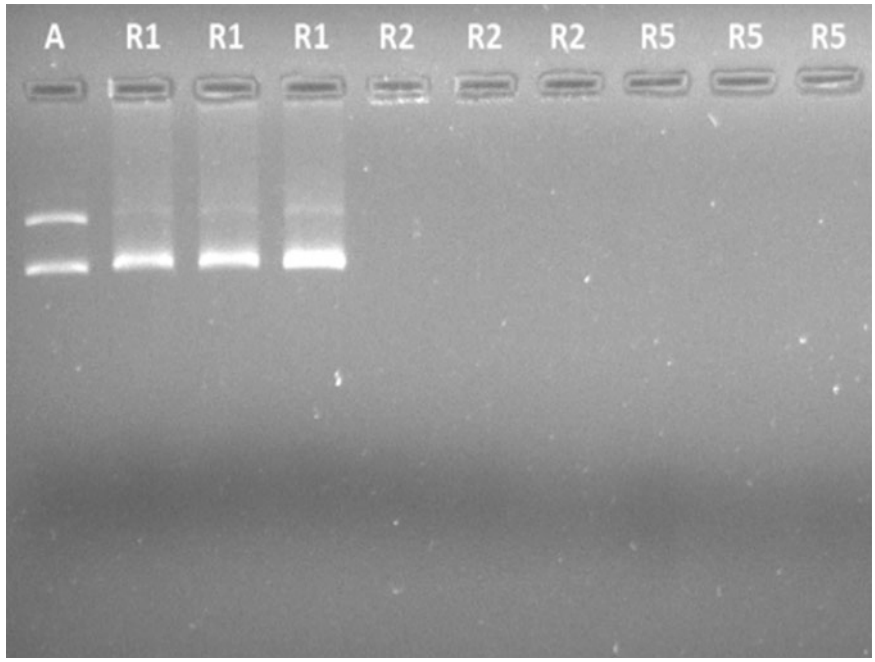

Fig. 2 Agarose gel electrophoresis for a set of 25 kDa PEI/pDNA polyplexes formulated at various N/P ratios (1, 2, and 5). A—Control pDNA sample. The samples were loaded at the application site at the upper end of the image and the lower end is the cathodic end

2. Measure out 1 g of agarose in 40 mL of TAE buffer 1× stained with 1 μg/mL of GreenSafe in a horizontal electrophoresis gel support and insert a well-forming comb (*see* **Note 15**).
3. Wait for 20–30 min to let it polymerize (until to become opaque). Carefully remove the comb and put the gel in the electrophoresis tank, with the sample wells oriented to the negative electrode, with enough TAE buffer 1× to submerge the gel.
4. Prepare 20 μL of each sample with 5 μL of loading buffer and load 20 μL of one sample to each well, as well as 5 μL of molecular weight standard to one lane of the gel.
5. Connect the electrophoresis apparatus to the power supply and perform electrophoresis at 100 V, for approximately 30 min.
6. Put the gel in a transilluminator and visualize with the ultraviolet system (Fig. 2) (*see* **Note 16**).

3.2.3 FTIR

1. Before spectrum acquisition, all the PEI/pDNA systems should be lyophilized (*see* **Note 17**).
2. Prepare KBr pellets. Mix 1% of the sample with 250 mg KBr powder and then finely pulverize and place into a pellet-forming die. A force of around 8 tons is applied under vacuum for 10 min, to form transparent pellets (*see* **Note 18**). Eliminate air by degassing.

3. Before forming the KBr powder into pellets, pulverize it to 200 mesh maximum and then dry at approximately 110 °C for 2 h. After, drying the powder, store it in a desiccator.
4. Acquire the spectra by using a FTIR spectrophotometer and consider an average of 120 scans, a spectral width ranging from 4000 and 525 cm^{-1} and a spectral resolution of 4 cm^{-1}.
5. For comparative purposes, also acquire the spectra from PEI and pDNA.

The FTIR spectrum of PEI/pDNA-based nanoparticles is shown in Fig. 3 and illustrates the formation of polyplexes.

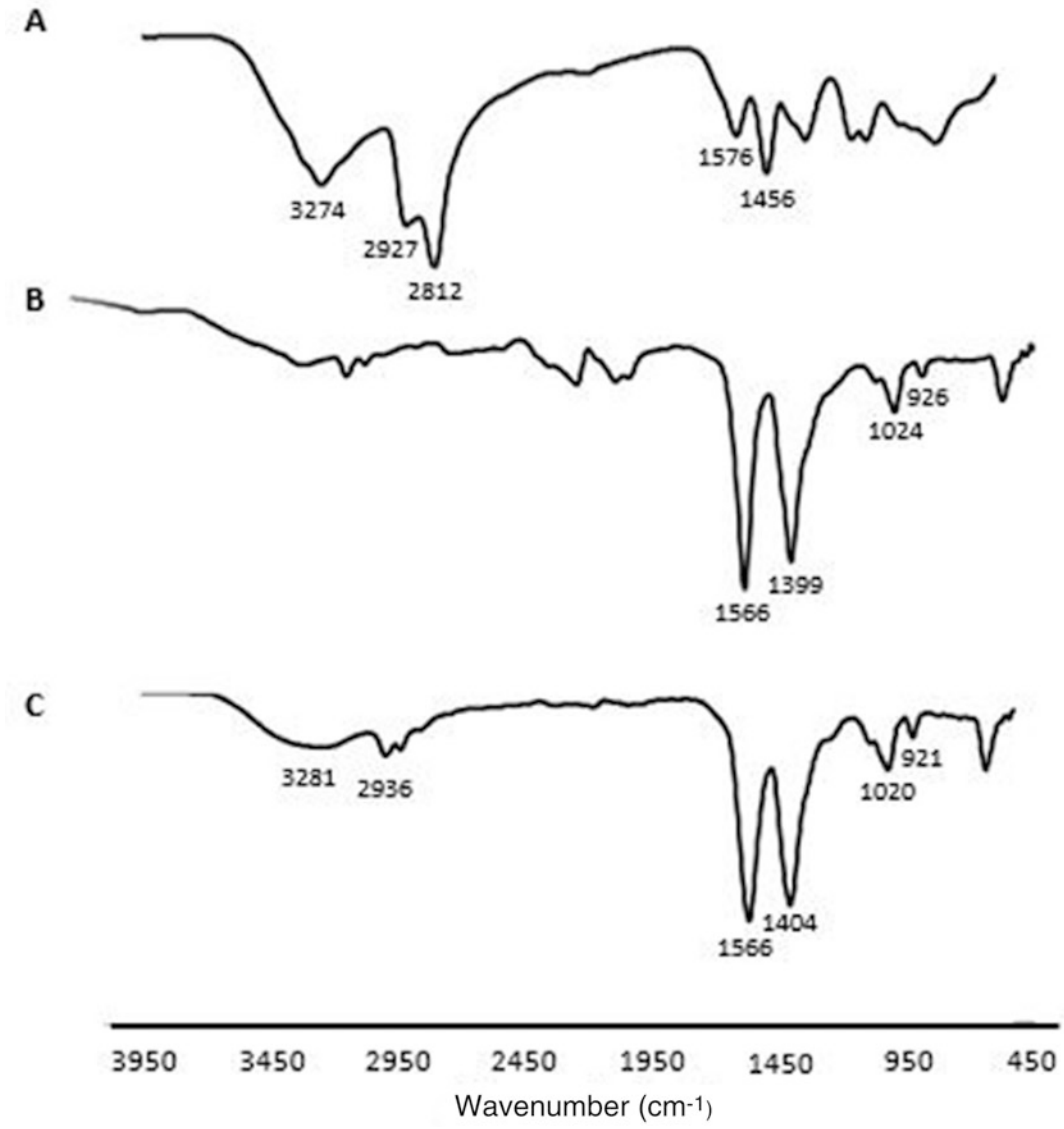

Fig. 3 FTIR spectra (transmittance versus wavenumber) of PEI (**a**), pDNA (**b**), and PEI/pDNA (**c**) based nanoparticles formulated at N/P ratio of 5

3.2.4 Size and Surface Charges

1. Determine the average particle size and the zeta potential of nanoparticles by DLS (*see* **Note 19**). Use a Zetasizer nano ZS equipped with a He-Ne laser.
2. Prepare the complexes at desired N/P ratios. Measure the particle diameters at 25 °C, with 173° scattering angle in fully automatic mode.
3. Determine the surface charges (zeta potential) of the prepared nanoparticles in disposable capillary cells and computed by using Henry's [F(Ka)1.5], and Smoluchowski models, at 25 °C (*see* **Note 19**).

3.3 Cellular Uptake and Internalization

3.3.1 FITC pDNA Labeling

1. Stain pDNA with FITC by assembly 8 μL of pDNA, 75 μL of labeling buffer (0.1 M sodium tetraborate, pH 8.5) and 2 μL of FITC (in sterile anhydrous dimethyl sulfoxide, 500 mg/mL).
2. Place the samples under constant stirring for 4 h at room temperature and protected them from light (*see* **Note 20**).
3. Add one volume of 3 M NaCl (85 μL) and 2.5 volumes of 100% ethanol (212.5 μL).
4. Incubate samples containing stained pDNA at −20 °C overnight.
5. Centrifuge the samples at 4 °C for 30 min, recover the pellet, and wash it with 75% ethanol.

3.3.2 Confocal Fluorescence Microscopy

1. Incubate cancer HeLa cells at 37 °C in a humidified atmosphere containing 5% CO_2 and maintained in Dulbecco's modified Eagle's medium with high glucose (DMEM-HG) supplemented with 10% heat inactivated FBS, 0.5 g/L sodium bicarbonate, 1.10 g/L HEPES, and 100 μg/mL of streptomycin-penicillin.
2. Grow HeLa cells in μ-slide with eight wells until 50–60% confluence is achieved.
3. To stain the nucleus, incubate the cells with 1 μM DAPI for 10 min (*see* **Note 21**).
4. Prepare the PEI nanoparticles using FITC-labeled pDNA.
5. Visualize real live transfection using a confocal laser scanning microscope under a 63× magnification and analyze with a laser scanning confocal microscope.
6. During the experiment, keep HeLa cells at 37 °C with 5% CO_2 (*see* **Note 22**).

The PEI/pDNA vectors transfection ability and intracellular co-localization in HeLa cells has been monitored by fluorescence confocal microscopy. Figure 4 shows a live-cell image of cancer cells 2 h after transfection mediated by PEI/pDNA and demonstrates the capacity of the developed complexes for cellular uptake and internalization with nucleus co-localization.

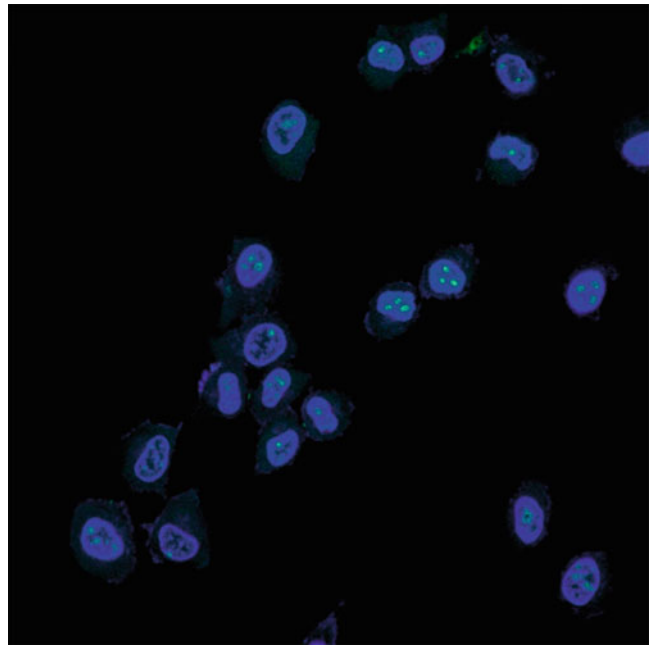

Fig. 4 Live-cell image of HeLa cells 2 h after transfection mediated by PEI/pDNA-based nanoparticles formulated at N/P ratio of 5. Scale bar = 5 μM

4 Notes

1. The working PEI solution should be stored at 4 °C in order to be stable for a long period of time.
2. The preparation of samples to be observed at scanning electron microscope must include procedures to increase their electrical conductivity. Non-conducting materials are generally coated with an electrically conducting material, such as, tungsten.
3. TAE buffer is prepared as a stock solution 50× concentrated (2 M Tris base, 1 M acetic acid, and 50 mM EDTA, pH 8.0). Mix 242.2 g of Tris base, 57.19 mL of acetic acid, and 17.91 g EDTA in a glass flask containing 800 mL of water. To dissolve EDTA faster, water should be warmed to 37 °C. However, before adjusting the pH, the solution should be cooled at room temperature. After the pH adjustment, the volume of 1 L should be completed with water, in a volumetric flask. Finally, to prepare 1 L of TAE 1× dilute 20 mL of TAE 50× with 980 mL of water.
4. GreenSafe is a nucleic acid stain that can be used as a safer alternative to traditional ethidium bromide for detecting DNA or RNA in agarose gels. It is sensitive as ethidium bromide and emits green fluorescence when bound to nucleic acids. It has two secondary fluorescence peaks (≈270 and ≈290 nm) and one strong excitation peak at 490 nm.

5. Bromophenol blue is a loading dye that allows controlling the migration front line, and glycerol makes the sample dense enough to sink to the bottom of the sample well.
6. The molecular weight DNA standard is composed of DNA fragments with known and different sizes that will be distributed throughout the electrophoresis gel according to the respective size. Normally, the standard is chosen with a similar size range to the molecules under study in order to identify the target DNA.
7. Infrared spectroscopy incorporates several types of methods to perform the measurements, such as the diffuse reflection method and attenuated total reflection method. When considering powder samples, two options arise: the KBr pellet method and the Nujol method. The KBr pellet method explores the property that alkali halides become plastic when subjected to pressure and turn themselves transparent in the infrared region. Potassium bromide (KBr) is the most common alkali halide used in the pellets.
8. To culture and grow cells, an adequate culture media should be used. Most cells, as cancer HeLa cells, can be grown on DMEM or RPMI culture media, with 10% FBS, glutamine, and antibiotics. Check which culture media and culture supplements the cell line you are using requires before starting cultures. Culture media and supplements should always be sterile. Purchase sterile reagents when possible, only use under aseptic conditions in a culture hood to ensure they remain sterile.
9. Concentrated HCl can be used first to reduce the gap from the starting pH to the required pH. Thereafter, it would be better to use a series of diluted HCl solutions with lower ionic strengths to prevent a sudden drop in pH below the required pH.
10. FITC is the most widely used fluorescent probe for the preparation of conjugates with biological molecules. pDNA can easily be labeling with FITC, emitting green fluorescence. This FITC stain tool is very useful to monitor the biological activity of pDNA in confocal microscopy experiments.
11. DAPI is a blue fluorescent probe that fluoresces brightly upon selectively binding to the minor groove of double-stranded DNA, where its fluorescence is approximately 20-fold greater than in the nonbound state. It exhibits a high selectivity for DNA, which along with its significant cell permeability allows efficient staining of nuclei with little cytoplasm background. DAPI is effective for fixed-cell staining and quantitation of DNA content, and it is ideal for use alongside detection of specific targets with fluorescent antibodies for fluorescence microscopy or high-content screening (HCS).

12. PEI-pDNA complexes were prepared at various nitrogen/phosphate (N/P) ratios, considering the mass per charge ratio of DNA (330 g/mol, relative to one phosphate group) and PEI (44 g/mol, correspondent to one amine group), and the pK_a value of the polymer. The calculation of the N/P ratio for the PEI/DNA formulations is defined as the molar relation of amine groups in the PEI molecule which represent the positive charges, to phosphate groups in the DNA, which represent the negative charges. Note that for this calculation, only primary amines have been considered, as both secondary and tertiary amines exhibit very low pK_a values.
13. For the formation of PEI/DNA complexes at various N/P ratios, the following considerations and calculations were made:
    For DNA, 330 g/mol corresponds to one phosphate atom.
    1 μg × 330 g/1 μg = 1 mol phosphate.
    1 μg DNA = 1 mol phosphate × 10^{-6}/330.
    1 μg DNA = 3.03 × 10^{-9} mol phosphate.
    For PEI, the number of *N* atom in 25 kDa of PEI = 25,000/43.1 = 580.0464 ≈ 580.05.
    If the researcher, for instance, intends to prepare nanoparticles at *N/P* ratio of 5, it must be considered $N = 5 \times P$ and $N = 5 \times 30.3 \times 10^{-9} = 151.5 \times 10^{-9}$.
    To determine the number of moles of PEI correspondent:
    151.5 × 10^{-9}/580.05 = 0.26 × 10^{-9} mol of PEI, and the respective mass can be determined by multiplying the number of moles to 25,000 g/mol.
14. The sputter coating sample preparation technique can be used to improve image quality and resolution. Due to its high conductivity, gold coating strategy can increase the signal-to-noise ratio during SEM imaging and therefore produce better quality images. Sputtered films for SEM typically have a thickness range of 2–20 nm.
15. Agarose gel concentration defines the size of three-dimensional pores formed after agarose polymerization. For the well resolution of nucleic acids ranging in size from 1000 to 10,000 kbp, 1% agarose is recommended. The nucleic acids move toward the positive pole (anode) of the electrophoresis apparatus according to the negative charge of the phosphate residues in the molecule backbone, size, and conformation.
16. UV transilluminators are used in molecular biology labs to visualize DNA (or RNA) that has been separated by electrophoresis through an agarose gel. During or immediately after electrophoresis, the agarose gel is stained with a fluorescent dye which binds to nucleic acid. Exposing the stained gel to a UV

light source causes the DNA/dye to fluoresce and become visible. This technique is used to easily and quickly visualize the DNA- or RNA-based sample, for example, sizing a PCR product, purifying DNA segment after a restriction enzyme digest, quantifying DNA, or verifying RNA integrity after extraction.

17. FTIR spectra can be used to identify a wide range of compounds by comparing the measured spectra to spectral databases. For proteins, FTIR spectra from wavenumbers 1700–1500 cm^{-1} can be used to determine structural properties. Measuring protein absorbance over these wavenumbers gives two absorption bands, conventionally called Amide I and Amide II and lying between wavenumbers 1700–1600 and 1600–1500 cm^{-1}, respectively. The Amide I band is due to C=O stretching vibrations of the peptide bonds, which are modulated by the secondary structure (α-helix, β-sheet, etc.). Water can interfere with FTIR measurements of protein samples, because it strongly absorbs in the Amide I region. Consequently, FTIR is best suited for lyophilized (freeze-dried) protein samples.
18. To prepare a KBr pellet, follow the guidelines:
    (a) The powder sample and KBr must be ground to reduce the particle size to less than 5 mm in diameter. Otherwise, large particles scatter the infrared beam and cause a slope baseline of spectrum.
    (b) Add a spatula full of KBr into an agate mortar and grind it to fine powder until crystallites can no longer be seen, and it becomes somewhat "pasty" and sticks to the mortar.
    (c) Take a small amount of powder sample (about of 0.1–2% of the KBr amount) and mix with the KBr powder. Subsequently grind the mixture for 3–5 min.
    (d) Assemble the die-set as shown in the drawing. When assembling the die, please add the powder to a 7 mm collar. Press the powder for 2 min to form a pellet. A good KBr pellet is thin and transparent.
    (e) Disassemble the die set and take out the 7 mm collar. Put the collar together with the pellet onto the sample holder.
19. DLS sometimes referred to as Quasi Elastic Light Scattering (QELS) is a well-established technique for measuring the size and size distribution of molecules and particles typically in the submicron region, and lower than 1 nm. DLS allows for the characterization of particles, emulsions, or molecules which have been dispersed or dissolved in a liquid. The Brownian motion of particles or molecules in suspension causes laser light to be scattered at different intensities. Analysis of these intensity fluctuations yields the velocity of the Brownian

motion and hence the particle size using the Stokes–Einstein relationship. Zeta potential is the charge on a particle at the shear plane. This value of surface charge is useful for understanding and predicting interactions between particles in suspension. Manipulating zeta potential is a method of enhancing suspension stability for formulation work. Electrophoretic light scattering exploits the fact that a charged particle responds to an applied electric field. The particle motion due to the applied electric field is measured by light scattering. The particles are illuminated with laser light and therefore the particles scatter light. The frequency of the scattered light is a function of particle velocity due to the Doppler shift. A second beam of light (the reference beam) is mixed with the scattered beam in order to sensitively extract the frequency shift in the scattered light. From the known applied electric field and measured particle velocity, the particle mobility is readily determined. Zeta potential is then calculated from mobility by using a model, frequently the Smoluchowski model. The parameters required for determining zeta potential are liquid dielectric constant, refractive index, and viscosity. This makes the technique rapid and reliable.

20. To ensure FITC fluorescence levels, samples should be stored in the dark.
21. A DAPI stock solution should be prepared. Add 2 mL of deionized water (diH_2O) or dimethylformamide (DMF) to the entire contents of the DAPI vial to make a 14.3 mM (5 mg/mL) DAPI stock solution. DAPI has poor solubility in water, so sonicate as necessary to dissolve. The 5 mg/mL DAPI stock solution may be stored at 2–6 °C for up to 6 months or at ≤ -20 °C for longer periods. Add 2.1 μL of the 14.3 mM DAPI stock solution to 100 μL PBS to make a 300 μM DAPI intermediate dilution. Dilute the 300 μM DAPI intermediate dilution 1:1000 in PBS as needed to make the appropriate concentrated DAPI stain solution.
22. Live-cell imaging has become a requisite analytical tool in most cell biology laboratories, as well as a routine methodology that is practiced in the wide ranging fields of biomedical research. Among the most significant technical challenges for performing successful live-cell imaging experiments is to maintain the cells in a healthy state and functioning normally on the microscope stage while being illuminated in the presence of synthetic fluorophores. Tight control of the environment is one of the most critical factors in successful live-cell imaging experiments. The conditions under which cells are maintained on the microscope often dictate the success of a particular experiment. Aspects of the environment that are readily manipulated include the physical parameters of the chamber

in which the cells are grown and imaged, the localized degree of temperature control, atmospheric conditions (gas mixture and humidity), nutritional supplements, growth medium buffering (pH), and osmolarity of the culture medium. For most cell lines, conditions of temperature and humidity should be 37 °C and 5% CO_2.

References

1. Sun W, Shi Q, Zhang H et al (2019) Advances in the techniques and methodologies of cancer gene therapy. Disc Med 146:45–55
2. McCrudden CM, McBride JW, McCaffrey J et al (2018) Gene therapy with RALA/iNOS composite nanoparticles significantly enhances survival in a model of metastatic prostate cancer. Cancer Nano 9:5
3. Hinderer C, Katz N, Buza EL et al (2018) Severe toxicity in nonhuman primates and piglets following high-dose intravenous administration of an AVV vector expressing human SMN. Hum Gene Ther 29:285–298
4. Rey-Rico A, Cucchiarini M (2019) Supramolecular cyclodextrin-based hydrogels for controlled gene delivery. Polymers 11:514–523
5. Costa D, Albuquerque T, Queiroz JA et al (2019) A co-delivery platform based on plasmid DNA peptide-surfactant complexes: formation, characterization and release behaviour. Colloids Surf B Biointerfaces 178:430–438
6. Coutinho E, Batista C, Sousa F et al (2017) Mitochondrial gene therapy: advances in mitochondrial gene cloning, plasmid production and nanosystems targeted to mitochondria. Mol Pharm 14:626–638
7. Du B, Gu X, Han X et al (2017) Lipid-coated gold nanoparticles functionalized by folic acid as gene vectors for targeted gene delivery in vitro and in vivo. ChemMedChem 12:1768–1775
8. Costa D, Briscoe WH, Queiroz JA (2015) Polyethylenimine coated plasmid DNA-surfactant complexes as potential gene delivery systems. Colloids Surf B Biointerfaces 133:156–163
9. Temprana CF, Prieto MJ, Igartúa DE et al (2017) Diacetylenic lipids in the design of stable lipopolymers able to complex and protect plasmid DNA. PLoS One 12:e0186194
10. Chang H, Zhang J, Wang H et al (2017) A combination of guanidyl and phenyl groups on a dendrimer enables efficient siRNA and DNA delivery. Biomacromolecules 18:2371–2378
11. Zhang Y, Liu L, Lin L et al (2017) In-situ dual-crosslinked nanoparticles for tumor targeting gene delivery. Acta Biomater 65:349–362
12. Appelbe OK, Kim BK, Rymut N et al (2018) Radiation-enhanced delivery of plasmid DNA to tumors utilizing a novel PEI polyplex. Cancer Gene Ther 25:196–206
13. Dai Z, Wu C (2012) How does DNA complex with polyethylenimine with different chain lengths and topologies in their aqueous solution mixtures? Macromolecules 45:4346–4353
14. Costa D, Valente AJM, Queiroz JA et al (2018) Finding the ideal polyethylenimine-plasmid DNA system for co-delivery of payloads in cancer therapy. Colloids Surf B Biointerfaces 170:627–636
15. Tay CY, Menon N, Leong DT et al (2015) Molecular architecture governs cytotoxicity and gene transfection efficacy of polyethylenimine based nanoplexes in mammalian cell lines. J Inorg Organomet Polym 25:30–311
16. Utsuno K, Kono H, Tanaka E et al (2016) Low molecular weight branched PEI binding to linear DNA. Chem Pharm Bull 64:1484–1491
17. Nam JP, Nah JW (2016) Target gene delivery from targeting ligand conjugated chitosan-PEI copolymer for cancer therapy. Carbohydr Polym 135:153–161
18. Sousa A, Faria R, Albuquerque T et al (2020) Design of experiments to select triphenylphosphonium-polyplexes with suitable physicochemical properties for mitochondrial gene therapy. J Mol Liq 302:112488. https://doi.org/10.1016/j.molliq.2020.112488
19. Salatin S, Maleki Dizaj S, Yari A (2015) Effect of the surface modification, size and shape on cellular uptake of nanoparticles. Cell Biol Int 39:881–890
20. Liu X, Wu F, Tian Y et al (2016) Size dependent cellular uptake of rod-like bionanoparticles with different aspect ratios. Sci Rep 6:24567

Chapter 16

Main Features of DNA-Based Vectors for Use in Lactic Acid Bacteria and Update Protocols

Nina D. Coelho-Rocha, Fernanda A. L. Barroso, Laísa M. Tavares, Ester S. S. dos Santos, Vasco Azevedo, Mariana M. Drumond, and Pamela Mancha-Agresti

Abstract

DNA vaccines have been used as a promising strategy for delivery of immunogenic and immunomodulatory molecules into the host cells. Although, there are some obstacles involving the capability of the plasmid vector to reach the cell nucleus in great number to promote the expected benefits. In order to improve the delivery and, consequently, increase the expression levels of the target proteins carried by DNA vaccines, alternative methodologies have been explored, including the use of non-pathogenic bacteria as delivery vectors to carry, deliver, and protect the DNA from degradation, enhancing plasmid expression.

Key words DNA vaccines, Delivery vectors, Lactic acid bacteria (LAB), *Lactococcus lactis* sp., Mucosal delivery

1 Introduction

DNA vaccines are the most recent platform of vaccination, and it is an interesting alternative for antigen presentation to immune system. The standard DNA vaccine delivered by bacteria consists in a plasmid formed by two regions: a prokaryotic propagation region and an eukaryotic expression region, responsible for encoding one or more vaccine antigen [1].

The prokaryotic propagation region consists in an origin of bacterial replication, which allows the propagation and amplification of plasmids into bacteria, and a selection marker responsible for the plasmid stability and maintenance into bacterial cell. The selection markers are usually an antibiotic resistance gene, food-grade selection markers like an auxotrophic complementation gene or markers which confer immunity to bacteriocin, resistance to heavy metals, etc. [1, 2]. The eukaryotic expression region, in counterpoint, contains the transcription unit composed of a

Ângela Sousa (ed.), *DNA Vaccines: Methods and Protocols*, Methods in Molecular Biology, vol. 2197,
https://doi.org/10.1007/978-1-0716-0872-2_16,

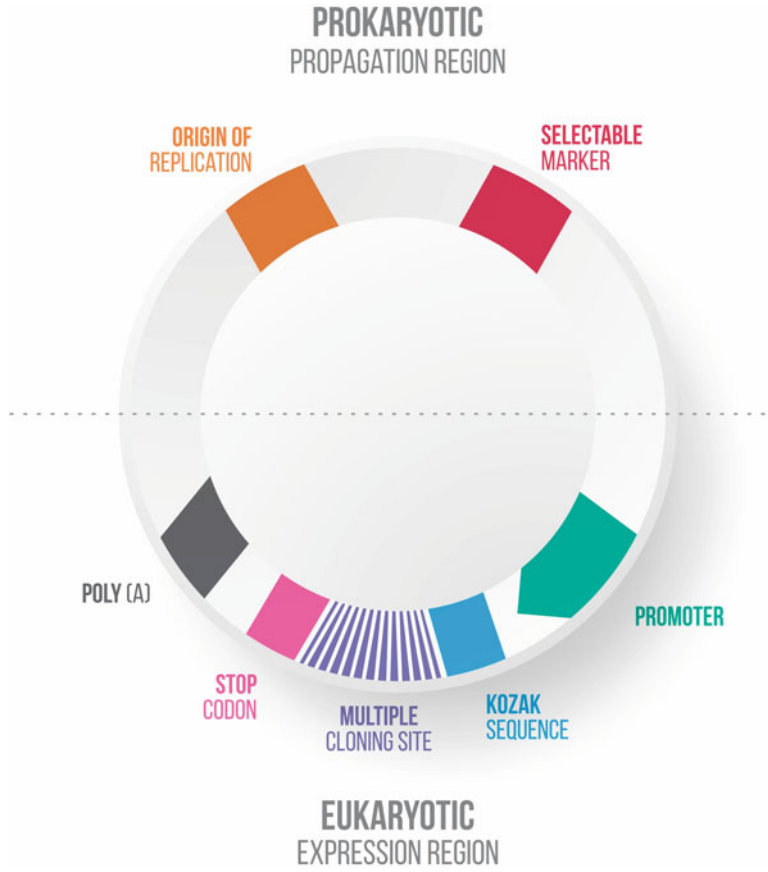

Fig. 1 Plasmid DNA vaccine schematic representation: at the top of the figure is represented the prokaryotic propagation region, which is responsible for the propagation and maintenance of the vaccinal plasmid in the bacterial cell. This region contains a prokaryotic origin of replication and a selection marker. At the bottom of the figure is the eukaryotic expression region which is composed of the promoter, the Kozak sequence, the multiple cloning site (MCS), the stop codon, and the polyadenylation signal sequence (poly-A tail)

promoter, usually a constitutive viral promoter that gives a high level of protein expression in eukaryotic cells, the transgene of interest, and a specific consensus sequences like Kozak sequence, stop codon, and the Poly (A) tail for post-transcriptional processing [3] (Fig. 1).

There are many methods by which DNA vaccines can be administrated, such as intramuscular [4], epidermic delivery by biobalistic [5], and electroporation [6]. Although, the biggest challenge is to deliver high amounts of DNA to stimulate immune responses, avoiding its degradation inside the host organism [7]. Thus, a potential way of administration, recommended by World Health Organization (WHO), is the mucosa surface, for being economically viable and secure. The mucosal way can be accessed basically

by intranasal or oral administration, promoting both systemic and mucosa immune responses [8]. The oral way maybe the most advantageous, once the gastrointestinal tract (GIT) houses the largest number of immune cells, being the most dynamic immunological site [9]. This region can be reached by many bacterial strains, thus, in the context of DNA vaccines, transforming bacteria with DNA plasmids could be a promising tool to optimize the delivery of immunogenic and immunomodulatory molecules [10].

About four decades ago, it was demonstrated, for the first time, in in vitro test, that DNA can be transferred from bacteria into eukaryotic cells [11]. Since then, several studies have been conducted using attenuated intracellular pathogens such as *Listeria*, *Salmonella*, and *Shigella* for such purpose [12–14]. Nevertheless, a major safety concern regarding the use of attenuated pathogens is the residual risk associated with the possibility of reversion to pathogenic phenotype form [15]. Consequently, considering this risk, the use of non-pathogenic bacteria, such as the lactic acid bacteria (LAB) group, is an attractive alternative for use as mucosal vaccine carriers [16].

The LAB group has been used for centuries by human for food preservation and fermentation, and so, most of these microorganisms have the GRAS (Generally Recognized as Safe) status and consequently are safe for consume [17]. Beyond this safety, some LAB strains can also exert health benefits to the host when administered in adequate amounts, been referred as probiotics [18, 19].

LAB strains have some key features which allows their use as a promising delivery vector for DNA vaccines, such as resistance to the adversities of the gastrointestinal tract, being able to reach the intestine in relatively high amounts, absence of lipopolysaccharides (LPS) in their membrane, eliminating the risk of endotoxin shock and low immunogenicity, being tolerable to the organism [20]. Concerning the LAB group, *Lactococcus lactis* is considered the model microorganism, being the most studied and well characterized [21]. Although these bacteria are generally recognized to be incapable of invading eukaryotic cells, Guimarães et al. (2006) showed that the co-incubation of Caco-2 cells with *L. lactis* MG1363 strain, harboring an expression cassette encoding bovine β-lactoglobulin (BLG) cDNA under the transcriptional control of the human cytomegalovirus eukaryotic promoter (Pcmv), results in the transfer of the plasmid and expression of the BLG protein into these cells [22]. In vivo studies also verified the presence of BLG protein in mice enterocytes [23].

Nowadays, some groups are involved in the development of DNA vaccine vectors using *L. lactis* and other LABs as delivery vehicles, such as pValac [24, 25], pLKV1 [26], pExu [27, 28], and pPERDBY [29, 30].

Thus, the present chapter will describe some techniques required to transform plasmid DNA, codifying sequences of interest, into LAB bacteria, more specifically, *Lactococcus lactis* sp., and techniques to analyze and confirm the protein expression by eukaryotic cells.

2 Materials

2.1 Confection and Test of Escherichia coli (E. coli) Electrocompetent Cells (See Note 1)

1. Culture stock of *E. coli* cells.
2. 50 mL tubes.
3. Erlenmeyer.
4. Luria-Bertani (LB) broth: 5 g/L yeast extract, 10 g/L sodium chloride, and 10 g/L casein enzymatic hydrolysate in distilled water (*see* **Note 2**). Store at 4 °C.
5. Orbital shaker, 37 °C.
6. Spectrophotometer.
7. Refrigerated centrifuge.
8. 10% glycerol: 100 mL/L glycerin in distilled water (*see* **Note 2**). Store at 4 °C.
9. 200 μL microtubes.
10. −80 °C ultra-freezer.

2.1.1 Efficiency Test of Electrocompetent E. coli Cells (See Note 1)

1. Plasmid DNA used for test (usually a high copy number plasmid, 100 ng approximately).
2. Electrocompetent *E. coli* cells.
3. Pulser cuvette (0.1 cm electrode gap).
4. Electroporator.
5. LB broth.
6. 1.5 mL microtubes.
7. Water bath, 37 °C.
8. Incubator, 37 °C.
9. Petri dishes (25 mL).
10. LB agar: prepare LB broth as described in Subheading 2.1, **item 4**, and add 1.5% of bacteriological agar (*see* **Notes 2** and **3**).
11. Antibiotic or another character required for selection.

2.2 Transformation of E. coli Electrocompetent Cells (See Note 1)

The materials involved in this subheading are the same required for testing efficiency (Subheading 2.1.1), using the DNA plasmid of interest to proceed the tests.

2.3 Plasmid Extraction (Alkaline Lysis) (See Note 1)

1. LB broth.
2. Antibiotic (ATB) or another character required for selection.
3. Incubator, 37 °C.
4. 2 mL microtubes.
5. 80% glycerol: 80 mL glycerin; 20 mL of distilled water (*see* **Note 2**). Stored at 4 °C.
6. −80 °C ultra-freezer.
7. Microtube centrifuge.
8. Solution I: 1 mL of 50 mM sucrose, 0.25 mL 25 mM Tris–HCl (pH 8.0), 0.20 mL of 10 mM EDTA (pH 8.0) in 10 mL of distilled water (final volume).
9. Solution II: 0.2 mL of 5 M NaOH, 0.25 mL 1% SDS in 5 mL of distilled water (final volume) (*see* **Notes 4** and **5**).
10. Solution III: 30 mL of 5 M potassium acetate, 5.75 mL of acetic acid glacial in 50 mL of distilled water (final volume). Store at 4 °C.
11. RNAse.
12. 1.5 mL microtubes.
13. Isopropanol.
14. −20 °C freezer.
15. Ethanol 70%.
16. Incubator, 37 °C.
17. Ultrapure water.
18. 200 μL microtubes.
19. Electrophoresis equipment.
20. Spectrophotometer.

2.4 Clone Confirmation

2.4.1 Polymerase Chain Reaction (PCR)

1. Plasmid obtained in the DNA extraction.
2. Specific primers designed for amplification of the open reading frame (ORF) of interest.
3. 10× buffer (according to the manufacturer's specifications of the DNA polymerase).
4. 200 μM dNTPs (50 μM of each of the four nucleotides).
5. 5 mM Mg^{2+}.
6. 20–50 pmol of each primer.
7. DNA polymerase.
8. Ultrapure water.
9. Thermocycler.
10. Reagents and equipment for agarose gel electrophoresis.

2.4.2 Enzymatic Digestion

1. Plasmid obtained in the DNA extraction.
2. Buffer (according to manufacturer specifications of the restriction enzymes).
3. Restriction enzymes.
4. Ultrapure water.
5. Reagents and equipment for agarose gel electrophoresis.

2.4.3 Sequencing

1. Plasmid obtained in the DNA extraction.
2. Specific primers designed for amplification of the ORF of interest.
3. 5× buffer (according to manufacturer specifications of the DNA polymerase).
4. Big dye mix (contains dNTPs, ddNTPs, AmpliTaq DNA polymerase, $MgCl_2$, and Tris–HCl buffer).
5. 3.3 pmol of each primer.
6. Ultrapure water.
7. 96-Well PCR microplate.
8. Thermocycler.
9. Automated sequencer.

2.5 Plasmid Expression Confirmation

*2.5.1 Culture of Caco-2 Cells (See **Note 1**)*

1. Caco-2 cells cultures.
2. Liquid nitrogen.
3. Bovine serum albumin (BSA).
4. Dulbecco's modified Eagle's medium (DMEM) supplemented with 20% of fetal bovine serum.
5. 15 mL tubes.
6. Dimethyl sulfoxide (DMSO).
7. 15 mL centrifuge.
8. 75 cm^2 cell culture flask.
9. Incubator, 37 °C with 5% of CO_2.
10. 0.25% trypsin with 0.53 mM EDTA.

*2.5.2 Lipofection of Eukaryotic Cells with the Plasmid (See **Note 1**)*

1. Plasmid DNA of interest.
2. 0.22 μm filters.
3. 5 mL syringe.
4. Coverslips.
5. Plate for cell culture.
6. Cell culture medium for specific eukaryotic cells.
7. Neubauer chamber, hemocytometer, or automatic cell counter.
8. Incubator, 37 °C with 5% of CO_2.
9. Liposomal reagent (cationic lipids) chosen.

2.5.3 Confocal Microscopy

1. 0.01 M PBS (1 L): 8 g NaCl, 0.2 g KCl, 1.15 g Na $_2HPO_4$, 0.2 g of KH_2PO_4 in 1 L of distilled water (*see* **Note 2**). Store at 4 °C.
2. 4% paraformaldehyde: 0.4 g paraformaldehyde dissolved in 10 mL of 0.01 M PBS 25 μL of 5 M NaOH (*see* **Note 5**).
3. 0.1 mL Triton X-100 in 100 mL of 0.01 M PBS (*see* **Note 5**).
4. Primary monoclonal antibody of the respective protein.
5. 1% BSA/PBS: 1 g bovine serum albumin (BSA) in 100 mL of 0.01 M PBS. Solution stored at 20 °C.
6. Humid chamber.
7. Secondary antibody of the respective protein diluted in 1% BSA/PBS.
8. Fluorochrome DAPI (2 μg/mL 4′,6-diamidino-2-phenylindole).
9. Microscope slides.
10. Buffered glycerin: 9 mL glycerin, 1 mL bicarbonate buffer (for bicarbonate buffer, mix 0.53 g of Na_2CO_3 and 0.54 g of $NaHCO_3$ in 23 mL in distilled water). Adjust pH to 9.0 (*see* **Note 5**).
11. Confocal microscope.

*2.5.4 Flow Cytometry (See **Note 1**)*

1. Trypsin.
2. 96 round bottom well plate.
3. Plate centrifuge.
4. Fixation concentrate buffer.
5. 4 °C freezer.
6. Permeabilization concentrate buffer.
7. 1% BSA/PBS.
8. Primary antibody.
9. Secondary antibody labeled with fluorochrome.
10. 0.01 M PBS.
11. Cytometry tubes.
12. Flow cytometry equipment.

2.6 Confection of Electrocompetent* Lactococcus *sp. Cells (See Note 1)

1. *L. lactis* sp. cells stock culture.
2. M17 broth: 0.05% ascorbic acid, 0.5% lactose, 0.025% magnesium sulfate, 0.5% meat extract, 0.25% meat peptone (peptic), 1.9% sodium glycerophosphate, 0.5% soya peptone (papainic), 0.25% tryptone, 0.25% yeast extract in 500 mL of distilled water (*see* **Note 2**).

3. M17 broth + 0.5% glucose (M17-Glu): Prepare M17 broth according to **item 2** in this subheading and after autoclavation, add glucose solution at a final concentration of 0.5% into M17 broth medium (*see* **Note 6**).
4. 1 M sucrose solution: 85.5 g of sucrose; 250 mL of distilled water.
5. 2× concentrated M17 broth: prepare M17 broth according to **item 2** in this subheading in 250 mL of distilled water instead of 500 mL.
6. M17 broth + 0.5 M sucrose + 0.5% glucose (M17-Sac-Glu): In laminar flow hood, mix M17 broth (2×) with sucrose 1 M. Add glucose, at a final concentration of 0.5% (*see* **Notes 6** and **7**). Store the solution at 4 °C.
7. 50, 15, and 1.5 mL tubes.
8. 500 mL Erlenmeyer.
9. Incubator, 30 °C.
10. Refrigerated centrifuge.
11. 0.5 M sucrose + 10% glycerol: 171.1 g/L sucrose, 100 mL/L glycerin; complete with 500 mL of distilled water (*see* **Note 2**). Solution stored at 4 °C.
12. 30% polyethylene glycol (PEG) 3000 + 10% glycerol: 3 g of PEG3000, 1 mL glycerin in 10 mL of distilled water (*see* **Note 2**). Solution stored at 4 °C.
13. 200 µL microtubes.

2.7 Transformation in L. lactis *Electrocompetent Cells (See Note 1)*

1. DNA plasmid.
2. Electrocompetent *L. lactis* cells.
3. Pulser cuvettes (0.1 cm electrode gap).
4. M17 + Glu.
5. Antibiotic (ATB) or another character required for selection.
6. 1.5 mL microtubes.
7. Incubator, 30 °C.
8. Petri dishes 25 mL.
9. M17 + Glu agar (prepare M17 broth as described in Subheading 2.6, **item 3**, and add 1.5% of bacteriological agar) (*see* **Notes 2** and **3**).
10. Electroporator.

2.8 Plasmid Extraction (See Note 1)

The materials involved in this subheading are the same required for plasmid extraction from *E. coli* (Subheading 2.3), and including the following:

1. M17-Glu broth.

2. Incubator, 30 °C.
3. Tris–EDTA buffer TE-LYS: 500 μL of TE buffer (stock solution 100 mL of 1 M Tris–HCl; 20 mL of 0.5 M EDTA); 100 mg lysozyme in 10 mL of distilled water. Solution stored at −20 °C.

2.9 Plasmid Verification

1. Plasmid obtained in the DNA extraction.
2. Specific primers designed for the amplification of the open reading frame (ORF) of interest.
3. Polymerase chain reaction (PCR) reagents.
4. Thermocycler.
5. Restriction enzymes reagents.

2.10 Dose Preparation for Gavage (See Note 1)

1. Culture stock of *Lactococcus* sp.
2. M17-Glu broth.
3. ATB or another character required for selection.
4. Incubator, 30 °C.
5. Spectrophotometer.
6. 50 mL tubes.
7. 50 mL centrifuge.
8. 0.01 M PBS.
9. −80 °C ultra-freezer.

3 Methods

3.1 Confection of Electrocompetent E. coli Cells (See Notes 1 and 8)

1. Inoculate 50 μL of an *E. coli* culture stock in 5 mL of LB medium.
2. Incubate the pre-inoculum at 37 °C for 18 h and 10 × *g* in the orbital shaker. The control is made with LB medium without bacteria.
3. After this time, add 3 mL of the pre-inoculum into 300 mL of LB medium.
4. Incubate at 37 °C under agitation in an orbital shaker until it reaches the optical density at 600 nm ($OD_{600\ nm}$) between 0.4 and 0.5 (*see* **Note 9**).
5. When achieving the appropriate OD, distribute equally 40 mL of the culture on tubes with capacity of 50 mL and maintain it on ice for 20 min (*see* **Note 10**).
6. Centrifuge the tubes at 1500 × *g* for 15 min at 4 °C.
7. After centrifugation, discard the supernatant and resuspend the pellet with 40 mL of 10% glycerol, mix the tubes gently to wash the cells.

8. Centrifuge again at 1500 × *g* for 15 min at 4 °C.
9. Repeat **steps 7** and **8** for three times.
10. After the last centrifugation, unify the pellet in one tube and resuspend it in 1 mL of 10% glycerol solution.
11. Divide the content in aliquots of 100 μL and stock at −80 °C.

3.2 Efficiency Test of E. coli *Electrocompetent Cells (See Note 1)*

1. Defrost an aliquot (100 μL) of electrocompetent cells on ice for 15 min.
2. Add the DNA plasmid used for test (usually 100 ng of a high copy number plasmid) and reserve on ice for 10 min. A negative control is made using no plasmid.
3. Transfer the mixture of cells and plasmid to pre-cooled pulser cuvette and submit it to a 1800 V pulse (25 μF capacitance and 200 Ω resistance), using an electroporator.
4. Immediately after the pulse, add 900 μL of LB medium to the cuvettes, homogenize, and transfer the content to a 1.5 mL microtube.
5. Incubate for 2–3 h at 37 °C in water bath.
6. After this time, perform serial dilution of 10^{-1} to 10^{-6} and plate 100 μL of 10^{-4}, 10^{-5}, and 10^{-6} in LB agar dishes with the respective antibiotic or selection character for 18 h at 37 °C (*see* **Note 11**).

3.3 Transformation in Electrocompetent E. coli *Cells (See Note 1)*

1. Follow the same transformation steps for efficiency test described in Subheading 3.2.
2. After **step 6**, perform the selection of the clones on the dishes, collecting the colonies, and expanding it in liquid LB medium (3–5 mL) with the respective antibiotic for stockage, plasmid extraction, and cloning confirmation.

3.4 Plasmid Extraction (See Note 1)

1. Expand each colony obtained after the transformation is in LB medium.
2. Incubate for 18 h at 37 °C under agitation.
3. Collect 1 mL of the aliquots and add glycerol at a final concentration of 40%.
4. Stock in −80 °C.
5. Place 2 mL of the remained growth culture in 2 mL tubes to perform plasmid extraction.
6. Centrifuge at 16,000 × *g* for 5 min.
7. Resuspend the pellet in 200 μL of solution I; with 0.5 μL of RNAse.
8. Wait for 5 min and add 200 μL of solution II.
9. Immediately, add 200 μL of solution III.

10. Invert the tubes about 4–6 times.
11. Centrifuge at 13,500 × *g* for 15 min.
12. Collect the supernatant and place it in new 1.5 mL tubes.
13. Add 420 μL of isopropanol and incubate the tubes at −20 °C for 30–40 min for DNA precipitation.
14. Centrifuge at 16,000 × *g* for 15 min.
15. After that, add 500 μL of 70% ethanol.
16. Centrifuge at 13,500 × *g* for 15 min.
17. Discard the supernatant and place the tube opened at 37 °C until all the residue of alcohol evaporate.
18. In the end, resuspend the DNA pellet in 20 μL of ultrapure water.
19. The quality of the extracted plasmids is verified by electrophoresis and the quantification is measured using a spectrophotometer and applying the 260/280 ratio (*see* **Note 12**).

3.5 Clone Confirmation

3.5.1 Polymerase Chain Reaction

1. Add 5 μL of 10× buffer.
2. Add 1 μL of 10 mM dNTPs.
3. Add 1.5 mM Mg^{2+} (*see* **Note 13**).
4. Add 1 μL of each 20 μM primers forward and reverse.
5. Add 0.5–2.5 U of DNA polymerase per 50 μL reaction according to the manufacturer's specifications.
6. Complete the final volume with ultrapure water (50 μL approximately).
7. Perform the PCR reaction in thermocyclator according to primers specification and DNA polymerase manufacturer instructions.
8. After reaction, confirm the amplification of the respective ORF through DNA migration in 0.8–1% agarose gel by electrophoresis.

3.5.2 Enzymatic Digestion

1. Add the concentration of the buffer according to enzyme specifications.
2. Add DNA of interest (about 5–10 μg).
3. Add approximately 1 U of each enzyme per μg of DNA.
4. Complete the final volume with ultrapure water (50 μL approximately).
5. Incubate at specific temperature for specific time, according to enzymes specifications (*see* **Note 14**).
6. After reaction, confirm digestion of the respective plasmid though DNA migration in 0.8% agarose gel by electrophoresis (*see* **Note 15**).

3.5.3 Sequencing

1. Prepare the mix according to the number of samples by adding to each sample: 2.0 μL 5× buffer; 1.0 μL big dye mix; 2.0 μL primer forward or reverse (1.6 pmoles/μL); 4.0 μL of ultrapure water.
2. Using a 96-well PCR microplate, add in each well 9.0 μL of mix and 1.0 μL of DNA of interest (30–50 ng).
3. After amplification reaction on thermocycler, the reaction must be precipitated with the addition of ethanol 100% and 125 mM EDTA, centrifuged and washed with 70% ethanol, as indicated by the manufacturer, and resuspended in highly deionized formamide.
4. Perform sequencing on automated DNA sequencer according to the manufacturer's instructions.

3.6 Plasmid Expression Confirmation

*3.6.1 Culture of Caco-2 Cells (See **Notes 1** and **16**)*

1. Defrost cell cultures of Caco-2 cells, stocked at −196 °C in liquid nitrogen in DMEM with 5% of DMSO (for cryopreservation) and place it in 15 mL tubes with 3 mL of DMEM.
2. Centrifuge the cells at 90 × *g* for 5 min and discard the supernatant for elimination of DMSO.
3. Add 10 mL of DMEM supplemented with 20% of bovine serum albumin (BSA) and transfer to a cell culture flask of 75 cm^2.
4. Incubate it at 37 °C with 5% of CO_2 until it reaches a confluence of 80–90%.
5. For sub-culturing, discard the medium, add 1 mL of trypsin–EDTA solution and incubate it at 37 °C for 3–6 min.
6. Add 6–8 mL of DMEM medium and aspirate the cell suspension with a pipette.
7. Add aliquots of the cell suspension to new culture flasks with sub-cultivation ratio of 1:4–1:6 (1×10^4 viable cells).
8. Renew medium 1–2 times per week until use.

*3.6.2 Lipofection of Eukaryotic Cells with the Plasmid (See **Note 1**)*

1. Proceed the DNA extraction of the plasmid from the recombinant *E. coli* as mentioned on Subheading 3.4.
2. Sterilize the DNA using 0.22 μm filters.
3. Deposit a coverslip in the bottom of each well (for future confocal microscopy analysis).
4. Count the cells culture and add about 200,000 cells to each well of a 6-well plate with 2 mL of medium (*see* **Note 17**).
5. Incubate the plates at 37 °C with 5% of CO_2 until it reaches the confluency of 80–90%.
6. Change the medium and add about 4 μg of DNA together with specially designed cationic lipids (such as DEAE-dextran,

polyethyleneimine, lipofectin, DOTAP, lipofectamine, and DOTMA) according to the specifications of the manufacturer.

7. Incubate the plate at 37 °C with 5% of CO_2 for 24–72 h depending on cell type and plasmidial transfection (*see* **Note 18**).

*3.6.3 Confocal Microscopy (*See ***Note 1****)*

Forty-eight hours after lipofection, the coverslips were treated to make slides to detect the desired protein.

1. Remove culture medium from the wells.
2. Wash the cells twice with 1 mL of 0.01 M PBS.
3. Fix the cells with 700 μL of 4% paraformaldehyde for 15 min without shaking.
4. Wash the cells again with 1 mL of 0.01 M PBS.
5. Permeabilize the cells by adding 700 μL of Triton X-100 (0.1% in 0.01 M PBS) and incubate for 10 min at room temperature.
6. Add 100 μL of the primary monoclonal antibody of the respective protein in 1% BSA/PBS according to the antibody specifications.
7. Wait for an hour or two in humid chamber at room temperature.
8. Wash (5×) the coverslip with 1 mL of 0.01 M PBS with soft agitation.
9. Incubate posteriorly with 100 μL of the secondary antibody in 1% BSA/PBS according to the antibody specifications.
10. Wait an hour in humid chamber at room temperature.
11. Label the nucleus by adding the fluorochrome DAPI (2 μg/mL 4′,6-diamidino-2-phenylindole).
12. Wash (5×) with 1 mL of 0.01 M PBS.
13. Place the coverslips on slides with buffered glycerin and sealed for later microscopic observation.
14. Analyze the treated transfected cells in a confocal microscope for visualization of fluorescence.

*3.6.4 Flow Cytometry (*See ***Note 1****)*

1. After 48 h post-transfection adds trypsin (the concentration of trypsin will be depend on the eukaryotic cell studied) to the plate to remove the cells.
2. Place the cells into a round-bottomed 96-well plate (1×10^6 cells per well).
3. Centrifuge the plate at 4 °C, 140 × *g* for 10 min.
4. Discard the supernatant.
5. Resuspend the pellet in 200 μL of fixation buffer according to the manufacturer.

6. Incubate for 30 min at 4 °C.
7. Centrifuge the plate at 4 °C, 140 × *g* for 10 min.
8. Discard the supernatant and resuspend the pellet with 150 μL of permeabilization buffer according to the manufacturer.
9. Centrifuge the plate at 4 °C, 140 × *g* for 10 min.
10. Repeat **steps 8** and **9**.
11. Discard the supernatant and wash the cells with 200 μL of 1% BSA/PBS.
12. Centrifuge it for 8 min at 4 °C, 140 × *g*.
13. Discard the supernatant and add 10 μL of the primary antibody.
14. Incubate the plate at room temperature for 30 min.
15. Wash the cells twice with 200 μL of 1% BSA/PBS and centrifuge at 4 °C, 140 × *g*, for 10 min.
16. Add 10 μL of the secondary antibody labeled with fluorochrome in a proportion according to the manufacturer specifications.
17. Incubate it at room temperature for 30 min.
18. Repeat **step 15**.
19. Discard the supernatant and resuspend the pellet with 200 μL of 0.01 M PBS.
20. Transfer this content to adequate cytometry tubes.
21. Analyze the samples in a flow cytometry equipment with about 30,000 events to be plotted.
22. Delimitate the most homogenous cell population to be analyzed based on granularity and fluorescence for evaluation of the expression of the protein of interest by the eukaryotic cell.

3.7 Confection of Electrocompetent Lactococcus *sp. Cells (See Note 1)*

1. Prepare a pre-inoculum previously by adding 50 μL of *L. lactis* sp. stock culture in 10 mL of M17-Glu and incubate it at 30 °C, without shaking.
2. On the second day, add 10 mL of the pre-inoculum to 200 mL of M17-Sac-Gli medium with glycine 1% ($OD_{600\ nm} = 0.1$).
3. Incubate at 30 °C without shaking until it reaches an $OD_{600\ nm}$ between 0.4 and 0.6 (*see* **Note 9**).
4. Distribute the culture in 50 mL tubes and centrifuge at 4 °C, 1500 × *g*, for 15 min (*see* **Note 10**).
5. Discard the supernatant and resuspend the pellet in 40 mL of a sterile solution of pre-cooled sucrose 0.5 M and glycerol 10%.
6. Centrifuge at 4 °C, 1500 × *g*, for 15 min.

7. Repeat **steps 5** and **6** for three times transferring the pellet from tube to tube until it reaches one tube on the last centrifugation.
8. Resuspend the final pellet in 1 mL of sterile solution of PEG 3000 + glycerol 10%.
9. Distribute aliquots of 100 μL in microtubes and stock it at −80 °C until the moment of transformation.

3.8 Transformation of Electrocompetent Lactococcus *sp. Cells (See Note 1)*

1. Mix carefully the confirmed plasmid with 100 μL of competent cells and incubate on ice for 5 min.
2. After that, transfer all this content to electroporation cuvettes and submit it to a 2500 V pulse (25 μF capacitance and 200 Ω resistance).
3. After the pulse, add 900 μL of M17 + Glu medium and the respective antibiotic, if necessary, and incubate it at 30 °C for 2 h.
4. Subsequently, plate 100 μL of this content in M17 + Glu agar medium and ATB, if necessary, on serial dilutions (10^{-4}, 10^{-5}, and 10^{-6}) and incubate at 30 °C for 24 h.
5. Select the clones on the dishes collecting the colonies and expanding it in M17 + Gli and ATB, if necessary, liquid medium for stockage, plasmid extraction, and cloning confirmation.

3.9 Plasmid Extraction

1. Expand each colony obtained after the transformation in M17-Glu medium.
2. Incubate for 18 h at 30 °C without agitation.
3. Collect 1 mL of the aliquots and add glycerol at final concentration of 25% and maintain it at −80 °C.
4. Place 2 mL of the remained growth culture in 2 mL tubes to perform plasmid extraction.
5. Centrifuge at 16,000 × *g* for 5 min.
6. Discard the supernatant.
7. Add 250 μL of a TE-LYS buffered solution.
8. Incubated the mixture for 1 h at 37 °C.
9. Follow the same methodology for plasmid extraction in *E. coli* (as described in Subheading 3.4 from **steps 7–19**).

3.10 Plasmid Verification

1. The presence of the plasmid vector in to *L. lactis* is verified by amplification of the insert by PCR (as described in Subheading 3.5.1), using specific primers.
2. Then, enzymatic digestion (as described in Subheading 3.5.2) is performed (*see* **Note 19**).

3.11 Doses Preparation for Gavage (See Note 1)

1. Expand 50 μL of the stocked culture in 5 mL of M17-Glu with the respective antibiotic and maintain it overnight at 30 °C with no agitation.
2. On the next day, inoculate the pre-inoculum in M17-Glu with the respective antibiotic at a 1:20 proportion (1 of the pre-inoculum for 19 of medium) and wait until it reaches the $OD_{600\ nm}$ which refers to 1×10^9 CFU/mL.
3. Divide the content in 50 mL tubes and centrifuge at 1500 × *g* for 15 min at 4 °C (*see* **Note 10**).
4. Wash the pellet with sterile 0.01 M PBS twice.
5. Discard the supernatant and add 140 μL of sterile 0.01 M PBS for each dose (*see* **Note 20**).
6. Store at −80 °C for 3 or 4 days until administrate to the animals (*see* **Notes 21–24**).

4 Notes

1. The materials and solutions in this subheading must be sterilized, as well as all procedures performed in a sterile workplace to avoid contamination.
2. Sterilize solution by autoclaving at 121 °C for 15 min.
3. When it is at room temperature add the ATB or the other selection character. Place the medium in the Petri dishes and wait until solidify.
4. To avoid foaming, do not shake the solution.
5. To avoid degradation of the solution compounds, prepare at the time of use.
6. To prepare the glucose at 50%, add 50 × g of anhydrous glucose to 100 mL of distilled water. Sterilize solution by filtering with 0.22 μm filter or autoclaving at 110 °C for 10 min.
7. The M17 broth 2× concentrated with sucrose 1 M 50% results in 1× M17 broth, 0.5 M sucrose.
8. Usually, recombinant DNA is first transformed into *E. coli* to facilitated laboratory proceed. *E. coli* are Gram-negative bacteria, with a peptidoglycan layer less thick than Gram-positive ones, which makes it easier to extract internal plasmids, and also, their rate grow is 20 min per generation under typical growth conditions. There are two main techniques for making competent *E. coli*, electro and chemically, which were addressed in this chapter.

9. The optical density at 600 nm of 0.4–0.6 refers to the exponential (log) phase of bacterial growth curve. At this phase, the cells are dividing by binary fission and duplicating in numbers after each generation time; log phase is the most metabolic active phase where there is a great number of viable cells.
10. Maintain the cells on ice all the time.
11. The efficiency is calculated as the following formula and a good efficiency corresponds to more than 1×10^7 CFU/mL:

$$\text{Efficiency} = \frac{\text{number of collonies}}{[\,]\text{DNA (μg)}} \times \frac{\text{plated volume (μl)}}{\text{total volume (μl)}} \times \text{dilution factor}$$

where:

Efficiency is given in CFU (colony-forming unit).

Number of colonies = number of colonies counted on the dishes.

[] DNA = plasmid concentration used in the transformation.

Plated volume = volume of the mixture of the transfection that was plated (generally is 100 μL).

Total volume = total volume of the transformation.

Dilution factor = dilution of each plate. E.g.: 10^{-4}, 10^{-5}, 10^{-6}.

12. The 260/280 nm absorbance ratio is used for estimate the purity of both DNA and RNA extraction. A 260/280 ratio of ~1.8 is accepted as "pure" for DNA, a ratio of ~2.0 is generally accepted as "pure" for RNA. If the ratio is lower than these values, it possibly indicates contamination with protein, phenol, or other contaminants that absorb strongly at or near 280 nm.
13. Add only if it is not present in the buffer. The enzyme Taq polymerase needs Mg^{+2} to become functional and reveal its activity.
14. Some restriction enzymes may have "star activity" also known as off-target cleavage, is an unwanted but intrinsic characteristic of them which happen after a long time of incubation, which may cleave similar sequences but not identical to the recognition sequence. *See* very carefully the enzyme's specification and, if they present "star activity," use as few units as possible to perform digestion, do not incubate the reaction overnight, only the specified time in the datasheet, and lower the pH of the buffer up to 7.0.

15. If the digestion is well succeeded, it will be possible to observe two bands in agarose gel, one regarding the plasmid vector and the other the released ORF.
16. In order to confirm in vitro expression, the DNA vaccine construction must be able to be transcribed, translated, and processed in the host eukaryotic cell to express the respective protein. In that way, in vitro tests with eukaryotic cells should be performed in order to analyze the expression of the intended protein by confocal microscopy and flow cytometry.
17. Cell counts are performed using either Neubauer chamber (in this case, add Trypan Blue 0.4% diluted 10× to label inviable cells), an automated counter or a hemocytometer.
18. It is important to make a transfection kinetic at different times (e.g., 12, 24, 48 h) to find the best interval to see protein expression after transfection.
19. By then, the plasmid is ready to have its expression confirmed in vivo using adequate animal models.
20. For each dose, 2 mL of expanded bacteria is used at $OD_{600\ nm} = 1.0$, which corresponds to 2×10^9 CFU for *Lactococcus lactis*. By the end of the process, 140 μL of 0.01 M PBS is added to each one. To make the process more practical, all doses are prepared together, and the separation of each dose is made only at the final of the process. In other words, if 10 doses are required, a volume of 20 mL of culture must be used, centrifuged, washed, and resuspended at the end with 1.4 mL of 0.01 M PBS (140 μL × 10).
21. The most studied animal model for expression analysis of DNA vaccines is the mice. The number of animals required for the experiment must be carefully analyzed before the experiment in order to provide statistically relevant results. The anesthesia and euthanasia methods chosen must be adequate to the specifications of the project, and previously approved by the ethics committee. Also, the mucosal way by which the dose containing the recombinant bacteria will be administered must be chosen in agreement with the intended objective of the study. Oral administration is the most common, although intranasal is also applied.
22. For oral administration, doses are prepared according to the Subheading 3.11 and administered via gavage (100 μL up to 500 μL). For nasal administration 2×10^9 CFU must be administered in a volume of 10 μL in each nostril.
23. The delineation of in vivo tests will depend on the main objective of the work. For the analysis of immunostimulatory effects after oral administration for therapy, the doses must be given after or during induction of the disease, and then, the blood

must be collected for the measurement of immunoglobulins, cytokines, and analysis of immune cellular responses, as well as histopathological analysis of affected organs. If the objective is to analyze the prophylactic potential, then doses must be administered before induction of the disease (*see* **Note 5**).

24. It is important to denote that in this chapter the methods described were related to immunization experiments, being possible the stimulation of immune responses. Another application may involve co-localization studies of two or more bacterial strains by cloning fluorescent proteins and analyzing its expression in vitro by the techniques described before and in vivo by confocal microscopy.

References

1. Ingolotti M, Kawalekar O, Shedlock DJ et al (2010) DNA vaccines for targeting bacterial infections. Expert Rev Vaccines 9:747–763
2. Landete JM (2017) A review of food-grade vectors in lactic acid bacteria: from the laboratory to their application. Crit Rev Biotechnol 37:296–308
3. Hobernik D, Bros M (2018) DNA vaccines—how far from clinical use? Int J Mol Sci 19:3605
4. Kutzler MA, Weiner DB (2008) DNA vaccines: ready for prime time? Nat Rev Genet 9:776–788
5. Fuller DH, Loudon P, Schmaljohn C (2006) Preclinical and clinical progress of particle-mediated DNA vaccines for infectious diseases. Methods 40:86–97
6. Vasan S, Hurley A, Schlesinger SJ et al (2011) In vivo electroporation enhances the immunogenicity of an HIV-1 DNA vaccine candidate in healthy volunteers. PLoS One 6:e19252
7. Wang S, Zhang C, Zhang L et al (2008) The relative immunogenicity of DNA vaccines delivered by the intramuscular needle injection, electroporation and gene gun methods. Vaccine 26:2100–2110
8. Pereira VB, Saraiva TDL, Souza BM et al (2015) Development of a new DNA vaccine based on mycobacterial ESAT-6 antigen delivered by recombinant invasive Lactococcus lactis FnBPA+. Appl Microbiol Biotechnol 99:1817–1826
9. Mowat AM, Agace WW (2014) Regional specialization within the intestinal immune system. Nat Rev Immunol 14:667–685
10. Wyszyńska A, Kobierecka P, Bardowski J et al (2015) Lactic acid bacteria—20 years exploring their potential as live vectors for mucosal vaccination. Appl Microbiol Biotechnol 99:2967–2977
11. Schaffner W (1980) Direct transfer of cloned genes from bacteria to mammalian cells. Proc Natl Acad Sci U S A 77:2163–2167
12. Courvalin P, Goussard S, Grillot-Courvalin C (1995) Gene transfer from bacteria to mammalian cells. C R Acad Sci III 318:1207–1212
13. Pilgrim S, Stritzker J, Schoen C et al (2003) Bactofection of mammalian cells by *Listeria monocytogenes*: improvement and mechanism of DNA delivery. Gene Ther 10:2036–2045
14. Daudel D, Weidinger G, Spreng S (2007) Use of attenuated bacteria as delivery vectors for DNA vaccines. Expert Rev Vaccines 6:97–110
15. Dunham SP (2002) The application of nucleic acid vaccines in veterinary medicine. Res Vet Sci 73:9–16
16. Wells JM, Mercenier A (2008) Mucosal delivery of therapeutic and prophylactic molecules using lactic acid bacteria. Nat Rev Microbiol 6:349–362
17. Bermúdez-Humarán LG, Aubry C, Motta J-P et al (2013) Engineering lactococci and lactobacilli for human health. Curr Opin Microbiol 16:278–283
18. Sanders ME (2003) Probiotics: considerations for human health. Nutr Rev 61:91–99
19. Hill C, Guarner F, Reid G et al (2014) The International Scientific Association for Probiotics and Prebiotics consensus statement on the scope and appropriate use of the term probiotic. Nat Rev Gastroenterol Hepatol 11:506–514
20. Mercenier A, Müller-Alouf H, Grangette C (2000) Lactic acid bacteria as live vaccines. Curr Issues Mol Biol 2(1):17–25

21. Faudzi H, Faroque H, Chia SL et al (2018) Lactococcus lactis: LAB model organism for bacteria-mediated therapeutic strategies. Asia-Pacific J Mol Biol Biotechnol 26(1):1–10
22. Guimarães VD, Innocentin S, Lefevre F et al (2006) Use of native Lactococci as vehicles for delivery of DNA into mammalian epithelial cells. Appl Environ Microbiol 72:7091–7097
23. Chatel J-M, Pothelune L, Ah-Leung S et al (2008) In vivo transfer of plasmid from food-grade transiting lactococci to murine epithelial cells. Gene Ther 15:1184–1190
24. Guimarães V, Innocentin S, Chatel J-M et al (2009) A new plasmid vector for DNA delivery using lactococci. Genet Vaccines Ther 7:4
25. Chiabai MJ, Almeida JF, de Azevedo MGD et al (2019) Mucosal delivery of Lactococcus lactis carrying an anti-TNF scFv expression vector ameliorates experimental colitis in mice. BMC Biotechnol 19:38
26. Tao L, Pavlova SI, Ji X et al (2011) A novel plasmid for delivering genes into mammalian cells with noninvasive food and commensal lactic acid bacteria. Plasmid 65:8–14
27. Mancha-Agresti P, Drumond MM, Carmo FLR d et al (2017) A new broad range plasmid for DNA delivery in eukaryotic cells using lactic acid bacteria: in vitro and in vivo assays. Mol Ther Methods Clin Dev 4:83–91
28. Coelho-Rocha ND, de Castro CP, de Jesus LCL et al (2018) Microencapsulation of lactic acid bacteria improves the gastrointestinal delivery and in situ expression of recombinant fluorescent protein. Front Microbiol 9:2398
29. Yagnik B, Padh H, Desai P (2016) Construction of a new shuttle vector for DNA delivery into mammalian cells using non-invasive Lactococcus lactis. Microbes Infect 18:237–244
30. Yagnik B, Sharma D, Padh H et al (2018) In vivo delivery of pPERDBY to BALB/c mice by LacVax® DNA-I and comparison of elicited immune response with conventional immunization methods. Gene Ther 25:485–496

Part V

DNA Vaccine Transfer to Clinical Trials

Chapter 17

Ethics of DNA Vaccine Transfer for Clinical Research

Ana Cristina Ramalhinho and Miguel Castelo-Branco

Abstract

Several experimental human DNA vaccines are currently undergoing Phase I, II, and III clinical trials in order to investigate their efficacy and safety. Human clinical trials must follow guidelines and procedures that have been approved by the regulatory authorities and ethics committees. Ethical clinical research is much more than applying an informed consent to participants. In this chapter we will review the ethical standards and provide a framework to evaluate and design ethical clinical research. Despite being universal standards supported by universal guidelines, they must be adapted to the conditions in each country where the clinical research is being conducted.

Key words Benefits, DNA vaccines, Ethics, Informed consent, Risk

1 Introduction

DNA vaccines work by causing the body to translate the injected DNA sequences into pathogenic proteins. The body then creates antibodies specific to the proteins, which confers immunity without causing infection. This is important for immune-compromised patients, including those infected by HIV. These vaccines are also easier to distribute than traditional vaccines because they are more stable, avoid the risk of accidental infection by the pathogen, and require no refrigeration. These features are appealing to practitioners in the developing world, burdened with disease-susceptible populations, and lack of proper infrastructure for maintaining traditional vaccines [1]. Several experimental human DNA vaccines are currently undergoing Phase I, II, and III clinical trials in order to investigate their efficacy and safety (in clinicaltrials.gov). Among the vaccines being tested include DNA vaccines that could offer protection against infectious diseases such as malaria, HIV, influenza, tuberculosis, zika, and Ebola virus, as well as antitumor and gene therapy vaccines. The main safety concern with DNA vaccines is related to unwanted side effects in the vaccinated organism. Unwanted side effects include the development of autoimmunity,

Ângela Sousa (ed.), *DNA Vaccines: Methods and Protocols*, Methods in Molecular Biology, vol. 2197,
https://doi.org/10.1007/978-1-0716-0872-2_17,

host cell genome integration, injection site inflammation, antibiotic resistance due the presence of antibiotic resistance genes within the construct, and tissue destruction due to cytotoxic responses [2].

Several regulatory agencies such as European Medicines Agency (EMA), the World Health Organization (WHO), and Food and Drug Administration (FDA) have published guidelines for DNA vaccines. Also, many countries have national regulations, including those on gene technology, which must be taken into consideration before undergoing clinical trial phase and receive marketing authorization. This chapter will highlight the ethical guidelines for the development of DNA vaccines, including the regulatory framework.

2 Ethical Issues for the Development of DNA Vaccines: Oversight and Regulatory Framework

The global objective of clinical research is to develop universal knowledge to improve health and/or increase understanding of human biology. By placing some people at risk of harm for the benefit of others, clinical research has the potential for the exploitation of human subjects. The legal–ethical issues connected with research in DNA vaccines pertain to the development of the vaccine, study design, population on which the vaccine is tested, and the location of the trial. The issues involved in assessing the safety of a DNA vaccine concern primarily the possible side effects, quality, and freedom from contamination. A DNA vaccine would be unsafe if it caused illness, disease, injury, or harm to the recipient [3]. The DNA platform is conceptually safer and more stable than are conventional vaccine approaches. Plasmids are non-live systems, which leaves little risk for reversion to a disease-causing state or secondary infection. The original concerns associated with the DNA platform were the potential for genomic integration and development of anti-DNA immune responses. Exhaustive research has found little evidence of integration, and the risk for integration appears to be significantly lower than that associated with naturally occurring mutations. Induction of anti-DNA immune responses after DNA vaccination has been monitored in multiple NHP studies and clinical trials, but evidence of increased production of such responses or changes in other clinical markers of autoimmunity has not been reported. Overall, multiple studies have reported the DNA platform to be well tolerated and to have an enviable safety record [4].

Before seeking approval to market the vaccine, research companies must conduct animal studies and Phase I to Phase III clinical trials to ascertain the safety and efficacy of the vaccine. Many times, there is a conflict of interest between the researchers and institutes testing the vaccine for its safety and efficacy; this can compromise

the vetting system of medical research. Research involves financial intertwining between the pharmaceutical companies, medical research professionals, academic institutions conducting the research, and government agencies. Due to financial interests, the truth about the vaccine safety, effectiveness, and efficacy is often compromised, misrepresented, and suppressed [5].

The study design may also raise legal–ethical issues sometimes. DNA vaccines intended for human use have to undergo a clinical development program, which include investigation and data gathering on immune response, persistence of immunity, appropriate dose, and vaccination procedure. In randomized controlled trials, the gold standard for evaluating the safety and efficacy of new interventions is the use of a placebo control arm or a no-treatment arm, even where standard treatment is available. International ethical guidelines require that the placebo control arm or no treatment arm should be used sparingly and only in cases in which there is a no-treatment option [6].

Human clinical trials must follow guidelines and procedures that have been approved by the regulatory authorities and ethics committees (*see*, e.g., EU Directive 2001/83/EC and Code of Federal Regulations Title 21—FDA, 2016). WHO has published a guideline for national authorities and vaccine manufacturers regarding the clinical assessment of vaccines (Guidelines for assuring the quality and nonclinical safety evaluation of DNA vaccines, Annex 1, WHO Technical Report Series No. 941, 2004). In this guideline, an outline of the international regulatory expectations to the different stages of vaccine development and for marketing approval is described. In addition, most countries demand that clinical trials be performed in line with good clinical practice (GCP) (International Conference on Harmonization, 1997; EMA, 2007 and 2012a; EU Directive 2001/20/EC) and according to the Declaration of Helsinki (1966) [2].

3 Population and Location Selection

Vaccines should be tested in varied populations to understand their efficacy and safety in populations of different ethnicity. Vaccines for children must first be tested on adults, and only then on children. Ethical and legal issues are generally raised when vaccines are tested on vulnerable populations or directly on children without providing them any safety or protection, or without following the norms of informed consent [7].

The location of the trials is of much importance as several ethical issues arise when interventions are researched in developed countries and then tested in the developing countries. It is mandatory to make sure that the ethical standards of research followed in the developed country are followed in the developing country, even

if the latter has a weak regulatory system. Also, factors such as the availability of healthcare facilities at the location where the trials take place, and the availability of screening and treatment at these locations can pose a challenge in developing countries. The ethical conduct of trials can be affected if such facilities are not available and advantage is taken of the vulnerability of those participating in the trial [8].

4 Definition of Benefits and Risks in Clinical Trials

Respect (autonomy), beneficence, non-maleficence, and justice are all involved in the conduct of clinical trials. Of the four primary pillars of health ethics, one is therefore particularly crucial for the study of DNA vaccines: beneficence. DNA vaccines can be of such great benefit that failing to put money and effort into developing and testing them is unethical [9].

Uncertainty about risks and benefits is inherent to clinical research, and it can only be justified if the potential risks to individual subjects are minimized, the potential benefits to individual subjects are improved, and the potential benefits to individual subjects and society are proportionate to or compensate the risk. This is called a favorable risk–benefit ratio. Assessment of the potential risks and benefits of clinical research by researchers and institutional review boards (IRB) typically involves multiple steps and is not a thigh procedure (Table 1) [10].

First, risks are identified and, within the context of good clinical practice, minimized by using procedures which are consistent with sound research design and do not necessarily expose subjects to risk, and whenever appropriate, by using procedures already being performed on the subjects for diagnostic or treatment purposes.

Table 1
Risks and benefits identified by IRB members [10]

Type of risk	Expected or unexpected side effects and toxicity Degree of invasiveness of the treatments (Frequency of) visits to and stays in hospital and extra tests Psychological and social risks Decrease in quality of life Burden, inconvenience, and risks to participating patients
Type of benefit	Possible treatment effect Increase in quality of life Psychological benefits Benefits to future patients Benefits to medical science

Second, potential benefits in health improvement to individual subjects are delineated and enhanced. And lastly, risks and potential benefits of the clinical research interventions to individuals are compared. In general, the more likely and/or severe the potential risks the greater in likelihood and/or magnitude the prospective benefits must be [11].

The revision of the International Conference on Harmonization (ICH) Good Clinical Practice (GCP) guideline, and specifically its addendum E6 (R2), was released in 2016. This regulatory document added new concepts to the existing ICH GCP guideline. The topic that was expanded upon the most in the GCPA document was quality management. GCPA fully embraces the quality-by-design and risk-based approaches. Quality management (QM) hinges on the quality-by-design concept, which infers that the quality of a clinical trial must be ensured through careful and fact-driven planning. In the new version, it is stated for the first time in the context of ICH GCP that QM is expected to be risk-based. The risk-based approach is based on the following criteria: critical process and data identification; risk identification; risk evaluation; risk control (mitigation actions); risk communication; periodical risk review; risk reporting. The analytic part of risk evaluation occurs with the help of the three main risk properties: likelihood that a risk or failure mode materializes; impact on subject's safety, rights and data integrity and reliability; and detectability—extent to which such threats or errors are detectable [12–14].

5 Informed Consent

Informed consent is an ethical and legal requirement for research involving human participants. It is the process where a participant is informed about all aspects of the trial, which are important for the participant to make a decision, and after studying all aspects of the trial, the participant voluntarily confirms his/her willingness to participate in a particular clinical trial and significance of the research for advancement of medical knowledge and social welfare. As no individual has right to infract fundamental rights of another person for the sake of fulfilling his own purpose, so an important tool called "informed consent" came into existence. The informed consent is described in ethical codes and regulations for human subject's research: Nuremberg Code, The Declaration of Helsinki, and The Belmont Report [15]. The purpose of informed consent is to ensure that individuals control whether or not they enroll in clinical research and participate only when the research is consistent with their values, interests, and preferences [11].

Table 2
Challenges during the informed consent process [16]

Research team	Poor communication technique Lack of time for the consent process Inability to detect lack of patient comprehension Legal outlook toward consent process
Patients	Anxiety and fear of new procedures Health status (terminal, debilitating diseases) Cognitive impairment (neurological disorders, elderly) Denial of disease state
Informed consent document	Complex language Medical terminologies Legal nature Lengthy consent documents

An informed consent process can be termed as complete, valid, and meaningful if all four criteria of information disclosure, competence, comprehension, and voluntariness are effectively satisfied. It is essential to consider here that competence or capacity of an individual to make decision depends on his/her ability to understand relevant information, to appreciate the nature of situation along with its consequence, to reason the given information, and the ability to communicate choice [16](Table 2).

To provide informed consent, individuals must be accurately informed of the purpose, methods, risks, benefits, and alternatives to the research, understand this information, and its bearing on their own clinical situation, and make a un-coerced decision whether to participate. Each of these elements is necessary to ensure that individuals make rational and free determinations of whether the research trial is consonant with their interests. Informed consent embodies the need to respect persons and their autonomous decisions. To enroll individuals in clinical research without their authorization is to treat them merely as a means to purpose and ends they may not endorse and deny them the opportunity to choose what projects they will pursue [11].

According to EMA and FDA, the following information must be included in the informed consent form:

(a) A statement that the study involves research subjects and an explanation of the research purposes.

(b) The expected duration of the subject's participation.

(c) A description of the procedures to be followed/of the medicine that is going to be tested, and an identification of any procedures which are experimental.

(d) A statement that participation is voluntary.

(e) Information about who is organizing and funding the research.

(f) A description of any reasonably foreseeable risk, discomfort, or disadvantages.

(g) A description of any benefits to the subject or to others which may reasonably be expected from the research avoiding inappropriate expectations.

(h) A disclosure of appropriate alternative procedures for treatment/diagnosis, if any, that might be advantageous to the subject.

(i) A statement describing the procedures adopted for ensuring data protection/confidentiality/privacy including duration of storage of personal data.

(j) A description of how incidental findings are handled.

(k) A description of any planned genetic tests.

(l) For research involving more than minimal risk, an explanation as to whether there are any treatments or compensation if injury occurs and, if so, what they consist of, or where further information may be obtained.

(m) Insurance coverage should be mentioned.

(n) A reference to whom to contact for answers to pertinent questions about the research and research subjects' rights, and whom to contact in the event of a research-related injury to the subject.

(o) A statement offering the subject the opportunity to ask questions and to withdraw at any time from the research without consequences.

(p) An explanation of what will happen with the data or samples at the end of the research period and if the data/samples are retained or sent/sold to a third party for further research.

(q) Information about what will happen to the results of the research.

There are also requirements for obtaining the informed consent from the participant [15](Table 3):

(a) The investigator or a person designated by the investigator must obtain the informed consent.

(b) Informed consent must be obtained before non-routine screening procedures are performed and/or before any change in the subject's current medical therapy is made for the purpose of the clinical trial.

(c) The subject/subject's legally acceptable representative should not be forced to sign on consent or participate/continue to participate in the trial.

Table 3
Obligations of all informed consent stakeholders [15]

Investigator	Design informed consent form Make sure that consent form includes all elements required by regional regulatory body Submit the designed consent form to IR for approval/make any change required by IRB Use the IRB approved informed consent form to discuss and explain trial related risks, benefits, and other aspects with the potential participant or its legal representative before the trail begins Provide the participant time and opportunity to clarify any doubts about the trial, and discuss it with other persons Not obligate or influence subjects to participate or to continue participations against their will Obtain a signed and dated voluntary informed consent from participants Inform the participant of their right to withdraw from the ongoing study without penalty, repercussions, or reason Keep subject informed about new findings of the ongoing trial, which may affect their decision Present information in language that subjects can understand
Sponsor	Elaborate a site-specific informed consent form with investigators Confirm that informed consent is properly required by the investigators, before the beginning of the trial Ensure that investigators use only IRB-approved informed consent forms
Subjects	Should properly understand all relevant aspects before signing the form Must comprehend the relevant information Feel free to clarify doubts Should consent voluntarily Should be aware of their rights when they agree for participating in the study
Regulatory authorities	Audit investigator site Ensure the quality and integrity of data obtained from clinical trials Protect the rights and welfare of participants

(d) The subject/legally acceptable representative and individual obtaining consent must personally sign with date the form. The signature of the prospective subject/legally acceptable representative on informed consent document indicated that content of informed consent document has been adequately discussed and the subject/subject's legally acceptable representative freely gave the informed consent.

6 Independent Review and Conflict of Interests

Investigators inherently have multiple, legitimate interests—interests to conduct high-quality research—complete the research promptly, protect research subjects, obtain funding, and advance their careers. These diverse interests can generate conflicts that may

unintentionally distort the judgment of investigators regarding the design, conduct, and analysis of research [11]. One of the hallmarks of a trustworthy clinical research is a comprehensive process for disclosure of interests (DOI) and management of conflicts of interest (COIs) [17]. Independent review of research protocols by individuals who do not relate with the clinical research helps minimize the potential impact of conflict of interest. Review should be done by a full committee of individuals with a range of expertise who have the authority to approve, amend, or terminate a study. Also, independent review of a study's compliance with ethical requirements assures members of society that people who enroll in trials will be treated ethically and that some segments of society will not benefit from the mistreatment of other human beings. Review also assures people that if they enroll in clinical research, the trial is ethically designed, and the risk–benefit ratio is favorable [11].

A conflict of interest (COI) occurs when an individual who is involved in multiple interests has one interest that interferes with another. The terms "conflict of interests" and "competing interests" are used interchangeably. Another way of describing a COI is: "*A conflict of interest is a set of circumstances that creates a risk that professional judgement or actions regarding a primary interest will be unduly influenced by a secondary interest.*" A COI occurs in many professions but has serious impact in medical practice and medical research, as a patient's life is often at stake. The mere presence of a COI does not imply an impropriety but suggests the risk of one, and if detected or declared in time, the impropriety can be prevented or at least its impact minimized. In clinical research, the aim of the therapeutic studies is to verify the safety and establish the efficacy of new drugs/devices. Though this is the primary aim of the study, the safety and well-being of the participants is more important than the eventual benefit of the drug to the society. According to the good clinical practice (GCP) guidelines of the International Conference on Harmonization (ICH), the health and medical care of the participants is the responsibility of the investigator; hence, any COI of the investigator is a risk for the participant. At a higher tier, the ethics committee (EC) provides oversight to the trial at the site, and hence, any COI affecting a member of the EC is a potential risk, though the level of risk could be lower than that of the investigator. Nonetheless, it is a risk, and hence, all efforts should be made to identify and eliminate it. For a fair and honest review by the EC, it is necessary to ascertain that no COI exists for the members approving and reviewing studies [17].

References

1. Zhang A (2015) DNA vaccines: scientific and ethical barriers to the vaccines of the future. Harvard College Global Health Review, Cambridge
2. Myhr AI (2017) DNA vaccines: regulatory considerations and safety aspects. Curr Issues Mol Biol 22:79–88
3. Spier RE (2004) Ethical aspects of the methods used to evaluate the safety of vaccines. Vaccine 22:2085–2090
4. Plotkin S (2011) Clinical applications of DNA vaccines: current progress. Clin Infect Dis 53:296–302
5. Parents Requesting Open *Vaccine* Education (PROVE) (2000) Conflicts of interest in vaccine policy making. Majority Staff Report, Committee on Government Reform, U.S. House of Representatives
6. Doussau A, Grady C (2016) Deciphering assumptions about step wedge designs: the case of Ebola vaccine research. J Med Ethics 42:797–804
7. Bhanot N, Mehta K (2012) Wrong at every step: the licensing of HPV vaccines. Mainstream Weekly 32
8. Johari V (2017) Identifying ethical issues in the development of vaccines and in vaccination. Indian J Med Ethics 2(2):88–93
9. Molyneux M (2017) New ethical considerations in vaccine trials. Hum Vaccin Immunother 13:2160–2163
10. van Luijn HEM, Musschenga AW, Keus RB et al (2002) Assessment of the risk/benefit ratio of phase II cancer clinical trials by Institutional Review Board (IRB) members. Ann Oncol 8:1307–1313
11. Emanuel EJ, Wendler D, Grady C (2000) What makes clinical research ethical. JAMA 283:2701–2711
12. ICH (2015) Integrated addendum to ICH E6 (R1): Guideline for Good Clinical Practice E6 (R2)
13. EMA (2013) Reflection paper on risk-based quality management in clinical trials
14. Piantadosi S (2013) Clinical trials: a methodologic perspective. John Wiley & Sons, Hoboken, NJ
15. Nijhawan LP, Janodia MD, Muddukrishna BS et al (2013) Informed consent: issues and challenges. J Adv Pharm Technol Res 4:134–140
16. Kadam RA (2017) Informed consent process: a step further towards making it meaningful! Perspect Clin Res 8:107–112
17. Ghooi RB (2015) Conflict of interest in clinical research. Perspect Clin Res 6:10–14

Chapter 18

Preparation of an Academic Clinical Trial

Ana Cristina Ramalhinho and Miguel Castelo-Branco

Abstract

Clinical trials are research studies performed in humans to evaluate the efficacy and safety of an intervention. They are the primary method by which researchers discover if a new treatment (drug, diet, medical device) is safe and effective in humans. DNA vaccines are considered, by definition, advanced therapy medicinal products (ATMPs). ATMPs are medicines for human use that are based on genes, tissues, or cells. They offer groundbreaking new opportunities for the treatment of disease and injury. Clinical trials using ATMPs are subject to specific regulatory requirements. This chapter will describe the most important steps when planning a clinical trial with DNA vaccines, such as regulatory and submission requirements, designing of a successful clinical trial protocol, stakeholders' responsibilities, and feasibility assessment.

Key words Advanced therapy medicinal products, Clinical trial, Feasibility, Protocol, Regulatory agencies, Stakeholders

1 Introduction

Universally, clinical trials are defined as research studies performed in humans that aim to evaluate a medical, surgical, or behavioral intervention. They are the primary methods by which researchers discover if a new treatment, like a new drug or diet or a medical device (e.g., a pacemaker), is safe and effective in humans. Often a clinical trial is used to gain knowledge if a new treatment is more effective and/or has less harmful side effects than the standard treatment.

Clinical trials advance through four phases to test a treatment, find the appropriate dosage, and investigate side effects. If, after the first three phases, researchers find a drug or other intervention to be safe and effective, the regulatory agency (the European Medicines Agency (EMA) in Europe and the Food and Drug Administration (FDA) in USA) approves it for clinical use and continues to monitor its effects.

Phase I corresponds to the initial safety trials on a new medicine, and first application in humans. The goal is to establish the

Ângela Sousa (ed.), *DNA Vaccines: Methods and Protocols* , Methods in Molecular Biology, vol. 2197,
https://doi.org/10.1007/978-1-0716-0872-2_18,

dose range tolerated in healthy volunteers for single and multiple doses. Phase I trials may be conducted in severely ill patients (e.g., in the field of cancer), when no other therapeutic alternative exists, or in less ill patients when pharmacokinetic issues are addressed [1].

Phase II trials begin after the successful completion of Phase I. During Phase II, the investigational medicinal product is tested for efficacy and safety. The studies conducted during Phase II, also known as therapeutic exploratory studies, try to discover whether the medicine treats the intended disease or condition. When an investigational medicinal product fails, it is usually because Phase II trials show that it does not work as expected or has unforeseen toxic effects in patients. Phase II trials can be divided into Phase IIa and Phase IIb. Phase IIa trials are pilot clinical trials to evaluate efficacy (and safety) in selected populations of patients with the disease or condition to be treated, diagnosed, or prevented. Objectives may focus on dose–response, type of patient, frequency of dosing, or numerous other characteristics of safety and efficacy. Phase IIb are well controlled trials to evaluate efficacy (and safety) in patients with the disease or condition to be treated, diagnosed, or prevented. These clinical trials usually represent the most rigorous demonstration of a medicine's efficacy. Sometimes referred to as pivotal trials and proof of concern [2].

Phase III clinical trial is the study that will test the safety and how well a new treatment works compared with a standard treatment. For example, Phase III clinical trials may compare which group of patients has better survival rates or fewer side effects. In most cases, treatments move into Phase III clinical trials only after they meet the goals of Phase I and Phase II clinical trials. Phase III clinical trials may include hundreds of people. They can be divided into Phase IIIa and Phase IIIb. Phase IIIa trials are conducted after efficacy of the medicine is demonstrated, but prior to regulatory submission of a new drug application (NDA) or another dossier. These clinical trials are conducted in patient populations for which the medicine is eventually intended. Phase IIIa clinical trials generate additional data on both safety and efficacy in relatively large numbers of patients in both controlled and uncontrolled trials. Clinical trials are also conducted in special groups of patients (e.g., renal failure patients) or under special conditions dictated by the nature of the medicine and disease. These trials often provide much of the information needed for the package insert and labeling of the medicine. Phase IIIb clinical trials are conducted after regulatory submission of an NDA or other dossier, but prior to the medicine's approval and launch. These trials may supplement earlier trials, complete earlier trials, or may be directed toward new types of trials (e.g., quality of life, marketing) or Phase IV evaluations. This is the period between submission and approval of a regulatory dossier for marketing authorization [3].

Phase IV clinical trial is based on studies or trials conducted after a medicine is marketed to provide additional details about the medicine's efficacy or safety profile, also known as Post Marketing Surveillance Trials. Different formulations, dosages, durations of treatment, medicine interactions, and other medicine comparisons may be evaluated. New age groups, races, and other types of patients can be studied. Detection and definition of previously unknown or inadequately quantified adverse reactions and related risk factors are an important aspect of many Phase IV studies. If a marketed medicine is to be evaluated for another (i.e., new) indication, then those clinical trials are considered Phase II clinical trials. The term "post-marketing surveillance" is frequently used to describe those clinical studies in Phase IV (i.e., the period following marketing) that are primarily observational or non-experimental in nature, to distinguish them from well-controlled Phase IV clinical trials or marketing studies [4].

This chapter will describe the steps involved when planning a clinical trial with DNA vaccines, considered advanced therapy medicinal products (ATMPs). Will be included regulatory and submission requirements, designing of a successful clinical trial protocol, stakeholders' responsibilities, and feasibility assessment.

Note: The information presented in this chapter is intended to outline the general processes, principles, and concepts of the healthcare product development lifecycle. Since regulatory requirements are ever-changing, it is current only as of the date of publication and not intended to provide detailed instructions for product development. Every healthcare product is unique, and therefore, so is its associated product development lifecycle. Specific advice should be sought from a qualified healthcare or other appropriate professional.

2 Clinical Trials of Investigational Medicinal Products (IMPs) and Advanced Therapy Medicinal Products (ATMPs)

An investigational medicinal product (IMP) is a pharmaceutical form of an active substance or placebo being tested or used as a reference in a clinical trial, including products already with a marketing authorization but used or assembled (formulated or packaged) in a way different from the authorized form, or when used for an unauthorized indication, or when used to gain further information about the authorized form [5]. Medicinal products with a marketing authorization (MA) are classified as IMPs when they are to be used as the test substance or reference substance in a clinical trial, provided they are used or assembled (formulated or packaged) in a way different from the authorized form, or used for an unauthorized indication, or used to gain further information about the authorized form. On this basis, provided that the requirement(s) are met, reference products used as comparators should be considered as IMPs [6]. A Non-Investigational

Medicinal Product (NIMP) is a medicinal product which is not classed as an IMP in a trial, but may be taken by subjects during the trial. Examples include concomitant or rescue/escape medication used for preventive, diagnostic, or therapeutic reasons and/or medication given to ensure that adequate medical care is provided for the subject during a trial [7].

Advanced therapy medicinal products (ATMPs) are medicines for human use that are based on genes, tissues, or cells. They offer groundbreaking new opportunities for the treatment of disease and injury.

ATMPs can be classified into three main types:

(a) Gene therapy medicines: These contain genes that lead to a therapeutic, prophylactic, or diagnostic effect. They work by inserting "recombinant" genes into the body, usually to treat a variety of diseases, including genetic disorders, cancer, or long-term diseases. A recombinant gene is a stretch of DNA that is created in the laboratory, bringing together DNA from different sources.

(b) Somatic-cell therapy medicines: These contain cells or tissues that have been manipulated to change their biological characteristics or cells or tissues not intended to be used for the same essential functions in the body. They can be used to cure, diagnose, or prevent diseases.

(c) Tissue-engineered medicines: These contain cells or tissues that have been modified, so they can be used to repair, regenerate, or replace human tissue.

In addition, some ATMPs may contain one or more medical devices as an integral part of the medicine, which are referred to as combined ATMPs. An example of this is cells embedded in a biodegradable matrix or scaffold (*see* Regulation (EC) No 1394/2007 [8] and Directive 2001/83/EC) [9].

3 Designing the Clinical Trial Protocol

Writing a research proposal is probably one of the most challenging and difficult task. Clinical research is conducted according to a plan (a protocol) or an action plan. The protocol demonstrates the guidelines for conducting the trial. It illustrates what will be made in the study by explaining each essential part of it and how it is carried out. It also describes the eligibility of the participants, the length of the study, the medications, and the related tests. A well-designed protocol must result in a short but comprehensive document that clearly summarizes the project. Thus, the protocol proposal must be clear, free of typographical errors, accurate, and easy to read [10]. Based on the International Conference on Harmonization, GCP Guidelines for Clinical Trial Protocol development, to

draft a sound scientific design of a clinical research study, it is recommended that the following information be included in a research protocol (Table 1) [11].

The information included in this table when writing the clinical trial protocol will help facilitate the application submission process and study approval from the Institutional Review Boards and other competent authorities. Note that the protocol should adequately answer the research question. It should provide enough detail that can allow another investigator to do the study and arrive at comparable conclusions. The proposed number of participants should be reasonably justified and the scientific design must be adequately described [10].

The first methodological step of the protocol design should be the formulation of a research question. Decisions made about the research question will dictate future decisions on research design. Both clinical experience and a thorough understanding of the current state of evidence are required. To do this, many investigators will start by mastering the literature, most commonly by performing systematic literature reviews and meta-analyses, and attending conferences to comprehend current issues. These activities naturally lead to a research question. When assessing a good research question, the investigator should remember that it should be *feasible* to carry out, be an *interesting* topic, be a *novel* idea to confirm and/or contribute information that will further the field, be *ethical* to carry out, and most importantly, have *relevance* to the scientific community such that it may influence clinical management, health policy, or provide new ideas for research. These five criteria can be remembered by the mnemonic, *FINER—Feasible*, *I*nteresting, *N*ovel, *E*thical, *R*elevant (Table 2) [12].

4 Stakeholders' Responsibilities

From the several parts involved in a clinical trial, investigators and promoters (or sponsors) share the major part of responsibilities and duties of all stakeholders. Usually, the clinical trial promoter (and/or sponsor) is considered to be the company or organization which conducts a clinical trial. But when we are leading with academic trials, the role of the promoter may be assumed by the principal investigator. In definition, a promoter is an individual, institution, company, or organization (e.g., a contract research organization) that takes the responsibility to initiate, manage, or finance the clinical trial [11] but does not actually conduct the investigation. A sponsor-investigator, on the other hand, takes on the responsibility as a clinical study sponsor and *also* conducts or oversees the clinical trial. Thus, a sponsor-investigator must comply with the applicable regulatory requirements that pertain to both the sponsor and the investigator [5, 13].

Table 1
Information to be addressed in a successful clinical trial protocol

Study summary
Study summary should include the following: • Protocol title (the title on related IRB submissions (e.g., applications for new study, changes in procedure, research progress reports) must match the title of the protocol) • Study phase • Duration of the study • Methodology • Study site • Approximate number of subjects • Name, title, address, and telephone number of the PI, co-PI, sponsors, and study coordinators • Investigator's affiliation
List of abbreviations
• Provide a list of abbreviation used in the study protocol
Background information/significance
• Name and description of the investigational product, and in case of retrospective reviews, justification for the chart and medical record reviews • Summary of results from prior clinical studies and clinical data to date • Human subjects' risks and benefits • Description of the population to be studied • Description and justification for the dosing regimen and treatment period • A paragraph stating that the clinical study will be conducted in compliance with the protocol, SOPs, and the federal, state, and local regulations • Citations from the references and data relevant to the study that also provides background for the trial
Objectives/rationale/research question
• Include a detailed description of the primary and secondary objectives and the purpose of the study and clearly state your research hypothesis or your question • Discuss the project's feasibility • Give details of resources, skills, and experience to complete the study • Include any pilot study information
Clinical study design
• Primary and secondary endpoints, if any, to be measured during the study • Include the information that is needed to answer the research question • Include the study design, e.g., single, double-blind, observational, randomized, and retrospective. A schematic diagram of the study design would be helpful • Include the amount of dosage, dosing regimen of the drug, packaging, and labeling of the experimental drug • Explain how the study drug will be stored and dispensed • Include the expected duration of the study and subject's participation and a description of the sequence and duration of all study periods • Include any follow-up visits • Describe when a subject's participation in the trial may be discontinued • Maintenance of randomization codes and confidentiality • Describe the potential risks and steps taken to minimize the risks • Identify possible benefits of the study

(continued)

Table 1
(continued)

Inclusion and exclusion criteria of the subjects
• Include subjects' inclusion criteria • Include subjects' exclusion criteria. Women of childbearing potential may not be routinely excluded from participating in research; however, pregnant women should be excluded unless there is a clear justification to include them • Include enrollment of persons of diverse racial and ethnic backgrounds to ensure that the benefits of the research study are distributed in an equitable manner
Informed consent form process: • Provide information about the regulatory requirements of the consent form and which languages will be used • Include a discussion of additional safeguards taken if potentially vulnerable subjects will be enrolled in the study, e.g., children, prisoners, cognitively impaired, and critically ill subjects • Specify code of ethics under which consent will be obtained • Include a copy of the proposed informed consent along with the protocol
Adverse event reporting
• Describe your plan to report any adverse event • Anticipated adverse events should be clearly documented • Identify the type and duration of follow-up and treatment for subjects that experience an adverse event
Assessment of safety and efficacy
• Be specific about the efficacy parameters • Include the methods and timing for assessing, recording, and analyzing efficacy parameters • Specify the safety parameters • Record and report properly all the adverse events and inter current illnesses
Treatment of subjects
• List all the treatments to be administered including product's name, dose, route of administration, and the treatment period for subjects • Include all medication permitted before and during the clinical trial • Include the procedures for monitoring subject compliance
Data collection plan
• Define the type of data collection instrument that will be used and list all the variables • Specify if computerized databases will be used • Identify what software will be used • Explain precautionary steps taken to secure the data
Data access
• Inform who will have access to the data and how the data will be used. If data with subject identifiers will be released, specify the person(s) or agency to whom the information will be released and the purpose of the release • Address all study-related monitoring, audits, and regulatory inspections
Statistical methods
• Describe the statistical methods in detail • Include the number of subjects you are planning to enroll. For multi-center studies, include the total number of sites expected and the total number of subjects to be enrolled across all sites

(continued)

Table 1
(continued)

• Provide the rationale for the sample size, the calculations on the power of the trial, and the clinical justification • Procedure of accounting for missing, unused, and spurious data • Procedures for reporting deviations from the original statistical plan • Include the selections of subjects to be included in the analyses
Conflict of interest
• Identify and document clearly any consultative relationship that the principal or co-investigators has with a non-USF entity related to the protocol that might be considered a real or apparent conflict of interest
Publication and presentation plans
• List any meetings or conference you will be presenting the data and the results of your study
Timeline
• A short paragraph stating when you plan to start and complete the study • Include a description, e.g., subject enrollment within a month, data collection within 6 months
References
• List all the references used in the background section at the end of the protocol

Table 2
FINER mnemonic to formulate a good clinical research question

F	*Feasible*	Adequate number of subjects, adequate technical expertise and resources, affordable in time and money, manageable in scope, *attainable objectives*
I	*I*nteresting	To the investigator, to the scientific community, to society, to funding agencies
N	*N*ovel	Confirms or refutes previous findings extends previous findings provides new findings
E	*E*thical	Ethical concerns with recruitment, safety, incentives, benefits, risks, confidentiality, anonymity
R	*R*elevant	To scientific knowledge, to clinical and health policy, to future research directions

There are specific regional requirements for a clinical study sponsor. Generally, a sponsor is responsible for selecting the investigator(s); providing investigator(s) with the necessary information to conduct the clinical trial; ensuring proper monitoring of the clinical study; ensuring all the necessary ethic review(s) and approval(s) are obtained; preparing and submitting clinical trial application(s) and amendment(s) to the appropriate regulatory agencies; ensuring that any reviewing ethics board and regulatory agencies are promptly informed of any significant new information (e.g., important findings that affect product safety) in a clinical study, ensuring compliance with labeling, reporting, and record-keeping requirements; refraining from engaging in promotional activities and other prohibited activities such as commercializing an investigational medical device; and ensuring that the clinical

study is conducted in accordance with Good Clinical Practice (GCP) (*see* the ICH HARMONISED GUIDELINE FOR GOOD CLINICAL PRACTICE ICH E6(R2)) [11].

The responsibilities of an investigator generally include protecting the rights, safety, and welfare of subjects in the clinical study; ensuring that informed consent is properly obtained from clinical trial subjects and kept all along the trial; conducting the clinical study (i.e., directly overseeing the administration of the test products to the subject); ensuring that the clinical trial is conducted in accordance with the signed agreement and the investigational plan; controlling the products under investigation (e.g., supervising medical device use and disposal); ensuring proper record-keeping; and reporting requirements are met (e.g., mandatory safety reporting). In situations where there is a team of researchers, the investigator will act as the team leader.

When the investigator acts simultaneously as sponsor, some additional considerations also apply. Sponsor-investigators also generally need to manage the following: securing funding for the clinical trial; applying for the appropriate insurance; generating the appropriate clinical trial documentation (e.g., informed consent, protocols) and submissions (e.g., ethics and/or regulatory submissions); ensuring adequate resources are available for the duration of the trial (e.g., experienced staff, investigational and control products, clinical and medical supplies, an analytical laboratory); creating appropriate written procedures (e.g., standard operating procedures related to GCP); and meeting all the applicable regulatory requirements such as obtaining and maintaining necessary approvals from the relevant ethics review boards and regulatory agencies. Also, sponsor-investigators will need to execute several administrative tasks to initiate a clinical trial. Research the regulatory requirements pertaining to the applicable submissions. Make good use of regulatory agency websites and professional organizations as well as related publications, seminars, and training. Contact the relevant regulatory agency via formal or informal means. Formal means may take the form of a request for a pre-submission meeting with the agency. Informal means may include contacting them with general questions. Prepare and submit the application based on the format and content relevant to the specific submission. Make sure that any comments or feedbacks received at the pre-submission meeting are incorporated in the submission dossier. After a submission is approved, ensure that all the post-approval requirements are fulfilled, such as any required safety reporting, annual reporting, and amendment submissions relating to significant changes to the products or study plan. Make certain that you fulfill your responsibilities as a sponsor as well as an investigator according to applicable regulatory requirements [13].

5 Regulatory Submission

The European Medicines Regulatory System (EMRS) operates through a pyramid, beginning from the Common European Union legislations and guidelines and ending in each Member State national procedures, regulations, and authorizations (Fig. 1).

The European Medicines Agency (EMA) co-exists with over 40 National Competent authorities in the EU/EEA, forming an integrated network. A centralized procedure for Marketing Authorization co-exists with procedures at national level (de-centralized procedure/mutual recognition procedure). EMA coordinates the existing scientific resources in Member States and provides an interface between all parties and works toward harmonization of regulatory and technical requirements within the EU. EMA scientific guidelines apply regardless as to the marketing authorization procedure used.

All clinical trials concerning IMPs require authorization from each country Medicines Regulatory Agencies (e.g., Medicines and Healthcare products Regulatory Agency (MHRA) in the United Kingdom). You can find a list of Global Regulatory Authority websites in https://www.pda.org/scientific-and-regulatory-affairs/regulatory-resources/global-regulatory-authority-websites and a list of European National Competent Authorities in https://www.ema.europa.eu/en/partners-networks/eu-partners/eu-member-states/national-competent-authorities-human. Usually application is made through informatics systems, after paying a standard application fee. Other fees may be applied for any amendments submitted after the initial approval until trial completion. For non-commercial trials, as sponsor-investigators driven trials, fees may not be applicable.

For advanced therapy medicinal products like DNA vaccines, the scope of centralized procedure is mandatory since 2008, so The

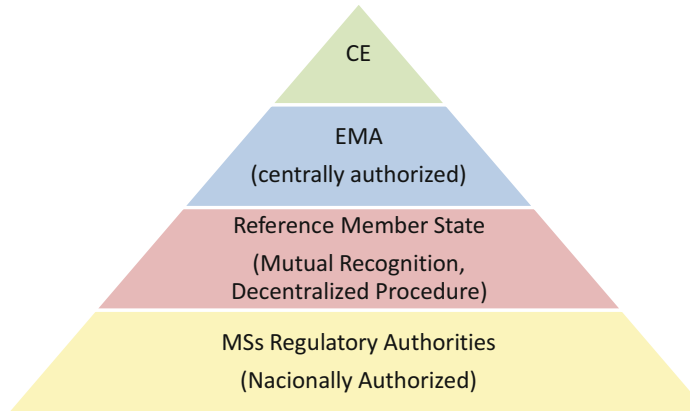

Fig. 1 European Medicines Regulatory System (EMRS)

Table 3
Summary of the contents of the clinical trials authorization application

Part I—Scientific and medicinal product documentation	Part II—National- and patient-level documentation
Application form	Patient materials: informed consent, patient information leaflet
Protocol	Compensation arrangements
Investigators brochure	Recruitment arrangements
GMP documentation	Investigators and facilities suitability
IMPD/AMPD	Damage compensation
Scientific advice	Data protection rules (Note: The precise content will be determined by each member state)
Pediatric Investigation Plan decision	
IMP/auxiliary labels	

European Medicines Agency (EMA) is responsible for the scientific evaluation of marketing authorization applications for all advanced therapy medicinal products (ATMPs) in the European Economic Area. As all advanced therapy medicines are authorized centrally via the European Medicines Agency (EMA), they benefit from a single evaluation and authorization procedure. As with all medicines, the Agency continues to monitor the safety and efficacy of advanced therapy medicines after they are approved and marketed. The Agency also gives scientific support to developers to help them design pharmacovigilance and risk management systems used to monitor the safety of these medicines. Under the European Union Clinical Trial Regulation (Regulation (EU) No 536/2014), sponsors are required to apply via a EU portal for authorization to conduct an interventional clinical trial with medicines in Europe. Table 3 summarizes the contents of the application for clinical trials in EU.

Most National Regulatory Agencies state that applications for clinical trial authorization should comply with the European Commission's guideline "Detailed guidance on the request to the competent authorities for authorization of a clinical trial on a medicinal product for human use, the notification of substantial amendments and the declaration of the end of the trial (CT-1)" in Chapter 1 of Volume 10 of EudraLex. Before an application can be submitted to the Regulatory Agency, sponsors must obtain a EudraCT number by logging onto the EudraCT website and following the instructions to obtain a security code and to apply for the EudraCT number. The sponsor should then use this unique EudraCT number to create a EudraCT application form. EudraCT is the European Clinical Trials Database of all clinical trials. Registration is compulsory for every clinical trial with at least one site in the European Community and provides a unique identification number for the trial, the EudraCT Number. EudraCT number can be obtained online at https://eudract.ema.europa.eu. Besides EudraCT register, most journals require many studies to have been listed on an independent, free to access, validated public register. These include trials whose primary

purpose is to affect clinical practice, trials providing evidence of clinical effectiveness or adverse effects, investigations of the biology of disease, collection of preliminary data that may lead to larger clinical trials and device trials. The trial must be registered before the first patient is recruited. Acceptable registries include ClinicalTrials.gov (www.clinicaltrials.gov) and International Standard Randomized Controlled Trial Number Register (ISRCTN). There may be a charge for registration.

6 Feasibility Assessment

In general terms, clinical trial feasibility is a process of evaluating the possibility of conducting a particular clinical program/trial in a particular geographical region with the overall objective of optimum project completion in terms of timelines, targets, and cost. Conducting clinical trial feasibility is one of the first steps in clinical trial conduct. This process includes assessing internal and environmental capacity, alignment of the clinical trial in terms of study design, dose of investigational product, comparator, patient type, with the local environment, and assessing potential of conducting clinical trial in a specific country. A robust feasibility also ensures a realistic assessment and capability to conduct the clinical trial. For local affiliates of pharmaceutical organizations, and contract research organizations, this is a precursor to study placement and influences the decision of study placement [14].

Traditionally, feasibility assessment is based on the answer of the investigator in each site to the following questions:

(a) What regulatory hurdles can we expect to encounter in the countries being considered for the study?

(b) Is the study design consistent with the standard of care in the various regions?

(c) Is there a large enough patient population to justify inclusion of particular countries and sites?

(d) Are the sites able to get the right infrastructure and staff in place to support the trial?

(e) How many patients can a given site enroll in a specified time frame?

Thus, the investigator is asked for input via questionnaires on how many patients who fit the study criteria an investigator could expect to recruit for an upcoming trial. However, there are limitations of relying on feedback from investigators, as they tend to overestimate their enrollment capability, hoping they will appear more attractive to sponsors and CROs and get selected for the trial. So, sponsors of drugs in development and the Contract Research Organizations (CROs) working on their behalf are often caught off guard by the difficulties they experience in enrolling subjects into

trials. Indeed, timelines for the majority of trials must be extended in order to fulfill their patient quotas. Recently, an evidence-based approach to conducting clinical trial feasibility assessments was proposed, which incorporates patient insights, draws on commercially available data, and uses statistical modeling to improve the predictability of patient enrollment [15]. This comprehensive feasibility assessment involves gathering information as detailed below (Table 4) and then using statistical modeling to incorporate and manage it all.

Table 4
Comprehensive feasibility assessment proposed by Johnson, 2015 [15]

Gauging patient availability. The first step in the process is to estimate the number of patients who will be eligible to participate in the trial. This calculation will be based on a breakdown, by country, of the incidence/prevalence of the disease and competing trials in the same therapeutic area; the study inclusion/exclusion criteria; the treatment guidelines and procedures; electronic medical records (EMRs), prescription, and/or integrated medical claims databases should be mined to understand how many patients are being treated for the particular disease and where they are located. These databases can be searched by diagnostic and procedure codes, as well as by various other inclusion/exclusion criteria
Gathering the patient perspective. At an early stage in the trial planning process, it is important to understand how the target patient population would respond to the protocol requirements. What would patients find appealing or objectionable about the approach? What motivational drivers would influence their participation decision? It is possible, for instance, that some aspect of the protocol could pose an unforeseen emotional or logistical hurdle for patients and be a risk to enrollment. A combination of primary research and social media monitoring should be used to validate assumptions made about patient attitudes, beliefs, and behaviors, so that the protocol can be evaluated through a patient's lens. When discovered early, any possible risks can either be mitigated or factored into enrollment estimates
Selecting countries with the most potential. The next step is to determine the optimal mix of countries based on their potential for enrolling patients. This is a matter of blending the information gathered above on patient counts, analogous historical trials, and competing trials with information on where sites operate by therapeutic area, indication, and specialty. A number of commercially available databases can reveal how many sites have the relevant experience, by country. The number of available patients can be affected by the number of competing trials in the same indication in a given country
Identifying the best investigators/sites. A major factor in enrollment success is site selection. Companies tend to turn repeatedly to a limited number of sites with which they have prior experience—an approach that often leads to disappointing results. A better approach is to use research and analytics to target the right sites that have
The required capabilities in terms of staff, experience, infrastructure, and equipment. Most protocols will require that sites have specific capabilities, whether it is expertise in the therapeutic area, familiarity with a particular technology, or access to specialized equipment. Analytical tools are available to profile sites on a range of dimensions, including their research activity, infrastructure, personnel, initiation timelines, and access to the targeted patient population
Sufficient capacity without competing trials. This can best be established by using the technique that sponsors have traditionally relied on to the exclusion of most others: Sending questionnaires to sites. Once sites have been identified that appear to meet the above criteria, they can be surveyed as to their availability in the proposed time period. Whether they are participating in competing trials can also be verified though publicly available and subscription trial intelligence databases

References

1. Dresser R (2009) First-in-human trial participants: not a vulnerable population, but vulnerable nonetheless. J Law Med Ethics 37:38–50
2. Johan PE, Karlberg JPE, Speers MA (2010) Reviewing clinical trials: a guide for the Ethics Committee, Clinical Trials Centre, The University of Hong Kong Hong Kong SAR, PR China
3. Umscheid CA, Margolis DJ, Grossman CE (2011) Key concepts of clinical trials: a narrative review. Postgrad Med 123:194–204
4. Cingi C, Muluk NB (2016) Quick guide to good clinical practice how to meet international quality standard in clinical research. Springer, New York
5. Directive 2001/20/EC of The European Parliament and of The Council on the approximation of the laws, regulations and administrative provisions of the Member States relating to the implementation of good clinical practice in the conduct of clinical trials on medicinal products for human use
6. European Commission Enterprise and Industry Directorate-General Consumer goods Pharmaceuticals Guidance on Investigational Medicinal Products (IMPs) and other medicinal products used in Clinical Trials to be included in The rules governing medicinal products in the European Union, vol 10: Clinical Trials Notice to Applicants Chapter V Additional Information (2011)
7. The rules governing medicinal products in the European Union, vol 10—Guidance documents applying to clinical trials guidance on investigational medicinal products (Imps) and 'Non Investigational Medicinal Products' (NIMPS) (2011)
8. Regulation (EC) No. 1394/2007 Regulation of the European Parliament and of the Council of 13 November 2007 on advanced therapy medicinal products
9. Directive 2001/83/EC of the European Parliament and of the Council of 6 November 2001 on the Community Code Relating to Medicinal Products for Human Use
10. Al-Jundi A, Sakka S (2016) Protocol writing in clinical research. J Clin Diagn Res 10: ZE10–ZE13
11. International Conference on Harmonization (1996) E6(R1): good clinical practice
12. Chung KC, Song JW, WRIST study group (2010) A guide on organizing a multicenter clinical trial: the WRIST study group. Plast Reconstr Surg 126:515–523
13. Kracov DA, Dwyer LM (2006) Regulatory requirements for clinical studies of medical devices and diagnostics. In: Becker KM, Whyte JJ (eds) Clinical evaluation of medical devices. Principles and case studies, 2nd edn. Humana Press, Totowa
14. Rajadhyaksha V (2010) Conducting feasibilities in clinical trials: an investment to ensure a good study. Perspect Clin Res 1:106–109
15. Johnson O (2015) An evidence-based approach to conducting clinical trial feasibility assessments. Clin Invest 5:491–499

INDEX

Ângela Sousa (ed.), *DNA Vaccines: Methods and Protocols*, Methods in Molecular Biology, vol. 2197, https://doi.org/10.1007/978-1-0716-0872-2,

D

E

F

G

H

I

L

M

N

O

P

R

S

T

U

V

W

Y

Z